Symmetry-based stability theory in fluid mechanics

Zur Erlangung des akademischen Grades Doktor-Ingenieur (Dr.-Ing.)
Genehmigte Dissertation von Tim Gebler aus Erlenbach a. Main
Tag der Einreichung: 22. April 2022, Tag der Prüfung: 21. Juni 2022

1. Gutachten: Prof. Dr.-Ing. Martin Oberlack
2. Gutachten: Prof. Dr. rer. nat. Amsini Sadiki
Darmstadt, Technische Universität Darmstadt

TECHNISCHE UNIVERSITÄT DARMSTADT

Mechanical Engineering Department

Fachgebiet für Strömungsdynamik

Symmetry-based stability theory in fluid mechanics

Accepted doctoral thesis by Tim Gebler

Date of submission: 22. April 2022
Date of thesis defense: 21. Juni 2022

Darmstadt, Technische Universität Darmstadt

Bitte zitieren Sie dieses Dokument als:
URN: urn:nbn:de:tuda-tuprints-237805
URL: http://tuprints.ulb.tu-darmstadt.de/23780
Jahr der Veröffentlichung auf TUprints: 2023

Dieses Dokument wird bereitgestellt von tuprints,
E-Publishing-Service der TU Darmstadt
http://tuprints.ulb.tu-darmstadt.de
tuprints@ulb.tu-darmstadt.de

Meinen Eltern und meinem Großvater

Erklärungen laut Promotionsordnung

§ 8 Abs. 1 lit. c PromO

Ich versichere hiermit, dass die elektronische Version meiner Dissertation mit der schriftlichen Version übereinstimmt.

§ 8 Abs. 1 lit. d PromO

Ich versichere hiermit, dass zu einem vorherigen Zeitpunkt noch keine Promotion versucht wurde. In diesem Fall sind nähere Angaben über Zeitpunkt, Hochschule, Dissertationsthema und Ergebnis dieses Versuchs mitzuteilen.

§ 9 Abs. 1 PromO

Ich versichere hiermit, dass die vorliegende Dissertation selbstständig und nur unter Verwendung der angegebenen Quellen verfasst wurde.

§ 9 Abs. 2 PromO

Die Arbeit hat bisher noch nicht zu Prüfungszwecken gedient.

Darmstadt, 22. April 2022

T. Gebler

Abstract

The present work deals with the stability theory of fluid flows. The central subject is the question under which circumstances a flow becomes unstable. Instabilities are a frequent trigger of laminar-turbulent transitions. Stability theory helps to explain the emergence of structures, e.g. wave-like perturbation patterns. In this context, the use of Lie symmetries allows the classification of existing and the construction of new solutions within the framework of linear stability theory. In addition, a new nonlinear eigenvalue problem (NEVP) is presented, whose derivation is completely based on Lie symmetries.
In classical linear stability theory, a normal ansatz is used for perturbations. Another ansatz that has been shown in early work is the Kelvin mode ansatz. In the work of Nold and Oberlack (2013) and Nold et al. (2015) it was shown that these ansätze can be traced back to the Lie symmetries of the linearized perturbation equations.
Interestingly, knowledge of the symmetries also allows for the construction of new ansatz functions that go beyond the known ansätze. For a plane rotational shear flow, in addition to the normal mode ansatz, an algebraic mode ansatz with algebraic behavior in time t^s (eigenvalue s) can be constructed. The flow is stable according to Rayleigh's inflection point criterion, which is also confirmed by the algebraic mode ansatz. Furthermore, exact solutions of the eigenfunctions can be found and new stable modes can be determined by asymptotic methods. Thereby, spiral-like structures of the vorticity can be recognized, which propagate in the region with time.
Another key result of this work is the formulation and solution of an NEVP based on the Lie symmetries of the Euler equation. It can is shown that an NEVP can be formulated for a class of flows with a constant velocity gradient. These include, for example, linear shear flows, strained flows, and rotating flows.
The NEVP for linear shear flows shows a relation to experimental data from turbulent shear flows. It can be theoretically shown that the turbulent kinetic energy scales exponentially with the eigenvalue of the NEVP. The eigenvalue is determined numerically using a parallel spectral solver. Initially, nonlinear terms are neglected. The determined eigenvalues are in the range of known literature values for turbulent shear flows. Furthermore, the NEVPs for plane flows with pure rotation and pure strain are solved. It is shown that the flow is invariant to rotation, while oscillatory eigenfunctions are found in the case of strain. In addition, an algorithm to solve the NEVP including the nonlinear terms is presented. The results allow an exciting insight into a new stability theory and form the basis for further investigation and understanding of the full nonlinear dynamics of the fluid flows based on the NEVP.

Zusammenfassung

Die vorliegende Arbeit beschäftigt sich mit der Stabilitätstheorie von Strömungen. Zentraler Gegenstand ist die Fragestellung, unter welchen Umständen eine Strömung instabil wird. Instabilitäten sind ein häufiger Auslöser laminar-turbulenter Transitionen. Die Stabilitätstheorie hilft ferner die Entstehung von Strukturen, z.B. wellenartigen Störungsmustern, zu erklären. Die Verwendung von Lie-Symmetrien erlaubt dabei die Klassifizierung bestehender und die Konstruktion neuer Lösungsansätze im Rahmen der linearen Stabilitätstheorie. Zudem wird ein neues nichtlineares Eigenwertproblem (englisch: nonlinear eigenvalue problem, kurz: NEVP) vorgestellt, dessen Herleitung vollständig auf Lie-Symmetrien basiert.
In der klassischen linearen Stabilitätstheorie werden Störungen in Form von Normal-Moden als Ansatz verwendet. Ein weiterer Ansatz, der bereits in frühen Arbeiten gezeigt wurde, ist der Kelvin-Moden-Ansatz. In der Arbeit von Nold und Oberlack (2013) und Nold et al. (2015) konnte gezeigt werden, dass sich diese Ansätze auf die Lie-Symmetrien der linearisierten Störungsgleichungen zurückführen lassen.
Interessanterweise erlaubt die Kenntnis der Symmetrien zudem die Konstruktion neuer Ansatzfunktionen, die über die bekannten Ansätze hinausgehen. Für eine ebene rotationssymmetrische Strömung mit Geschwindigkeitsprofil in Umfangsrichtung kann neben dem Normal-Moden-Ansatz ein weiterer Ansatz mit einem algebraischen Verhalten in der Zeit t^s (Eigenwert s) konstruiert werden. Die Strömung ist dabei stabil gemäß dem Wendepunktkriterium von Rayleigh, was auch durch den algebraischen Ansatz bestätigt wird. Weiterhin können exakte Lösungen der Eigenfunktionen gefunden werden. Mit Hilfe asymptotischer Methoden lassen sich zudem neue stabile Moden bestimmen. Dabei sind spiralartige Strukturen der Wirbelstärke zu erkennen, die sich mit der Zeit im Gebiet ausbreiten.
Ein weiteres zentrales Ergebnis dieser Arbeit ist die Formulierung und Lösung eines NEVP basierend auf den Lie-Symmetrien der Euler-Gleichung. Es kann gezeigt werden, dass für eine Reihe von Grundströmungen mit einem konstanten Geschwindigkeitsgradienten ein NEVP formuliert werden kann. Dazu zählen beispielsweise lineare Scherströmungen, Strömungen unter Kontraktion und Expansion oder rotierende Strömungen.
Das NEVP für lineare Scherströmungen zeigt dabei einen Bezug zu experimentellen Daten aus turbulenten Scherströmungen. Es kann theoretisch gezeigt werden, dass die turbulente kinetische Energie exponentiell mit dem Eigenwert des NEVP skaliert. Der Eigenwert wird numerisch mit Hilfe eines parallelen Spektrallösers bestimmt. Dabei werden zunächst nichtlineare Terme vernachlässigt. Die ermittelten Eigenwerte liegen im Bereich von Literaturwerten turbulenter Scherströmungen. Außerdem werden NEVP für ebene rotierende und ebene gestreckte Strömungen gelöst. Dabei zeigt sich, dass die Strömung invariant gegenüber ebener Rotation ist, während im Fall ebener Streckung oszillierende Eigenfunktionen gefunden werden. Abschließend werden nichtlineare Terme berücksichtigt und diesbezüglich ein Lösungsalgorithmus entwickelt. Zusammenfassend erlauben die Ergebnisse einen spannenden Einblick in eine neue Stabilitätstheorie und bilden die Basis für weitere Untersuchung und das Verständnis der vollständigen nichtlinearen Dynamik von Strömungen auf Basis des NEVP.

Danksagung

Die vorliegende Arbeit entstand während meiner Tätigkeit als wissenschaftlicher Mitarbeiter am Fachgebiet Strömungsdynamik der Technischen Universität Darmstadt unter der Leitung von Herrn Prof. Dr.-Ing. Martin Oberlack. An erster Stelle möchte ich mich daher bei ihm für die Unterstützung und das Vertrauen in meine Arbeit bedanken. Dabei denke ich an viele wertvolle Diskussionen zurück, die diese Arbeit maßgeblich vorangebracht haben.

Bei Herrn Prof. Dr. rer. nat. Amsini Sadiki möchte ich mich für die Übernahme des 2. Gutachtens und für das Interesse an meiner Arbeit bedanken.

Das vorliegende Ergebnis wäre nicht möglich gewesen ohne die gute Zusammenarbeit und Arbeitsatmosphäre am Fachgebiet Strömungsdynamik. Dabei möchte ich zunächst Herrn Prof. Dr.-Ing. Yongqi Wang ein Dank aussprechen für die Zusammenarbeit im Rahmen von Lehrveranstaltungen. Bei allen Kollegen möchte ich mich für die gute Zeit bedanken, namentlich bei Florian für die Beantwortung meiner Fragen zur Numerik und die Pflege der IT-Infrastruktur sowie bei Ruth für alle organisatorischen Fragen. Es war mir eine große Freude mit Alparslan nicht nur ein Büro zu teilen, sondern darüber hinaus auch auf viele gemeinsame Erlebnisse während Konferenzen und nach Feierabend zurückblicken zu können. Gefreut hat mich auch, dass Jie meine Bürokollegin war und wir dadurch häufiger auch mal Chinesisch essen waren. Ich denke auch an die riesige Geduld von Dominik während unserer Diskussionen für die gemeinsame Publikation. Vielen Dank euch für diese schöne Zeit!

Ein besonderer Dank gilt auch Herrn Prof. Volker Mehrmann (TU Berlin) für seine Zeit und Unterstützung bei Fragen rund um die numerische Lösung von Eigenwert-Problemen. Ein weiterer Dank gilt Herrn Prof. Hans-Dieter Alber (TU Darmstadt) und Herrn Prof. Sergio Hoyas (Universität Valencia) für weitere hilfreiche Diskussionen. Vielen Dank auch an das Team vom HRZ der TU Darmstadt für die Unterstützung bei der Verwendung des Lichtenberg-Clusters. Bei allen Studierenden, deren Master- oder Seminararbeit ich betreut habe, möchte ich mich zudem für ihre Arbeit und die spannenden Diskussionen bedanken.

Für das sorgfältige Lesen des Manuskripts danke ich (in alphabetischer Reihenfolge) Alparslan, Anna, Dario, Jie, Maurits und Simon. Eure Kommentare waren sehr hilfreich und haben zur Qualität dieser Arbeit beigetragen.

In besonderer Weise möchte ich mich bei meinen Eltern und meinen Freunden für die Unterstützung und den Rückhalt während der Promotionsphase und darüber hinaus bedanken.

Ein Teil der Rechnungen wurde auf dem Hochleistungsrechner Lichtenberg der TU Darmstadt durchgeführt. Diese Arbeit wurde vom Ministerium für Bildung und Forschung (BMBF) und dem Bundesland Hessen als Teil des NHR-Programms gefördert.

Contents

List of Abbreviations **xix**

1. Introduction **1**
1.1. Motivation . . . 1
1.2. Symmetry-based stability theory . . . 1
1.3. Outline of the thesis . . . 3

2. Governing equations **5**
2.1. Navier-Stokes and Euler equations . . . 5
2.2. Lie symmetries of the Navier-Stokes and Euler equations . . . 5

3. Generalization of modal stability theory using symmetries **9**
3.1. Stability theory with normal modes . . . 10
3.1.1. Viscous flows . . . 10
3.1.2. Inviscid flows . . . 12
3.1.3. From modal theory to a non-modal theory . . . 14
3.2. Review of some special ansatz functions . . . 15
3.2.1. Kelvin modes . . . 15
3.2.2. Görtler-Hämmerlin modes . . . 17
3.3. Extension of normal mode stability using symmetry methods . . . 18
3.4. Example: stability analysis of rotational shear flow . . . 23
3.5. Summary and discussion . . . 33

4. A new nonlinear eigenvalue problem in stability analysis **35**
4.1. Flows with constant velocity gradient . . . 36
4.1.1. Symmetry analysis of the velocity decomposition . . . 37
4.1.2. Construction of an invariant solution . . . 38
4.1.3. Derivation of an eigenvalue problem . . . 39
4.2. Linear shear . . . 40
4.3. Pure Strain . . . 47
4.3.1. Irrotational (planar) strain . . . 48
4.3.2. Axisymmetric strain . . . 50
4.4. Pure Rotation . . . 52
4.5. Wall-bounded shear flows (log law) . . . 53
4.6. Summary and outlook . . . 58

5. Numerical method for the linearized eigenvalue problem **59**
5.1. Spectral collocation . . . 60
5.1.1. Chebyshev polynomials . . . 61
5.1.2. Hermite polynomials . . . 64

5.2. Eigenvalue solver . . . 64
5.2.1. Full spectrum . . . 66
5.2.2. Iterative solver . . . 66
5.3. Filtering of spurious modes . . . 68
5.4. Implementation . . . 70
5.5. Test cases . . . 71
5.5.1. Choice of mapping parameter (1D) . . . 72
5.5.2. Multidimensional examples (2D and 3D) . . . 74
5.5.3. Eigenvalue filtering . . . 76
5.6. Summary . . . 78

6. Results for the linearized eigenvalue problem **81**
6.1. Two-dimensional flows . . . 81
6.1.1. Linear shear . . . 81
6.1.2. Pure strain . . . 85
6.1.3. Pure rotation . . . 88
6.2. Three-dimensional flows . . . 89
6.2.1. Linear shear . . . 89
6.3. Summary . . . 91

7. Towards a solution for the nonlinear eigenvalue problem **93**
7.1. Newton-Kantorovich method . . . 93
7.2. Examples of non-linear eigenvalue problems . . . 95
7.3. Algorithm for the non-linear eigenvalue problem . . . 97
7.4. Future work . . . 100

8. Conclusion **101**

A. Implementation details for Chebyshev collocation **103**
A.1. Chebyshev differentiation matrices . . . 103
A.2. Transform of differentiation matrices under mapping . . . 103
A.3. Approximation of Chebyshev coefficients in 2D . . . 104

B. Derivations for the non-linear eigenvalue problem **105**
B.1. Derivation of common term $\mathcal{M}$ . . . 105
B.1.1. Divergence . . . 105
B.1.2. Divergence of $\mathcal{M}$ . . . 105
B.1.3. Laplacian of $\mathcal{M}$ . . . 105
B.1.4. Rotation . . . 105

Bibliography **107**

List of Figures

1.1. Reynolds' pipe flow experiment . . . 2
1.2. Stable and unstable states of a ball . . . 2

3.1. Channel flow between two walls . . . 10
3.2. Linear shear flow . . . 15
3.3. Stagnation point flow . . . 17
3.4. Algebraic mode, inviscid flow: $f(x)/x$ . . . 29
3.5. Algebraic mode, inviscid flow: real part of the u_r disturbances . . . 29
3.6. Algebraic mode, viscous flow, $m = 0$: real part $f'(x)$ . . . 32
3.7. Algebraic mode, temporal vorticity evolution . . . 34

4.1. A flow with constant velocity gradient: linear shear, pure rotation, pure strain 37
4.2. Characteristics from the eigenvalue problem for linear shear . . . 47
4.3. Analytical solution of the eigenvalue equation for pure strain . . . 50

5.1. Test case (1D): influence of mapping parameter . . . 73
5.2. Test case (1D): influence of collocation points and mapping parameter . . . 73
5.3. Test case (1D): difference between mapped Chebyshev collocation and Hermite collocation . . . 74
5.4. Test case (2D): convergence of error norm . . . 76
5.5. Test case (3D): convergence of error norm . . . 77
5.6. Approximated Chebyshev coefficients of the filtered eigenfunction . . . 78

6.1. Linear shear (2D): full spectrum, $N = 141$ Chebyshev collocation points . . . 82
6.2. Linear shear (2D): filtering metric r(nearest) . . . 83
6.3. Linear shear (2D): filtered spectrum . . . 83
6.4. Linear shear (2D): filtered eigenfunction . . . 85
6.5. Linear shear (2D): slice of the filtered eigenfunction along the x_1 axis . . . 86
6.6. Pure strain (2D): filtered spectrum . . . 86
6.7. Pure strain (2D): numerical eigenfunction for $\lambda = 1.0$ . . . 87
6.8. Pure rotation 2D: filtered spectrum . . . 88
6.9. Linear shear (3D): calculated eigenvalues . . . 91

7.1. Bratu's equation: bifurcation of the solution . . . 95
7.2. Bratu's equation: bifurcation curve, obtained using a path following routine . 96

List of Tables

5.1. Five eigenvalues with the best filtering metrics 77

6.1. Linear shear (3D): three eigenvalues with the best filtering metric 90

List of Abbreviations

ASBL asymptotic suction boundary layer

BC boundary condition

BVP boundary value problem

CAS computer algebra system

CFD computational fluid dynamics

DNS direct numerical simulation

EVP eigenvalue problem

GEVP generalized eigenvalue problem

GH Görtler-Hämmerlin

MPI message passing interface

NEVP nonlinear eigenvalue problem

ODE ordinary differential equation

OS Orr-Sommerfeld

PDE partial differential equation

RHS right-hand side

SQ Squire

WRM weighted residual method

1. Introduction

The scope of the present work is the stability analysis of fluid flows based on the Lie symmetries of the underlying mathematical equations.

1.1. Motivation

Stability theory gives fundamental insight into instability mechanisms and provides mathematical tools to predict instabilities. From an engineering point of view, it is important to understand instabilities in flows as they are a trigger for turbulence. Turbulent flows have higher drag than laminar flows. From a global perspective, about five percent of the worldwide CO_2 emissions are due to wall-bounded turbulence (Jiménez, 2013). In other words, understanding instabilities can help delay the laminar-turbulent transition for some flows and save energy. An important example is the reduction of drag for aircraft. There are numerous attempts to design airfoils, which leave the flow laminar even for cruise speeds of commercial aircraft. Such airfoils would allow for significant reductions in fuel consumption for commercial flight scenarios (Joslin, 1998; Green, 2008; Spalart and McLean, 2011). It is therefore important to understand the instability mechanisms and to find ways to circumvent them or delay the transition.
There has been a growing interest in understanding the instabilities in fluids since the middle of the 19th century. An important and illustrative experiment was conducted by Reynolds (1883). He used a transparent water pipe into which a dye was inserted. For moderate flow velocities, the dye is simply convected by the flow. For higher velocities, there was a breakup of the dye and small eddies and vortices could be observed (see Figure 1.1). The flow becomes unstable for higher flow velocities. This leads to the famous Reynolds number, which is a gross measure of the inertial force compared to the viscous force. Reynolds' experiment is a classical example in textbooks and lectures on fluid mechanics. However, the pipe flow is stable according to linear stability theory, which is not consistent with the findings from the experiment. Thus, there is ongoing research on finding alternative ways to explain stability and to develop theories that better match the experimental findings (Eckhardt et al., 2007). Further work has to be done and the pipe flow is only one example. Another important class of flows is linear shear, which is the focus of the present thesis. It is shown how Lie symmetry methods can help to extend classical stability theories.

1.2. Symmetry-based stability theory

A definition of the terms *stability* and *symmetry* is given in the following. The term *stability* in mechanics describes how the equilibrium of a body changes under perturbations. If the body stays in the same position, the state is called stable. If the body moves away from the original position, such a state is unstable. Neutrally stable states are also possible (Hahn, 1967). Figure

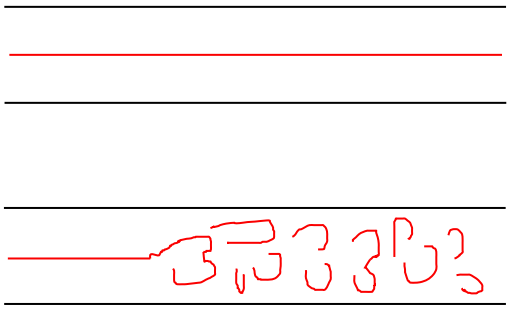

Figure 1.1.: Reynolds' pipe flow experiment: low Reynolds number (top), high Reynolds number (bottom), adapted from Reynolds (1883).

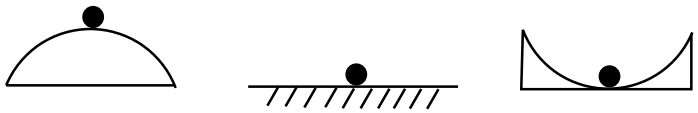

Figure 1.2.: Stability of a ball under infinitesimal perturbations: unstable (left), neutral (center), stable (right), adapted from Kundu et al. (2012).

1.2 shows the stability of a ball under very small (so-called *infinitesimal*) perturbations. The trajectories of the ball can be used to characterize the stability. In nonlinear stability theory, the trajectories are often analyzed in phase space, which also allows tracing the branching of solutions (bifurcation) (Kambe, 2007; Marsden and Ratiu, 1999). The concept of stability can also be applied in fluid mechanics. Therefore, a basic state (comparable to an equilibrium) of a flow is considered. The quantity of interest is the perturbation. In linear stability theory, these perturbations are of smaller order than the base flow and linearized equations are considered. If the perturbations grow in time or space, the flow is temporally or spatially unstable, respectively. Usually, the kinetic energy of the perturbations is a measure of the instability, cf. Schmid and Henningson (2001).
Hydrodynamic stability theory dates back to the 1870s with mathematical and experimental studies. Since then, ongoing research of both theoretical and experimental nature has led to a large body of knowledge which was also fostered by the use of computational fluid dynamics (CFD) in the second half of the 20th century. The present work considers *symmetry-based stability theory*. We are aware that different concepts that make use of *symmetries* to study the stability of fluids. The literature shows that both symmetries of the governing equations, as well as those of the flow geometry (e.g. a pipe with rotational symmetry, a channel with reflection symmetry), are considered, cf. Holmes et al. (2012). Geometrical symmetries are used in bifurcation theory, e.g. by Golubitsky and Schaeffer (1985) and Schecter (1976). A general

observation is that flows with geometrical symmetries (i.e. a reflection or rotation symmetry) have in general more complicated bifurcations than non-symmetric systems. In addition, new states can arise, which have fewer symmetries (symmetry-breaking) and usually have more complicated dynamics (Crawford and Knobloch, 1991). Symmetries are also used to determine energy stability, which is part of the nonlinear stability theory. Here, symmetry properties of the differential operators are used to make formal predictions of the eigenvalue spectrum (Straughan, 2004). The use of symmetries also plays a role in Hamiltonian formulations for classical mechanics and some applications in fluid mechanics (Bluman et al., 2010; Marsden and Ratiu, 1999; Olver, 1986).
In this work we consider the use of Lie symmetries to formulate eigenvalue problems in the context of stability theory. Therefore we understand the term *symmetry-based* in the sense of employing the *Lie symmetries* of the governing equations. Lie symmetries are named after Sophus Lie, who dedicated his entire research life to studying continuous symmetries (Cantwell, 2002). An introduction to Lie symmetries is given in various textbooks (cf. Bluman et al., 2010; Olver, 2000; Hydon, 2000; Cantwell, 2002). In the context of fluid mechanics, Birkhoff (1960) gave the first general introduction to symmetries and group theory. There are several applications of Lie symmetries, including rigorous theory building, solution of differential equations, or the construction of conservation laws, see Bluman et al. (2010) and Sundermeyer (2014) for an introduction.
In this work, symmetries are used as follows. First, it is possible to generalize the existing *normal mode ansatz* by using the symmetries of the stability equations. The related concept is a separation of variables using symmetries (cf. Burde et al., 2007; Zhalij et al., 2006; Nold and Oberlack, 2013; Nold et al., 2015; Hau et al., 2017).
Second, the Lie symmetries of the inviscid flow equations (Euler equations) give rise to a novel eigenvalue problem. This eigenvalue problem is nonlinear in the eigenfunctions and is referred to as a *nonlinear eigenvalue problem* (NEVP) throughout the present work. This idea is part of ongoing research and was introduced recently by Oberlack (2018) and Oberlack (2020). The results of this thesis are part of ongoing research on symmetry-based turbulence theory, which also involves turbulence modeling (Klingenberg et al., 2020) and scaling laws in turbulent flows (Rosteck, 2014; Oberlack et al., 2022).
For the sake of completeness, we note that the mentioned Hamiltonian formulation with application to stability theory in fluid mechanics has a close link to Lie symmetries, cf. Cantwell (2002) and Swaters (2000). Indeed, there is a correspondence between Lie symmetry groups and conservation laws by Noether's theorem (Noether, 1918; Anco and Bluman, 2002). However, stability theory based on a Hamiltonian formulation is not studied in the present thesis.

1.3. Outline of the thesis

Chapter 2 presents the Navier-Stokes and Euler equations, which describe the dynamics of incompressible fluids. In addition, the Lie symmetries of the Navier-Stokes and Euler equations are presented.
Chapter 3 is dedicated to the linear stability theory based on eigenvalue problems. Chapter 3.1 gives a review of linear stability theory using the normal mode ansatz. The Orr-Sommerfeld equation is derived for a shear flow. In addition, extensions of the normal mode theory, such as the non-modal theory are mentioned. An observation is that there are modes besides the normal mode ansatz, which are presented in Chapter 3.2. The relevance of Lie symmetries to generalize the normal mode approach is shown in Chapter 3.3 with various examples. Finally,

their application to a rotational shear flow is presented in Chapter 3.4.
In Chapter 4, a new eigenvalue problem is derived based on the symmetries of the Euler equations. This problem is nonlinear in its eigenfunctions and is referred to as a nonlinear eigenvalue problem (NEVP) in the following. It is possible to derive the NEVP for a class of flows in an unbounded domain having a constant velocity gradient, which is shown in Chapter 4.1. The equations for the cases of linear shear (Chapter 4.2), pure strain (Chapter 4.3), and pure rotation (Chapter 4.4) are derived in detail. In addition, an NEVP for a wall-bounded flow can be formulated (Chapter 4.5).
The NEVP is solved numerically by using a spectral collocation method, which is explained in Chapter 5. Details on the collocation method using Chebyshev and Hermite polynomials are given in 5.1. Chapter 5.2 explains of the numerical routines to solve eigenvalue problems. The succeeding Chapter 5.3 summarizes methods to identify non-physical eigenvalues in the computed spectrum. Implementation details are given in Chapter 5.4. The test cases in Chapter 5.5 show that the equations are successfully implemented.
The numerical solution of the linearized NEVP is presented in Chapter 6. Special attention is drawn to the case of linear shear flow, which is studied in 2D and 3D. The effects of strain and rotation in 2D are also discussed.
Chapter 7 is dedicated to the solution of the NEVP including the nonlinear terms. To this end, the Newton-Kantorovich method is described in Chapter 7.1. To better understand possible effects in nonlinear equations, two examples are studied in Chapter 7.2. The final nonlinear algorithm is given in Chapter 7.3.
A summary of the results of this thesis and an outlook are given in Chapter 8.

2. Governing equations

The motion of fluid flows is described by the Navier-Stokes and continuity equations. Physically, these equations describe the conservation of momentum and mass, respectively. The present work investigates incompressible flows with a constant density ρ. The velocity is denoted by $\boldsymbol{u}(\boldsymbol{x}, t)$ and the pressure by $p(\boldsymbol{x}, t)$. In the notation, (u, v, w) denote the (x, y, z)-components of the velocity. Alternatively, index notation is used for a more compact notation. In that case, u_i denotes the component of the velocity corresponding to the x_i-direction ($i = 1, 2, 3$) for three-dimensional flows.

2.1. Navier-Stokes and Euler equations

The Navier-Stokes equations are given by

$$\rho \left(\frac{\partial \boldsymbol{u}}{\partial t} + (\boldsymbol{u} \cdot \nabla) \boldsymbol{u} \right) = -\nabla p + \mu \Delta \boldsymbol{u} + \boldsymbol{f}, \tag{2.1}$$

and the continuity equation reads

$$\nabla \cdot \boldsymbol{u} = 0, \tag{2.2}$$

where μ is the dynamic viscosity, and $\boldsymbol{f}$ denotes the forcing term. When the flow is described in a rotating system with constant rotation $\boldsymbol{\Omega}$ around the origin, additional non-inertial terms appear. These are the centrifugal and Coriolis forces. Centrifugal forces can be absorbed in the pressure term and the Coriolis terms can be written as an external forcing $\boldsymbol{f} = -2\boldsymbol{\Omega} \times \boldsymbol{u}$. The equations (2.1) and (2.2) can be written in dimensionless form, denoted by a tilde, as

$$\frac{\partial \tilde{\boldsymbol{u}}}{\partial \tilde{t}} + \left(\tilde{\boldsymbol{u}} \cdot \widetilde{\nabla} \right) \tilde{\boldsymbol{u}} = -\widetilde{\nabla} \tilde{p} + \frac{1}{\mathrm{Re}} \Delta \tilde{\boldsymbol{u}} + \tilde{\boldsymbol{f}}, \tag{2.3}$$

$$\widetilde{\nabla} \cdot \tilde{\boldsymbol{u}} = 0, \tag{2.4}$$

where the Reynolds number is defined by $\mathrm{Re} = (\rho u_0 l_0)/\mu$ as a ratio of the inertial and viscous forces with a characteristic length l_0 and velocity u_0. For the sake of readability, the tilde is omitted in the following. For inviscid flows ($\mu = 0$), the momentum equations (2.3) in a non-rotating frame, i.e. $\boldsymbol{\Omega} = 0$, the Navier-Stokes equations (2.3) simplify to the Euler equations which are given by

$$\frac{\partial \boldsymbol{u}}{\partial t} + (\boldsymbol{u} \cdot \nabla) \boldsymbol{u} = -\nabla p. \tag{2.5}$$

2.2. Lie symmetries of the Navier-Stokes and Euler equations

The Lie symmetries of the Euler and Navier-Stokes equations are considered. We start with a precise definition of a Lie symmetry (transformation) (Oberlack, 2001). We consider a system

of partial differential equations $\boldsymbol{F}$ with variables $\boldsymbol{y}$ and $\boldsymbol{z}$ given as

$$\boldsymbol{F}(\boldsymbol{y}, \boldsymbol{z}) = 0. \tag{2.6}$$

A transformation of the variables is given by

$$\boldsymbol{y} \to \tilde{\boldsymbol{y}}, \qquad \boldsymbol{z} \to \tilde{\boldsymbol{z}}, \tag{2.7}$$

where $\tilde{\boldsymbol{y}}$ and $\tilde{\boldsymbol{z}}$ are the transformed variables. Any transformation which leaves the form of the equation invariant, i.e.

$$\boldsymbol{F}(\boldsymbol{y}, \boldsymbol{z}) = 0 \quad \Leftrightarrow \quad \boldsymbol{F}(\tilde{\boldsymbol{y}}, \tilde{\boldsymbol{z}}) = 0 \tag{2.8}$$

is called a symmetry (transformation) (Oberlack, 2000). If not indicated otherwise, we refer to Lie symmetries whenever the word *symmetry* is used in the present thesis. The symmetries of an ordinary differential equation (ODE), or partial differential equation (PDE) can be calculated in an algorithmic way by hand or by using a computer algebra system (CAS), see e.g. Bluman et al. (2010) and Cheviakov (2010).
The symmetries of the Navier-Stokes equation were first derived by Puhnachev (1960) for two-dimensional flows and by Bitev (1972) for three-dimensional flows (Boisvert et al., 1983). The symmetries of the Euler equations (2.5), as presented by Oberlack (2000), are given by

$$T_1: \quad \tilde{t} = t + a_1, \tilde{\boldsymbol{x}} = \boldsymbol{x}, \tilde{\boldsymbol{u}} = \boldsymbol{u}, \tilde{p} = p, \tag{2.9}$$

$$T_2: \quad \tilde{t} = t, \tilde{\boldsymbol{x}} = e^{a_2}\boldsymbol{x}, \tilde{\boldsymbol{u}} = e^{a_2}\boldsymbol{u}, \tilde{p} = e^{2a_2}p, \tag{2.10}$$

$$T_3: \quad \tilde{t} = e^{a_3}t, \tilde{\boldsymbol{x}} = \boldsymbol{x}, \tilde{\boldsymbol{u}} = e^{-a_3}\boldsymbol{u}, \tilde{p} = e^{-2a_3}p, \tag{2.11}$$

$$T_4 - T_6: \quad \tilde{t} = t, \tilde{\boldsymbol{x}} = \boldsymbol{a} \cdot \boldsymbol{x}, \tilde{\boldsymbol{u}} = \boldsymbol{a} \cdot \boldsymbol{u}, \tilde{p} = p, \tag{2.12}$$

$$T_7 - T_9: \quad \tilde{t} = t, \tilde{\boldsymbol{x}} = \boldsymbol{x} + \boldsymbol{f}(t), \tilde{\boldsymbol{u}} = \boldsymbol{u} + \frac{d\boldsymbol{f}}{dt}, \tilde{p} = p - \boldsymbol{x} \cdot \frac{d^2\boldsymbol{f}}{dt^2}, \tag{2.13}$$

$$T_{10}: \quad \tilde{t} = t, \tilde{\boldsymbol{x}} = \boldsymbol{x}, \tilde{\boldsymbol{u}} = \boldsymbol{u}, \tilde{p} = p + f_4(t). \tag{2.14}$$

The parameters a_i denote the group parameters. The term $\boldsymbol{a}$ is a constant rotation matrix with $\boldsymbol{a} \cdot \boldsymbol{a}^T = \boldsymbol{a}^T \cdot \boldsymbol{a} = \mathsf{I}$ where I is the identity matrix and $|\boldsymbol{a}| = 1$. The function $f_4(t)$ is differentiable in time and $\boldsymbol{f} = (a_4 f_1(t), a_5 f_2(t), a_6 f_3(t))^T$ is twice differentiable in time. The symmetry T_1 describes a translation in time. The transformations T_2 and T_3 are the scaling symmetries in space and time. In addition, the equations are invariant under a finite rotation as described by the symmetries $T_4 - T_6$. The symmetries $T_7 - T_9$ are due to Galilean invariance, i.e. a translation of the frame with a constant velocity. Finally, the symmetry T_{10} shows that any time-dependent function (or constant) can be added to the pressure, as only the pressure gradient appears in the Euler equations (2.5).
For two-dimensional flows, i.e. $\boldsymbol{u} = \boldsymbol{u}(x_1, x_2, t)$, the Euler equations (2.5) have an additional symmetry given by

$$\begin{aligned} T_{11}: \tilde{t} = t, \quad \tilde{x}_1 &= x_1 \cos(a_8 t) - x_2 \sin(a_8 t), \quad \tilde{x}_2 = x_1 \sin(a_8 t) + x_2 \cos(a_8 t), \\ \tilde{u}_1 &= u_1 \cos(a_8 t) - u_2 \sin(a_8 t) - a_8 x_1 \sin(a_8 t) - a_8 x_2 \cos(a_8 t), \\ \tilde{u}_2 &= u_1 \sin(a_8 t) + u_2 \cos(a_8 t) + a_8 x_1 \cos(a_8 t) - a_8 x_2 \sin(a_8 t), \\ \tilde{p} &= p + 2a_8 \int_Q (u_2 dx_1 - u_1 dx_2) + \frac{1}{2} a_8^2 \left(x_1^2 + x_2^2\right). \end{aligned} \tag{2.15}$$

The symmetry T_{11} is called *2D material frame indifference*, we refer to Oberlack (2000) and Silvis (2020) for a detailed explanation. It is possible to combine two symmetries. For example, the translation in time T_1 (2.9) and the scaling in space T_2 (2.10) can be combined to a new symmetry described by the two parameters a_1 and a_2:

$$T_1 + T_2 : \quad \tilde{t} = t + a_1, \quad \tilde{\boldsymbol{x}} = e^{a_2}\boldsymbol{x}, \quad \tilde{\boldsymbol{u}} = e^{a_2}\boldsymbol{u}, \quad \tilde{p} = e^{2a_2}p. \tag{2.16}$$

The Navier Stokes equations (2.1) have a reduced set of symmetries compared to the Euler equations. This is due to the the viscous term (a constant viscosity $\nu = \mu/\rho$ is assumed). The symmetries T_1 and $T_4 - T_{10}$ remain. Combination of the scaling symmetries T_2 (2.10) and T_3 (2.11) gives (Oberlack, 2000)

$$\tilde{t} = e^{2a}t, \quad \tilde{\boldsymbol{x}} = e^{a}\boldsymbol{x}, \quad \tilde{\boldsymbol{u}} = e^{-a}\boldsymbol{u}, \quad \tilde{p} = e^{-2a}p. \tag{2.17}$$

Note that there are usually two representations of Lie symmetries used in this work. The symmetries in (2.9) to (2.15) are global transformations. It is also possible to define an infinitesimal generator X to describe the transformations. Those two representations are equivalent and can be converted to another representation, which is explained later in Chapter (4). For more details, the reader is referred to Oberlack (2000) and Bluman et al. (2010).
In addition, the Navier-Stokes and Euler equations further have discrete symmetries. The spatial reflection, as presented by Oberlack (2000), reads

$$T_{D1} : \quad \tilde{t} = t,\ \tilde{x}_\alpha = -x_\alpha,\ \tilde{u}_\alpha = -u_\alpha,\ \tilde{x}_\beta = x_\beta,\ \tilde{u}_\beta = u_\beta,\ \tilde{p} = p \quad \text{with } \beta \neq \alpha \tag{2.18}$$

where $\alpha \in \{1, 2, 3\}$ corresponds to the reflection of the spatial coordinate x_α and the remaining directions β are unaltered. In addition, the Euler equations show a reversibility in time, which follows from a reflection in time and velocity by

$$T_{D2} : \quad \tilde{t} = -t, \quad \tilde{\boldsymbol{x}} = \boldsymbol{x}, \quad \tilde{\boldsymbol{u}} = -\boldsymbol{u}, \quad \tilde{p} = p. \tag{2.19}$$

Note that this latter reflection symmetry does not exist for the Navier-Stokes equations, which from this point are not reversible due to viscosity (Oberlack, 1997; Oberlack, 2000). It is important to note that the discrete symmetries (2.18) and (2.19) are not Lie symmetries. Both Lie symmetries and discrete symmetries are sometimes referred to as an *invariance* or an *invariant transformation* in the literature, cf. Pope (2000).

3. Generalization of modal stability theory using symmetries

In this chapter, we show how Lie symmetries can help to systematize classical stability theory. Furthermore, it is shown how classical ansatz functions such as the normal mode ansatz can be extended by symmetry methods. We start with an introduction to hydrodynamic stability and present some important results for channel flows, including the Orr-Sommerfeld (OS) equation. We show how several alternative ansatz functions can be constructed by using Lie symmetries. In addition, we present a stability analysis for rotational shear flows using a novel ansatz function which is referred to as the algebraic mode ansatz.

Stability theory in fluid mechanics

Hydrodynamic stability theory is part of many textbooks (cf. Lin, 1955; Chandrasekhar, 1961; Schmid and Henningson, 2001; Drazin, 2002; Criminale et al., 2003; Drazin and Reid, 2004; Georgescu, 2010; Charru, 2011; Yaglom, 2012). There are different approaches to studying the occurrence of instabilities, which can be classified as linear or nonlinear theories. Based on a literature review, we briefly explain the main idea and systematize the different branches of stability theory.

Linear stability theory Linear stability theory covers the understanding of linearized stability equations. The stability equations can be derived directly from the Navier-Stokes equations by superposition of fluctuations and omitting nonlinear terms. In classical work, the initial-value problem for the perturbations is transformed into an eigenvalue problem by assuming an exponential time dependence. This is referred to as the normal mode ansatz. In general, the perspective of stability as an eigenvalue problem instead of an initial-value problem is called a modal (eigenvalue) analysis (Schmid, 2007). If all directions unless one are inhomogeneous, this leads to the so-called normal mode approach. For more than one inhomogeneous direction, some methods have been proposed, e.g. bi-global, tri-global methods, cf. Theofilis (2003). The various latter methods are called global, whereas the normal mode ansatz is considered a local method (Juniper et al., 2014). The normal mode fails to predict the stability of some flows. For example, a plane Couette flow is stable to infinitesimal perturbations for all Reynolds numbers (Schmid, 2007). However, experiments clearly show instabilities (Avila et al., 2011). Since the 1990s, the initial-value formulation of stability problems has attracted growing attention. This is usually called *nonmodal* stability theory or theory of *transient growth*. The main idea is to study the response of an initial-value problems with different initial conditions and to understand the interaction of different (non-orthogonal) modes (Schmid, 2007).

Nonlinear stability theory If the perturbations grow in amplitude, nonlinear terms can no longer be neglected (Schmid and Henningson, 2001). The most general way to study nonlinear

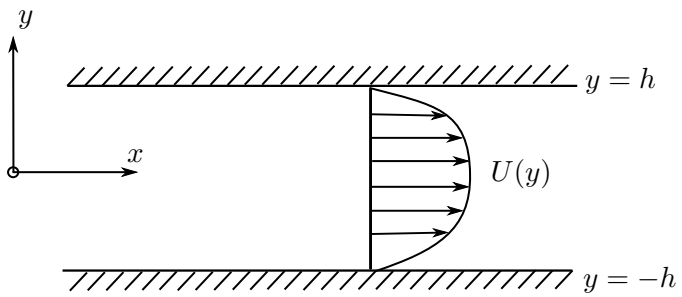

Figure 3.1.: Channel flow between two walls at $y = \pm h$ with a laminar base flow $U(y)$, adapted from Schmid and Henningson (2001).

stability is to define an energy norm $E(t)$ for the initial state and consider the growth of the perturbation energy in time (Kerswell, 2018). From a mathematical point, there is no longer a simple (linear) superposition principle of mode solutions. In a physical picture, we can observe wave interactions (Schmid and Henningson, 2001). Moreover, nonlinear equations are associated with bifurcation (Kambe, 2007). There are several different nonlinear methods so we can only mention the most frequent approaches here, cf. Schmid and Henningson (2001). Weakly-nonlinear techniques allow using series expansions and perturbation methods to analytically solve the stability equations. The energy method studies the evolution of the energy $E(t)$ (Schmid and Henningson, 2001). There is also an extension of the non-modal theory to a full nonlinear initial-value problem (nonlinear nonmodal theory) (Kerswell, 2018). In addition, there are nonlinear methods, which rather consider the stability problem in state space, cf. Skufca et al. (2006) and Eckhardt et al. (2007).
This chapter mainly considers modal stability theory, i.e. the formulation of corresponding eigenvalue problems for the stability. While studying stability problems, it is important to keep the assumptions of a problem in mind. The stability results may differ if two- or three-dimensional perturbations are considered. Furthermore, the effect of viscosity and the choice of the boundary condition (BC) can alter the stability results.

3.1. Stability theory with normal modes

In this section, we show the basic steps for a temporal stability analysis for a channel flow. As a classical example, we consider a parallel shear flow in a channel. We consider linear stability theory based on normal modes. This is a part of the so-called modal stability theory. In the following, we consider a channel flow which is depicted in Figure 3.1. The channel is bounded by two walls at $y = \pm h$. It is assumed that the base flow only depends on the wall-normal coordinate y, i.e. $(U, V, W) = (U(y), 0, 0)$. Possible base flows satisfying these conditions are the Poiseuille flow or the Couette flow (walls moving in opposite directions).

3.1.1. Viscous flows

We present a stability analysis for viscous flows. The derivations in this section are based on Schmid and Henningson (2001) if not indicated else wise. The starting point is a given

basic state of the Navier-Stokes equations. Usually, an exact solution of the unperturbed flow equations is used, so analytical techniques can be used to conduct the stability analysis. In a next step, perturbations are added to the base flow so that the instantaneous velocities (u, v, w) are given by

$$(u, v, w)^T = (U + u', v', w')^T, \qquad p = P + p' \tag{3.1}$$

For sake of readability, the primes are omitted in the following. For a base flow $U(y)$, the momentum equation can be written as

$$\frac{\partial u}{\partial t} + U\frac{\partial u}{\partial x} + vU' = -\frac{\partial p}{\partial x} + \frac{1}{\mathrm{Re}}\nabla^2 u, \tag{3.2}$$

$$\frac{\partial v}{\partial t} + U\frac{\partial v}{\partial x} = -\frac{\partial p}{\partial y} + \frac{1}{\mathrm{Re}}\nabla^2 v, \tag{3.3}$$

$$\frac{\partial w}{\partial t} + U\frac{\partial w}{\partial x} = -\frac{\partial p}{\partial z} + \frac{1}{\mathrm{Re}}\nabla^2 w. \tag{3.4}$$

Here U' and U'' denotes the first and second derivative of $U(y)$ with respect to y. The continuity equation is given by

$$\frac{\partial u}{\partial x} + \frac{\partial v}{\partial y} + \frac{\partial w}{\partial z} = 0. \tag{3.5}$$

By taking the divergence of the momentum equations, a Poisson equation for the pressure can be derived

$$\nabla^2 p = -2U'\frac{\partial v}{\partial x} \tag{3.6}$$

Inserting the pressure from (3.6) into the momentum equation for v, given by (3.3), and neglecting all nonlinear terms in the fluctuations gives

$$\left[\left(\frac{\partial}{\partial t} + U\frac{\partial}{\partial x}\right)\nabla^2 - U''\frac{\partial}{\partial x} - \frac{1}{\mathrm{Re}}\nabla^4\right] v = 0. \tag{3.7}$$

In the context of wall-bounded flows, this is referred to as the wall-normal velocity. By using the wall-normal vorticity

$$\eta = \frac{\partial u}{\partial z} - \frac{\partial w}{\partial x}, \tag{3.8}$$

it is possible to derive an equation for the wall-normal vorticity from ∂_z(3.2) $- \partial_x$(3.4) which gives

$$\left[\frac{\partial}{\partial t} + U\frac{\partial}{\partial x} - \frac{1}{\mathrm{Re}}\nabla^2\right]\eta = -U'\frac{\partial v}{\partial z}. \tag{3.9}$$

The main question in stability theory is, if the perturbations grow in time. Therefore a normal mode ansatz can be used to reduce the PDE problem from (3.7) and (3.9) to an ODE. The ansatz reads

$$v(x, y, z, t) = \hat{v}(y)e^{i(\alpha x + \beta z - \omega t)}, \tag{3.10}$$

$$\eta(x, y, z, t) = \hat{\eta}(y)e^{i(\alpha x + \beta z - \omega t)} \tag{3.11}$$

with an assumption of Fourier modes in space ($\alpha, \beta \in \mathbb{R}$) and a exponential growth or decay rate ($\omega \in \mathbb{C}$) in time. The criterion for temporal stability is based on ω_i, which is the imaginary part of ω

$$\omega_i = \begin{cases} < 0 & \text{stable} \\ = 0 & \text{neutrally stable} \\ > 0 & \text{unstable} \end{cases} \tag{3.12}$$

The flow is unstable if and only if there is one unstable mode. Consequently, the stability equations have to be solved for the eigenvalue ω_i. By inserting the ansatz into (3.7) and (3.9), we obtain the following system

$$\left[(-i\omega + i\alpha U)\left(\mathcal{D}^2 - k^2\right) - i\alpha U'' - \frac{1}{\mathrm{Re}}\left(\mathcal{D}^2 - k^2\right)^2\right]\hat{v} = 0, \tag{3.13}$$

$$\left[(-i\omega + i\alpha U) - \frac{1}{\mathrm{Re}}\left(\mathcal{D}^2 - k^2\right)\right]\hat{\eta} = -i\beta U'\hat{v}, \tag{3.14}$$

where $\mathcal{D}$ denotes a differentiation with respect to y and $k^2 = \alpha^2 + \beta^2$. The BCs at the solid walls are

$$\hat{v} = \frac{d\hat{v}}{dy} = \hat{\eta} = 0, \quad \text{for } y = \pm h. \tag{3.15}$$

The system of (3.13) and (3.14) together with the BCs (3.15) constitutes an eigenvalue problem for ω. Equation (3.13) does not contain the vorticity and therefore decouples from the equation for the normal vorticity (3.14). Consequently, the OS equation (3.13) must be solved first and the solution can be inserted as a particular solution to (3.14). The solution gives an eigenvalue ω and a set of corresponding eigenfunctions $\hat{v}, \hat{\eta}$. There are two types of solutions. First, we have OS modes

$$\{\hat{v}, \hat{\eta}, \omega\} \tag{3.16}$$

These modes can be found by solving the homogeneous equation for $\hat{v}$ and using the solution as inhomogeneity to solve for the vorticity $\hat{\eta}$. The second type of solutions are the Squire (SQ) modes which are a solution in the case of $\hat{v} = 0$

$$\{\hat{v} = 0, \hat{\eta}, \omega\} \tag{3.17}$$

The OS equation is usually solved numerically using spectral methods. For an introduction the reader is referred to Schmid and Henningson (2001) and Canuto et al. (2007). Another question is, whether it makes a difference if two-dimensional or three-dimensional perturbations are considered. Squire (1933) showed that for unstable three-dimensional flows there is critical Reynolds number which is lower for two-dimensional perturbations.

3.1.2. Inviscid flows

For inviscid flows, the viscous term in stability equation (3.7) disappears and the equation for v from (3.3) simplifies to

$$\left[\left(\frac{\partial}{\partial t} + U\frac{\partial}{\partial x}\right)\nabla^2 - U''\frac{\partial}{\partial x}\right]v = 0, \tag{3.18}$$

and for the vorticity follows from (3.9)

$$\left(\frac{\partial}{\partial t} + U\frac{\partial}{\partial x}\right)\eta = -U'\frac{\partial v}{\partial z}. \tag{3.19}$$

Using the normal mode ansatz (3.10), it is possible to derive the following Rayleigh equation

$$(U-c)\left(\mathcal{D}^2 - k^2\right)\hat{v} - U''\hat{v} = 0, \tag{3.20}$$

with the BC $\hat{v} = 0$ on the wall and c defined as

$$\omega = \alpha c. \tag{3.21}$$

Although the Rayleigh equation (3.20) is only a second order equation compared to the OS equation (3.13), the solution is not necessarily easier. One reason is that the equation has a variable coefficient in leading order (Yaglom, 2012). In addition, there is a singularity in the equation for $U = c$ (Drazin, 2002).

Rayleigh's inflection point criterion

An important finding for the stability is Rayleigh's inflection point criterion, which can be directly derived from the Rayleigh equation (3.20). Following the arguments of Squire (1933), the two-dimensional modes can be used as a proxy to study three-dimensional instability, cf. Drazin (2002). The two-dimensional Rayleigh equation reads

$$(U-c)\left(\mathcal{D}^2 - \alpha^2\right)\hat{v} - U''\hat{v} = 0, \tag{3.22}$$

and can be rewritten as

$$\hat{v}'' - \alpha^2\hat{v} - \frac{U''}{U-c}\hat{v} = 0. \tag{3.23}$$

Here $\hat{v}''$ is the second derivative of $\hat{v}$ with respect to y. We consider a possibly unstable mode with $c_i > 0$. Multiplying (3.23) by the complex conjugate $\hat{v}^*$ of $\hat{v}$ and integrating the equation from y_1 to y_2 (for the channel flow this would be $y_1 = -h$ to $y_2 = h$) we obtain

$$\int_{y_1}^{y_2}\left(|\hat{v}'| + \alpha^2|\hat{v}|^2\right)dy + \int_{y_1}^{y_2}\frac{U''}{U-c}|\hat{v}|^2 dy = 0, \tag{3.24}$$

where the imaginary part reads

$$c_i\int_{y_1}^{y_2}\frac{U''}{|U-c|^2}|\hat{v}|^2 dy = 0. \tag{3.25}$$

From the assumption $c_i > 0$ follows that U'' must change sign in that interval. Note that the inflection point is only a necessary criterion for instability of flows (Drazin, 2002).
Using a similar theoretical approach, Fjørtoft (1950) and Howard (1961) proposed relevant extensions to Rayleigh's criterion for some special cases. The interested reader is referred to Schmid and Henningson (2001) for more information.
An important result of Rayleigh's criterion is that classical flows such as the plane Couette flow or the Blasius boundary layer flow are stable under inviscid perturbations according to this theory (Mack, 1984; Charru, 2011). It should be noted that this result also holds for unbounded flows, where the fluctuations vanish in the far field (Drazin, 1958; Lin, 2003; Sun, 2007). For flows with no inflection point, it is necessary to consider the viscous stability. However, some theoretical results from normal mode stability are not in line with observations from experiments. This motivated the non-modal theory which is explained in the next section.

3.1.3. From modal theory to a non-modal theory

Stability theory using normal mode helps to understand instabilities and to calculate critical Reynolds numbers. It is reported that the results for flows with thermal (e.g. Rayleigh-Bérnard) or centrifugal (e.g. Taylor-Couette) instabilities match reasonably well with experiments. However, the results for shear-driven flows deviate from theory (Trefethen et al., 1993). Two prominent examples are the plane Poiseuille and the plane Couette flow. The critical Reynolds number for Poiseuille flows from theory is of order $\mathrm{Re} = 5300$ while instabilities are observed for even smaller Reynolds numbers. The plane Couette flow is stable for all Reynolds numbers, however instabilities are observed in experiments (Daviaud et al., 1992; Trefethen et al., 1993).

An important observation is that the differential operators of the thermal and centrifugal instabilities are normal, while those for linear shear flows are non-normal. By definition an operator (or matrix) is non-normal if its adjoint $L^\dagger$ does not commute (Kerswell, 2018)

$$\mathsf{L}\mathsf{L}^\dagger \neq \mathsf{L}^\dagger\mathsf{L}. \tag{3.26}$$

A new perspective on stability problems emerged by considering possible non-normal effects. The stability problem is written as an initial-value problem. A combination of certain non-normal modes can lead to a short time growth of the perturbation energy. This is called transient growth (Yaglom, 2012).
We present a short example to illustrate the idea of non-modal stability theory. This example was initially proposed by Trefethen et al. (1993) and frequently used in other publications (Schmid and Henningson, 1994; Kerswell, 2005; Eckhardt and Pandit, 2003; Grossmann, 2000). The following explanation is mainly based on Kerswell (2005). Consider a two-dimensional evolution equation

$$\frac{d}{dt}\begin{pmatrix} x \\ y \end{pmatrix} = \mathsf{L}\begin{pmatrix} x \\ y \end{pmatrix} := \begin{pmatrix} -\frac{1}{\mathrm{Re}} & 0 \\ 1 & -\frac{2}{\mathrm{Re}} \end{pmatrix}\begin{pmatrix} x \\ y \end{pmatrix}. \tag{3.27}$$

The eigenvalues of the linear operator L are $\lambda_1 = -1/\mathrm{Re}$ and $\lambda_2 = -2/\mathrm{Re}$. Both eigenvalues are negative and the eigenfunctions $(1, \mathrm{Re})^T$ and $(0, 1)^T$ are stable modes according to the normal mode stability theory. Note however that the operator L is non-Hermitian (see definition (3.26)) and therefore non-modal growth can occur. The eigenvector basis together with the initial condition $(x, y)^T = (1, 0)^T$ can be expanded for small times using a Taylor series (for technical details refer to Farrell and Ioannou, 1996), which gives

$$\begin{pmatrix} x(t) \\ y(t) \end{pmatrix} = \begin{pmatrix} 1 \\ \mathrm{Re} \end{pmatrix} e^{-t/\mathrm{Re}} - \begin{pmatrix} 0 \\ 1 \end{pmatrix} e^{-2t/\mathrm{Re}} \approx \begin{pmatrix} 1 - \frac{t}{\mathrm{Re}} + \mathcal{O}\left(\frac{t}{\mathrm{Re}}\right)^2 \\ t + \mathcal{O}\left(\frac{t}{\mathrm{Re}}\right)^2 \end{pmatrix}. \tag{3.28}$$

This shows an algebraic growth until $t = \mathcal{O}(\mathrm{Re})$. This example indicates several consequences of the non-modal approach. First, even two modes which are stable (in a sense that both have stable eigenvalues) can interact and lead to a growth of perturbation energy. This mechanism can trigger nonlinear instabilities if the perturbation energy exceeds a certain threshold. In that way, one can seek for a combination of modes or an initial condition such that this growth is maximized (optimal growth theory) (Kerswell, 2005; Kerswell, 2018).
Further, in non-modal theory, there is an interaction between the modes. Therefore the shape of the modes can change in time. This contrasts with the normal mode stability theory, where the spatial structure of the modes does not change in time (Kerswell, 2018). It is also reported

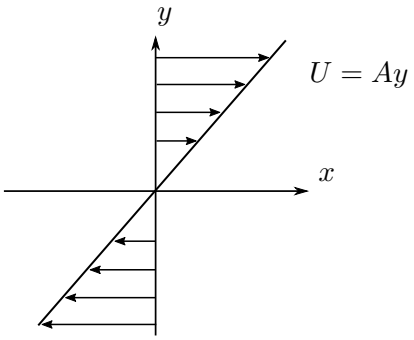

Figure 3.2.: Linear shear flow with a constant shear rate A in an unbounded domain $y \to \pm\infty$

that flows with 3D instabilities can have larger amplifications of the instabilities than 2D perturbations. This contrasts with the classical Squire criterion, which states that the most unstable modes are two-dimensional (Trefethen et al., 1993).

3.2. Review of some special ansatz functions

In linear (modal) stability theory, there are two important examples ansätze which are different from the normal mode ansatz (compare (3.10) and (3.10)). The first examples are the Kelvin modes in shear flows, the second example are Görtler-Hämmerlin (GH) modes in stagnation point flows. One important question is if the stability results are different from the normal mode case or if there are instabilities which can be only observed with these alternative modes (Yaglom, 2012). We present these two examples in the following and explain their relevance in stability theory.

3.2.1. Kelvin modes

The Kelvin modes can be observed in unbounded linear shear flows. Such a flow is depicted in figure 3.2, where the shear rate A is constant. This solution was first presented by Kelvin (1887) and further examined by Orr (1907a) and Orr (1907b). It is argued, that the term Kelvin mode or Kelvin wave may be misleading as this might evoke different concepts in fluid mechanics (Sagaut and Cambon, 2018). Here we use the term Kelvin modes to describe solutions of linear shear flows in unbounded domains according to Kelvin's work.
The stability equation (3.3) together with the Poisson equation (3.6) can be written as a scalar equation for v in (3.7). In the case of linear shear $U = Ay$, the second derivative of U with respect to y is zero ($U'' = 0$). Using this result, it is possible to rewrite (3.7) as a system of second order PDE

$$\left[\frac{\partial}{\partial t} + Ay\frac{\partial}{\partial x}\right]\sigma = \frac{1}{\mathrm{Re}}\nabla^2\sigma \tag{3.29}$$

where

$$\sigma = \nabla^2 v. \tag{3.30}$$

For inviscid flows ($1/\mathrm{Re} \to 0$), Kelvin (1887) proposed the ansatz

$$\sigma = f(x - Ayt), \tag{3.31}$$

where f is an arbitrary function. For viscous flows, the ansatz

$$\sigma = T(t) e^{i(k_x x + (k_y - k_x A t) y + k_z z)} \tag{3.32}$$

is used by Kelvin, where $T(t)$ is an arbitrary function of the time t and k_x, k_y, k_z denote the spatial wavenumbers. Inserting (3.32) into (3.29) gives an ODE for $T(t)$

$$\frac{dT}{dt} = -\frac{1}{\mathrm{Re}} \left[k_x^2 + (k_y - k_x A t)^2 + k_z^2 \right] T, \tag{3.33}$$

which can be solved by

$$T(t) = C e^{-\frac{1}{\mathrm{Re}} t \left(k_x^2 + k_y^2 + k_z^2 - k_y k_x A t + \frac{k_x^2}{3} A^2 t^2 \right)}, \tag{3.34}$$

where C is a constant of integration. The perturbation velocity v can be obtained from (3.30) together with the ansatz (3.32) and $T(t)$ defined in (3.34) and reads

$$v = -T(t) \frac{e^{i(k_x x + (k_y - k_x A t) y + k_z z}}{k_x^2 + (k_y - k_x A t)^2 + k_z^2}. \tag{3.35}$$

The ansatz (3.31) has some interesting physical properties. For the solution (3.32) we see that there is a time-dependent wave number. The time-dependent transformation is a Galilean transformation with the constant shear rate A, i.e. $U = Ay$ (Drazin, 2002). Sagaut and Cambon (2018) recommend therefore to call the solution *Fourier modes advected by the mean* or *mean-Lagrangian Fourier modes*. The Galilean transformation for shear flows has several applications in fluid mechanics, see e.g. Yaglom (2012) for a detailed explanation. Examples are the Rogallo transformation (Rogallo, 1981) or a corresponding transformation in Rapid Distortion theory (Moffatt, 1965; Goldstein, 2020).
Note that the the denominator in the solution (3.35) behaves as t^{-2} for large t. It is interesting to see that the solution has an algebraic decay in time. This contrasts with the normal mode solutions, which have an exponential decay rate (Yaglom, 2012).
In stability theory, Kelvin mode solution have received little attention for a long time. It even seems that these ideas were forgotten, cf. Craik and Criminale (1986) and Yaglom (2012). This changed around 100 years after Kelvin's discovery, mainly with the work of Craik and Criminale (1986). The authors studied an initial-value problem for linear shear and used Kelvin mode solutions. This was studied by other researchers at this time, e.g. (Farrell, 1987; Criminale, 1991; Criminale and Drazin, 1990), leading to an increasing interest in Kelvin mode solutions. For a detailed review the reader is referred to Yaglom (2012) or Hau (2016). In addition, it was further shown, that Kelvin modes are the natural choice for non-Hermitian operators (Yoshida, 2005).

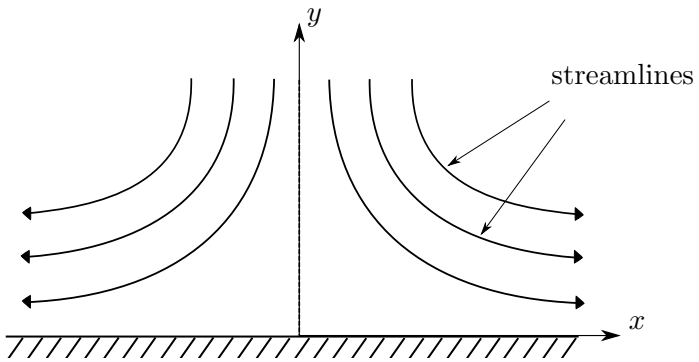

Figure 3.3.: Stagnation point flow, the stagnation point is at the origin $(0, 0)$ of the coordinate system, based on Kundu et al. (2012)

3.2.2. Görtler-Hämmerlin modes

A second example for special ansatz functions are the so-called Görtler-Hämmerlin (GH) modes, compare (Theofilis et al., 2003) (in earlier works they are sometimes called Hämmerlin modes, e.g. in Hall et al. (1984)). These modes play an important role in the stability analysis of stagnation point flows. The GH modes should not be confused with the Görtler problem, which describes vortices along a concave wall (centrifugal instability) (Görtler, 1940). For the GH modes, it is assumed that the perturbations have a similar form as the base flows. For this reason, we start with an analytical solution for stagnation point flows and proceed with the stability theory afterwards. A stagnation point flow is shown in figure 3.3. The (unperturbed) stagnation point flow was studied in a classical work by Hiemenz (1911) and numerically by Howarth (1934). For the inviscid case, the velocities are given by $U = ax, V = -ay$. For viscous flows the ansatz

$$U = kxf'(\zeta), \qquad V = -(\nu a) f(\zeta) \qquad \zeta = z (a/\nu)^{1/2} \tag{3.36}$$

allows to reduce the x-component of the Navier-Stokes equation to an ODE

$$f''' + ff'' + f'^2 + 1 = 0 \tag{3.37}$$

with BCs $f(0) = f'(0) = 0$ and $f'(\infty) = 1$, e.g. (Görtler, 1955; Rosenhead, 1963; Schlichting and Gersten, 2006). Note that the ansatz for U has the factor of x in front of the first derivative f'.

The idea of Görtler (1955) and Hämmerlin (1955) was to study the stagnation point flow under three-dimensional disturbances. Periodic disturbances were assumed in the z-direction. The authors proposed an ansatz for the stability equations which has the same form as the ansatz (3.36) and also contains the factor x for the streamwise component. The ansatz reads

$$(u, v, w) = (x\hat{u}(y), \hat{v}(y), \hat{w}(y))\, e^{i(\beta z - ct)} \tag{3.38}$$

This ansatz (3.38) is referred to as the GH ansatz. It should be noted that Görtler (1955) used a different notation. For consistency with the normal mode ansatz, we used a different notation in (3.38), compare e.g. (Lin and Malik, 1996).

The stability analysis reveals a spectrum of neutrally stable modes whose eigenfunctions decay

algebraically in y-direction as well. In addition, there is a discrete spectrum of eigenvalues with exponentially decaying eigenfunctions that decay in y-direction (Hämmerlin, 1955) . The extension to three-dimensional stagnation point flows was later done by Hall et al. (1984). The GH ansatz plays a major role in the stability analysis of flows around aircraft wings. There is a high interest in understanding the instability and transition mechanisms for swept wings. The possible instability mechanisms are attachement line, streamwise, centrifugal, or cross-flow instabilities (Saric et al., 2003). The work by GH provides the basis for the so called *attachement line instability*, or alternatively *leading-edge boundary-layer theory*, cf. Theofilis et al. (2003). Consequently, the GH modes were used in many works (cf. Hall et al., 1984; Lin and Malik, 1996; Theofilis, 1998; Obrist and Schmid, 2003a; Obrist and Schmid, 2003b; Theofilis et al., 2003). The stability analysis shows that the GH mode corresponds to the most unstable mode. Other modes are also found, but they are less unstable (i.e. they have smaller temporal growth rates) than the GH mode (Theofilis et al., 2003). This shows that the normal mode ansatz alone does not always predict the most unstable mode. Thus, it can be valuable to consider alternative ansätze besides the normal mode ansatz to study the stability of a flow.

3.3. Extension of normal mode stability using symmetry methods

The Kelvin modes (3.31) and the GH ansatz (3.38) show that there are alternative ways besides the normal mode ansatz to formulate eigenvalue problems.
There are different approaches in systematizing them. For example, the Kelvin mode solution shows an algebraic growth in time, which is different from the exponential growth for the normal mode solution. Algebraic growth rates are also observed in non-modal stability theory due to non-Hermitian operators, compare chapter 3.1.3. Using the term *non-modal* for Kelvin modes might be misleading, as still an eigenvalue problem rather than an initial-value problem is considered, e.g. compare to the definition of *non-modal* in Schmid (2007).
In the author's opinion, it is more appropriate to systematize the Kelvin modes and GH modes as a *generalized modal approach* (note that this term was already used for Kelvin modes in a less regarded work by Volponi and Yoshida (2002)).
A common property of Kelvin, GH, and normal modes are that they reduce an PDE to an ODE for the eigenvalue. Interestingly, there is a link between the subsequently introduced Lie symmetries of the equation and this property. We explain this aspect in the following.

Lie symmetries and stability

There is a link between separation of variables and Lie symmetries, which was described by Miller (1977) in a monograph "Symmetry and separation of variables". However, this idea was already known, and mentioned earlier, e.g. in Winternitz and Fris (1965) (Miller, 1977). The examples in the book showed a separation of variables for different equations in theoretical physics, e.g. the Schrödinger equation. The application to linear hydrodynamic stability theory was done by Burde et al. (2007) and Zhalij et al. (2006). In earlier works by these authors, they considered the separation of equations from theoretical physics (cf. Zhalij, 1999; Zhdanov and Zhalij, 1999a; Zhdanov and Zhalij, 1999b; Zhalij, 2002). In their hydrodynamic stability studies, they essentially considered non-parallel flows. They showed that ansatz functions consisting of algebraic and exponential terms can be used to study the stability of a flow between two concentric cylinders. Due to a time-dependent spatial coordinate, they used permeable walls with transpiration and moving walls. These problems were solved analytically

for some special cases and numerically. Unstable modes were found for the three-dimensional case (Zhalij et al., 2006; Burde et al., 2007).
Nold and Oberlack (2013) realized that the concept of separation is linked to Lie symmetries. They showed that Lie symmetry methods can be applied to calculate the symmetries and to systematically derive ansatz functions.
They found that the normal mode ansatz is based on classical symmetries (translation in space and time and a scaling symmetry of the dependent variable). Their idea is to use the general algorithms for finding symmetries to find the symmetries of the linearized flow equations. They showed that a combination of classical symmetries leads to the normal mode ansatz. If the stability equations have additional symmetries it is possible to construct alternative ansatz functions. This is not always the case, as some flow profiles or BC can be symmetry-breaking. This method was also applied successfully to compressible shear flows (Hau, 2016), the asymptotic suction boundary layer (Yalcin et al., 2021) and to rotational shear flows (Gebler et al., 2021). We present these results in the following.

Linear shear flows

In this section we summarize the results from Nold and Oberlack (2013) and Nold et al. (2015). The stability of a two-dimensional flow $(U(y),0)^T$ with perturbations $(u',v')^T$ is considered. By using a stream function Ψ for the perturbations

$$u' = \frac{\partial \Psi}{\partial y}, \qquad v' = -\frac{\partial \Psi}{\partial x}, \tag{3.39}$$

the linearized stability equation in terms of the stream function reads

$$\frac{\partial}{\partial t}\Delta\Psi + U\frac{\partial}{\partial x}\Delta\Psi - U''\frac{\partial \Psi}{\partial x} = \nu\Delta^2\Psi. \tag{3.40}$$

A symmetry analysis of (3.40) for a general base flow $U(y)$ gives the following symmetries

$$X_0 = \Psi_0\frac{\partial}{\partial \Psi}, \qquad X_1 = \frac{\partial}{\partial x}, \qquad X_2 = \frac{\partial}{\partial t}, \qquad X_3 = \Psi\frac{\partial}{\partial \Psi}, \tag{3.41}$$

and a symmetry X_0 due to the superposition principle for linear differential equations and $\Psi_0(x,y,t)$ solves (3.40). The symmetry X_1 is a translation in space, X_2 is a translation in time, X_3 is a scaling symmetry. The symmetries $X_1 - X_3$ are classical symmetries. For linear shear flows, i.e. $U(y) = Ay$ an additional symmetry X_4 exists

$$X_4 = At\frac{\partial}{\partial x} + \frac{\partial}{\partial y} \tag{3.42}$$

The symmetries can be combined by a linear combination

$$X = a_1X_1 + a_2X_2 + a_3X_3 + a_4X_4. \tag{3.43}$$

In general, the coefficients are complex numbers $a_i \in \mathbb{C}, i = 1,2,3$. Based on the combination of symmetries according to (3.43) it is possible to construct different ansatz functions. A combination of the classical symmetries (translation in space and time and scaling of the dependent variable) gives

$$X = a_1\frac{\partial}{\partial x} + a_2\frac{\partial}{\partial t} + a_3\Psi\frac{\partial}{\partial \Psi} \tag{3.44}$$

We use an invariance condition for the solution $\Psi = \Psi(x, y, t)$ given by

$$X\left(\Psi - \Psi(x, y, t)\right)|_{\Psi=\Psi(x,y,t)} = 0, \tag{3.45}$$

which yields

$$a_3\Psi - a_1\frac{\partial\Psi}{\partial x} - a_2\frac{\partial\Psi}{\partial t} = 0. \tag{3.46}$$

This condition can be solved using the method of characteristics for $a_2 \neq 0$ which gives

$$\Psi(x, y, t) = f(\xi, y)e^{\frac{a_3}{a_2}t}, \tag{3.47}$$

where

$$\xi = x - \frac{a_1}{a_2}t. \tag{3.48}$$

The ansatz (3.47) can be inserted into the linearized stability equation (3.40) and we obtain the following differential equation

$$\left(U - \frac{a_1}{a_2}\right)\frac{\partial}{\partial\xi}\Delta f + \frac{a_3}{a_2}\Delta f - U''\frac{\partial}{\partial\xi}f = \nu\Delta^2 f. \tag{3.49}$$

A symmetry analysis of (3.49) shows that the equation has two symmetries

$$X = b_1\frac{\partial}{\partial\xi} + b_2 f\frac{\partial}{\partial f}. \tag{3.50}$$

By using the invariant surface condition (see (3.45)) a second time, it is possible to find the following ansatz, assuming $b_1 \neq 0$

$$f(\xi, y) = g(y)e^{\frac{b_2}{b_1}\xi} \tag{3.51}$$

Combining the ansätze (3.47) and (3.51) we find

$$\Psi(x, y, t) = g(y)\exp\left(\frac{b_2}{b_1}x + \frac{a_3b_1 - a_1b_2}{a_2b_1}t\right). \tag{3.52}$$

Using a different notation with $\alpha = b_2/b_1$ and $c = a_1/a_2 - (a_3b_1)/(a_2b_2)$ (here it is assumed that all parameters are real values) we obtain

$$\Psi(x, y, t) = g(y)e^{i\alpha(x-ct)}. \tag{3.53}$$

We see that by a successive use of symmetries from (3.44)and (3.50) we can recover the normal mode ansatz. In addition, the Orr-Sommerfeld equation can be also derived directly from the Lie symmetries.
Moreover, it is possible to construct two distinct modes using a different combination of symmetries including X_4. Note that the symmetry X_4 only exists for linear shear.

- Kelvin mode approach X_1, X_2, X_4

  $$\Psi(x, y, t) = g(t)e^{ik_x(x-Ayt)+ik_y y} \tag{3.54}$$

  with wavenumbers k_x and k_y for the two-dimensional flow.

- New invariant solution using symmetries X_1, X_2, X_3, X_4

$$\Psi(x,y,t) = g\left(\kappa y - \frac{t}{T}\right) \exp\left(i\kappa\left(x - \frac{At^2}{2\kappa T}\right) + cxt\right) \tag{3.55}$$

  where the coefficients κ, T, c depend on the coefficients of the symmetries, i.e. on a_i for a linear combination of the symmetries. The coefficient κ is real and c is proportional to κ but can take complex values. T is a time scale such that $(\kappa T)^{-1}$ is constant. The modes of the new invariant solution are periodic in stream-wise direction and travel with a constant speed $(\kappa T)^{-1}$ in cross-stream direction.

Asymptotic suction boundary layer

In stability theory there is an interesting extension to wall-bounded flows with permeable walls (wall suction). This allows for crossflows relative to the streamwise velocity. The displacement thinkness δ_1 (a measure for the boundary layer thickness) is asymptotically constant for distances large enough from the inflow (i.e. the leading edge of the flat plate). This is referred to as the asymptotic suction boundary layer (ASBL) in the literature, cf. Hughes and Reid (1965). We consider a wall-bounded flow with a constant suction at the wall with a constant velocity V_0. The base flow is given by

$$(U, Y, W) = \left(U_\infty\left(1 - e^{\frac{yV_0}{\nu}}\right), -V_0, 0\right). \tag{3.56}$$

A critical Reynolds number was found to be $\mathrm{Re} = 54.370$ (Hocking, 1975). However, numerically the transition to turbulence could be shown for Reynolds numbers of order $\mathrm{Re} \approx 300$ (Schlatter and Örlü, 2011). For further numerical work the reader is referred to e.g. Fransson and Alfredsson (2003) and Khapko et al. (2013). This section is a summary of a recent work by Yalcin et al. (2021). The stability equation can be derived in a similar way as the Orr-Sommerfeld equation. However, there is an additional term due to the suction which scales with Re^{-1} (refer to Yalcin et al. (2021) for details). For the 2D inviscid case the stability equation in terms of a streamfunction reads

$$\left[\frac{\partial}{\partial t} + \left(1 - e^{-y}\right)\frac{\partial}{\partial x} - \frac{1}{\mathrm{Re}}\frac{\partial}{\partial y}\right]\Delta\Psi + e^{-y}\frac{\partial\Psi}{\partial x} = 0, \tag{3.57}$$

where the Reynolds number is defined as

$$\mathrm{Re} = \frac{U_\infty}{V_0}. \tag{3.58}$$

A symmetry analysis gives the following symmetries (Mirzayev, 2016)

$$X_1 = \frac{\partial}{\partial t}, \qquad X_2 = \frac{\partial}{\partial x}, \qquad X_3 = \Psi\frac{\partial}{\partial\Psi}, \tag{3.59}$$

$$X_4 = e^{1/\mathrm{Re}}\left[\frac{\partial}{\partial t} + \frac{\partial}{\partial x} - \frac{1}{\mathrm{Re}}\frac{\partial}{\partial y}\right], \qquad X_0 = \Psi_0\frac{\partial}{\partial\Psi}. \tag{3.60}$$

The symmetries $X_1 - X_3$ are the classical symmetries and X_4 is a special symmetry which only exists for inviscid flows. The symmetry X_0 gives the superposition principle for linear differential equations, where $\Psi_0(x,y,t)$ solves (3.57). The combination of the symmetries reveals three ansatz functions.

- The normal mode ansatz (2D) is based on the symmetries X_1, X_2, X_3 and is given by

$$q(x, y, t) = \hat{q}(y) e^{i(\alpha x - \omega t)}. \tag{3.61}$$

  A stability analysis reveals unstable normal modes. The reader is referred to Yalcin et al. (2021) for more details.

- The double-exponential ansatz function arises from the symmetries X_2, X_3, X_4 and reads

$$\Psi(x, y, t) = \Phi\left(\mathrm{Re} y + t\right) e^{\mathrm{Re}\omega e^{\frac{t}{\mathrm{Re}}} + \alpha x + \mathrm{Re}\alpha y}, \tag{3.62}$$

  where the time-dependency can be interpreted as a travelling wave solution.

- The alternative exponential ansatz function with symmetries X_1, X_2, X_3, X_4 is given by

$$\Psi(x, y, t) = \varphi\left(y(1-\lambda)\mathrm{Re} + t - \lambda x\right) e^{\alpha(\mathrm{Re} y + x)}. \tag{3.63}$$

  The stability analysis shows that all modes from (3.63) are stable.

Rotational shear flows

Another interesting class of flows are rotational shear flows. One example are flows confined by two concentric cylinders. For the viscous case $V(r) = Ar + B/r$ is an exact solution. For inviscid flows, any profile $V(r)$ is a solution (Chandrasekhar, 1961). If three dimensional perturbations are allowed, this leads to the Taylor Couette experiment (Taylor, 1923). The study of the plane rotational shear flow reveals new stable modes, which are presented in the following.
The Navier-Stokes equations (2.3) with perturbations are written in cylindrical coordinates (r, φ) with velocities u_r, u_φ in a stationary frame (without any forcing terms). The streamfunction ψ for the two-dimensional perturbations u'_r, u'_φ is defined by

$$u'_r = \frac{1}{r}\frac{\partial \psi}{\varphi}, \qquad u'_\varphi = -\frac{\partial \psi}{\partial r}. \tag{3.64}$$

The linearized stability equation for a general base flow

$$V(r) = Ar + B/r \tag{3.65}$$

reads

$$\left[\frac{\partial}{\partial t} + \left(A + \frac{B}{r^2}\right)\frac{\partial}{\partial \varphi}\right]\Delta\Psi = \frac{1}{\mathrm{Re}}\Delta^2\Psi, \tag{3.66}$$

where the Reynolds number is defined as $\mathrm{Re} = B/\nu$. In the following, we consider the case $B = 1$. The symmetries of the equation (3.66) are given as follows (these symmetries were first presented by Sanjon (2005))

$$X_1 = \frac{\partial}{\partial t}, \qquad X_2 = \frac{\partial}{\partial \varphi}, \qquad X_3 = \Psi\frac{\partial}{\partial \Psi}, \qquad X_4 = r\frac{\partial}{\partial r} + 2t\frac{\partial}{\partial t} + At\frac{\partial}{\partial \varphi} \tag{3.67}$$

The symmetries $X_1 - X_3$ are the classical symmetries, namely the translation in time, space and the scaling symmetry. In addition, X_4 is a special symmetry. There are two types of modes

- normal mode ansatz with symmetries X_1, X_2, X_3

$$\psi(r, \varphi, t) = g(r) e^{i(m\varphi - \omega t)} \tag{3.68}$$

- algebraic mode ansatz with symmetries X_1, X_2, X_3, X_4

$$\psi(r, \varphi, t) = f\left(\frac{r}{\sqrt{\bar{t}}}\right) e^{im(\varphi - At)} \bar{t}^s \tag{3.69}$$

  Due to the coordinate transform $r/\sqrt{t}$, there is a singularity for $t = 0$. However, the symmetry X_1 admits a translation in time, which allows to shift the origin of time, i.e. $\bar{t} \to t + t_0$ to avoid this singularity. The term $\bar{t}^s$ implies an algebraic growth in time. Therefore we refer to ansatz (3.69) as the *algebraic mode* ansatz in the following.

The base flow $V(r) = Ar + 1/r$ covers a large class of flows. The base flow profile is a plane analogue to the flow between two concentric cylinders. For three-dimensional perturbations this corresponds to the Taylor-Couette experiment (Taylor, 1923). However, only two-dimensional perturbations are considered here. In the case of a vanishing A the base flow reduces to a point vortex flow.
An interesting extension to base flows with $V(r) = r^{-n}$ is given in Kleinjung (2019). The symmetries $X_1 - X_3$ from (3.67) are preserved. However, the symmetry X_4 can be written more generally as

$$X_4 = r\frac{\partial}{\partial r} + (n+1)t\frac{\partial}{\partial t}, \tag{3.70}$$

which reduces to the special case for X_4 from (3.67) for $A = 0$ and $n = 1$. The corresponding ansatz function to the symmetries X_2, X_3 from (3.67) with symmetry X_4 from (3.70) reads

$$\psi(r, \varphi, t) = f\left(\frac{r}{t^{\frac{1}{n+1}}}\right) e^{im\varphi} t^s. \tag{3.71}$$

For $n = 2$ we obtain a base flow $V(r) = r^{-1/2}$ which is known as a Keplerian velocity profile. The flow profile is used to model accretion disks in astrophysics. Accretion is seen as a key process in the growth of new stars (Shariff, 2009). Interestingly, the mass fluxes in accretion disks indicate that the flow is turbulent, however the flow profile is stable to classical analysis (Shakura, 2018). Several extensions including magneto-hydrodynamic effects were proposed (Shariff, 2009). Though, this still bears several open questions for the hydrodynamic stability theory (cf. Ji et al., 2006; Balbus, 2011; Avila, 2012; Balbus, 2017; Shi et al., 2017). In the following we present a full stability analysis using the novel algebraic mode ansatz with a base flow $V(r) = r^{-1}$ (point vortex flow).

3.4. Example: stability analysis of rotational shear flow

This section is based on the publication "Algebraic Stability Modes in Rotational Shear Flow" by T. Gebler, D. Plümacher, J. Kahle, and M. Oberlack (2021). The results, equations, and figures are based on the publication mentioned.
We consider a rotational base flow $V(r) = r^{-1}$. Physically, this can be interpreted as a point vortex. The base flow has a singularity at the center $r = 0$. Special attention is therefore needed

for the BCs and physical quantities (e.g. perturbation velocity or vorticity) near the center. The stability criteria are different for this flow under two- or three-dimensional perturbations. This work addresses two-dimensional instability. Here Rayleigh's inflection point theorem for rotational flows holds (cf. Rayleigh (1879), which is similar to the Rayleigh's inflection point criterion for plane flows in (3.23) to (3.25)). The theorem states that the necessary condition for instability is a change of sign for the base flow vorticity, cf. Drazin and Reid (2004) and Kerswell (2015). Therefore the point vortex is stable according to classical stability analysis. For the stability analysis under three-dimensional instabilities, the reader is referred to Rayleigh (1917), Synge (1938), and Billant and Gallaire (2005).
In the present work, we investigate if there are any instabilities using the algebraic mode ansatz. In addition, we discuss how the stability criterion from a normal mode ansatz can be generalized and applied to the algebraic mode ansatz.

Formulation of the eigenvalue problem

Inserting the algebraic mode ansatz (3.69) into the linearized stability equation (3.66) gives the following equation for the eigenvalue s

$$\left(\frac{im}{x^2} + s - 1 - \frac{x}{2}\frac{d}{dx}\right)\mathcal{L}f(x) = \frac{1}{\mathrm{Re}}\mathcal{L}^2 f(x), \tag{3.72}$$

where

$$\mathcal{L} = \left(\frac{d^2}{dx^2} + \frac{1}{x}\frac{d}{dx} - \frac{m^2}{x^2}\right). \tag{3.73}$$

Note that due to the coordinate transform $x = r/\sqrt{t}$, the new coordinate x is implicitly time-dependent. The derivative with respect to r transforms as

$$\frac{\partial}{\partial r} = \frac{1}{\sqrt{t}}\frac{\partial}{\partial x}. \tag{3.74}$$

The velocity can be obtained from the definition of the stream function and the algebraic mode ansatz as follows

$$u_r = \lim_{x\to\infty} t^{s-\frac{1}{2}}\frac{f(x)}{x}\mathrm{e}^{im\varphi} im, \tag{3.75}$$

$$u_\varphi = \lim_{x\to\infty} t^{s-\frac{1}{2}} f'(x)\mathrm{e}^{im\varphi}. \tag{3.76}$$

Vanishing velocities in the limit $r \to \infty$ for all times t are applied as BC. With (3.75) and (3.76), the outer BCs therefore read

$$\lim_{r\to\infty} u_r = \lim_{x\to\infty} t^{s-\frac{1}{2}}\frac{f(x)}{x}\mathrm{e}^{im\varphi} im = 0, \tag{3.77}$$

$$\lim_{r\to\infty} u_\varphi = \lim_{x\to\infty} t^{s-\frac{1}{2}} f'(x)\mathrm{e}^{im\varphi} = 0. \tag{3.78}$$

For the inner BCs, Batchelor and Gill (1962) proposed conditions for smooth and bounded solutions for the velocity given by (Khorrami et al., 1989)

$$\lim_{r\to 0}\frac{\partial \boldsymbol{u}}{\partial \varphi} = 0, \tag{3.79}$$

or written component-wise as

$$\lim_{r\to 0}\left[\left(\frac{\partial u_r}{\partial\varphi}-u_\varphi\right)\mathbf{e}_r+\left(u_r+\frac{\partial u_\varphi}{\partial\varphi}\right)\mathbf{e}_\varphi\right]=0. \tag{3.80}$$

By using the definition of the stream function (3.64) and the algebraic mode ansatz (3.69) the condition (3.80) can be rewritten as

$$\lim_{r\to 0}\left(\frac{f(x)}{x}m^2-f'(x)\right)=0, \tag{3.81}$$

$$\lim_{r\to 0}\left(\frac{f(x)}{x}im-f'(x)im\right)=0. \tag{3.82}$$

Special attention must be paid to the case $m=0$ as there are two dependent BCs (Khorrami et al., 1989). By using the continuity equation we can derive an additional condition

$$2\left(\frac{f(x)}{x}\right)'-f''(x)=0. \tag{3.83}$$

The resulting BCs read

$$m=0: \qquad \frac{f(x)}{x} \text{ finite},\ f'(x)=0, \tag{3.84}$$

$$m=1: \qquad \frac{f(x)}{x}-f'(x)=0, \quad 2\left(\frac{f(x)}{x}\right)'-f''(x)=0, \tag{3.85}$$

$$m\geq 2: \qquad \frac{f(x)}{x}=f'(x)=0. \tag{3.86}$$

The eigenvalue equation (3.72) and the BCs (3.84)-(3.86) constitute an eigenvalue problem for the stability of the rotational shear flow.

Stability criterion for algebraic modes

According to (temporal) stability theory using normal modes, a flow is unstable if there exists at least one mode (wave-like disturbance) which is not damped for large times (Yaglom, 2012). If we consider an unstable mode with $\omega_i>0$, the kinetic perturbation energy of the mode grows as $E\sim\exp(2\omega_i t)$ (Canuto, 1988). In that way, we see that the kinetic energy E of the perturbations is defined in general by

$$E=\frac{1}{2}\int_V u_i u_i dV \tag{3.87}$$

and can be taken as a criterion for the longtime stability, cf. Schmid and Henningson (2001). In (3.87), the square of the perturbation velocities u_i is integrated over the domain V. As the rotational shear flow is defined on an infinite domain, the integration has to be done over $r=[0,\infty[$, or written in transformed variables over $x=[0,\infty[$. In addition, the eigenfunctions f from (3.72) with corresponding BCs are in general complex valued. As the perturbation velocities can be obtained directly from the eigenfunctions (cf. (3.75) and (3.76)), the velocities are in general also complex valued. Therefore, the complex conjugate $\overline{f}$ of f is used to obtain

the (real valued) kinetic energy. For the algebraic mode ansatz (3.69), the perturbation energy from (3.87) can be written as

$$E(t) = \frac{1}{2} t^{2s_R} \int_0^\infty \int_0^{2\pi} \left(\frac{m^2}{x^2} f\overline{f} + f'\overline{f}' \right) x d\varphi dx = \frac{1}{2} t^{2s_R} E_0, \tag{3.88}$$

where E_0 is the initial kinetic energy. It follows directly that a necessary criterion for a temporal growth of energy is $s_R > 0$, where s_R is the real part of the eigenvalue s. The stability therefore only depends on the real part of s. Note that only the real part of s, i.e. s_R remains in (3.88) due to the use of complex conjugate quantities. In addition, it can be shown that the stability equation (3.66) has a discrete symmetry $(m, s) \rightarrow (-m, \bar{s})$ and is invariant under a change of sign of the wavenumber in a two-dimensional analysis. In three-dimensional stability analysis, for example, vortices with an axial flow, the stability results may depend on the sign of the wavenumber, e.g. (Ash and Khorrami, 1995). As the energy $E(t)$ has to be bounded at all times, the integral in (3.88) has to be bounded. Therefore the eigenfunctions $f(x)/x$ and $f'(x)$ must decay as x^{-1} or faster to have bounded results. This gives an additional condition for a physically realizable solution and has to be checked for any possibly unstable mode. It can be discussed if other quantities, such as the vorticity ($\boldsymbol{\eta} = \nabla \times \boldsymbol{u}$) or enstrophy ($\epsilon = \int |\boldsymbol{\eta}|^2 dV$, integrated over the corresponding volume V) should be bounded as well.
The vorticity η for the two-dimensional flows in polar coordinates reads

$$\eta = \frac{1}{r} \frac{\partial}{\partial r} (r u'_\varphi) - \frac{1}{r} \frac{\partial u'_r}{\partial \varphi} = -\Delta \psi. \tag{3.89}$$

Transforming the expression (3.89) from (r, φ, t) to (x, φ, t) and using the definition of the velocity fluctuations from (3.75) and (3.76) gives

$$\eta = t^{s-1} e^{im\varphi} \left(f''(x) + \frac{f'(x)}{x} + m^2 \frac{f(x)}{x^2} \right), \tag{3.90}$$

where $f''(x)$ denotes the second derivative with respect to x. Using the result for the vorticity from (3.90), the enstrophy

$$\epsilon = \int_V \eta^2 dV \tag{3.91}$$

can be calculated by multiplying the vorticity η from (3.90) with its complex conjugate and integrating the expression over the infinite domain, which gives

$$\epsilon = t^{2s_R - 2} \int_0^\infty \int_0^{2\pi} \left(f'' + \frac{f'}{x} + m^2 \frac{f}{x^2} \right) \left(\overline{f}'' + \frac{\overline{f}'}{x} + m^2 \frac{\overline{f}}{x^2} \right) x d\varphi dx. \tag{3.92}$$

In order that the integral (3.92) is bounded, its integrand must decay faster than x^{-1}. Expanding the product of the integrand leads to an expression of nine terms. For the case that bounded enstrophy is used as an additional criterion together with the bounded energy (3.88), we can use the result that f/x and f' must decay as x^{-1} or faster (see section below (3.88)). For the remaining terms follows the condition that that f'' and $\overline{f}''$ have to decay faster than x^{-1}. Throughout the present work, the behavior for large arguments, i.e $x \rightarrow \infty$ is discussed based on asymptotic expansions. These expansions admit a series representation as polynomials. In general, if the polynomial for the asymptotic of f' has a decay rate of x^{-1} or faster, its

derivative, i.e. the polynomial for the asymptotic of f'' decays with x^{-2} or faster. The same arguments also holds for the complex conjugate $\overline{f}''$. Therefore, the enstrophy criterion (3.92) does not give further limitations on the decay of the solutions if it is used in addition to the energy criterion (3.88). However, in the following, we restrict the present study to the kinetic energy of the perturbation and therefore only force the expression (3.88) to be bounded.

Stability analysis for inviscid flows

The stability equation (3.72) simplifies for inviscid perturbations to

$$\left(\frac{im}{x^2} + s - 1 - \frac{x}{2}\frac{d}{dx}\right)\mathcal{L}f(x) = 0, \tag{3.93}$$

where $\mathcal{L}$ is defined in (3.73). The solution for for the axisymmetric case reads

$$f(x) = C_1 \ln(x) + C_2 x^{2s} + C_3. \tag{3.94}$$

With respect to the BCs (3.78) and (3.84) it follows that only the trivial solution $f(x) = 0$ exists for the axisymmetric case. For the non-axisymmetric case ($m \neq 0$) the solution of (3.93) is

$$f(x) = C_3 x^m + C_2 x^{-m} + C_1 x^{2s}\left(\frac{\mathrm{e}^{-\frac{z}{2}}}{2m}\sum_{j=1}^{2}(-1)^j z^{-\frac{\kappa_j}{2}}\frac{\mathrm{W}\left[\frac{\kappa_j}{2}, \frac{\kappa_j}{2}+\frac{1}{2}, z\right]}{\kappa_j(1+\kappa_j)} - \frac{\mathrm{e}^{-z}}{2\kappa_1\kappa_2}\right), \tag{3.95}$$

where W is the Whittaker function with the following parameters

$$\kappa_1 = -s - \frac{m}{2}, \qquad \kappa_2 = -s + \frac{m}{2}, \qquad z = \frac{im}{x^2}. \tag{3.96}$$

We perform an analytic investigation of the solution. The Whittaker function has a singularity if its second argument is a negative integer. In addition, the denominator is singular if $\kappa_j = 0$ or $\kappa_j + 1 = 0$. These cases have to be considered separately. In the following, an analysis for the non-singular case $|m| \neq 2s$ is performed.

By using the limit $x \to \infty$ of (3.95) and with the asymptotic limits for the Whittaker function given by Olver (2010) we obtain

$$\frac{f(x)}{x} \sim C_1 x^{2s-1}\left(\hat{\kappa}x^{-2} - \frac{1}{2\kappa_1\kappa_2}\right) + C_3 x^{m-1} + C_2 x^{-(m+1)}, \tag{3.97}$$

where

$$\hat{\kappa} = \frac{i}{2}\left(\frac{1}{\kappa_2(\kappa_2+1)} - \frac{1}{\kappa_1(\kappa_1+1)}\right). \tag{3.98}$$

The term x^{2s-1} with coefficient C_1 in (3.97) converges to zero if $s_R < 1/2$. However, to ensure sufficient decay, the condition $s_R < 0$ is necessary. Otherwise, C_1 must be set to zero. In the following analysis, positive wavenumbers are assumed. The term x^{m-1} with coefficient C_3 in (3.97) is therefore critical. For any wavenumber $m \geq 1$, it follows directly that $C_3 = 0$ must hold.
The limit of (3.95) for $x \to 0$ gives

$$f(x) = (C_3 - C_1\alpha)\, x^m + (C_2 - C_1\beta)\, x^{-m} - \frac{C_1 i}{2m^2}\gamma e^{-im/x^2} x^{2(s+2)}, \tag{3.99}$$

with

$$\alpha = -\frac{\Gamma(\kappa_2)}{2m}(im)^{-\kappa_2}, \qquad \beta = \frac{\Gamma(\kappa_1)}{2m}(im)^{-\kappa_1}. \tag{3.100}$$

We use the conditions for smoothness and boundedness for $r \to 0$. For perturbations with higher modes $m \geq 2$ the BC (3.86) is used, giving

$$\lim_{x\to 0} \frac{f(x)}{x} = (C_3 - C_1\alpha)\, x^{m-1} + (C_2 - C_1\beta)\, x^{-(m+1)} - \frac{C_1 i}{2m^2}\gamma e^{-im/x^2} x^{2s+3} = 0, \tag{3.101}$$

$$\begin{aligned}\lim_{x\to 0} f'(x) = {} & (C_3 - C_1\alpha)\, m x^{m-1} + (-C_2 + C_1\beta)\, m x^{-(m+1)} \\ & + C_1\gamma e^{-im/x^2}\left(\frac{1}{m}x^{2s+1} - \frac{i(s+2)}{m^2}x^{2s+3}\right) = 0.\end{aligned} \tag{3.102}$$

The constant γ arises from the asymptotic limit of the Gamma function. The term x^{-m-1} is singular for positive wavenumbers ($m \geq 2$). The contributions vanish for a linear combination of the coefficients, i.e.

$$C_2 = C_1\beta. \tag{3.103}$$

The exponential term e^{-im/x^2} in (3.102) and (3.101) has a purely imaginary argument and thus has unit amplitude. The terms

$$\frac{1}{m}x^{2s+1} - \frac{i(s+2)}{m^2}x^{2s+3} \tag{3.104}$$

which are given between the brackets in (3.102) are of order x^{2s+1} and x^{2s+3}. Any choice $s_R > -1/2$ satisfies the BC (3.86). From the analysis for $x \to \infty$, we find the condition $s_R < 0$. It follows that under condition (3.103), the solution (3.95) admits a continuous spectrum.

For mode-one perturbations ($m = 1$) the inner BCs from (3.85) yield

$$\lim_{x\to 0}\left[\frac{f(x)}{x} - f'(x)\right] = 2(C_2 - C_1\beta)x^{-2} + C_1\gamma e^{-i/x^2}x^{2s+1}\left(1 + \mathcal{O}(x^2)\right) = 0 \tag{3.105}$$

$$\lim_{x\to 0}\left[2\left(\frac{f(x)}{x}\right)' - f''(x)\right] = -6(C_2 - C_1\beta)x^{-3} + C_1\gamma i e^{-i/x^2}x^{2s-2}\left(1 + \mathcal{O}(x^2)\right) = 0 \tag{3.106}$$

To avoid singularities due to the terms x^{-2} and x^{-3} their contribution must vanish by a linear combination of of the coefficients C_1 and C_2, i.e. $C_2 - C_1\beta = 0$. The condition (3.105) gives $s_R \geq -1/2$ while (3.106) requires $s_R > 1$. Therefore (3.105) and (3.106) can not be fulfilled at the same time. As a consequence, C_1 must be zero and it follows that only the trivial solution ($f(x) = 0$) exists for $m = 1$.
It can be shown that also in the singular case $m = 2s$, only a trivial solution $f(x) = 0$ exists, see Gebler et al. (2021) for more details. To summarize, all inviscid eigenfunctions are stable with wavenumber $m \geq 2$. For wavenumber $m = 0$ and $m = 1$ there are only trivial solutions ($f(x) = 0$). The corresponding eigenfunction $f(x)/x$ for $m = 2$ is shown in Figure 3.4. It can be seen that there is an oscillation near $r = 0$. The real part of the velocity component u_r is shown in Figure 3.5, which reveals a spiral-like structure of the velocity field.

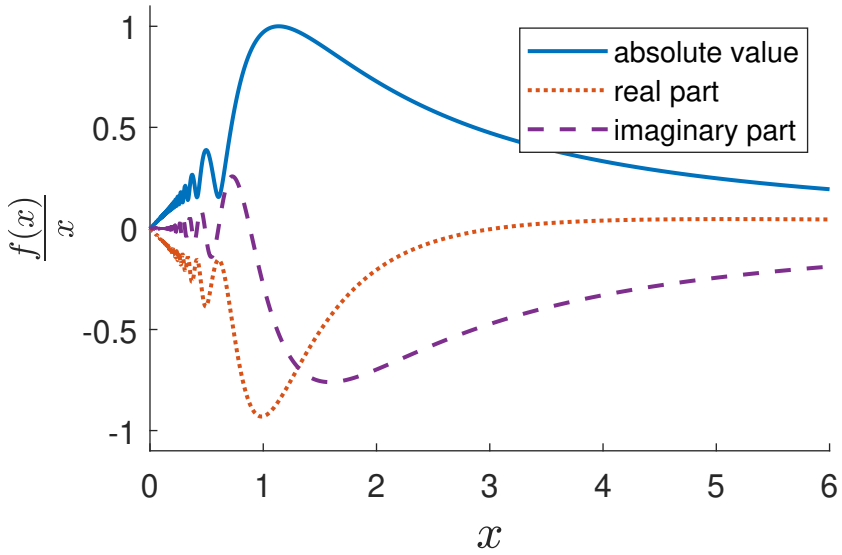

Figure 3.4.: Algebraic mode, inviscid flow: $f(x)/x$ from definition (3.95) ($s = -1/4, m = 2$) with absolute value, real part and imaginary part. The domain is truncated at $x = 6$. The functions are rescaled by the maximum of the absolute value

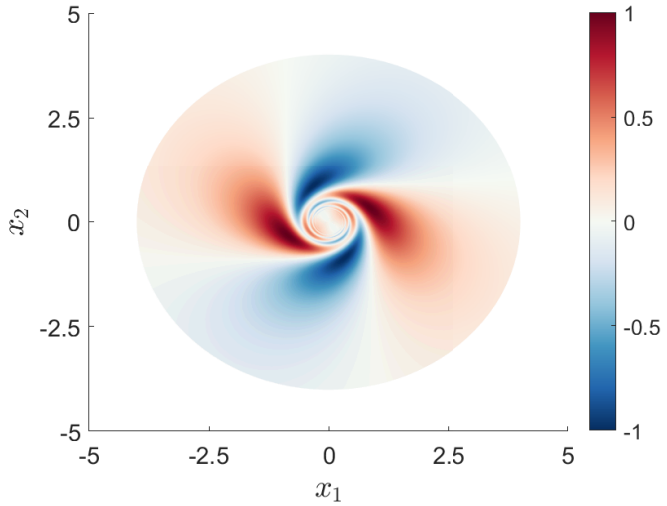

Figure 3.5.: Algebraic mode, inviscid flow: real part of the u_r disturbances for ($s = -1/4, m = 2, t = 1$) in polar coordinates (r, φ). The domain is truncated at $r = 6$.

Stability analysis for viscous flows (non-axisymmetric perturbations)

The solution of (3.72) for viscous flows is given by

$$\begin{aligned} f(x) =& C_3 x^m + C_4 x^{-m} \\ &+ C_1 \left[x^m \int_1^x \tilde{x}^{-m} e^{-\frac{\tilde{z}}{2}} \mathrm{M}\left[\kappa, \mu; \tilde{z}\right] d\tilde{x} - x^{-m} \int_1^x \tilde{x}^m e^{-\frac{\tilde{z}}{2}} \mathrm{M}\left[\kappa, \mu; \tilde{z}\right] d\tilde{x} \right] \\ &+ C_2 \left[x^m \int_1^x \tilde{x}^{-m} e^{-\frac{\tilde{z}}{2}} \mathrm{W}\left[\kappa, \mu; \tilde{z}\right] d\tilde{x} - x^{-m} \int_1^x \tilde{x}^m e^{-\frac{\tilde{z}}{2}} \mathrm{W}\left[\kappa, \mu; \tilde{z}\right] d\tilde{x} \right] \end{aligned} \tag{3.107}$$

with

$$z = \frac{\mathrm{Re}}{4} x^2, \quad \kappa = \frac{1}{2} - s, \qquad \mu = \frac{1}{2}\sqrt{m^2 + im\mathrm{Re}}. \tag{3.108}$$

Note that there is also a representation in terms of hypergeometric functions, cf. Kahle (2017) for more details. We use the solution representation (3.107), and perform an asymptotic analysis with respect to the BCs. First, the integrand is replaced by its asymptotic expansion and second, the integration is performed. This approach can be found in textbooks on asymptotic methods, see e.g. Olver (1974).

The limit of (3.107) for small x under non-axisymmetric perturbations reads

$$x \to 0: \quad f(x) = C_3 x^m + C_4 x^{-m} + x^{2+2\mu} C_1 a_1 + x^{2-2\mu} C_2 a_2, \tag{3.109}$$

with

$$a_1 = \left(\frac{\mathrm{Re}}{4}\right)^{1/2-\mu} \frac{2m}{(2+2\mu-m)(2+2\mu+m)}, \tag{3.110}$$

$$a_2 = \left(\frac{\mathrm{Re}}{4}\right)^{1/2-\mu} \frac{2m}{(2+2\mu-m)(-2+2\mu-m)}. \tag{3.111}$$

It can be easily verified that $\Re(\mu) > 1/2$. Thus, the term C_1 with $x^{2+2\mu}$ converges to zero. This contribution is therefore uncritical in the limit of $x \to 0$. The BC(3.85) for mode one solutions ($m = 1$) gives

$$\lim_{x\to 0} \left[\frac{f(x)}{x} - f'(x) \right] = a_2 \left(2\mu - 1\right) C_2 x^{1-2\mu} + 2\tilde{C}_4 x^{-2} = 0, \tag{3.112}$$

$$\lim_{x\to 0} \left[2\left(\frac{f(x)}{x} \right)' - f''(x) \right] = -2a_2(2\mu-1) C_2 \mu x^{-2\mu} - 6\tilde{C}_4 x^{-3} = 0. \tag{3.113}$$

The terms x^{-2} and $x^{1-2\mu}$ with $\Re(\mu) > 1/2$ are in general singular as $x \to 0$. A special case occurs for the Reynolds number $\mathrm{Re} = 12\sqrt{2}$ which gives exponents of the same order. However, it can be easily shown that this special case does not satisfy (3.112) and (3.113) at the same time. Therefore, the choice $C_2 = C_4 = 0$ is necessary.
For modes $m \geq 2$, the conditions from the terms C_3 are uncritical and we obtain from BC (3.86)

$$\lim_{x\to 0} \frac{f(x)}{x} = C_4 x^{-m-1} + x^{1-2\mu} C_2 a_2 = 0, \tag{3.114}$$

$$\lim_{x\to 0} f'(x) = -C_4 m x^{-m-1} + x^{1-2\mu} C_2 (2-2\mu) a_2 = 0. \tag{3.115}$$

Similar to the case with wavenumber $m = 1$ only a trivial choice ($C_2 = C_4 = 0$) is possible. Special care must be taken for limit $x \to \infty$. Here, the asymptotic depends on s_R and a case split is necessary. The asymptotic expansions read

$$\lim_{x\to\infty} \frac{f(x)}{x} \sim C_3 x^{m-1} + C_1 a_3 \gamma x^{m-1} \qquad \text{for } s_R < -\tfrac{m}{2}, \tag{3.116}$$

$$\lim_{x\to\infty} \frac{f(x)}{x} \sim C_3 x^{m-1} + C_1 a_3 \left(\gamma x^{m-1} - \ln(x) x^{-m-1}\right) \qquad \text{for } s_R = -\tfrac{m}{2}, \tag{3.117}$$

$$\lim_{x\to\infty} \frac{f(x)}{x} \sim C_3 x^{m-1} + C_1 a_3 \left(\gamma x^{m-1} - a_4 x^{2s-1}\right) \qquad \text{for } s_R \in]-\tfrac{m}{2}, 0[, \tag{3.118}$$

with a proportionality constant γ from the integration and the coefficients

$$a_3 = \left(\frac{\mathrm{Re}}{4}\right)^{s-1/2} \frac{\Gamma(1+2\mu)}{\Gamma(\frac{1}{2}+\mu-\kappa)}, \tag{3.119}$$

$$a_4 = \frac{1}{2s+m}. \tag{3.120}$$

For $s_R > 0$ there are only trivial solutions, therefore a detailed analysis is omitted here. The terms x^{m-1} vanish under a linear combination of C_3 and C_1. The contributions $\ln(x)x^{-m-1}$ and x^{2s-1} both have sufficient decay and satisfy the energy criterion (3.88). Therefore a non-trivial viscous eigenfunction is found based on (3.107).

Stability analysis for viscous flows (axisymmetric perturbations)

For axisymmetric perturbations ($m = 0$), the equation (3.72) simplifies and has the solution

$$\begin{aligned} f(x) = \quad & C_1 + C_2 \ln(x) \\ & + C_3 \left[\frac{x^2\mathrm{Re} + 4s}{x^2} e^{-\frac{z}{2}} \mathrm{M}(-s, \frac{1}{2}, z) + \frac{-4s+4}{x^2} e^{-\frac{z}{2}} \mathrm{M}(1-s, \frac{1}{2}, z)\right] \\ & + C_4 \left[\frac{x^2\mathrm{Re} + 4s}{x^2} e^{-\frac{z}{2}} \mathrm{W}(-s, \frac{1}{2}, z) - \frac{4}{x^2} e^{-\frac{z}{2}} \mathrm{W}(1-s, \frac{1}{2}, z)\right], \end{aligned} \tag{3.121}$$

The radial velocity vanishes (i.e. $u_r = 0$) in the axisymmetric case, which follows directly from the definition of the stream function (3.64). The azimuthal perturbations are proportional to $f'(x)$ and are obtained by differentiation of (3.121) with respect to x

$$f'(x) = \frac{C_2}{x} + C_3 \frac{2s\mathrm{Re}}{x} e^{-\frac{z}{2}} \mathrm{M}\left(-s, \frac{1}{2}, z\right) + C_4 \frac{2s\mathrm{Re}}{x} e^{-\frac{z}{2}} \mathrm{W}\left(-s, \frac{1}{2}, z\right). \tag{3.122}$$

The asymptotic analysis of $x \to \infty$ reads

$$f'(x) \sim \frac{C_2}{x} + C_3 \frac{2s\mathrm{Re}}{\Gamma(1+s)} \left(\frac{\mathrm{Re}}{4}\right)^{s} x^{2s-1} + C_4 2s\mathrm{Re} \left(\frac{\mathrm{Re}}{4}\right)^{-s} x^{-2s-1}, \tag{3.123}$$

and it follows that

$$C_4 = 0 \quad \text{for} \quad s_R < 0, \qquad \text{or} \qquad C_3 = 0 \quad \text{for} \quad s_R > 0. \tag{3.124}$$

In addition, C_2 has to be set to zero because of the energy criterion (3.88) which demands a decay faster than x^{-1}. In the limit of $x \to 0$, we find for the expression (3.122)

$$f'(x) \sim \frac{C_2}{x} + C_3 \frac{s\mathrm{Re}^2}{2} x + C_4 \frac{2s\mathrm{Re}}{\Gamma(1+s)} \frac{1}{x}. \tag{3.125}$$

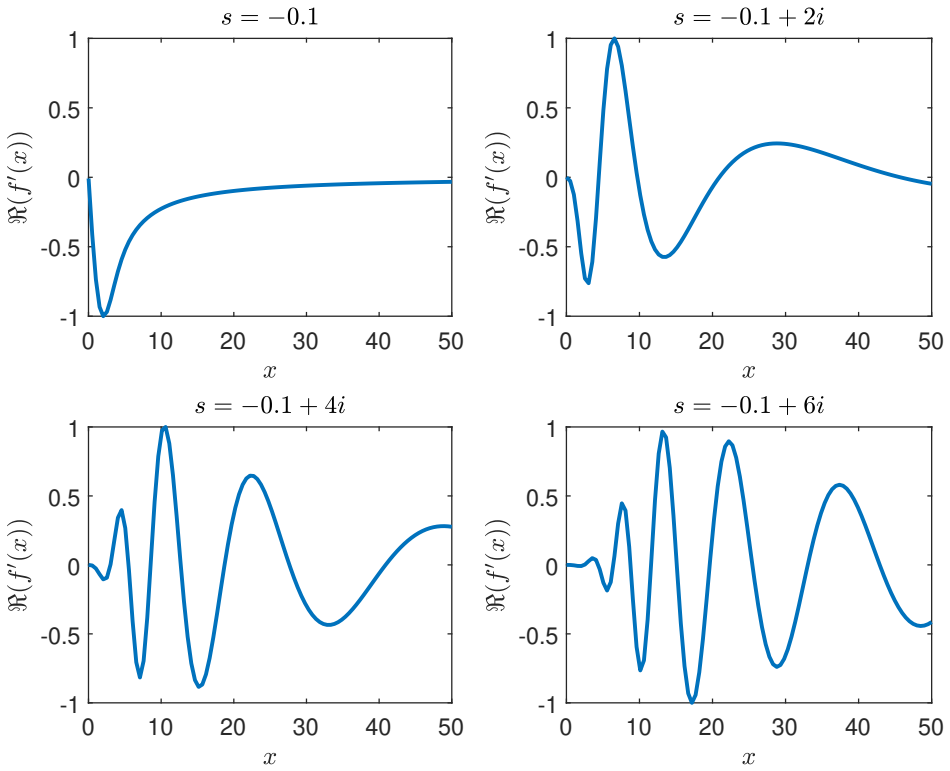

Figure 3.6.: Algebraic mode, viscous flow, $m = 0$: real part $f'(x)$ from (3.126). The eigenvalue is $s_R = -0.1$ and different values of s_I, scaled to unity.

In general, the condition (3.125) could be satisfied for a linear combination of C_2 and C_4, so that the singular term x^{-1} annihilates. However, the constant C_2 has to be zero to satisfy the energy criterion (3.88) as can be seen from (3.123). The only non-trivial solution is the contribution due to the term with constant C_3. The corresponding modes are given by

$$f'(x) = C_3 \frac{2s\mathrm{Re}}{x} e^{-\frac{z}{2}} \mathrm{M}\left(-s, \frac{1}{2}, \frac{\mathrm{Re}}{4}x^2\right), \quad s_R \in]-\infty, 0[\setminus \{-1, -2, ...\}, \tag{3.126}$$

which are stable for all s_I. Figure 3.6 shows the real part of the eigenfunction (3.126) for different choices of stable eigenvalues s. The stability limit is $s_R = 0$. The eigenfunctions decay faster as $x \to \infty$ for smaller s_R. For the inviscid flow, only trivial solutions for the vorticity can be found due to the presence of a singularity at $x \to 0$. The stability analysis using algebraic modes confirms the results of the normal mode theory and shows that only stable modes exist.

Vorticity evolution for viscous flows

The vorticity for this two-dimensional flow is given by (3.89). Using the algebraic mode ansatz (3.69) the vorticity for viscous flows can be obtained by solving

$$\eta = -t^{s-1} e^{im(-At+\varphi)} \mathcal{L}f(x). \tag{3.127}$$

Solving the viscous equation (3.72) for $\mathcal{L}f$ gives

$$\mathcal{L}f(x) = C_1 \frac{e^{-z/2}}{x} \mathrm{M}(\kappa, \mu; z) + C_2 \frac{e^{-z/2}}{x} \mathrm{W}(\kappa, \mu; z), \tag{3.128}$$

with the definition for z, κ, and μ from (3.108). The limit of (3.128) for $x \to 0$ reads

$$\eta \sim \tilde{C}_1 x^{-2s+2} + \tilde{C}_2 x^{2s}. \tag{3.129}$$

Note that constants from the asymptotic limit are taken into $\tilde{C}_j$. It is shown in the analysis of the velocity eigenfunctions that solutions only exist for $s_R < 0$. As a consequence $C_2 = 0$ is chosen to eliminate the singularity at $x = 0$. The limit $x \to \infty$ yields

$$\eta \sim \hat{C}_1 x^{-2+2s}, \tag{3.130}$$

where $\hat{C}_1$ contains coefficients from the asymptotic limit. With the condition $s_R < 0$ in (3.130), the vorticity has a sufficiently fast decay with x^{-2} for large x. The temporal vorticity evolution of (3.128) is shown in Figure 3.7. For a wavenumber $m = 2$, there are two pairs of low and high vorticity that evolve in time. The temporal evolution has an algebraic decay rate. Furthermore, the figure illustrates that the spiral structures are diffusive and its maximum amplitude decays. Note that the solid body rotation in the general velocity profile $V(r) = 1/r + Ar$ (cf. general solution (3.65)) is suppressed by setting $A = 0$. Otherwise, a rotation would be superposed on these structures.

3.5. Summary and discussion

Classical linear stability theory uses a normal mode decomposition, which gives the famous Orr-Sommerfeld equation. Kelvin (1887) showed that for linear shear, there are also solutions with time-dependent wave number (Kelvin modes). Both the normal and algebraic modes can be systematized by a Lie symmetry analysis. Further, it is shown that new ansatz functions can be derived for linear shear flows by using additional symmetries.
For rotational shear flows, it is shown that an algebraic mode ansatz exists. This ansatz allows finding new modes with an algebraic decay. Only stable solutions are found, which is in line with the normal mode result.
Still, the relation between the GH modes and the Lie symmetries is not elucidated. The GH modes are based on the solution of the Hiemenz flow (Hall et al., 1984). The Hiemenz flow has a more complicated group-theoretical explanation. The solution of the (unsteady) stagnation point flow can be explained by partially invariant solutions (Kuznetsov and Pukhnachev, 2009; Pukhnachev, 2021). For details, the reader is referred to Olver (1992) and Ondich (1995) for an introduction. Alternatively, the ansatz can be explained as a nonlinear separation of variables. It is shown that the Hiemenz flow solution can be systematically obtained from the Navier-Stokes equation (Polyanin, 2001; Polyanin and Zhurov, 2022).

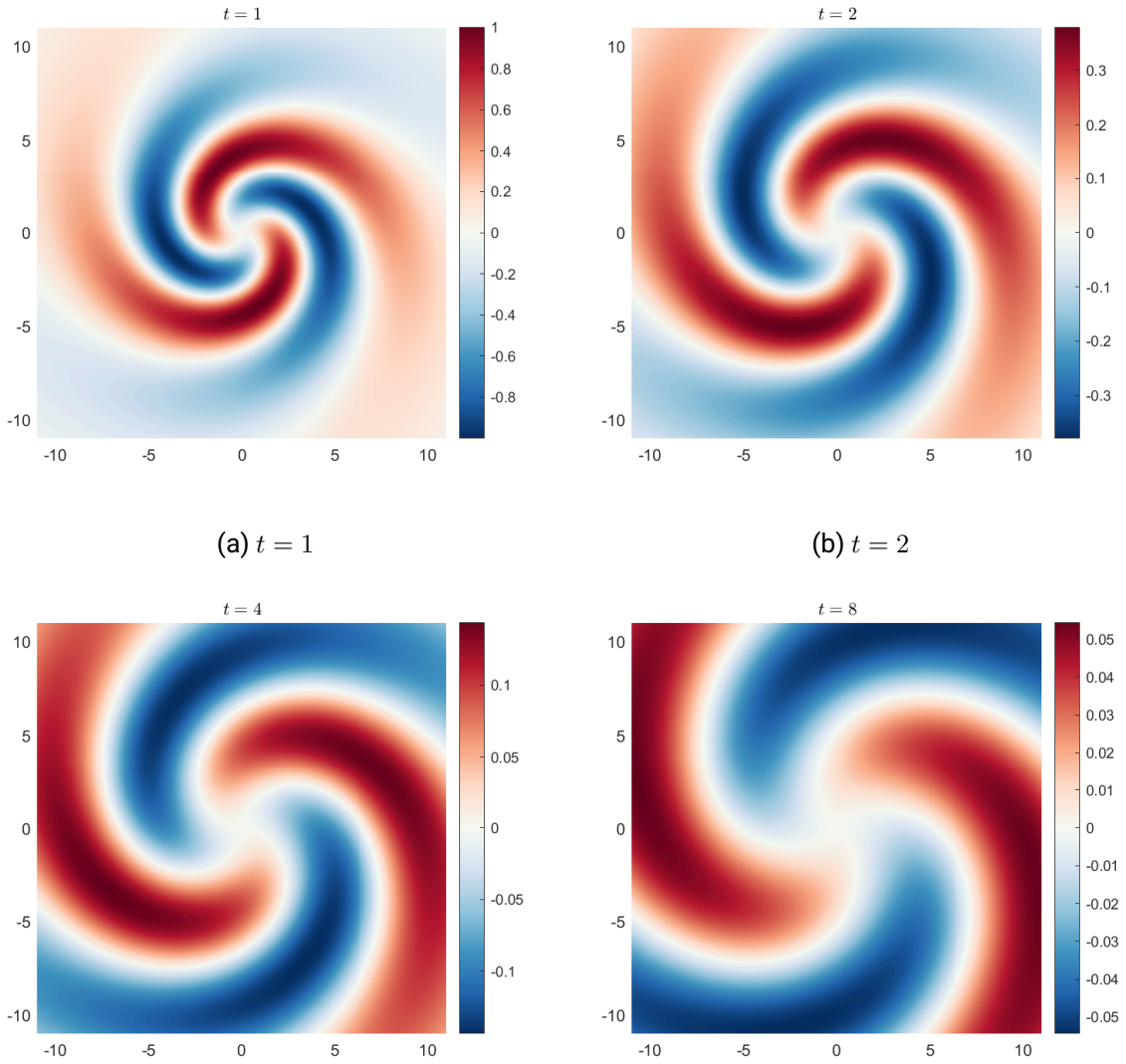

(a) $t = 1$

(b) $t = 2$

(c) $t = 4$

(d) $t = 8$

Figure 3.7.: Vorticity evolution for algebraic mode, viscous ($m = 2$, $\mathrm{Re} = 1$, $s = -0.2 + 2i$) for four different time steps $t = [1, 2, 4, 8]$ in physical space (r, φ).

4. A new nonlinear eigenvalue problem in stability analysis

Contributions:
The formulation of a nonlinear eigenvalue problem (NEVP) is based on an idea by M. Oberlack and was raised in a proposal for the German Research Foundation (Deutsche Forschungsgemeinschaft, DFG, see Oberlack (2018)). The derivations were done by M. Oberlack and A. Yalcin. The derivation of the NEVP (chapter 4.1), the formulation of the Rayleigh quotient (chapter 4.2), and the derivation for wall-bounded flows (chapter 4.5) are based on private communications, cf. Yalcin (2018).

Motivation Recently, a novel idea for an eigenvalue problem in stability theory has been proposed (Oberlack, 2018; Oberlack, 2020). This approach also uses the Lie symmetries of the underlying equations but goes beyond the classical modal approach (see Chapter 3 for an overview). Based on the Lie symmetries of the Euler equations an invariant solution for the following velocity decomposition

$$\boldsymbol{u} = \overline{\boldsymbol{u}} + \boldsymbol{u}' = \boldsymbol{e}_x A y + e^{\lambda A t}\tilde{\boldsymbol{u}}'(\tilde{\boldsymbol{x}}), \qquad \tilde{\boldsymbol{x}} = \boldsymbol{x} e^{-\lambda A t} \tag{4.1}$$

for an unbounded linear shear flow. Here, A is the constant shear rate and λ is a parameter arising from the symmetries. The inverse of the shear rate A^{-1} is called the shear time scale (Sagaut and Cambon, 2018). The fluctuation velocities scale as

$$\boldsymbol{u}' = e^{\lambda A t}\tilde{\boldsymbol{u}}'. \tag{4.2}$$

In general, the turbulent kinetic energy is defined as

$$k(t) = \frac{1}{2}\overline{u_i' u_i'}, \tag{4.3}$$

where u_i' are the turbulent fluctuations and the overbar denotes a Reynolds average (which is in general an ensemble average, cf. Pope (2000) and Sagaut and Cambon (2018)). As a consequence, the scaling in (4.2) implies a growth of the kinetic energy of the fluctuations $k(t)$ as

$$k(t) \sim e^{2\lambda A t}. \tag{4.4}$$

The velocity decomposition (4.1) can be interpreted as base flow $\overline{u}$ and perturbations $\boldsymbol{u}'$. Alternatively, in the view of turbulence theory, (4.1) corresponds to a Reynolds decomposition in mean flow and fluctuations (see e.g. Pope (2000) for more details).
Interestingly, a similar exponential scaling as (4.4) is observed in turbulence research. Experiments (e.g. (Tavoularis and Corrsin, 1981) and direct numerical simulation (DNS) (e.g.

Brethouwer (2005) and Isaza and Collins (2009)) of linear shear flows also show an exponential growth of the turbulent kinetic energy in an asymptotic regime $At \geq 25$, where At is a dimensionless quantity. The reader is referred to Briard et al. (2016) and Sagaut and Cambon (2018) for an overview. It should be noted that the community usually uses the letter γ or σ to describe the exponential growth, i.e. $\exp(\gamma At)$ (Sagaut and Cambon, 2018). It is found that the value is nearly constant for flows of high Reynolds numbers. Typical values are $\sigma \approx 0.07 - 0.33$ (Briard et al., 2016). This indicates, that λ acts as a kind of eigenvalue for linear shear flows.

We show that a nonlinear eigenvalue problem (NEVP) for the eigenvalue λ can be derived based on the symmetries of the Euler equations. In other words, the NEVP establishes a theory to calculate the exponent λ of the growth of kinetic energy (4.4) and may help to better understand the flow dynamics. In particular, a detailed derivation of the result from (4.1) is shown. Moreover, this theory can be applied to flows having a constant velocity gradient, in particular flows under strain or with rotation. The extension to these cases is also part of the present chapter.

4.1. Flows with constant velocity gradient

In the introductory example, the velocity decomposition (4.1) for a linear shear flow is shown. However, it is possible to formulate an eigenvalue problem for other base flows that have a constant velocity gradient. A general form for the velocity decomposition reads

$$u_i = \overline{u}_i + u_i' = A_{ij} x_j + u_i', \quad p = \overline{p} + p', \tag{4.5}$$

where A_{ij} is the velocity-gradient tensor defined as

$$A_{ij} = \frac{\partial \overline{u}_i}{\partial x_j}. \tag{4.6}$$

The tensor A_{ij} can be split into a symmetric part S_{ij} and an antisymmetric part Ω_{ij}

$$A_{ij} = S_{ij} + \Omega_{ij}, \tag{4.7}$$

where $S_{ij} = (A_{ij} + A_{ji})/2$ and $\Omega_{ij} = (A_{ij} - A_{ji})/2$. The tensor A_{ij} has nine entries for the three-dimensional case. Due to tensor invariants, A_{ij} only has five independent entries, which are denoted by $(A_{11}, A_{12}, A_{13}, A_{22}, A_{23})$ in the following (Meneveau, 2011). The general tensor can thus be written as (Mishra and Girimaji, 2015)

$$A_{ij} = \begin{pmatrix} A_{11} & A_{12} & A_{13} \\ -A_{12} & A_{22} & A_{23} \\ -A_{13} & -A_{23} & -A_{11} - A_{22} \end{pmatrix}. \tag{4.8}$$

The continuity equation is satisfied by $A_{ii} = 0$, cf. tensor invariants in (4.8). There are some canonical cases concerning the choice of A_{ij}. These include the case of (pure) linear shear, (pure) strain, and (pure) rotation (Oberlack, 1994; Sagaut and Cambon, 2018). We depict the three different types in Figure 4.1.

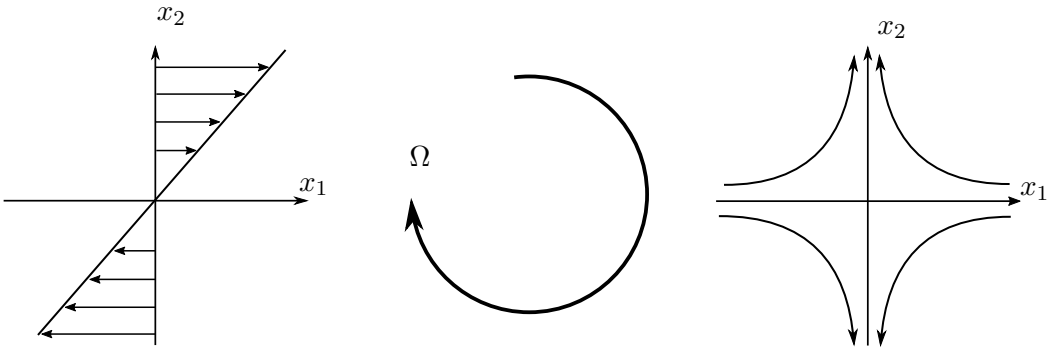

Figure 4.1.: Three different types of base flows with constant velocity gradient: linear shear (left), pure rotation (center), and pure strain (right), based on a representation by Takagi and Strickler (2020)

4.1.1. Symmetry analysis of the velocity decomposition

The following derivation (in particular (4.10) to (4.34)) is based on Oberlack (2018) and Yalcin (2018). In a first step, we consider the invariance of the velocity decomposition (4.5) under Lie symmetries. The starting point are the Euler equations given in (2.5) and restated here in a index notation

$$\frac{\partial u_i}{\partial t} + u_j \frac{\partial u_i}{\partial x_j} = -\frac{\partial p}{\partial x_i}. \tag{4.9}$$

The corresponding Lie symmetries for the Euler equation are presented in (2.9)-(2.15). We use the scaling symmetries in space (2.10) and time (2.11) given by

$$\tilde{t} = e^{a_3} t, \quad \tilde{x}_i = e^{a_2} x_i, \quad \tilde{u}_i = e^{a_2 - a_3} u_i, \quad \tilde{p} = e^{2a_2 - 2a_3} p. \tag{4.10}$$

We start with the velocity decomposition for linear shear (constant shear rate A), i.e. $\overline{\boldsymbol{u}}^T = (Ax_2, 0, 0)^T$. Therefore (4.5) reads

$$u_i = \overline{u}_i + u_i' = Ax_2\delta_{i1} + u_i'. \tag{4.11}$$

Using the symmetries (4.10) in (4.11) yields

$$\tilde{u}_i e^{-a_2 + a_3} = A\tilde{x}_2 e^{-a_2}\delta_{i1} + \tilde{u}_i' e^{-a_2 + a_3}. \tag{4.12}$$

Multiplying with $\exp(a_2 - a_3)$ simplifies the expression to

$$\tilde{u}_i = A\tilde{x}_2 e^{-a_3}\delta_{i1} + \tilde{u}_i'. \tag{4.13}$$

In order that (4.13) is invariant to (4.11) with respect to the symmetry groups a_2 and a_3, it follows directly that $a_3 = 0$, i.e. the linear shear term is symmetry-breaking for the scaling in time. The symmetries from (4.10) with $a_3 = 0$ are therefore simply

$$\tilde{t} = t, \quad \tilde{x}_i = e^{a_2} x_i, \quad \tilde{u}_i = e^{a_2} u_i, \quad \tilde{p} = e^{2a_2} p. \tag{4.14}$$

It is also possible to show that the velocity decomposition for the more general base flow

$$u_i = A_{ij} x_j + u_i' \tag{4.15}$$

is also invariant under the symmetry groups. Using the definition of A_{ij} from (4.6) explicitly in (4.15) and applying the scaling symmetry in space from (4.14) gives

$$\tilde{u}_i e^{-a_2} = e^{a_2} \frac{\partial \tilde{\overline{u}}_i e^{-a_2}}{\partial \tilde{x}_j} \tilde{x}_j e^{-a_2} + e^{-a_2} \tilde{u}'_i, \tag{4.16}$$

which simplifies to

$$\tilde{u}_i = \frac{\partial \tilde{\overline{u}}_i}{\partial \tilde{x}_j} \tilde{x}_j + \tilde{u}'_i. \tag{4.17}$$

Therefore the velocity decomposition (4.15) for a general base flow is also invariant under the scaling symmetry in space (4.14).

4.1.2. Construction of an invariant solution

The aim is to construct an invariant solution. Therefore we use the symmetry for scaling in space (2.10) with group parameter a_2 and the translation in time (2.9) with group parameter a_1. The translation in time does not affect the invariance of the velocity decomposition shown in (4.16). The two-parameter symmetry group reads

$$\tilde{t} = t + a_1, \quad \tilde{x}_i = e^{a_2} x_i, \quad \tilde{u}_i = e^{a_2} u_i, \quad \tilde{p} = e^{2a_2} p. \tag{4.18}$$

The corresponding infinitesimal operator is given by

$$X = a_2 x_i \frac{\partial}{\partial x_i} + a_1 \frac{\partial}{\partial t} + a_2 u_i \frac{\partial}{\partial u_i} + 2a_2 p \frac{\partial}{\partial p}. \tag{4.19}$$

Using the invariant surface condition

$$XF|_{F=0} = 0, \tag{4.20}$$

and applying the *method of characteristics* (see e.g. Schneider (1978) for an introduction to this method) we obtain the following system of equations

$$d\tau = \frac{dx_i}{a_2 x_i} = \frac{dt}{a_1} = \frac{du_i}{a_2 u_i} = \frac{dp}{2a_2 p}. \tag{4.21}$$

We collect the independent variables (x_i, t) which gives

$$\frac{dx_i}{dt} = \frac{a_2}{a_1} x_i. \tag{4.22}$$

The expression (4.22) can be integrated and the constant of integration is the invariant $\tilde{x}_i$. Analogously, the expressions for u_i and p are integrated, so that the set of invariant variables reads

$$x_i = \tilde{x}_i e^{\frac{a_2}{a_1} t}, \qquad u_i(\boldsymbol{x}) = \tilde{u}_i(\tilde{\boldsymbol{x}})\, e^{\frac{a_2}{a_1} t}, \qquad p(\boldsymbol{x}) = \tilde{p}(\tilde{\boldsymbol{x}})\, e^{\frac{2a_2}{a_1} t}. \tag{4.23}$$

For sake of simplicity, we introduce the variable λ as a ratio of the two group parameters a_1 and a_2 by

$$\lambda := \frac{a_2}{a_1}. \tag{4.24}$$

By using the definition for λ from (4.24), the expression (4.23) can be rewritten as

$$x_i = \tilde{x}_i e^{\lambda t}, \quad u_i = \tilde{u}_i(\tilde{\boldsymbol{x}}) e^{\lambda t}, \quad p = \tilde{p}(\tilde{\boldsymbol{x}}) e^{2\lambda t}. \tag{4.25}$$

4.1.3. Derivation of an eigenvalue problem

In the following, the derivation of an eigenvalue problem for λ and the eigenfunctions (fluctuations) $\tilde{u}_i'$ and $\tilde{p}'$ around a base flow profile $\overline{u}_i = A_{ij}x_j$ is presented. The velocity decomposition (4.5) based on the result (4.25) reads

$$u_i = A_{ij}x_j + \tilde{u}_i'(\tilde{\boldsymbol{x}})e^{\lambda t}. \tag{4.26}$$

The decomposition of the pressure (4.5) from (4.25) is

$$p = \overline{p} + \tilde{p}'(\tilde{\boldsymbol{x}})e^{2\lambda t}, \tag{4.27}$$

Note that the mean quantities $(\overline{u}_i, \overline{p})$ are solutions of the Euler equation (4.9). By inserting these quantities into the Euler equation (4.9), it follows that the mean pressure gradient

$$\frac{\partial \overline{p}}{\partial x_i} = -\overline{u}_j \frac{\partial \overline{u}_i}{\partial x_j} \tag{4.28}$$

$$= -A_{jl}x_l \frac{\partial}{\partial x_j}\left(A_{ik}x_k\right) \tag{4.29}$$

$$= -A_{jl}x_l A_{ij} \tag{4.30}$$

is a function of the mean velocity-gradient tensor A_{ij} and the spatial variables x_j. By integrating (4.28), the mean pressure $\overline{p}$ reads

$$\overline{p} = -\int \overline{u}_j \frac{\partial \overline{u}_i}{\partial x_j} dx_i + C, \tag{4.31}$$

where C is a constant of integration. Note that the mean pressure for a linear shear flow $\overline{\boldsymbol{u}}^T = (Ax_2, 0, 0)^T$ is a constant, i.e. $\overline{p} = C$. This can be directly shown by inserting the mean velocity profile into (4.31). However, for flows under strain and rotation the mean pressure depends in general on the velocity-gradient tensor A_{ij} and on the spatial variables x_j. For example, for a planar strain flow with $\overline{\boldsymbol{u}}^T = (-Sx_1, Sx_2, 0)^T$ it can be shown with (4.31) that the mean pressure is

$$\overline{p} = -\frac{1}{2}S^2\left(x_1^2 + x_2^2\right) + C. \tag{4.32}$$

The derivation of the eigenvalue problem is based on the Euler equation (4.9), which needs to be transformed to $\tilde{x}_i$ and $\tilde{t}$, where $\tilde{t} = t$ holds. The chain rule for $\tilde{x}_i = \tilde{x}_i(x_i, t)$ and $\tilde{t} = \tilde{t}(x_i, t)$ gives

$$\frac{\partial}{\partial x_i} = \frac{\partial}{\partial \tilde{x}_i}\frac{\partial \tilde{x}_i}{\partial x_i} + \frac{\partial}{\partial \tilde{t}}\frac{\partial \tilde{t}}{\partial x_i} = \exp(-\lambda t)\frac{\partial}{\partial \tilde{x}_i}, \tag{4.33}$$

$$\frac{\partial}{\partial t} = \frac{\partial}{\partial \tilde{x}_i}\frac{\partial \tilde{x}_i}{\partial t} + \frac{\partial}{\partial \tilde{t}}\frac{\partial \tilde{t}}{\partial t} = -\lambda \tilde{x}_i \frac{\partial}{\partial \tilde{x}_i} + \frac{\partial}{\partial \tilde{t}}. \tag{4.34}$$

Inserting the decomposition for the velocity (4.26) and the pressure (4.27) into the Euler equation (4.9) gives

$$\frac{\partial}{\partial t}\left(A_{ij}x_j + \tilde{u}_i'(\tilde{\boldsymbol{x}})e^{\lambda t}\right) + \left(A_{jl}x_l + \tilde{u}_j'(\tilde{\boldsymbol{x}})e^{\lambda t}\right)\frac{\partial}{\partial x_j}\left(A_{ik}x_k + \tilde{u}_i'(\tilde{\boldsymbol{x}})e^{\lambda t}\right) = -\frac{\partial}{\partial x_i}\left(\overline{p} + \tilde{p}'e^{2\lambda t}\right). \tag{4.35}$$

Subtracting the Euler equation (4.9) for the mean quantities $(\overline{u}_i, \overline{p})$ from (4.35) gives an equation for the fluctuations $(\tilde{u}_i', \tilde{p}')$ which reads

$$\frac{\partial}{\partial t}\left(\tilde{u}_i'(\tilde{\boldsymbol{x}})e^{\lambda t}\right) + A_{jl}x_l\frac{\partial}{\partial x_j}\tilde{u}_i'(\tilde{\boldsymbol{x}})e^{\lambda t} + \tilde{u}_j'(\tilde{\boldsymbol{x}})e^{\lambda t}\frac{\partial}{\partial x_j}\left(A_{ik}x_k\right) + \tilde{u}_j'(\tilde{\boldsymbol{x}})\frac{\partial}{\partial x_j}\tilde{u}_i'(\tilde{\boldsymbol{x}})e^{2\lambda t} = -\frac{\partial \tilde{p}' e^{2\lambda t}}{\partial x_i}. \tag{4.36}$$

Applying the transform of the variables (4.25), as well as the transform of the derivatives from (4.33)-(4.34), we can rewrite (4.36) as

$$\begin{aligned}&\left(-\lambda\tilde{x}_k\frac{\partial}{\partial\tilde{x}_k} + \frac{\partial}{\partial\tilde{t}}\right)\left(\tilde{u}_i'(\tilde{\boldsymbol{x}})e^{\lambda t}\right)\\ &+ A_{jl}\tilde{x}_l\frac{\partial\tilde{u}_i'(\tilde{\boldsymbol{x}})}{\partial\tilde{x}_j}e^{\lambda t} + \tilde{u}_j'(\tilde{\boldsymbol{x}})A_{ij}e^{\lambda t} + \tilde{u}_j'(\tilde{\boldsymbol{x}})\frac{\partial\tilde{u}_i'(\tilde{\boldsymbol{x}})}{\partial\tilde{x}_j}e^{\lambda t} = -\frac{\partial\tilde{p}'}{\partial\tilde{x}_i}e^{\lambda t}.\end{aligned} \tag{4.37}$$

Differentiating, and multiplying by $\exp(-\lambda t)$ gives

$$-\lambda\tilde{x}_k\frac{\partial}{\partial\tilde{x}_k}\tilde{u}_i'(\tilde{\boldsymbol{x}}) + \lambda\tilde{u}_i'(\tilde{\boldsymbol{x}}) + A_{jl}\tilde{x}_l\frac{\partial\tilde{u}_i'(\tilde{\boldsymbol{x}})}{\partial\tilde{x}_j} + \tilde{u}_j'(\tilde{\boldsymbol{x}})A_{ij} + \tilde{u}_j'(\tilde{\boldsymbol{x}})\frac{\partial\tilde{u}_i'(\tilde{\boldsymbol{x}})}{\partial\tilde{x}_j} = -\frac{\partial\tilde{p}'}{\partial\tilde{x}_i}. \tag{4.38}$$

Note that we have also used that $\tilde{u}_i'$ and $\tilde{p}'$ are not a function of $\tilde{t}$. In addition, from the continuity equation follows that

$$\frac{\partial\tilde{u}_i'}{\partial\tilde{x}_i} = 0. \tag{4.39}$$

The set of equations (4.38) and (4.39) already constitutes an eigenvalue problem for λ if supplied by suitable boundary conditions. However, we have not discussed the role of $\tilde{u}_i'$ and $\tilde{p}'$ for this eigenvalue problem. This is done in the following for different base flows.

4.2. Linear shear

In Chapter 3, some interesting properties of the stability of linear shear flows are discussed, including the Kelvin mode solution and new alternative modes. The velocity-gradient tensor for a base flow $(\overline{u}, 0, 0) = (Ax_2, 0, 0)$ reads

$$A_{ij} = \begin{pmatrix}0 & A & 0\\ 0 & 0 & 0\\ 0 & 0 & 0\end{pmatrix}. \tag{4.40}$$

The transformed velocities from (4.5) are given by

$$\tilde{u}_1 = A\tilde{x}_2 + \tilde{u}_1', \qquad \tilde{u}_2 = \tilde{u}_2', \qquad \tilde{u}_3 = \tilde{u}_3', \qquad \tilde{p} = \tilde{p}', \tag{4.41}$$

where the prime quantities denote the fluctuations. The expression (4.41) can be written in a compact way using

$$\tilde{u}_i = A\tilde{x}_2\delta_{1i} + \tilde{u}_i', \tag{4.42}$$

where the unity tensor is defined as

$$\delta_{ij} = \begin{cases} 0 & i \neq j \\ 1 & i = j. \end{cases} \tag{4.43}$$

Inserting the base flow given by (4.40) into the transformed Euler equations (4.38) gives

$$\lambda \tilde{u}_i' - \lambda \tilde{x}_k \frac{\partial \tilde{u}_i'}{\partial \tilde{x}_k} + \tilde{u}_j' \frac{\partial \tilde{u}_i'}{\partial \tilde{x}_j} + \frac{\partial \tilde{p}'}{\partial \tilde{x}_i} + A\tilde{u}_2' \delta_{1i} + A\tilde{x}_2 \frac{\partial \tilde{u}_i'}{\partial \tilde{x}_1} = 0. \tag{4.44}$$

For the continuity equation from (4.39) we find with (4.42) that

$$\frac{\partial \tilde{u}_i'}{\partial \tilde{x}_i} = 0. \tag{4.45}$$

The BC for the system (4.44) and (4.45) are given by vanishing perturbation in the far-field, i.e.

$$\tilde{u}_i' \to 0, \quad \tilde{p}' \to 0 \qquad \text{for} \quad |\tilde{x}_j| \to \infty \qquad \text{and } i, j \in \{1, 2, 3\} \tag{4.46}$$

Properties of the nonlinear eigenvalue problem

The problem (4.44), (4.45) with BC (4.46) is a nonlinear eigenvalue problem for λ. The nonlinearity refers to the eigenfunction $\tilde{u}_i$, which is nonlinear, however, the eigenvalue appears linearly. It is possible to gain a first insight into the problem. We start with the physical interpretation of the velocity, which can be interpreted from two perspectives. First, the velocity decomposition (4.42) can be seen as a stability problem (base flow with perturbations), or second, as a turbulent flow (Reynolds decomposition of the flow). We present some consequences and physical interpretations of the equations, which are based on a turbulence perspective. As shown in (4.4), the turbulent kinetic energy defined in (4.3) scales as $k \sim \exp(2\lambda A t)$. Such a scaling is observed in experiments for homogeneous turbulence (Pope, 2000). However, the precise value of the exponential growth rate has not been determined precisely (Isaza and Collins, 2009). The new theory might help use first principles to find a value.

Further information on λ can be gained. Multiplying (4.44) with $\tilde{u}_i'$ gives

$$\lambda \tilde{u}_i'^2 - \lambda \tilde{x}_k \frac{\partial \tilde{u}_i'}{\partial \tilde{x}_k} \tilde{u}_i' + \tilde{u}_j' \frac{\partial \tilde{u}_i'}{\partial \tilde{x}_j} \tilde{u}_i' + \frac{\partial \tilde{p}'}{\partial \tilde{x}_i} \tilde{u}_i' + A\tilde{u}_2' \delta_{1i} \tilde{u}_i' + A\tilde{x}_2 \frac{\partial \tilde{u}_i'}{\partial \tilde{x}_1} \tilde{u}_i' = 0. \tag{4.47}$$

The first two terms in (4.47) can be rewritten as

$$\lambda \tilde{u}_i'^2 - \lambda \tilde{x}_k \frac{\partial \tilde{u}_i'}{\partial \tilde{x}_k} \tilde{u}_i' = \lambda \left(\tilde{u}_i'^2 - \frac{1}{2} \tilde{x}_k \frac{\partial \tilde{u}_i^2}{\partial \tilde{x}_k} \right). \tag{4.48}$$

It is easy to verify that

$$\frac{\partial \left(\tilde{x}_k \tilde{u}_i^2 \right)}{\partial \tilde{x}_k} = 3\tilde{u}_i^2 + \tilde{x}_k \frac{\partial \tilde{u}_i^2}{\partial \tilde{x}_k}. \tag{4.49}$$

A direct consequence from (4.49) is that

$$\frac{1}{2} \tilde{x}_k \frac{\partial \tilde{u}_i'}{\partial \tilde{x}_k} = \frac{1}{2} \left(\frac{\partial x_k \tilde{u}_i'}{\partial \tilde{x}_k} - 3\tilde{u}_i' \right). \tag{4.50}$$

Using the finding (4.50) for (4.48) gives

$$\lambda\tilde{u}_i'^2 - \lambda\tilde{x}_k\frac{\partial\tilde{u}_i'}{\partial\tilde{x}_k}\tilde{u}_i' = \frac{5}{2}\tilde{u}_i'^2 - \frac{1}{2}\frac{\partial\tilde{x}_k\tilde{u}_i'^2}{\partial\tilde{x}_k}. \tag{4.51}$$

The third and fourth term in (4.47) can be rewritten using the continuity equation as

$$\tilde{u}_j'\frac{\partial\tilde{u}_i'}{\partial\tilde{x}_j}\tilde{u}_i' + \frac{\partial\tilde{p}'}{\partial\tilde{x}_i}\tilde{u}_i' = \frac{1}{2}\frac{\partial\tilde{u}_i'^2\tilde{u}_j'}{\partial\tilde{x}_j} + \frac{1}{2}\frac{\partial\tilde{p}'\tilde{u}_i'}{\partial\tilde{x}_i}. \tag{4.52}$$

The fifth and sixth term in (4.47) (both terms scale with A) can be rewritten as

$$A\tilde{u}_2'\delta_{1i}\tilde{u}_i' + A\tilde{x}_2\frac{\partial\tilde{u}_i'}{\partial\tilde{x}_1}\tilde{u}_i' = A\tilde{u}_1'\tilde{u}_2' + \frac{1}{2}A\frac{\tilde{x}_2\tilde{u}_i'^2}{\partial\tilde{x}_1}. \tag{4.53}$$

Using the results from (4.51), (4.52), and (4.53) in (4.47) and integrating over a volume Ω gives

$$\int_\Omega \frac{5}{2}\lambda\tilde{u}_i'^2 - \frac{1}{2}\lambda\frac{\partial\tilde{x}_k\tilde{u}_i'^2}{\partial\tilde{x}_k} + \frac{1}{2}\frac{\partial\tilde{u}_i'^2\tilde{u}_j'}{\partial\tilde{x}_j} + \frac{1}{2}\frac{\partial\tilde{p}'\tilde{u}_i'}{\partial\tilde{x}_i} + A\tilde{u}_1'\tilde{u}_2' + \frac{1}{2}A\frac{\tilde{x}_2\tilde{u}_i'^2}{\partial\tilde{x}_1}dV = 0. \tag{4.54}$$

The divergence theorem (Gauss's theorem) can be used to rewrite the volume integrals containing expressions under a divergence as a surface integral. As the problem is defined on an unbounded domain $\Omega = \mathbb{R}^3$ the surface terms disappear due to vanishing fluctuations in the far field by (4.46). The remaining terms are given by

$$\lambda\int_\Omega \frac{5}{2}\tilde{u}_i'^2 dV = -\int_\Omega A\tilde{u}_1'\tilde{u}_2' dV. \tag{4.55}$$

This gives the following nonlocal relation for λ

$$\lambda = -\frac{2}{5}A\frac{\int_\Omega \tilde{u}_1'\tilde{u}_2' d\tilde{V}}{\int_\Omega \tilde{u}_j'\tilde{u}_j' d\tilde{V}}, \tag{4.56}$$

with $\Omega = \mathbb{R}^3$ (Oberlack, 2018). The eigenvalue λ scales linearly with the shear rate A. The expression (4.56) is related to a variational formulation or the Rayleigh-Ritz quotient in mechanics. The reader is referred to Jost and Li-Jost (1998) for an introduction. Note that in turbulence research, $(\overline{u_1'u_2'})/(\overline{u_i'u_i'})$ describes the ratio of production of kinetic energy (which is proportional $\overline{u_1'u_2'}$) to the kinetic energy (4.3) (the overbar denotes the Reynolds average). In experiments on turbulent shear flows, this quantity is found to be constant (Sagaut and Cambon, 2018). Interpreting the Reynolds average as a spatial average corresponds to a constant λ according to (4.56).
Still, the shape and dynamics of the eigenfunctions (modes) are an open question. To further study the equations (4.44), (4.45) with BC (4.46), a velocity-vorticity formulation is derived, similar to the linear stability problem with a normal mode ansatz, as shown in Chapter 3.1.1.

Velocity equation

The starting point is the system of equations given by (4.44) and (4.45). We perform two main steps to eliminate the pressure for the momentum equations.

- The divergence of (4.44) gives a Poisson equation for the pressure (the continuity equation (4.45) can be used to simplify the expression afterward).
- The Poisson equation is inserted in the expression $\Delta(4.44)_2$ (subscript 2 denotes the second component) to find a pressure-free equation for the normal velocity $\tilde{u}_2'$.

For sake of readability, we introduce the terms $\mathcal{M}_j$ and $\mathcal{S}_j$. The momentum equation (4.44) can be expressed as

$$\mathcal{M}_j + \mathcal{S}_j = 0. \tag{4.57}$$

Here $\mathcal{M}_j$ denotes the common terms for the j-th component. The common terms arise purely due to the decomposition of the flow equation in mean and fluctuation quantities. The calligraphic letter $\mathcal{S}_j$ describes the special terms due to the base flow (e.g. linear shear). The term should not be confused with the symmetric part of the strain tensor S or S_{ij}. The common terms read

$$\mathcal{M}_i = \lambda\tilde{u}_i' - \lambda\tilde{x}_k\frac{\partial\tilde{u}_i'}{\partial\tilde{x}_k} + \tilde{u}_k'\frac{\partial\tilde{u}_i'}{\partial\tilde{x}_k} + \frac{\partial\tilde{p}'}{\partial\tilde{x}_i}. \tag{4.58}$$

And the terms $\mathcal{S}$ for linear shear are

$$\mathcal{S}_1 = A\tilde{u}_2' + A\tilde{x}_2\frac{\partial\tilde{u}_1'}{\partial\tilde{x}_1}, \qquad \mathcal{S}_2 = A\tilde{x}_2\frac{\partial\tilde{u}_2'}{\partial\tilde{x}_1}, \qquad \mathcal{S}_3 = A\tilde{x}_2\frac{\partial\tilde{u}_3'}{\partial\tilde{x}_1}. \tag{4.59}$$

This notation facilitates the derivation of the velocity-vorticity formulation. To take the divergence of (4.44) we can use the following result (for details we refer to Appendix (B.1))

$$\nabla\cdot\mathcal{M} = \frac{\partial}{\partial\tilde{x}_i}\left(\tilde{u}_k'\frac{\partial\tilde{u}_i'}{\partial\tilde{x}_k}\right) + \frac{\partial^2\tilde{p}'}{\partial\tilde{x}_i\partial\tilde{x}_i}. \tag{4.60}$$

After some calculations using the incompressibility condition (4.45), we find

$$\nabla\cdot\mathcal{S} = 2A\frac{\partial\tilde{u}_2'}{\partial\tilde{x}_1}. \tag{4.61}$$

Rearranging the terms from (4.60) and (4.61) in $\nabla\cdot(\mathcal{M}+\mathcal{S}) = 0$ gives the Poisson equation for the pressure

$$\Delta\tilde{p}' = -2A\frac{\partial\tilde{u}_2'}{\partial\tilde{x}_1} - \frac{\partial}{\partial\tilde{x}_i}\left(\tilde{u}_k'\frac{\partial\tilde{u}_i'}{\partial\tilde{x}_k}\right). \tag{4.62}$$

In the next step, we apply the Laplacian (Δ) to the second component of the momentum equation (i.e. the momentum equation for $\tilde{u}_2'$) (4.44), i.e.

$$\Delta\left(\mathcal{M}_2 + \mathcal{S}_2\right) = 0. \tag{4.63}$$

The term $\Delta\mathcal{M}_2$ with $\mathcal{M}_2$ defined in (4.58) reads

$$\Delta\mathcal{M}_2 = \Delta\left(\lambda\tilde{u}_2' - \lambda\tilde{x}_k\frac{\partial\tilde{u}_2'}{\partial\tilde{x}_k} + \tilde{u}_k\frac{\partial\tilde{u}_2'}{\partial\tilde{x}_k} + \frac{\partial\tilde{p}'}{\partial\tilde{x}_2}\right). \tag{4.64}$$

The Laplacian can be applied on the second term on the RHS in (4.64) which gives

$$\Delta\left(\lambda\tilde{x}_k\frac{\partial\tilde{u}_2'}{\partial\tilde{x}_k}\right)=\lambda\tilde{x}_k\frac{\partial\Delta\tilde{u}_2'}{\partial\tilde{x}_k}+2\lambda\Delta\tilde{u}_2', \tag{4.65}$$

and therefore the expression for $\Delta\mathcal{M}_2$ from (4.64) can be rewritten as

$$\Delta\mathcal{M}_2=-\lambda\Delta\tilde{u}_2'-\lambda\tilde{x}_k\frac{\partial\Delta\tilde{u}_2'}{\partial\tilde{x}_k}+\Delta\left(\tilde{u}_k'\frac{\partial\tilde{u}_2'}{\partial\tilde{x}_k}\right)+\frac{\partial}{\partial\tilde{x}_2}\Delta\tilde{p}'. \tag{4.66}$$

Note that the sign in front of the first term $\lambda\Delta\tilde{u}_2'$ in (4.66) changes to a negative sign. The term $\Delta\mathcal{S}_2$ from (4.59) reads

$$\Delta\mathcal{S}_2=A\Delta\left(\tilde{x}_2\frac{\partial\tilde{u}_2'}{\partial\tilde{x}_1}\right) \tag{4.67}$$

$$=A\tilde{x}_2\frac{\partial^3\tilde{u}_2'}{\partial\tilde{x}_1^3}+2A\frac{\partial^2\tilde{u}_2'}{\partial\tilde{x}_2\partial\tilde{x}_1}+\tilde{x}_2A\frac{\partial\tilde{u}_2'}{\partial\tilde{x}_1\partial\tilde{x}_2^2}=0 \tag{4.68}$$

$$=2A\frac{\partial\tilde{u}_2'}{\partial\tilde{x}_2\partial\tilde{x}_1}+A\tilde{x}_2\frac{\partial}{\partial\tilde{x}_1}\Delta\tilde{u}_2'. \tag{4.69}$$

Using the results (4.66) and (4.69) in (4.63) gives

$$-\lambda\Delta\tilde{u}_2'-\lambda\tilde{x}_k\frac{\partial\Delta\tilde{u}_2'}{\partial\tilde{x}_k}+\Delta\left(\tilde{u}_k'\frac{\partial\tilde{u}_2'}{\partial\tilde{x}_k}\right)+\frac{\partial}{\partial\tilde{x}_2}\Delta\tilde{p}'+2A\frac{\partial\tilde{u}_2'}{\partial\tilde{x}_2\partial\tilde{x}_1}+A\tilde{x}_2\frac{\partial}{\partial\tilde{x}_1}\Delta\tilde{u}_2'=0. \tag{4.70}$$

Substituting the pressure from (4.62) in (4.70) gives

$$\begin{aligned}&-\lambda\Delta\tilde{u}_2'-\lambda\tilde{x}_k\frac{\partial\Delta\tilde{u}_2'}{\partial\tilde{x}_k}+\Delta\left(\tilde{u}_k'\frac{\partial\tilde{u}_2'}{\partial\tilde{x}_k}\right)+\frac{\partial}{\partial\tilde{x}_2}\left(-2A\frac{\partial\tilde{u}_2'}{\partial\tilde{x}_1}-\frac{\partial}{\partial\tilde{x}_i}\left(\tilde{u}_k'\frac{\partial\tilde{u}_i'}{\partial\tilde{x}_k}\right)\right)\\&+2A\frac{\partial\tilde{u}_2'}{\partial\tilde{x}_2\partial\tilde{x}_1}+A\tilde{x}_2\frac{\partial}{\partial\tilde{x}_1}\Delta\tilde{u}_2'=0.\end{aligned} \tag{4.71}$$

Obviously, the term $2A(\partial\tilde{u}_2')/(\partial\tilde{x}_2\partial\tilde{x}_1)$ vanishes. The resulting equation for $\Delta\tilde{u}_2'$ from (4.71) reads

$$-\lambda\Delta\tilde{u}_2'-\lambda\tilde{x}_k\frac{\partial\Delta\tilde{u}_2'}{\partial\tilde{x}_k}+A\tilde{x}_2\frac{\partial}{\partial\tilde{x}_1}\Delta\tilde{u}_2'+\mathcal{N}_2=0, \tag{4.72}$$

where the nonlinear terms are given by

$$\mathcal{N}_2=\Delta\left(\tilde{u}_k'\frac{\partial\tilde{u}_2'}{\partial\tilde{x}_k}\right)-\frac{\partial}{\partial\tilde{x}_2}\frac{\partial}{\partial\tilde{x}_i}\left(\tilde{u}_k'\frac{\partial\tilde{u}_i'}{\partial\tilde{x}_k}\right). \tag{4.73}$$

Vorticity equation

An equation for the normal vorticity $\tilde{\eta}_2'$ (in the following simply denoted by η' as defined by (3.8)) can be obtained by

$$\frac{\partial}{\partial\tilde{x}_3}(4.44)_{(1)}-\frac{\partial}{\partial\tilde{x}_1}(4.44)_{(3)}=0. \tag{4.74}$$

Making use of the notation in terms of $\mathcal{M}$ from (4.58) and $\mathcal{S}$ from (4.59), the expression (4.74) can be rewritten as

$$\frac{\partial}{\partial \tilde{x}_3}\left(\mathcal{M}_1 + \mathcal{S}_1\right) - \frac{\partial}{\partial \tilde{x}_1}\left(\mathcal{M}_3 + \mathcal{S}_3\right) = 0. \tag{4.75}$$

For the divergence operator acting on the common terms $\mathcal{M}_1$ and $\mathcal{M}_3$ we find

$$\frac{\partial \mathcal{M}_1}{\partial \tilde{x}_3} - \frac{\partial \mathcal{M}_3}{\partial \tilde{x}_1} = -\lambda \tilde{x}_k \frac{\partial \eta'}{\partial \tilde{x}_k} + \tilde{u}_j \frac{\partial \eta'}{\partial \tilde{x}_j} - \eta \frac{\partial \tilde{u}_2'}{\partial \tilde{x}_2} + \frac{\partial \tilde{u}_2'}{\partial \tilde{x}_3}\frac{\partial \tilde{u}_1'}{\partial \tilde{x}_2} - \frac{\partial \tilde{u}_2'}{\partial \tilde{x}_1}\frac{\partial \tilde{u}_3'}{\partial \tilde{x}_2}. \tag{4.76}$$

Therefore we find for (4.75) the expression

$$-\lambda \tilde{x}_k \frac{\partial \eta'}{\partial \tilde{x}_k} + A\tilde{x}_2 \frac{\partial}{\partial \tilde{x}_1}\eta' + A\frac{\partial \tilde{u}_2'}{\partial \tilde{x}_3} + \mathcal{N}_\eta = 0, \tag{4.77}$$

with

$$\mathcal{N}_\eta = \tilde{u}_j \frac{\partial \eta'}{\partial \tilde{x}_j} - \eta \frac{\partial \tilde{u}_2'}{\partial \tilde{x}_2} + \frac{\partial \tilde{u}_2'}{\partial \tilde{x}_3}\frac{\partial \tilde{u}_1'}{\partial \tilde{x}_2} - \frac{\partial \tilde{u}_2'}{\partial \tilde{x}_1}\frac{\partial \tilde{u}_3'}{\partial \tilde{x}_2}. \tag{4.78}$$

Consider the velocity-vorticity system given by (4.72) and (4.77) with BC

$$\tilde{u}_2' \to 0, \quad \eta' \to 0, \qquad \text{for} \quad |\tilde{x}_j| \to \infty. \tag{4.79}$$

If the nonlinear terms are neglected, it is possible to solve (4.72) for $(\tilde{u}_2', \lambda)$ in a first step. In the second step, the linearized equation (4.77) can be solved, which reduces to a boundary value problem, as λ is known from the solution of (4.72) in the previous step. This procedure is similar to solving stability problems in the context of the normal mode ansatz. The recovery of the velocities $\tilde{u}_1'$, $\tilde{u}_3'$ is done using the definition of the vorticity and the continuity equation. The starting point is the definition of the vorticity

$$\eta' = \frac{\partial \tilde{u}_1'}{\partial \tilde{x}_3} - \frac{\partial \tilde{u}_3'}{\partial \tilde{x}_1}. \tag{4.80}$$

Differentiating the equation (4.80) with respect to $\tilde{x}_3$ gives

$$\frac{\partial \eta'}{\partial \tilde{x}_3} = \frac{\partial^2 \tilde{u}_1'}{\partial \tilde{x}_3^2} - \frac{\partial^2 \tilde{u}_3'}{\partial \tilde{x}_1 \partial \tilde{x}_3}. \tag{4.81}$$

Using the continuity equation for the second term on the right hand side, i.e.

$$\frac{\partial \tilde{u}_3'}{\partial \tilde{x}_3} = -\frac{\partial \tilde{u}_1}{\partial \tilde{x}_1} - \frac{\partial \tilde{u}_2}{\partial \tilde{x}_2}, \tag{4.82}$$

gives an equation for $\tilde{u}_1'$ in terms of $\tilde{u}_2'$ and η'

$$\left(\frac{\partial^2}{\partial \tilde{x}_1^2} + \frac{\partial^2}{\partial x_3^2}\right)\tilde{u}_1' = \frac{\partial \eta'}{\partial \tilde{x}_3} - \frac{\partial^2 \tilde{u}_2'}{\partial \tilde{x}_1 \partial \tilde{x}_2}. \tag{4.83}$$

The velocity $\tilde{u}_3'$ can simply be obtained from the continuity equation with the result from (4.83)

$$\frac{\partial \tilde{u}_3'}{\partial \tilde{x}_3} = -\frac{\partial \tilde{u}_1'}{\partial \tilde{x}_1} - \frac{\partial \tilde{u}_2'}{\partial \tilde{x}_2}. \tag{4.84}$$

Analytical solution for the velocity $\tilde{u}_2'$

In this section, we discuss an analytical solution for $\tilde{u}_2'$. We consider the linearization of (4.72), i.e. with $\mathcal{N}_2 = 0$. If the fluctuations are infinitesimal, the linearization seems justified as shown in Chapter 3 regarding linear stability theory. The linearized equation reads

$$-\lambda \Delta \tilde{u}_2' - \lambda \tilde{x}_k \frac{\partial \Delta \tilde{u}_2'}{\partial \tilde{x}_k} + A\tilde{x}_2 \frac{\partial \Delta \tilde{u}_2'}{\partial \tilde{x}_1} = 0, \tag{4.85}$$

with the boundary conditions from (4.46) given by

$$|\tilde{u}_j| \to 0, \qquad \text{for} \quad |\tilde{x}_j| \to \infty. \tag{4.86}$$

Similar to the normal mode analysis, the system can be solved by calculating the eigenpair $(\tilde{u}_2, \lambda)$ and obtaining the vorticity η' by solving (4.77) afterward. Note that $\tilde{u}_2'$ appears always with the Laplacian operator (Δ). It is therefore possible to rewrite (4.85) as a system of equations

$$-\lambda q - \lambda \tilde{x}_k \frac{\partial q}{\partial \tilde{x}_k} + A\tilde{x}_2 \frac{\partial q}{\partial \tilde{x}_1} = 0, \tag{4.87}$$

$$\Delta \tilde{u}_2' = q, \tag{4.88}$$

where $q(\tilde{x}_1, \tilde{x}_2, \tilde{x}_3)$ is introduced as auxiliary function. Obviously, (4.88) states a Poisson equation. It can be easily shown that any harmonic function for $\tilde{u}_2'$ solves (4.88) on a square domain, e.g. $(x, y) \in [-1, 1]$. However, for an infinite domain, this problem is more involving. The harmonic functions, such as a sine or cosine do not satisfy the boundary conditions (4.46) and restated in (4.86). In general, the existence and uniqueness of elliptic problems on unbounded domains is a difficult topic, involving the definition of appropriate function spaces and norms. These aspects are not discussed here and the reader is referred to the literature (see e.g. Janßen (1986) and Mäulen and Werner (1983)).
The aim is to find a solution to (4.87) in a first step. For the linearized case, the shear rate A can be absorbed into the eigenvalue, i.e. $\lambda/A \to \lambda$. Writing the equation without index notation in the three-dimensional case $(\tilde{x}_1, \tilde{x}_2, \tilde{x}_3)$ and collecting the terms gives

$$(-\lambda \tilde{x}_1 + \tilde{x}_2) \frac{\partial q}{\partial \tilde{x}_1} - \lambda \tilde{x}_2 \frac{\partial q}{\partial \tilde{x}_2} - \lambda \tilde{x}_3 \frac{\partial q}{\partial \tilde{x}_3} = \lambda q. \tag{4.89}$$

Using the method of characteristics with parameter τ, the following system of ODEs can be derived

$$\frac{d\tilde{x}_1}{d\tau} = -\lambda \tilde{x}_1 + \tilde{x}_2, \quad \frac{d\tilde{x}_2}{d\tau} = -\lambda \tilde{x}_2, \quad \frac{d\tilde{x}_3}{d\tau} = -\lambda \tilde{x}_3, \quad \frac{dq}{d\tau} = \lambda. \tag{4.90}$$

The characteristics are easily obtained by integration. A general solution for $\Delta \tilde{u}_2'$ from (4.85) is found, which reads

$$\Delta \tilde{u}_2' \left(\tilde{x}_1, \tilde{x}_2, \tilde{x}_3\right) = F\left(\frac{\tilde{x}_2}{\tilde{x}_3}, \frac{2}{\lambda} \ln(\tilde{x}_2) + \frac{\tilde{x}_1}{\tilde{x}_2}\right) \frac{1}{\tilde{x}_2}, \tag{4.91}$$

where F is a free function depending on two characteristics. To obtain a physical solution, F should be continuous and give smooth solutions (no jumps, etc.) for $\Delta \tilde{u}_2'$ and $\tilde{u}_2'$. In addition, the solution for $\tilde{u}_2'$ should decay sufficiently fast at infinity (e.g. for boundedness

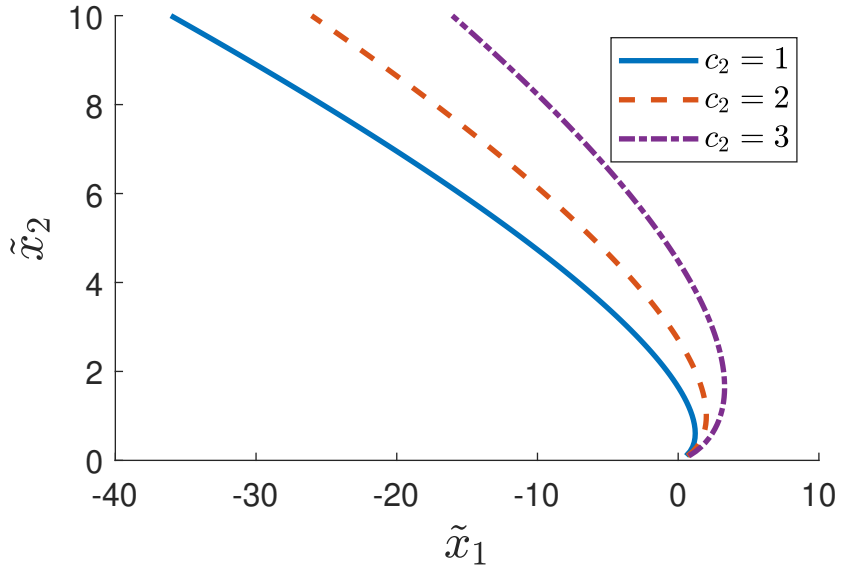

Figure 4.2.: Characteristic c_2 from (4.92) for different values of c_2

of kinetic energy). Assuming that the corresponding Green's integral exists, a solution for $\tilde{u}_2'$ from the Poisson equation (4.91) can be constructed. However, there is some doubt that the corresponding integral exists, which depends on the properties of F. To discuss possible choices of F, it is convenient to study the characteristics in (4.91). The characteristic $c_1 = \tilde{x}_2/\tilde{x}_3$ gives a linear relation between $\tilde{x}_2$ and $\tilde{x}_3$. The characteristic c_2 can be solved for $\tilde{x}_1$ to obtain:

$$\tilde{x}_1 = c_2\tilde{x}_2 - \frac{2}{\lambda}\ln(\tilde{x}_2)\,\tilde{x}_2 \tag{4.92}$$

The characteristics for different choices of c_2 are shown in Figure 4.2. The characteristics all diverge to infinity in $\tilde{x}_1$ for large $\tilde{x}_2$. Moreover, there is a singularity for $\tilde{x}_2 = 0$ due to the logarithmic term. Even a transform would still leave the singularity caused by the factor $1/\tilde{x}_2$ in (4.91). In that way, a function F should be chosen to eliminate this singularity.
Even after numerous attempts, it was not possible to find a function F such that the boundary conditions are satisfied. The use of canonical functions such as trigonometric functions or exponential functions as well as series expansions were considered without success. Consequently, (4.85) should be solved numerically using spectral methods (see Chapter 5 and Chapter 6 for more details).

4.3. Pure Strain

In the following we consider flows with strain. The most general form of a flow under strain is

$$A_{ij} = \begin{pmatrix} S_1 & 0 & 0 \\ 0 & S_2 & 0 \\ 0 & 0 & S_3 \end{pmatrix}, \tag{4.93}$$

while $S_1 + S_2 + S_3 = 0$ must hold (Sagaut and Cambon, 2018). We consider two special cases of (4.93) in the following. The first case is a pure irrotational strain (planar distortion) and the second case is axisymmetric (irrotational) strain.

4.3.1. Irrotational (planar) strain

The velocity gradient tensor for planar strain is given by

$$A_{ij} = \begin{pmatrix} -S & 0 & 0 \\ 0 & S & 0 \\ 0 & 0 & 0 \end{pmatrix}, \tag{4.94}$$

and therefore the velocities according to (4.5) read

$$\tilde{u}_1 = -S\tilde{x}_1 + \tilde{u}_1', \qquad \tilde{u}_2 = S\tilde{x}_2 + \tilde{u}_2', \qquad \tilde{u}_3 = \tilde{u}_3'. \tag{4.95}$$

The momentum equation for the fluctuations can be obtained by inserting A_{ij} from (4.94) into the general momentum equation (4.38). The terms $\mathcal{M}$ are given in (4.58) and are identical to the terms for linear shear. There are contributions due to strain for the $\tilde{x}_1$ and $\tilde{x}_2$-component which can be taken into the averaged pressure according to (4.31). The averaged pressure for planar strain reads

$$\tilde{\bar{p}} = -\frac{1}{2}S^2(\tilde{x}_1^2 + \tilde{x}_2^2). \tag{4.96}$$

The terms $\mathcal{S}$ as defined in (4.57) are given by

$$\mathcal{S}_1 = -S\tilde{x}_1\frac{\partial \tilde{u}_1'}{\partial \tilde{x}_1} - \tilde{u}_1'S + S\tilde{x}_2\frac{\partial \tilde{u}_1'}{\partial \tilde{x}_2}, \tag{4.97}$$

$$\mathcal{S}_2 = S\tilde{x}_2\frac{\partial \tilde{u}_2'}{\partial \tilde{x}_2} + \tilde{u}_2'S - S\tilde{x}_1\frac{\partial \tilde{u}_2'}{\partial \tilde{x}_1}, \tag{4.98}$$

$$\mathcal{S}_3 = -S\tilde{x}_1\frac{\partial \tilde{u}_3'}{\partial \tilde{x}_1} + S\tilde{x}_2\frac{\partial \tilde{u}_3'}{\partial \tilde{x}_2}, \tag{4.99}$$

where we have to keep in mind the difference between a calligraphic $\mathcal{S}$ and the strain rate S.

Velocity formulation in 2D

We try to find a velocity-vorticity formulation as in Section 4.2 for linear shear. The divergence of the momentum equations $\nabla \cdot (\mathcal{M} + \mathcal{S})$ yields the Poisson equation for the pressure

$$\Delta\tilde{p}' = -S\left(\frac{\partial \tilde{u}_2'}{\partial \tilde{x}_2} - \frac{\partial \tilde{u}_1'}{\partial \tilde{x}_1}\right) - \frac{\partial}{\partial \tilde{x}_i}\left(\tilde{u}_k\frac{\partial \tilde{u}_i'}{\partial \tilde{x}_k}\right). \tag{4.100}$$

At this point, we see that the latter equation contains the velocities $\tilde{u}_1'$ and $\tilde{u}_2'$. The derivative of (4.100) with respect to $\tilde{x}_2$ can inserted into the momentum equation for the component $\tilde{u}_2'$, i.e. $\mathcal{M}_2 + \mathcal{S}_2 = 0$. This procedure is analogous the the derivation for the linear shear case. Note that the linearized equation for irrotational strain would still contain $\tilde{u}_1'$ components. This contrasts with the linear shear case, where only $\tilde{u}_2'$-components occur, which allows to formulate a scalar equation for $\tilde{u}_2'$. Therefore, the derivation of a single scalar equation in not possible for the three-dimensional case.
However, for the two-dimensional case (planar strain with two-dimensional fluctuations) it is possible to use the continuity equation to rewrite (4.100) as

$$\Delta\tilde{p}' = -2S\left(\frac{\partial \tilde{u}_2'}{\partial \tilde{x}_2}\right) - \frac{\partial}{\partial \tilde{x}_i}\left(\tilde{u}_k\frac{\partial \tilde{u}_i'}{\partial \tilde{x}_k}\right). \tag{4.101}$$

The third term on the right-hand side (RHS) of (4.101) is a nonlinear term. However, by neglecting them, the remaining two terms on the RHS only depend on $\tilde{u}_2'$. For three-dimensional perturbations it is not possible to modify the Poisson equation, such that the linear terms on the RHS only depend on $\tilde{u}_2'$. Therefore it was not possible to find a velocity-vorticity formulation for the three-dimensional case. For the two-dimensional case, the Laplacian can be applied on the eigenvalue problem defined by the terms (4.58) and (4.97) to (4.99), i.e.

$$\Delta \left(\mathcal{M}_2 + \mathcal{S}_2 \right) = 0. \tag{4.102}$$

$\Delta \mathcal{M}_2$ is already given in (4.66), for $\Delta \mathcal{S}_2$ we find

$$\Delta \mathcal{S}_2 = S\tilde{x}_2 \frac{\partial}{\partial \tilde{x}_2} \Delta \tilde{u}_2' - S\tilde{x}_1 \frac{\partial}{\partial \tilde{x}_1} \Delta \tilde{u}_2' + 3S \frac{\partial^2 \tilde{u}_2'}{\partial \tilde{x}_2^2} - S \frac{\partial^2 \tilde{u}_2'}{\partial \tilde{x}_1^2}. \tag{4.103}$$

Inserting the Poisson equation (4.101) into (4.102) and simplifying the expression gives

$$\left(-\lambda + S\right) \Delta \tilde{u}_2' + \left(-\lambda - S\right) \tilde{x}_1 \frac{\partial \Delta \tilde{u}_2'}{\partial \tilde{x}_1} \left(-\lambda + S\right) \tilde{x}_2 \frac{\partial \Delta \tilde{u}_2'}{\partial \tilde{x}_2} - 2S \frac{\partial^2 \tilde{u}_2'}{\partial \tilde{x}_1^2} + \mathcal{N} = 0, \tag{4.104}$$

where the nonlinear terms are given by (4.73).

Analytical solutions

We consider the linearized form of (4.104) for the two-dimensional case, given by

$$\left(-\lambda + S\right) \Delta \tilde{u}_2' + \left(-\lambda - S\right) \tilde{x}_1 \frac{\partial \Delta \tilde{u}_2'}{\partial \tilde{x}_1} \left(-\lambda + S\right) \tilde{x}_2 \frac{\partial \Delta \tilde{u}_2'}{\partial \tilde{x}_2} - 2S \frac{\partial^2 \tilde{u}_2'}{\partial \tilde{x}_1^2} = 0. \tag{4.105}$$

In contrast to the case of linear shear, a substitution of $\Delta \tilde{u}_2' = q$ (cf. (4.87) and (4.88)) does not work here, as the last term on the left hand side does not contain $\Delta \tilde{u}_2'$. However, it is possible to find solution for a special case. For $\lambda = S$, the eigenvalue equation simplifies to a partial differential equation (or to a boundary value problem (BVP) if supplied with the corresponding BC)

$$\tilde{x}_1 \frac{\partial \Delta \tilde{u}_2'}{\partial \tilde{x}_1} + \frac{\partial^2 \tilde{u}_2'}{\partial \tilde{x}_1^2} = 0. \tag{4.106}$$

Similarly, the choice $\lambda = -S$ in (4.104) gives

$$\tilde{x}_2 \frac{\partial \Delta \tilde{u}_2'}{\partial \tilde{x}_2} + \frac{\partial^2 \tilde{u}_2'}{\partial \tilde{x}_2^2} = 0. \tag{4.107}$$

with a vanishing of $\tilde{u}_2'$ at infinity (compare BC (4.46)). Both equations (4.106) and (4.107) can be solved analytically (e.g. using CAS). The general solution of (4.106) can be obtained from MAPLE and be written as the real part $\Re$ of the following expression

$$\tilde{u}_2'(\tilde{x}_1, \tilde{x}_2) = \Re \left[F_1(\tilde{x}_2) - \frac{1}{2} \tilde{x}_1 \left(C_3 \sin\left(\alpha \tilde{x}_2\right) + C_4 \cos\left(\alpha \tilde{x}_2\right) \right) F_2(\tilde{x}_1, \tilde{x}_2) \right], \tag{4.108}$$

where F_2 is defined by

$$\begin{aligned} F_2(\tilde{x}_1, \tilde{x}_2) = & - C_2 \pi \mathrm{K}_0\left(\alpha \tilde{x}_1\right) \mathrm{L}_1\left(\alpha \tilde{x}_1\right) - C_1 \pi \mathrm{I}_0\left(\alpha \tilde{x}_1\right) \mathrm{L}_1\left(\alpha \tilde{x}_1\right) \\ & + C_1 \pi \mathrm{L}_0\left(\alpha \tilde{x}_1\right) \mathrm{I}_1\left(\alpha \tilde{x}_1\right) + C_2 \pi \mathrm{L}_0\left(\alpha \tilde{x}_1\right) \mathrm{K}_1\left(\alpha \tilde{x}_1\right) \\ & - 2C_2 \mathrm{K}_0\left(\alpha \tilde{x}_1\right) - 2C_1 \mathrm{K}_0\left(\alpha \tilde{x}_1\right). \end{aligned} \tag{4.109}$$

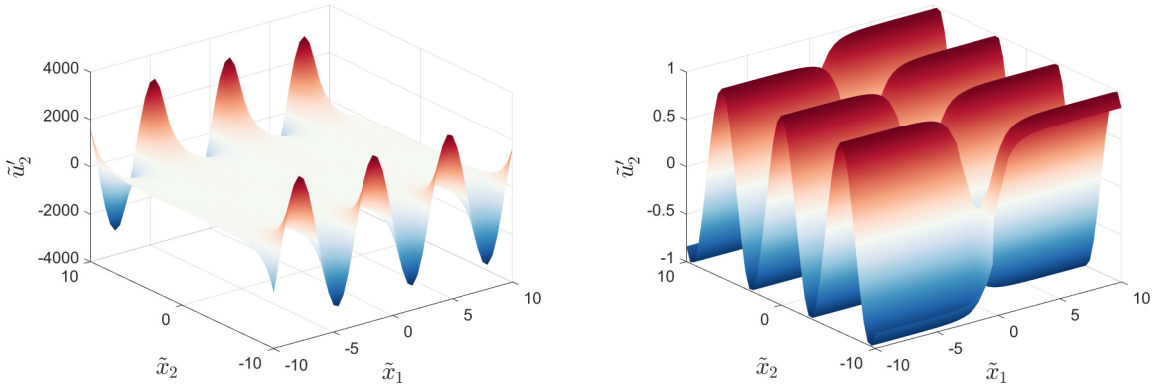

(a) $F_1 = 0, C_1 = C_3 = 1, C_2 = C_4 = 0, \alpha = 1$ (b) $F_1 = 0, C_1 = C_3 = 0, C_2 = C_4 = 1, \alpha = 1$

Figure 4.3.: Pure strain (2D): analytical solution for $\tilde{u}_2'$ from (4.108) with (4.109) for different values of the constants C_j and the wavenumber α.

Here $C_1, C_2, C_3, C_4, \alpha$ are constants, F_1 is an arbitrary function depending on $\tilde{x}_2$, I_n and K_n are n-th modified Bessel function, and L_n is n-th the modified Stuve function. An asymptotic analysis of the solution (4.108) is omitted here and it subject to future work. Figure 4.3 shows the analytic solutions (4.108) for two different sets of constants on a truncated domain.
The preliminary analysis of the solution (4.108) for the set of constants shown in Figure 4.3b indicates that the solution is periodic in $\tilde{x}_2$ even for large arguments in $\tilde{x}_1$. Therefore the this solution does not satisfy the BC (4.46) and is not an eigenfunction in a proper sense. It can be discussed, if the boundary conditions should be relaxed, by enforcing bounded values instead of vanishing (zero) values at infinity. This topic is addressed in detail in Chapter 6.1.2.

4.3.2. Axisymmetric strain

For three-dimensional axisymmetric strain, the velocity gradient tensor is given by

$$A_{ij} = \begin{pmatrix} -S/2 & 0 & 0 \\ 0 & -S/2 & 0 \\ 0 & 0 & S \end{pmatrix}. \tag{4.110}$$

The velocity decomposition (4.5) reads

$$\tilde{u}_1 = -\frac{S}{2}\tilde{x}_1 + \tilde{u}_1', \qquad \tilde{u}_2 = -\frac{S}{2}\tilde{x}_2 + \tilde{u}_2', \qquad \tilde{u}_3 = S\tilde{x}_3 + \tilde{u}_3' \tag{4.111}$$

with a mean pressure following from (4.31), which is given by

$$\tilde{\bar{p}} = -\frac{1}{8}S^2\tilde{x}_1^2 - \frac{1}{8}S^2\tilde{x}_2^2 - \frac{1}{2}S^2\tilde{x}_3^2. \tag{4.112}$$

The momentum equation with A_{ij} from (4.110) can be obtained from (4.38). The common terms are defined in (4.58), while the specific terms are given by

$$\mathcal{S}_1 = -\frac{S}{2}\tilde{x}_1\frac{\partial \tilde{u}_1'}{\partial \tilde{x}_1} - \frac{S}{2}\tilde{u}_1' - \frac{S}{2}\tilde{x}_2\frac{\partial \tilde{u}_1'}{\partial \tilde{x}_2} + S\tilde{x}_3\frac{\partial \tilde{u}_1'}{\partial \tilde{x}_3}, \tag{4.113}$$

$$\mathcal{S}_2 = -\frac{S}{2}\tilde{x}_1\frac{\partial \tilde{u}_2'}{\partial \tilde{x}_1} - \frac{S}{2}\tilde{x}_2\frac{\partial \tilde{u}_2'}{\partial \tilde{x}_2} - \frac{S}{2}\tilde{u}_2' + S\tilde{x}_3\frac{\partial \tilde{u}_2'}{\partial \tilde{x}_3}, \tag{4.114}$$

$$\mathcal{S}_3 = -\frac{S}{2}\tilde{x}_1\frac{\partial \tilde{u}_3'}{\partial \tilde{x}_1} - \frac{S}{2}\tilde{x}_2\frac{\partial \tilde{u}_3'}{\partial \tilde{x}_2} + S\tilde{x}_3\frac{\partial \tilde{u}_3'}{\partial \tilde{x}_3} + \tilde{u}_3' S. \tag{4.115}$$

Velocity equation

Taking the divergence of the $\mathcal{S}_j$ terms defined by (4.113) - (4.115) and using the result from $\nabla \cdot \mathcal{M}$ given in (4.60) yields the Poisson equation

$$\Delta\tilde{p}' = -2S\left(-\frac{1}{2}\frac{\partial \tilde{u}_1'}{\partial \tilde{x}_1} - \frac{1}{2}\frac{\partial \tilde{u}_2'}{\partial \tilde{x}_2} + \frac{\partial \tilde{u}_3'}{\partial \tilde{x}_3}\right) - \frac{\partial}{\partial \tilde{x}_i}\left(\tilde{u}_k'\frac{\partial \tilde{u}_i'}{\partial \tilde{x}_k}\right). \tag{4.116}$$

By using the continuity equation it is possible to rewrite the linear part of the Poisson equation entirely in terms of $\tilde{u}_3'$ as

$$\Delta\tilde{p}' = -3S\frac{\partial \tilde{u}_3'}{\partial \tilde{x}_3} - \frac{\partial}{\partial \tilde{x}_i}\left(\tilde{u}_k'\frac{\partial \tilde{u}_i'}{\partial \tilde{x}_k}\right). \tag{4.117}$$

Therefore we obtain a decoupled equation for the linear part of $\tilde{u}_3'$ given by

$$-\lambda\Delta\tilde{u}_3' - \lambda\tilde{x}_k\frac{\partial \Delta\tilde{u}_3'}{\partial \tilde{x}_k} - 3S\frac{\partial^2\tilde{u}_3'}{\partial \tilde{x}_3^2} - \frac{S}{2}\left(\tilde{x}_1\frac{\partial \Delta\tilde{u}_3'}{\partial \tilde{x}_1} + \tilde{x}_2\frac{\partial \Delta\tilde{u}_3'}{\partial \tilde{x}_2} - 2\tilde{x}_3\frac{\partial \Delta\tilde{u}_3'}{\partial \tilde{x}_3}\right) + S\Delta\tilde{u}_3' + \mathcal{N} = 0, \tag{4.118}$$

where the nonlinear term still depend on $\tilde{u}_1'$ and $\tilde{u}_2'$ and are given by

$$\mathcal{N} = \Delta\left(\tilde{u}_k'\frac{\partial \tilde{u}_3'}{\partial \tilde{x}_k}\right) - \frac{\partial}{\partial \tilde{x}_3}\frac{\partial}{\partial \tilde{x}_i}\left(\tilde{u}_k\frac{\partial \tilde{u}_i'}{\partial \tilde{x}_k}\right). \tag{4.119}$$

Vorticity equation

The velocity-vorticity formulation is usually based on the normal velocity and the normal vorticity, i.e. the components $\tilde{u}_2'$ and η_2. As the present formulation (4.118) is based on $\tilde{u}_3'$, the corresponding vorticity component η_3 is considered instead. This is done to be consistent with the formulations for $\tilde{u}_2'$. The vorticity component η_3 is defined by

$$\eta_3' = \frac{\partial \tilde{u}_2'}{\partial \tilde{x}_1} - \frac{\partial \tilde{u}_1'}{\partial \tilde{x}_2}. \tag{4.120}$$

A cross-differentiation is performed, i.e.

$$\frac{\partial}{\partial \tilde{x}_1}\left(\mathcal{M}_2 + \mathcal{S}_2\right) - \frac{\partial}{\partial \tilde{x}_2}\left(\mathcal{M}_1 + \mathcal{S}_1\right) \tag{4.121}$$

which gives after some reshaping

$$-\lambda\tilde{x}_k\frac{\partial\eta_3'}{\partial\tilde{x}_k}-\frac{S}{2}\tilde{x}_1\frac{\partial}{\partial\tilde{x}_1}\eta_3-\frac{S}{2}\frac{\partial}{\partial\tilde{x}_2}\eta_3'+S\tilde{x}_3\frac{\partial}{\partial\tilde{x}_3}\eta_3'-S\eta_3'+\mathcal{N}_{\eta_3}=0, \tag{4.122}$$

where the nonlinear term is given by

$$\mathcal{N}_{\eta_3}=\frac{\partial}{\partial\tilde{x}_1}\left(\tilde{u}_k'\frac{\partial\tilde{u}_2'}{\partial\tilde{x}_k}\right)-\frac{\partial}{\partial\tilde{x}_2}\left(\tilde{u}_k'\frac{\partial\tilde{u}_1'}{\partial\tilde{x}_k}\right). \tag{4.123}$$

4.4. Pure Rotation

The velocity-gradient tensor for a flow with pure (constant) rotation around the x_3-axis, i.e. $\boldsymbol{\Omega}=(0,0,\Omega)$ reads

$$A_{ij}=\begin{pmatrix}0&-\Omega&0\\\Omega&0&0\\0&0&0\end{pmatrix}. \tag{4.124}$$

However, it is easier to consider the flow in a rotating frame (Sagaut and Cambon, 2018). In this non-Galilean frame, the Coriolis force has to be taken into account. The case of a pure rotation has no base flow and therefore the velocity decompositions read

$$\tilde{u}_1=\tilde{u}_1',\quad \tilde{u}_2=\tilde{u}_2',\quad \tilde{u}_3=\tilde{u}_3'. \tag{4.125}$$

The corresponding eigenvalue problem is given by the transformed Euler equations (4.38) with velocity fluctuations (4.125) and an additional Coriolis force. Therefore we have

$$Eq.\,(4.38)+f_i=0, \tag{4.126}$$

with the Coriolis force

$$f_i=2\Omega\left(-\tilde{u}_2,\tilde{u}_1,0\right). \tag{4.127}$$

Pressure-free formulation

The aim is to find an expression where the pressure does not explicitly occur. This is comparable to the velocity-vorticity formulation for linear shear. Consistent with the notation, we have again common terms $\mathcal{M}$ and a term due to the Coriolis force given by $\mathcal{F}=f_i$ from (4.127). By taking the divergence of the transformed Euler equation in the rotating frame, i.e. $(\nabla\cdot(\mathcal{M}+\mathcal{F})=0$, we obtain the Poisson equation for the pressure

$$\Delta\tilde{p}'=2\Omega\frac{\partial\tilde{u}_2'}{\partial x_1}-2\Omega\frac{\partial\tilde{u}_1'}{\partial\tilde{x}_2}-\frac{\partial}{\partial\tilde{x}_i}\left(\tilde{u}_k\frac{\partial\tilde{u}_i'}{\partial\tilde{x}_k}\right). \tag{4.128}$$

Substituting into $\Delta\left(\mathcal{M}_2+\mathcal{F}_2\right)=0$ gives

$$-\lambda\Delta\tilde{u}_2'-\lambda\tilde{x}_k\frac{\partial\Delta\tilde{u}_2'}{\partial\tilde{x}_k}+\frac{\partial}{\partial\tilde{x}_2}\left(2\Omega\frac{\partial\tilde{u}_2'}{\partial x_1}-2\Omega\frac{\partial\tilde{u}_1'}{\partial\tilde{x}_2}\right)+2\Omega\Delta\tilde{u}_1+\mathcal{N}_2=0, \tag{4.129}$$

where the nonlinear terms read

$$\mathcal{N}_j = -\frac{\partial}{\partial \tilde{x}_j}\frac{\partial}{\partial \tilde{x}_i}\left(\tilde{u}_k \frac{\partial \tilde{u}_i'}{\partial \tilde{x}_k}\right) + \Delta\left(\tilde{u}_k' \frac{\partial \tilde{u}_j'}{\partial \tilde{x}_k}\right). \tag{4.130}$$

Note that explicitly contains $\tilde{u}_1'$ and $\tilde{u}_3'$. It was not possible to obtain a scalar equation in only one variable, e.g. $\tilde{u}_2'$. Instead, the pressure from (4.128) is substituted in $\Delta\left(\mathcal{M}_1 + \mathcal{F}_1\right) = 0$ giving

$$-\lambda\Delta\tilde{u}_1' - \lambda\tilde{x}_k\frac{\partial\Delta\tilde{u}_1'}{\partial\tilde{x}_k} + \frac{\partial}{\partial\tilde{x}_1}\left(2\Omega\frac{\partial\tilde{u}_2'}{\partial x_1} - 2\Omega\frac{\partial\tilde{u}_1'}{\partial\tilde{x}_2}\right) - 2\Omega\Delta\tilde{u}_2' + \mathcal{N}_1 = 0, \tag{4.131}$$

and in $\Delta\left(\mathcal{M}_3 + \mathcal{F}_3\right) = 0$ which yields

$$-\lambda\Delta\tilde{u}_3' - \lambda\tilde{x}_k\frac{\partial\Delta\tilde{u}_3'}{\partial\tilde{x}_k} + \frac{\partial}{\partial\tilde{x}_3}\left(2\Omega\frac{\partial\tilde{u}_2'}{\partial\tilde{x}_1} - 2\Omega\frac{\partial\tilde{u}_1'}{\partial\tilde{x}_2}\right) + \mathcal{N}_3 = 0. \tag{4.132}$$

The nonlinear terms $\mathcal{N}_1$ and $\mathcal{N}_3$ are defined by (4.130). The linearized equations (4.4) (4.131), (4.132) with $\mathcal{N}_j = 0$ can be written as a system in terms of the velocities $(\tilde{u}_1, \tilde{u}_2, \tilde{u}_3)^T$ which takes the form

$$\mathsf{A}\boldsymbol{u} = \lambda\mathsf{B}\boldsymbol{u}, \tag{4.133}$$

with

$$\boldsymbol{u} = \left(\tilde{u}_1', \tilde{u}_2', \tilde{u}_3'\right)^T, \tag{4.134}$$

and

$$\mathsf{A} = 2\Omega\begin{pmatrix} -\frac{\partial^2}{\partial\tilde{x}_1\partial\tilde{x}_2} & \left(\frac{\partial^2}{\partial\tilde{x}_1^2} - \Delta\right) & 0 \\ -\left(\frac{\partial^2}{\partial\tilde{x}_2^2} - \Delta\right) & \frac{\partial^2}{\partial\tilde{x}_1\partial\tilde{x}_2} & 0 \\ -\frac{\partial^2}{\partial\tilde{x}_2\partial\tilde{x}_3} & \frac{\partial^2}{\partial\tilde{x}_1\partial\tilde{x}_3} & 0 \end{pmatrix} \tag{4.135}$$

and

$$\mathsf{B} = \begin{pmatrix} -\Delta - \tilde{x}_k\frac{\partial\Delta}{\partial\tilde{x}_k} & 0 & 0 \\ 0 & -\Delta - \tilde{x}_k\frac{\partial\Delta}{\partial\tilde{x}_k} & 0 \\ 0 & 0 & -\Delta - \tilde{x}_k\frac{\partial\Delta}{\partial\tilde{x}_k} \end{pmatrix} \tag{4.136}$$

The matrices A from (4.136) and B from (4.136) contain differential operators. When using numerical methods (e.g. spectral collocation), the discretization of A leads to a singular (discretized) matrix for the three-dimensional case, since the third column is a zero vector. This can be circumvented by only considering plane (two-dimensional) fluctuations, which yields a non-singular matrix A.

4.5. Wall-bounded shear flows (log law)

In the previous sections, an NEVP for unbounded flows is derived. However, in engineering applications, flows are often bounded by solid walls. In the following, the symmetry-based approach is applied on wall-bounded flows. In comparison to unbounded flows, the distance to

the wall gives a length scale to the problem (Rotta, 2010; Jiménez, 2013). For wall-bounded turbulent flows, the velocity profile is logarithmic in the near-wall region (von Kármán, 1930; Prandtl, 1932; Millikan, 1939). This is referred to as the logarithmic law of the wall, or simply log law. The wall-normal distance is denoted by y^+ and the streamwise velocity by U^+. The superscript $+$ denotes that the quantities are normalized by using the friction velocity u_τ and the kinematic viscosity ν. The velocity in the range between $y^+ > 30$ and $y/\delta < 0.1 - 0.2$ (outer length scale δ: e.g. boundary layer thickness) can be described by

$$U^+ = \frac{1}{\kappa} \ln y^+ + B, \tag{4.137}$$

where κ is the van Kármán constant and B is an additive constant (Pope, 2000; Örlü et al., 2010). Based on a symmetry approach, an additional constant A is proposed in the argument of the logarithm (Oberlack, 2001)

$$U^+ = \frac{1}{\kappa} \ln \left(y^+ + A \right) + B. \tag{4.138}$$

However, the determination of the precise values of κ and B is difficult (Örlü et al., 2010; Marusic et al., 2010). The values are given by approximately $\kappa \approx 0.41$ and $B \approx 5.2$ (Pope, 2000). The value of κ seems to be universal in wall-bounded turbulence (Örlü et al., 2010). The value is not only interesting from a theoretical perspective. Moreover, numerical simulation of turbulent flows also depends on the choice of κ (George, 2007). However, to the author's knowledge, there is no precise value obtained from a first-principles theory.

Derivation of a nonlinear eigenvalue problem for κ

An interesting extension of the NEVP for boundary-layer flows, which also covers κ, was proposed by Oberlack (2020). The following derivation is based on private communications (Yalcin, 2018).
In the following, we consider a flow under the decomposition

$$u_i = \delta_{1i} \left(\frac{1}{\kappa} \ln(x_2) + B \right) + u_i'. \tag{4.139}$$

The starting point for the derivation of the eigenvalue problem is the combination of three symmetries of the Euler equation, namely scaling in space (2.10), scaling in time (2.11) and a generalized Galiean invariance (2.13). The infinitesimal generator reads

$$\begin{aligned} X = &\left(a_1 x_i + f_i(t)\right) \frac{\partial}{\partial x_i} + a_2 t \frac{\partial}{\partial t} + \left(\left(a_1 - a_2\right) u_i + \dot{f}_i(t) \right) \frac{\partial}{\partial u_i} \\ &+ \left(\left(a_1 - a_2\right) 2p - x_i \ddot{f}_i(t) \right) \frac{\partial}{\partial p}. \end{aligned} \tag{4.140}$$

where $\dot{f}_i$ and $\ddot{f}_i$ denotes the first and second derivative with respect to time, respectively. Using the invariant surface condition for u_i, i.e.

$$X \left(\boldsymbol{u} - \boldsymbol{u}(\boldsymbol{x}, t) \right) |_{\boldsymbol{u}(\boldsymbol{x},t)=\boldsymbol{u}} = 0, \tag{4.141}$$

leads to the following equation to determine the characteristics

$$\frac{dx_i}{a_1 x_i + f_i(t)} = \frac{dt}{a_2 t} = \frac{du_i}{(a_1 - a_2) u_i + \dot{f}_i(t)}. \tag{4.142}$$

The characteristics can be solved for x_i and u_i, which gives

$$x_i = t^{\frac{a_1}{a_2}} \left(\tilde{x}_i + \frac{1}{a_2} \int f_i(t) t^{-\frac{a_1+a_2}{a_2}} dt \right), \tag{4.143}$$

$$u_i = t^{\frac{a_1-a_2}{a_2}} \left(\tilde{u}_i + \frac{1}{a_2} \int \dot{f}_i(t) t^{-\frac{a_1}{a_2}} dt \right). \tag{4.144}$$

Accordingly, a symmetry transform of (4.139) in terms of transformed variables is given by

$$\tilde{u}_i = \delta_{i1} \left(\frac{1}{\kappa} \ln(\tilde{x}_2) + B \right) + \tilde{u}'_i. \tag{4.145}$$

By inserting the decomposition (4.145) into (4.144), the following ansatz is constructed

$$u_i = t^{\frac{a_1-a_2}{a_2}} \left(\delta_{i1} \left(\frac{1}{\kappa} \ln(\tilde{x}_2) + B \right) + \tilde{u}'_i(\tilde{\boldsymbol{x}}) + \delta_{i1} \frac{1}{a_2} \int \dot{f}_i(t) t^{-\frac{a_1}{a_2}} dt \right). \tag{4.146}$$

The aim of ansatz (4.146) is to determine the group parameters a_1, a_2 and the function f_i such that the logarithmic base flow is invariant under the transform. In order that the logarithmic profile in (4.146) is invariant under the symmetries according to (4.139), a first condition is

$$t^{\frac{a_1-a_2}{a_2}} = 1, \tag{4.147}$$

and it follows directly that

$$a_1 = a_2. \tag{4.148}$$

With (4.148), the transform $\tilde{x}_i$ from (4.143) simplies to

$$\tilde{x}_i = t^{-1} x_i - \frac{1}{a_2} \int f_i(t) t^{-2} dt. \tag{4.149}$$

Therefore $\ln(\tilde{x}_2)$ reads

$$\ln(\tilde{x}_2) = \ln \left(t^{-1} x_2 - \frac{1}{a_2} \int f_2(t) t^{-2} dt \right). \tag{4.150}$$

By comparison of coefficients with the base flow (4.139), the contribution of the second term in (4.150) must vanish and it follows that

$$f_2 = 0. \tag{4.151}$$

Consequently, the transform of $\tilde{x}_2$ from (4.143) simplifies to

$$\tilde{x}_2 = x_2 t^{-1}. \tag{4.152}$$

From the logarithmic identities we have

$$\ln(\tilde{x}_2) = \ln(x_2) - \ln(t). \tag{4.153}$$

With the findings (4.148), (4.151) and the identity (4.153), we can rewrite (4.146) as

$$u_i = \left(\delta_{i1} \left(\frac{1}{\kappa} \ln(x_2) + B \right) + \tilde{u}'_i(\tilde{\boldsymbol{x}}) - \delta_{i1} \frac{1}{\kappa} \ln(t) + \delta_{i1} \frac{1}{a_2} \int \dot{f}_i(t) t^{-1} dt \right). \tag{4.154}$$

Additionally, it follows from (4.154) that the condition

$$\frac{1}{\kappa}\ln(t) = \frac{1}{a_2}\dot{f}_1(t)t^{-1}dt \tag{4.155}$$

must hold. Integrating over t gives

$$\frac{a_2}{\kappa}t^{-1} = \dot{f}_1(t)t^{-1}. \tag{4.156}$$

Solving for $f_1(t)$ by integration gives

$$f_1(t) = \frac{a_2}{\kappa}t + C, \tag{4.157}$$

where C denotes a constant, which is set to zero in the following. The resulting transform for x_1 from (4.143) is therefore

$$x_1 = t\left(\tilde{x}_1 + \frac{1}{\kappa}\int t^{-1}dt\right) \tag{4.158}$$

$$= t\left(\tilde{x}_1 + \frac{1}{\kappa}\ln(t)\right). \tag{4.159}$$

Based on the ansatz (4.146), we do not obtain an explicit condition for f_3. However, by considering (4.143) and (4.144), we set $f_3 = 0$ for this base flow. Therefore, the transform of the spatial variables reads

$$x_1 = t\left(\tilde{x}_1 + \frac{1}{\kappa}\ln(t)\right), \quad x_2 = t\tilde{x}_2, \quad x_3 = t\tilde{x}_3. \tag{4.160}$$

The first derivatives with respect to these variables transform as

$$\frac{\partial}{\partial x_1} = t^{-1}\frac{\partial}{\partial \tilde{x}_1}, \quad \frac{\partial}{\partial x_2} = t^{-1}\frac{\partial}{\partial \tilde{x}_2}, \quad \frac{\partial}{\partial x_3} = t^{-1}\frac{\partial}{\partial \tilde{x}_3}. \tag{4.161}$$

To derive an eigenvalue problem for κ, we insert the velocity decomposition following from (4.154) with (4.157) and given by

$$u_i = \left(\delta_{i1}\left(\frac{1}{\kappa}\ln(x_2) + B\right) + \tilde{u}_i'(\tilde{\boldsymbol{x}})\right), \tag{4.162}$$

and the ansatz for the pressure (4.140)

$$p = \overline{p} + \tilde{p}', \tag{4.163}$$

into the Euler equation (4.9), which gives

$$\begin{aligned}&\frac{\partial}{\partial t}\left(\delta_{i1}\left(\frac{1}{\kappa}\ln(x_2) + B\right) + \tilde{u}_i'(\tilde{\boldsymbol{x}})\right)\\ &+ \left(\delta_{j1}\left(\frac{1}{\kappa}\ln(x_2) + B\right) + \tilde{u}_j'(\tilde{\boldsymbol{x}})\right)\frac{\partial}{\partial x_j}\left(\delta_{i1}\left(\frac{1}{\kappa}\ln(x_2) + B\right) + \tilde{u}_i'(\tilde{\boldsymbol{x}})\right) + \frac{\partial(\overline{p} + \tilde{p}')}{\partial x_i} = 0.\end{aligned} \tag{4.164}$$

Subtracting the Euler equation (4.9) for the base flow $(\overline{u}_i, \overline{p})$ from (4.164) gives

$$\frac{\partial}{\partial t}\left(\tilde{u}_i'(\tilde{\boldsymbol{x}})\right) + \tilde{u}_2'(\tilde{\boldsymbol{x}})\frac{\delta_{i1}}{\kappa x_2} + \left(\frac{1}{\kappa}\ln(x_2) + B\right)\frac{\partial}{\partial x_1}\tilde{u}_i'(\tilde{\boldsymbol{x}}) + \tilde{u}_j'(\tilde{\boldsymbol{x}})\frac{\partial}{\partial x_j}\tilde{u}_i'(\tilde{\boldsymbol{x}}) + \frac{\partial \tilde{p}'}{\partial x_i} = 0. \quad (4.165)$$

The next step is to rewrite the equation entirely in the transformed variables $\tilde{x}_i$. The transform of the spatial variables is given in (4.161). The time derivative can be expressed in terms of $\tilde{x}_i$ by the chain rule of differentiation which gives

$$\begin{aligned} &- t^{-1}\left(\tilde{x}_k\frac{\partial}{\partial \tilde{x}_k} + \frac{1}{\kappa}\ln(t)\frac{\partial}{\partial \tilde{x}_1} + \frac{1}{\kappa}\frac{\partial}{\partial \tilde{x}_1}\right)\tilde{u}_i'(\tilde{\boldsymbol{x}}) + t^{-1}\tilde{u}_2'(\tilde{\boldsymbol{x}})\frac{\delta_{i1}}{\kappa \tilde{x}_2} \\ &+ t^{-1}\left(\frac{1}{\kappa}\ln(\tilde{x}_2 t) + B\right)\frac{\partial}{\partial \tilde{x}_1}\tilde{u}_i'(\tilde{\boldsymbol{x}}) + t^{-1}\tilde{u}_j'(\tilde{\boldsymbol{x}})\frac{\partial}{\partial \tilde{x}_j}\tilde{u}_i'(\tilde{\boldsymbol{x}}) + t^{-1}\frac{\partial \tilde{p}'}{\partial \tilde{x}_i} = 0. \end{aligned} \quad (4.166)$$

By using the identity $\ln(\tilde{x}_2 t) = \ln(\tilde{x}_2) + \ln(t)$, the two contributions of $\ln(t)$ cancel. Multiplying with t yields

$$\begin{aligned} &- \left(\tilde{x}_k\frac{\partial}{\partial \tilde{x}_k} + \frac{1}{\kappa}\frac{\partial}{\partial \tilde{x}_1}\right)\tilde{u}_i'(\tilde{\boldsymbol{x}}) + \tilde{u}_2'(\tilde{\boldsymbol{x}})\frac{\delta_{i1}}{\kappa \tilde{x}_2} \\ &+ \left(\frac{1}{\kappa}\ln(\tilde{x}_2) + B\right)\frac{\partial}{\partial \tilde{x}_1}\tilde{u}_i'(\tilde{\boldsymbol{x}}) + \tilde{u}_j'(\tilde{\boldsymbol{x}})\frac{\partial}{\partial \tilde{x}_j}\tilde{u}_i'(\tilde{\boldsymbol{x}}) + \frac{\partial \tilde{p}'}{\partial \tilde{x}_i} = 0. \end{aligned} \quad (4.167)$$

Reordering of the terms finally gives

$$\frac{1}{\kappa}\left(\left(\ln(\tilde{x}_2) - 1\right)\frac{\partial \tilde{u}_i'(\tilde{\boldsymbol{x}})}{\partial \tilde{x}_1} + \delta_{i1}\frac{\tilde{u}_2'(\tilde{\boldsymbol{x}})}{\tilde{x}_2}\right) - \tilde{x}_k\frac{\partial}{\partial \tilde{x}_k}\tilde{u}_i'(\tilde{\boldsymbol{x}}) + B\frac{\partial \tilde{u}_i'(\tilde{\boldsymbol{x}})}{\partial \tilde{x}_1} + \frac{\partial \tilde{p}'}{\partial \tilde{x}_i} + \tilde{u}_j'(\tilde{\boldsymbol{x}})\frac{\partial \tilde{u}_i'(\tilde{\boldsymbol{x}})}{\partial \tilde{x}_j} = 0. \quad (4.168)$$

For the continuity equation follows that

$$\frac{\partial \tilde{u}_i'}{\partial \tilde{x}_i} = 0. \quad (4.169)$$

Note that (4.168) establishes an equation for the eigenvalue κ and the parameter B together with (4.169). Equation (4.168) is also non-linear in the eigenfunctions similar to the linear shear case (cf. (4.44)). The solution of (4.169) in combination with the boundary conditions gives a value for κ. The boundary condition for the domain are given by

$$\tilde{u}_i' = 0, \quad \tilde{p}' = 0 \qquad \text{on } \partial\,\Omega, \quad (4.170)$$

where $\partial\Omega$ denotes the boundary of the domain Ω. In particular, it follows that the fluctuations quantities vanish in the far field for $\tilde{y} \to \infty$.
Multiplying the equation (4.168) with $\tilde{u}_i'$, integrating over the domain Ω, and using the divergence theorem gives a Rayleigh quotient for κ (Oberlack, 2020)

$$\kappa = \frac{2}{3}\int_\Omega \frac{\tilde{u}_1'\tilde{u}_2'}{\tilde{x}_2}d\tilde{V} \Big/ \int_\Omega \tilde{\boldsymbol{u}}'^2 d\tilde{V}. \quad (4.171)$$

It should be noted that a Rayleigh quotient has also been derived for linear shear flows in a similar way, cf. (4.56). Interestingly, in (4.171) the constant B does not appear explicitly. However, the solution of (4.169) requires the solution for both unknown parameters or eigenvalues κ and B and for the corresponding eigenfunctions. Formally, if the eigenvalue is defined as a vector of κ and B, this would correspond to a multiparameter eigenvalue problem by the definition of Volkmer (1988). In addition, the similarity variable $\tilde{\boldsymbol{x}}$ from (4.160) is complicated as it involves a time-dependency. The study of the log law problem is subject to further research.

4.6. Summary and outlook

A novel NEVP was derived based on the symmetries of the Euler equation. The velocity field is decomposed in a mean flow and fluctuations, which can be interpreted both from a stability theory or turbulence perspective. In the latter case, the splitting of the velocity is effectively a Reynolds decomposition. The symmetries hold for a large class of unbounded flows having a constant velocity gradient. This allows studying problems with linear shear, strain, and rotation. In addition, there is an extension to the log law region in wall-bounded flows. The eigenvalue results from the group parameters of the symmetries. There is a strong indication that the eigenvalues have a deep physical meaning. For linear shear flows, the eigenvalue λ is related to the exponential growth rate of energy, while for the log law the eigenvalue κ is van Kármán's constant.
We have shown that for the linearized NEVP, it is possible to formally find a solution for the eigenfunctions in the linear shear case. However, the solution has a free function that could not explicitly be determined to satisfy the boundary conditions. Therefore, the NEVP is solved numerically in the following chapters.

5. Numerical method for the linearized eigenvalue problem

The aim is to numerically solve the NEVP from Chapter 4. In the first step, the nonlinear terms are neglected. The full nonlinear algorithm is presented in Chapter 7.

Classification of the problem To numerically solve the problem, it is convenient to choose a pressure-free formulation. This has the advantage that no explicit treatment of the pressure is necessary. In addition, the memory demand decreases. For example, with a velocity-vorticity formulation, only two variables have to be stored compared to four variables in a primitive formulation (formulation in velocity and pressure), cf. Canuto et al. (2007).
For linear shear, the linearized equation from (4.72) for the eigenpair $(\tilde{u}_2, \lambda)$ reads

$$-\lambda\Delta\tilde{u}_2' - \lambda\tilde{x}_k\frac{\partial\Delta\tilde{u}_2'}{\partial\tilde{x}_k} + \tilde{x}_2\frac{\partial\Delta\tilde{u}_2'}{\partial\tilde{x}_1} = 0. \tag{5.1}$$

The shear rate A has been absorbed in the eigenvalue $\lambda/A \to \lambda$. The eigenvalue equation (5.1) is scalar and only contains the dependent variable $\tilde{u}_2'$. The variables $\tilde{u}_1', \tilde{u}_3', \tilde{p}'$ have been eliminated by substitution (see Chapter 4 for details). The derivatives are up to order 3 and contain mixed derivatives in $\tilde{x}_1, \tilde{x}_2, \tilde{x}_3$. It should be noted that the independent variable occurs as a coefficient in front of the derivatives.
It is assumed that the perturbations are inhomogeneous in all three spatial directions. We refer to an inhomogeneous direction as a direction with non-periodic perturbations. In contrast, the classical normal mode ansatz (3.10) in three dimensions has two homogeneous directions in space (Fourier transform or wavelike disturbances in x_1- and x_3-direction) and one inhomogeneous direction (with an amplitude function depending on x_2). The base flow is unbounded, i.e. no walls are prescribed and the domain for the two- or three-dimensional flow is $\mathbb{R}^2$ or $\mathbb{R}^3$, respectively. The fluctuations vanish in the far-field, i.e. we have

$$\tilde{u}_2' \to 0, \qquad \text{for } |\tilde{\boldsymbol{x}}| \to \infty. \tag{5.2}$$

The problem (5.1) with BC (5.2) has the form of a generalized eigenvalue problem. This can be easily shown by discretizing the equation, which leads to a matrix system of the form $\mathsf{A}\boldsymbol{x} = \lambda\mathsf{M}\boldsymbol{x}$.

Outline of the chapter In this chapter, we present a spectral method (Chebyshev and Hermite collocation) to discretize the linearized NEVP, e.g. (5.1) with BC (5.2) for linear shear. As already mentioned, the discretized equation gives a generalized matrix eigenvalue problem. Appropriate numerical solvers are presented. In addition, different techniques are discussed to filter out non-physical eigenvalues. Finally, we perform some test cases which demonstrate that discretization, solver, and filter routines work properly.

5.1. Spectral collocation

We use a spectral collocation method. This method has been proven for the numerical solution of eigenvalue problems in fluid mechanics (Canuto et al., 2007). In general, spectral methods have better convergence properties than e.g. finite difference or finite volume schemes. We start with a short summary of spectral methods. An introduction to this topic is also given by Gottlieb and Orszag (1977), Canuto (1988), Canuto (2006), and Canuto et al. (2007). The work of Kopriva (2009), Boyd (2000), and Trefethen (2000) gives practical advice for the implementation.

Weighted residual method

The different types of spectral methods can be best explained by starting with the weighted residual method (WRM) (Fornberg, 1996; Shen et al., 2011). The following summary is based on Shen et al. (2011). Consider a boundary value problem for a solution $u(x)$ given by

$$\mathcal{L}u(x) = f(x), \qquad x \in \Omega, \tag{5.3}$$

where $\mathcal{L}$ is a linear differential operator and the right-hand side is given by $f(x)$. The differential equation (5.3) is defined on a domain Ω and appropriate boundary conditions are prescribed. The exact solution $u(x)$ is approximated by a numerical solution $u^N(x)$ as a finite sum

$$u(x) \approx u^N(x) = \sum_{k=0}^{N} a_k \phi_k(x), \tag{5.4}$$

with trial (or basis) functions ϕ_k. The coefficients a_k are called expansions coefficients and have to be determined in the following. Substituting the solution $u(x)$ in (5.3) by the approximate solution $u^N(x)$ defined in (5.4) gives

$$R^N(x) = \mathcal{L}u^N(x) - f(x) \neq 0. \tag{5.5}$$

Here R^N denotes the residual which is in general non-zero. The idea of the WRM is eliminate the residual R^N by enforcing the following expression

$$\left(R^N(x), \Psi_j\right)_\omega := \int_\Omega R^N(x)\Psi_j(x)\omega(x)dx = 0, \qquad 0 \leq j \leq N, \tag{5.6}$$

where the $\Psi_j(x)$ denotes the test function and $\omega(x)$ is a positive weight function. By defining a set of $N+1$ collocation points $x_k = x_0, x_1, ...x_N$ the quadrature of the integral (5.6) can be expressed as a finite sum

$$\langle R^N, \Psi_j \rangle_{N,\omega} = \sum_{k=0}^{N} R^N(x_k)\Psi_j(x_k)\omega_k(x_k) = 0, \qquad 0 \leq j \leq N, \tag{5.7}$$

which is evaluated at collocation points x_k and ω_k are the weights of the selected numerical quadrature formula. Using the definition of R^N from (5.5) and expressing the numerical solution $u^N(x)$ by (5.4) finally allows to determine the set of coefficients a_k at the cost of solving a linear system of equations.
Spectral methods use both global trial functions ψ_j and global test functions Ψ_j. This is the

main difference to finite-difference or finite-element methods which use local test functions. Common trial functions in spectral methods are orthogonal polynomials. The different methods are named after their trial functions, for example,

$$\phi_k(x) = e^{ikx} \qquad \text{Fourier spectral method} \tag{5.8}$$
$$\phi_k(x) = T_k(x) \qquad \text{Chebyshev spectral method} \tag{5.9}$$
$$\phi_k(x) = H_k(x) \qquad \text{Hermite spectral method} \tag{5.10}$$

where T_k, H_k are the Chebyshev, Hermite polynomials of degree k, respectively. Fourier polynomials are a natural choice for periodic problems. Chebyshev polynomials are usually used for non-periodic problems on finite domains, while Hermite polynomials are considered for infinite domains. It should be noted that there are more polynomials (e.g. Legendre, Laguerre, and Sinc) considered in the literature (e.g. Weideman and Reddy (2000)) but beyond the scope of the present thesis. With the chosen method, the approximate solution can be expressed as finite sum according to (5.4).
The spectral method is further characterized by the choice of the test function Ψ_j. A Galerkin method uses the same test and trial functions ($\Phi_k = \Psi_k$), while a collocation method evaluates the residuals pointwise at collocations points, i.e. the test function is only non-zero at certain collocation points x_j.
In this work, we use collocation methods, which allow for simple implementation and adaptation of the code, its implementation is best described in e.g. Trefethen (2000). Concerning the trial functions, the focus of the present work is on Chebyshev polynomials with mapping and Hermite polynomials.

5.1.1. Chebyshev polynomials

The ansatz for $u^N(x)$ using a Chebyshev collocation method can be easily found by using the finite sum approximation (5.4) together with definition of the Chebyshev trial function from (5.9). For the numerical solution of $u(x)$, the Chebyshev expansion is truncated at order p

$$u^N(x) \approx \sum_{k=0}^{p} \hat{u}_k T_k(x), \tag{5.11}$$

where T_k is the Chebyshev polynomial of degree k defined as

$$T_k(x) = \cos(k\theta), \quad \theta = \arccos x. \tag{5.12}$$

It is possible to use a transformation $x = \cos(t)$ to recast a Chebyshev series into a Fourier series $T_x(x) = \cos(nt)$, cf. Boyd, 2000. The Chebyshev polynomials can be computed by a three-term recurrence relation, which is numerically stable and with cost $\mathcal{O}(N)$, cf. (Boyd, 2000)

$$T_0 = 1; \quad T_1 = x; \quad T_{n+1} = 2xT_n - T_{n-1}, \quad n = 1, ... \tag{5.13}$$

The collocation points (Gauss-Lobatto points) are given by

$$x_j = \cos\frac{\pi j}{N}. \tag{5.14}$$

For numerical implementation, a differential operator can be expressed by a differentiation matrix $\tilde{D}^j$

$$\frac{\partial^j}{\partial x^j} \to \tilde{D}^j. \tag{5.15}$$

An explicit formula for $\tilde{D}^1$ is given in appendix A.1. Different implementations are proposed, in order to improve the numerical accuracy of the differentiation matrices (Canuto et al., 2007). Indeed, the round-off errors can become quite large, especially for higher-order derivatives, see Baltensperger and Trummer (2003) and Don and Solomonoff (1997) for an introduction to that topic. Higher-order derivatives ($\tilde{D}^2, \tilde{D}^3, ...$) can be constructed by matrix-matrix-multiplication (e.g. $\tilde{D}^2 = \tilde{D} \cdot \tilde{D}$) or by explicit formulas, see e.g. Canuto et al. (2007).

Mapping of the unbounded domain

The problem (5.1) and with BC (5.2) from the introduction is defined on an infinite domain, whereas the Chebyshev polynomials are defined on $[-1, 1]$. Therefore, we seek a way to solve the physical problem with a finite numerical basis. Several techniques are proposed in the literature, the interested reader is referred to Shen and Wang (2009) and Shen et al. (2011) for an introduction. There are two approaches which can be applied here. The first approach is a domain truncation to a finite domain $x \in [-x_{\max}, +x_{\max}]$

$$x = x_{\max}\xi, \quad \xi = \frac{x}{x_{\max}}, \quad \xi \in [-1, 1] \quad x \in [-x_{\max}, +x_{\max}], \tag{5.16}$$

where a simple linear map is used. Note that nonlinear maps are also possible to obtain a better distribution of grid points, which is in general problem-dependent. Note that the cutoff length x_{max} is an additional numerical parameter in the problem. In general, the domain truncation is favorable if the solution decays fast to zero so that after a certain length the domain can be truncated (Canuto et al., 2007).
The second approach is a mapping of the infinite domain to a finite domain $[-1, 1]$. Different mappings are possible, however, the algebraic and exponential map is frequently used. The following summary is based on Canuto et al. (2007). An algebraic map is given by

$$x = L\frac{\xi}{\sqrt{1-\xi^2}}, \quad \xi = \frac{x}{\sqrt{x^2+L^2}}, \quad \xi \in (-1, 1), x \in (-\infty, +\infty). \tag{5.17}$$

The algebraic map leads to so-called rational Chebyshev functions TB_n, which are related to the Chebyshev functions T_n, cf. (Boyd, 1987)

$$TB_n(x) := T_n(\xi) = T_n\left(\frac{x}{\sqrt{x^2+L^2}}\right) = \cos\left(n \cot^{-1}(x/L)\right) \tag{5.18}$$

As a consequence, a differential problem on the real line can be mathematically recast into a cosine transform. It should be noted that L has to be increased with N to obtain spectral accuracy (Boyd, 2000). An exponential map is given by

$$x = L \tanh^{-1}\xi, \quad \xi = \tanh\left(\frac{x}{L}\right), \qquad \xi \in (-1, 1), x \in (-\infty, +\infty). \tag{5.19}$$

In addition, a domain truncation and some non-linear maps (i.e. more complicated maps than in (5.16)) can be combined. However, this usually gives two additional numerical parameters (cutoff length and mapping parameter) besides the parameter N.

Boundary conditions

There are two important issues concerning the boundary conditions. First, the problem is defined on an infinite domain. Second, third-order derivatives require in general the implementation of three boundary conditions.
For problems on unbounded domains, one can distinguish between behavioral and numerical boundary conditions. Behavioral boundary conditions enforce a certain behavior of the solution. For example, periodic solutions have the same values at the endpoints for multiples of a period. Another example is an unbounded function which is zero at the endpoints. If the basis functions for the collocation have the same behavior, it is in general not necessary to explicitly implement the boundary conditions in the discretized matrices. However, there might be cases for which this approach does not work, e.g. due to singularities of the differential equation. Here, numerical boundary conditions have to be implemented explicitly for the differential equations (Boyd, 2000).
For the equation from example (5.1), the boundary conditions have to be enforced explicitly, as the variable x_j appears as a factor in front of the derivatives and this would lead to infinite values for the coefficients through the mapping.
The implementation of third-order boundary conditions needs special attention. Note that the majority of textbook examples only covers second or fourth order derivatives (e.g. Poisson-type equations, Orr-Sommerfeld equations in Trefethen (2000)). There are only a few examples with third order derivatives in textbooks, cf. Shen et al. (2011).
From an analytical perspective, any third order differential equation on a finite domain requires three boundary conditions for a unique solution. Let us consider a solution $u_2(x)$ on a domain $[-1, 1]$ for a third order differential equation. Here two Dirichlet conditions are used together with one Neumann condition

$$u_2(\pm 1) = u_2'(-1) = 0. \tag{5.20}$$

The Dirichlet conditions can be treated in the same ways as for a second order operator, e.g. by eliminating the first and last row and column in the discretized matrix, for details refer to (Trefethen, 2000; Weideman and Reddy, 2000) To impose the Neumann condition, modified polynomials $\tilde{T}$ of the form

$$\tilde{T}_n(x) = (1 + x)T_n(x) \tag{5.21}$$

are used (Heinrichs, 1999). By differentiating the expression (5.21), it can be easily shown that the boundary conditions are fulfilled. The use of modified polynomials for fourth order differential equations (e.g. Orr-Sommerfeld equation) is usually referred to as clamped boundary conditions (Trefethen, 2000).
Finally, special care must be taken for the implementation of the mapped modified polynomials. In general, the matrix operations involved for mapping and applying the BC do not commute. Formally a chain rule applies, compare Solomonoff (1992) for a similar problem.

Multidimensional expansion of Chebyshev collocation

So far we have only considered the Chebyshev method in one dimension. The method can be easily extended to higher dimensions, for example, the two-dimensional analog to (5.11) is

$$u^N(x, y) \approx \sum_{k_1=0}^{p_1} \sum_{k_2=0}^{p_2} \hat{u}_{k_1,k_2} T_{k_1,k_2}(x, y), \tag{5.22}$$

with an approximation to order p_1 and p_2 in each spatial direction. For the numerical implementation, Kronecker products of the differentiation are used (Canuto et al., 2007) and a differential operator can be extended in the following way

$$\frac{\partial^{i+j}}{\partial x_1^i x_2^j} = D^j \otimes D^i := D_{i,j}. \tag{5.23}$$

The extension to three dimensions is straightforward and not shown here. An early applications of multi-dimensional Chebyshev methods can be found for example in Lin and Pierrehumbert (1988). Note that the multidimensional Chebyshev collocation leads to large matrices, as the Kronecker product of two matrices of size $N \times N$ results in a matrix of size $N^2 \times N^2$ In contrast, stability theory based on normal mode usually applies Chebyshev collocation in only one inhomogeneous direction, while the periodic directions are discretized using Fourier methods.

5.1.2. Hermite polynomials

The Hermite polynomials are an example of eigenfunctions defined on the real line. They can therefore be used for problems on unbounded domains without mapping. In particular, they are eigenfunctions of the Hermite equation and therefore give a very good approximation for this class of problems (Boyd, 2000). As Hermite polynomials $H_k(x)$ have a difficult asymptotic for $x \to \infty$ (exception: $H_0(x)$ is constant), it is convenient to use so-called Hermite functions for numerical purposes (Shen and Wang, 2009). They form a basis set defined as

$$\psi_n(x) = e^{-x^2/2} H_n(x), \tag{5.24}$$

where $H_n(x)$ is the Hermite polynomial of degree n (Boyd, 2000). The factor $\exp(-x^2/2)$ is a weight function ω_k in the general framework of (5.7), cf. Weideman and Reddy (2000). The collocation points are the roots of the polynomials $H_n(x)$. Hermite functions also have a three-term recurrence, similar to (5.13) for Chebyshev polynomials (Shen and Wang, 2009). Similar to Chebyshev polynomials, it is possible to create differentiation matrices, for explicit formulas the reader is referred to Funaro (1992).
The endpoints of the collocation points are finite values and grow as $\mathcal{O}(N)$ for $N \to \infty$ (Weideman and Reddy, 2000). In general, neither mapping nor a domain truncation is necessary. In this work, a scaled weight function $w(x) = \exp(-x^2 b^2/2)$ is used, cf. Boyd (2000). This allows to scale the collocation points with x_k/b. Finally, the extension to higher dimensions is done by Kronecker products (compare (5.23)).

5.2. Eigenvalue solver

With the discretization techniques presented in Chapter 5.1, it is possible to discretize eigenvalue equation for linear shear flow (5.1). The discretized equation has the form of a generalized eigenvalue problem

$$\mathsf{A}\boldsymbol{x} = \lambda \mathsf{M}\boldsymbol{x}, \tag{5.25}$$

where $\lambda \in \mathbb{C}$ is the eigenvalue. The terms corresponding to the matrix A and M and the eigenvector $\boldsymbol{x}$ are explained in the following. For sake of clarity, the PDE (5.1) is rewritten in a

different order

$$\tilde{x}_2 \frac{\partial}{\partial \tilde{x}_1} \Delta \tilde{u}_2' = \lambda \left(\Delta + \tilde{x}_1 \frac{\partial \Delta}{\partial \tilde{x}_1} + \tilde{x}_2 \frac{\partial \Delta}{\partial \tilde{x}_3} + \tilde{x}_3 \frac{\partial \Delta}{\partial \tilde{x}_3} \right) \tilde{u}_2'. \tag{5.26}$$

Obviously, the terms on the left hand side are given by a linear operator acting on $\tilde{u}_2'$. On the right hand side, there is a product of the eigenvalue λ and a linear operator acting on $\tilde{u}_2'$. The spectral collocation is evaluated at the collocation points $\xi_{i,1}, ..., \xi_{i,N}$ in each direction. The vector $\boldsymbol{x}$ with dimension N^3 contains the solution $\tilde{u}_2'(\xi_{1,j}, \xi_{2,j}, \xi_{3,j})$ at the collocation points and therefore reads

$$\boldsymbol{x} = \left(\tilde{u}_2'(\xi_{1,1}, \xi_{2,1}, \xi_{3,1}), ..., \tilde{u}_2'(\xi_{1,N}, \xi_{2,N}, \xi_{3,N}) \right). \tag{5.27}$$

In the following, it is assumed that the disretizations are identical in each spatial direction, i.e. in each direction we have $\xi_i = \xi_1, ..., \xi_N$. The extension to different discretizations for the spatial directions is straight-forward and only a matter of bookkeeping. We define the matrix Q (of size $N \times N$) containing ξ_i at the diagonal

$$Q_{ij} = \begin{cases} \xi_i & \text{for } i = j \\ 0 & \text{else.} \end{cases} \tag{5.28}$$

For the case of different discretizations in each direction this would correspond to different Q for each direction. We define the matrices X_j of dimension $N^3 \times N^3$ given by

$$\mathsf{X}_1 = \mathsf{Q} \otimes \mathsf{I} \otimes \mathsf{I}, \quad \mathsf{X}_2 = \mathsf{I} \otimes \mathsf{Q} \otimes \mathsf{I}, \quad \mathsf{X}_3 = \mathsf{I} \otimes \mathsf{I} \otimes \mathsf{Q}, \tag{5.29}$$

where I is the identity matrix of dimension $N \times N$ and $\otimes$ denotes the Kronecker product. The discretized Laplacian L reads

$$\mathsf{L} = D_\xi^2 \otimes \mathsf{I} \otimes \mathsf{I} + \mathsf{I} \otimes D_\xi^2 \otimes \mathsf{I} + \mathsf{I} \otimes \mathsf{I} \otimes D_\xi^2, \tag{5.30}$$

where the second derivative with respect to ξ is denoted by D_ξ^2. The resulting matrices read

$$\mathsf{A} = \mathsf{X}_2 \left(\mathsf{D}_\xi \otimes \mathsf{I} \otimes \mathsf{I} \right) \mathsf{L}, \tag{5.31}$$

$$\mathsf{M} = \mathsf{L} + \left[\mathsf{X}_1 \left(D_\xi \otimes \mathsf{I} \otimes \mathsf{I} \right) + \mathsf{X}_2 \left(\mathsf{I} \otimes D_\xi \otimes \mathsf{I} \right) + \mathsf{X}_3 \left(\mathsf{I} \otimes \mathsf{I} \otimes D_\xi \right) \right] \mathsf{L}, \tag{5.32}$$

where a matrix-matrix product is implied and D_ξ is the discretized operator for the first derivative with respect to ξ. The matrices A and M are of dimension $N^3 \times N^3$.
The aim is to numerically solve the (discretized) generalized eigenvalue problem (5.25) with A and M defined in (5.31) and (5.32) and $\boldsymbol{x}$ defined in (5.27). From a numerical perspective, there are two groups of eigenvalue solvers. The first are direct methods (QR/QZ routines). The second are iterative solvers (Boyd, 2000). We give a short introduction and discuss the advantages of each method. The matrices are in general dense and non-symmetric. No particular structure (e.g. band-structured entries) can be observed. Therefore specific routines (e.g. routines for symmetric matrices or sparsity preserving routines) are not discussed here, the reader is referred to Golub and van der Vorst (2000) for an extensive review.

5.2.1. Full spectrum

A standard eigenvalue problem

$$\mathsf{A}\boldsymbol{x} = \lambda\boldsymbol{x} \tag{5.33}$$

with a matrix A of dimension N has N eigenvalues. To compute the full spectrum of all N eigenvalues, a QR routine for standard (5.33) or a QZ routine for generalized eigenvalue problems (5.25) can be used. The main idea of the QR routine is briefly sketched. Consider a standard eigenvalue problem (5.33) where $\mathsf{A} \in \mathbb{R}^{N\times N}$. A Schur decomposition of the matrix A is defined as

$$\mathsf{Q}^*\mathsf{A}\mathsf{Q} = \mathsf{R}, \tag{5.34}$$

where $\mathsf{Q} \in \mathbb{C}^{N\times N}$ is a unitary matrix and $\mathsf{R} \in \mathbb{C}^{N\times N}$ is an upper triangular matrix. This decomposition has the interesting property that the eigenvalues λ_i of A are located on the diagonal of R. The spectrum of the matrix A can therefore be directly extracted from R. The QR algorithm aims at finding a decomposition of the matrix A in terms of Q and R (Dahmen and Reusken, 2008).
The QZ algorithm is an equivalent routine to the QR routine with the difference that the decomposition is applied on $\mathsf{B}^{-1}\mathsf{A}$, given that the inverse B^{-1} of B exists. As this operation is internally implemented, the rounding errors are usually smaller than performing the matrix operation first and calling a QR routine afterward (Dahmen and Reusken, 2008). It can therefore be used for generalized eigenvalue problems. Both QR and QZ algorithms are available for numerical libraries such as LAPACK (Anderson et al., 1999). There are several particularities (e.g. row shifts, deflation) in the numerical implementation of QR/QZ routines. The reader is referred to Kressner (2005) and Golub and Van Loan (2013) for more details.
The QR/QZ routines are widely used for the computation of the eigenvalue spectrum for stability problems, for example in Orszag (1971). The advantage is that the full spectrum is resolved and branches in the spectrum can be directly detected. The drawbacks are high computational costs and storage requirements. The operations scale with $\mathcal{O}(N^3)$ for a matrix of size $N \times N$, which blows up the computational time for large eigenvalue problems (Boyd, 2000).

5.2.2. Iterative solver

For large matrices, iterative solvers are a better choice. In particular, a multidimensional Chebyshev expansion (compare (5.23)) leads to very large matrices, which can only be efficiently solved by iterative methods, cf. Theofilis et al. (2003).
The main idea is to compute only a portion of eigenvalues rather than the complete spectrum. Only a few eigenvalues are computed by a user-specified criterion, for example, eigenvalues having the largest magnitude or largest real part. The storage requirement to compute k eigenvalues is $N \cdot \mathcal{O}(k) + \mathcal{O}(k^2)$ (Lehoucq et al., 1997). It is reported that they are used up to problem size with 384 GB of memory, e.g. Timme (2020) and Theofilis (2011) with massively parallel computing. The withdrawal is that no information of the full spectrum is given, as eigenvalues are calculated locally for some part of the spectrum (Boyd, 2000). In stability theory using normal modes, this is often the spectrum near $\omega_i = 0$ as this defines stability on instability (compare (3.12)).
There are different types of solvers, which are mainly based on Krylov subspace methods. For

more details refer to Stewart (2002). In the following, we focus on the implicitly-restarted Arnoldi algorithm which is implemented in the ARPACK library. The following explanations are based on the ARPACK manual (Lehoucq et al., 1997) if not indicated otherwise.

Basic idea of the Arnoldi algorithm

The implicitly restarted Arnoldi algorithm belongs to a class of Krylov methods. Detailed introductions and explanations of that algorithm can be found in the literature (Golub and Van Loan, 2013; Meerbergen and Roose, 1996). We limit our explanation to important aspects of the use of the ARPACK package. Consider a standard eigenvalue problem (EVP) defined by

$$\mathsf{C}\boldsymbol{x} = \lambda\boldsymbol{x}. \tag{5.35}$$

The vector $\boldsymbol{x}$ is iterated from an initial guess until convergence. Therefore a repeated matrix-vector operation of an iterated vector on the matrix C is required

$$\boldsymbol{w} \leftarrow \mathsf{C}\boldsymbol{v}. \tag{5.36}$$

The matrix C is not affected or changed by the algorithm. The iteration stops if the computed eigenvalue satisfies a user-specified tolerance.
The repeated calls of the matrix-vector routine (5.36) make ARPACK an efficient tool when it comes to large structured matrices, where the number of floating-point operations $\mathcal{O}(N)$ of (5.36) can be reduced compared to unstructured (dense) matrices with $\mathcal{O}(N^2)$. Iteration of 100 or more are possible so that the matrix-vector multiplication can be the bottleneck for the computation time and should be a suspect candidate for code optimization.

Conversion to standard EVP

The discretization of the linearized NEVP for linear shear in (5.1) gives a generalized eigenvalue problem (GEVP). However, GEVPs are only supported in ARPACK if M and A are symmetric (or Hermitian for complex matrices). As the matrices in (5.1) are non-symmetric, it is necessary to convert (5.1) to a standard EVP of the form (5.35). For non-singular M (i.e. an inverse M^{-1} exists) this can be achieved by the following transform

$$\mathsf{M}^{-1}\mathsf{A}\boldsymbol{x} = \lambda\boldsymbol{x}, \tag{5.37}$$

which gives a standard EVP as in (5.35) with $\mathsf{C} = \mathsf{M}^{-1}\mathsf{A}$. It is not recommended to perform the operation in (5.37) directly. In general, this converts sparse problems to dense ones. Instead, the matrix-vector product (5.36) is replaced by a matrix-vector multiplication and a solution of a linear system

$$\boldsymbol{z} \leftarrow \mathsf{A}\boldsymbol{v} \tag{5.38}$$

$$\mathsf{M}\boldsymbol{w} = \boldsymbol{z} \tag{5.39}$$

The second step (5.39) can be efficiently implemented using a *LU*-decomposition of the matrix $\mathsf{M} = \mathsf{LU}$ with forward and backward substitution, cf. Bornemann (2016).

User-specified eigenvalue search

ARPACK includes predefined settings to compute k eigenvalues with a certain property, for example, those with the largest or smallest magnitude. However, one may be interested in eigenvalues in the interior of the spectrum. For a GEVP (A, M) with an eigenpair $(\boldsymbol{x}, \lambda)$ this can be achieved by a shift and invert spectral transformation

$$(\mathsf{A} - \sigma\mathsf{M})^{-1}\,\mathsf{M}\boldsymbol{x} = \boldsymbol{x}\nu, \qquad \text{where} \quad \nu = \frac{1}{\lambda - \sigma}. \tag{5.40}$$

This transformation allows finding eigenvalues near a user-specified shift $\sigma \in \mathbb{C}$. The eigenvalues have to be transformed back by

$$\lambda_j = \sigma + 1/\nu_j \tag{5.41}$$

Again, the matrix inversion in (5.40) should not be performed explicitly. A substitution similar to the one in (5.39) should be used instead (Lehoucq et al., 1997).

5.3. Filtering of spurious modes

A curse in solving eigenvalue problems is the occurrence of spurious modes (Gottlieb and Orszag, 1977; Weideman and Trefethen, 1988; Boyd, 2000; Manning et al., 2008). These modes are numerically correct as they are solutions to the discretized eigenvalue problem. However, these modes are nonphysical solutions. If a differential operator with an infinite number of modes is discretized, only a portion of the modes is correctly represented by the discretization. High-frequency modes lack poor resolution and lead to spurious solutions. A rule-of-thumb for a one-dimensional problem on a bounded domain is that about one-half of the modes are spurious. For problems on an infinite domain, the percentage of spurious modes is in general higher (Boyd, 2000).
Different approaches to handling spurious modes are presented in the literature. In the context of the Orr-Sommerfeld equation, modified polynomials are proposed (similar as shown in (5.21)), to reduce the number of spurious modes as e.g. implemented by Zebib (1987), McFadden et al. (1990), and Gardner et al. (1989). However, spurious modes may persist.
Another approach is to filter out spurious modes from the calculated spectrum. For a full spectrum (QZ-algorithm) the eigenvalues are therefore computed for two different resolutions. These two spectra are then compared and only the values which change little according to a certain metric are kept, for details refer to Boyd (2000) and Gheorghiu (2020a). Some spectral codes (e.g. *Chebfun*) already implement these filtering techniques by default, cf. Driscoll et al. (2008). In the following, we present some metrics from Boyd (1996) and Boyd (2000). The eigenvalues are sorted according to their magnitude and the absolute ordinal drift is calculated by

$$\delta_{j,\text{ordinal}} = \left|\lambda_j^{(N_1)} - \lambda_j^{(N_2)}\right|, \tag{5.42}$$

for two sets of numerical solutions, indicated by the superscript (N_1) and (N_2). For different resolutions, it can happen that spurious modes enter somewhere between these values. So it might be better to find the eigenvalues with the smallest difference between them (nearest neighbor), given by

$$\delta_{j,\text{nearest}} = \min_{k\in[1,N_2]} \left|\lambda_j^{(N_1)} - \lambda_k^{(N_2)}\right|. \tag{5.43}$$

In some eigenvalue problems, for example, the Legendre equation, there is a scaling of the j-th eigenvalue as $\mathcal{O}(j^2)$. Therefore a certain metric of how fast the eigenvalues grow can be used. This is named intermodal separation and is defined as (Boyd, 1996)

$$\sigma_j = \begin{cases} |\lambda_1 - \lambda_2| & j = 1 \\ \frac{1}{2}\left(|\lambda_j - \lambda_{j-1}| + |\lambda_{j+1} - \lambda_j|\right) & j > 1. \end{cases} \tag{5.44}$$

Boyd (1996) proposes to plot the r_j values to find eigenvalues that change little. A large value of r_j is an indicator that the mode is non-spurious. These values are given by

$$r_{j,\text{ordinal}} = \frac{\min(|\lambda_j|, \sigma_j)}{\delta_{j,\text{ordinal}}}, \tag{5.45}$$

$$r_{j,\text{nearest}} = \frac{\min(|\lambda_j|, \sigma_j)}{\delta_{j,\text{nearest}}}. \tag{5.46}$$

A third technique is to calculate the Chebyshev coefficients of the eigenfunction. This can be done by the so-called Chebyshev approximation formula, see e.g. Press (1996). If the solution is known as a closed analytical expression, e.g. as a polynomial, the calculation of the Chebyshev coefficients can be implemented using a fast Fourier transform (Gentleman, 1972; Townsend, 2014). For a discretized solution from a numerical solver, we can use the Chebyshev approximation formula. Given that we know the discretized solution of the eigenfunctions $u_2^N(x_k)$ with N collocation points in one dimension, we can calculate the Chebyshev coefficients by

$$c_j = \frac{2}{N} \sum_{k=1}^{N} u_2^N(x_k) T_j(x_k), \tag{5.47}$$

where the Chebyshev polynomials $T_j(x_k)$ can be easily obtained from (5.13). Further, it is possible to reconstruct the solution based on the Chebyshev coefficients as a Chebyshev series, which can give further insights. The eigenfunction can be approximated by

$$u_2 \approx \sum_{k=0}^{N-1} c_k T_k(x) - \frac{1}{2} c_0. \tag{5.48}$$

Note that the reconstruction in (5.48) can also be done by taking the sum including the N-th term. However, if the coefficients are characterized by an exponential decay (or at least a sufficiently fast decay), this contribution is usually very small.
The extension of (5.48) to higher dimensions is shown in Appendix A.3. The relation between the coefficients can also be expressed as matrix-vector products

$$\boldsymbol{u}^N = \mathsf{T}\boldsymbol{c}, \qquad \boldsymbol{c} = \mathsf{T}^{-1}\boldsymbol{u}^N, \tag{5.49}$$

where $\boldsymbol{c}$ is the vector containing the coefficients, and T is a matrix containing the Chebyshev polynomials of different orders evaluated at the collocation points, and $\boldsymbol{u}^N$ is the numerical solution (Peyret, 2002). In addition, the one-dimensional series in (5.48) differentiated symbolically (using CAS) and inserted into the differential equation to calculate a residual.
A different criterion without calculating (5.48) explicitly is to investigate the Chebyshev coefficients. Spurious modes are usually associated with non-decaying and oscillating coefficients

(Boyd, 2000).
There are other filtering techniques that are not used in this work. However, we mention them for sake of completeness. Another approach is to compute the orthogonality of the eigenvectors. This approach can also be used if the solution is not known a priori (Gheorghiu, 2018). To our knowledge, this was first used in Bailey et al. (1978) for Sturm-Liouville problems. A different approach is to use certain symmetries in the eigenvalue spectrum. For example, if the spectrum is a priori known to be symmetric, all the modes which do not have a symmetric counterpart can be rejected (Kitsios, 2010).

5.4. Implementation

To solve the eigenvalue problem defined in Chapter 4 it is convenient to design and implement a software framework. It is acknowledged that there are existing software packages (Driscoll et al., 2014) as well as Fortran and MATLAB routines (Canuto, 1988; Weideman and Reddy, 2000; Trefethen, 2000; Schmid and Henningson, 2001) publicity available for spectral eigenvalue problems. These codes provide the flexibility to study a large number of one-dimensional eigenvalue problems. In the context of stability theory, they can be used to discretize and solve the Orr-Sommerfeld equation.
On the contrary, the NEVP defined in Chapter 4 has some particularities as unbounded domains, variable coefficients depending on x_j, third-order derivatives, and two-or-three inhomogeneous directions. These aspects need careful implementation and testing. In addition, parallel computation with distributed memory is necessary to solve multidimensional problems. To the author's knowledge, there is no out-of-the-box solution for this problem type publicly available. Therefore, we decided to write our own software for this application. The three main goals are:

- High-performance computing: Multidimensional eigenvalue problems lead to large matrices with a large memory demand. It is therefore necessary for production runs to use a high-performance language (Fortran) with parallel computing standards (in particular the message passing interface (MPI) standard).
- Full user control of all parameters: the user has full access to all parameters of the discretization (polynomial, collocation points, mapping parameters), MPI parallel data distribution (number of cores, block sizes for distributed matrices), eigenvalue solver routines (full or iterative solver, number of iterations, tolerance), and filtering (metric, tolerance).
- Ease of use in implementing new equations: In Chapter 4 we show different applications of flows with constant velocity gradients. Differentiation matrices and Kronecker products are available from routines, such that new equations can be easily implemented.

Serial implementation A serial implementation in Fortran can be done as follows. For the discretization, existing MATLAB routines for Chebyshev (Trefethen, 2000) and Hermite (Weideman and Reddy, 2000) differentiation matrices were ported to Fortran. Linear algebra routines (e.g. matrix-vector multiplication) were called from the library LAPACK. The implementation was tested extensively against MATLAB code giving the same results up to machine epsilon. Note that MATLAB internally also implements LAPACK routines, cf. Bornemann (2016). The eigenvalue solvers for the full spectrum were called from LAPACK. The iterative solution of

the eigenvalue problem is done from ARPACK (Lehoucq et al., 1997). Note that generalized non-symmetric eigenvalue problems have to be transformed to standard eigenvalue problems which was done using LAPACK routines.

Parallel implementation The serial code is parallelized in Fortran using MPI. The parallel routines from ScaLAPACK (Blackford, 1997) and PARPACK (Maschho and Sorensen, 1996) were called instead of their serial implementations. The basic approach is as follows. The data is distributed over the processors with a block-cyclic layout. In other words, the global matrix is split into blocks that are distributed in a certain order over the processor grid. ScaLAPACK uses the BLACS communicator and provides MPI routines for data manipulation across the processor grid.
However, parallelization involves several challenges. To our knowledge, there is no simple routine available for the parallel Kronecker product from ScaLAPACK. Therefore the routines for the matrix assembly are written using elementary MPI communicators.
Concerning the eigenvalue solver for the full spectrum, there is only a parallel implementation for standard eigenvalue problems. Therefore conversion is necessary. Note that PARPACK uses a row-cycling layout. For performance reasons, matrix redistribution routines between a row-cyclic layout and block-cyclic layout are used. These routines are available from ScaLAPACK.
At run-time, there are two main issues. First, the choice of the block size impacts the parallel communication effort and therefore the performance. The block size is varied within the recommended range from literature (Choi et al., 1996; Blackford, 1997) to reduce computational time. Note that the optimal values also depend on other factors such as computational architecture and latency times.
Second, it is necessary to call linear solvers within this framework, for example, to calculate the velocity u_1 from u_2. Another application is the iterative solution of non-linear equations, where a linear system has to be solved in each iteration (the details are given in Chapter 7.3). However, the linear solvers from ScaLAPACK are direct solvers and have a poor scaling in performance for larger problems (Schäfer, 1999). As ScaLAPACK only contains direct solvers turned out to be a bottleneck at runtime, we decided to use iterative solvers from the PETSc library (Balay et al., 2021). In that way, it is also possible to call iterative eigenvalue solvers from the related SLEPc package (Hernandez et al., 2005).

Post-processing routines Routines for the post-processing of the data are provided within the software framework. This includes the filtering and the approximation of Chebyshev coefficients (cf. Chapter 5.3). Moreover, an interface to MAPLE (CAS) is provided to analytically reconstruct the Chebyshev series and calculate the residuals. In addition, some auxiliary routines are provided to track the memory demand on run time. The code can be compiled with a profiling option, which calls Score-P (Knüpfer et al., 2012) at runtime and allows for performance analysis after job completion.

5.5. Test cases

The software framework has been designed and implemented by the author. Most of the routines for the matrix assembly and eigenvalue filtering are based on code written by the author. Therefore all routines and functions have to undergo careful testing. The purpose of this section is two-fold. First, we show that the implementation works correctly. Second,

the findings help to select appropriate numerical parameters (number of collocation points, mapping parameter) and filtering routines.

5.5.1. Choice of mapping parameter (1D)

The code was tested for different 2nd order PDEs and EVPs on finite and infinite domains. The results from the literature could be successfully reproduced. In the following, we focus on third order differential equations defined on finite domains. A test case is constructed using the method of manufactured solutions, cf. Roache (2019). The BVP reads

$$u_{xxx} + u_x = \mathcal{F}, \qquad u(\pm\infty) = 0, \quad u'(\infty) = 0. \tag{5.50}$$

The forcing term on the RHS depends on the solution of $u(x)$. We use typical test cases (see e.g. Shen et al. (2011)) for the solutions with their specific RHS

$$u(x) = \exp(-x^2), \quad \mathcal{F} = 10xe^{-x^2} - 8x^3e^{-x^2}, \tag{5.51}$$

$$u(x) = \frac{1}{x^2+1}, \quad \mathcal{F} = -\frac{48x^3}{(x^2+1)^4} + \frac{24x}{(x^2+1)^3} - \frac{2x}{(x^2+1)^2}. \tag{5.52}$$

We denote (5.51) as the exponentially decaying and (5.52) as the algebraically decaying test case.

Influence of the mapping parameter For problems on unbounded domains, the quality of the numerical solution depends on the number of collocation points and the mapping parameter (Boyd, 2000). For Chebyshev collocation, an exponential map (5.19) formally maps the physical domain $x \in [-\infty, \infty]$ to a numerical basis $\xi \in (-1, 1)$. In the implementation, the points $\xi \pm 1$ are excluded (effectively they are Dirichlet BC). The reason is that for problems with coefficients depending on x (like the NEVP (5.1)), this would otherwise give infinite values.
A numerical solution shows that the mapping parameter has an important effect on the quality of the solution. This qualitative result is shown in Figure 5.1 for two different mapping parameters. The choice $L = 1.0$ gives good results, while the choice $L = 0.25$ does not approximate the analytical solution.
We consider the L_2-norm of the error $\|\boldsymbol{u} - \boldsymbol{u}^N\|_2$ evaluated at the collocation points. In Figure 5.2a we show how the error depends on the mapping parameter L. There seems to be a minimum the error for $L = 10$. This corresponds to an effective domain length of $\hat{L} \approx 41.63$ (magnitude of the outer points of the collocation grid). Note that the function 5.51, is already of order 10^{-16} for $x \approx 6$ and numerically zero at $\hat{L}$. The dependence of N is shown in the Figure 5.2b for a constant L. Interestingly, it was not possible to find an error as low as for the left figure. Moreover, the error grows for values The reasons can be that the collocation points are distributed in a way that they do not capture the main structure of the function, e.g. many points are located in a domain where the function is nearly zero. The second reason is rounding errors for larger differentiation matrices.
In that sense, it is not the right way to simply increase N but to wisely choose a corresponding scaling parameter L. If the solution is known as in this example, the domain width can be adjusted accordingly. However, if the solution is not known a priori, it is necessary to iterate both N and L to reduce the error (Boyd, 2000).

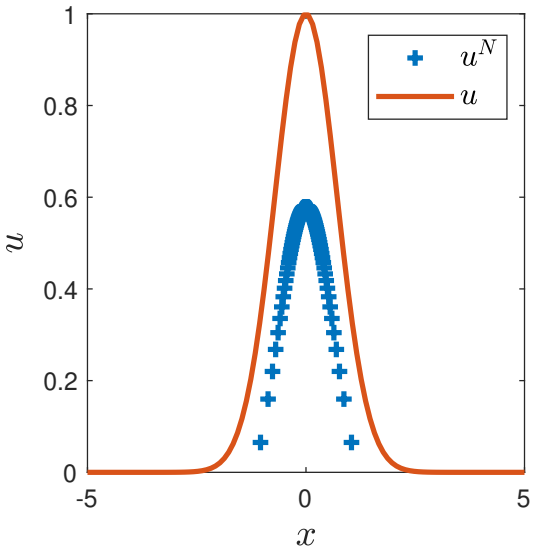

(a) $L = 0.25$

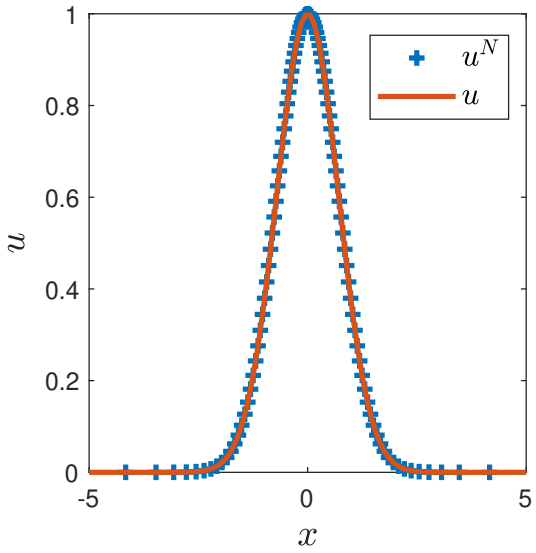

(b) $L = 1.0$

Figure 5.1.: Test case in 1D: Chebyshev collocation with exponential mapping, $N = 101$ with different mapping parameter L.

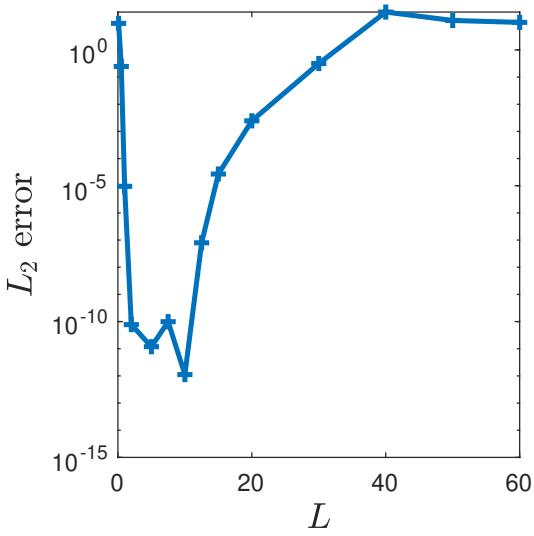

(a) Variation of $L = 0.1 - 60$ with constant $N = 101$

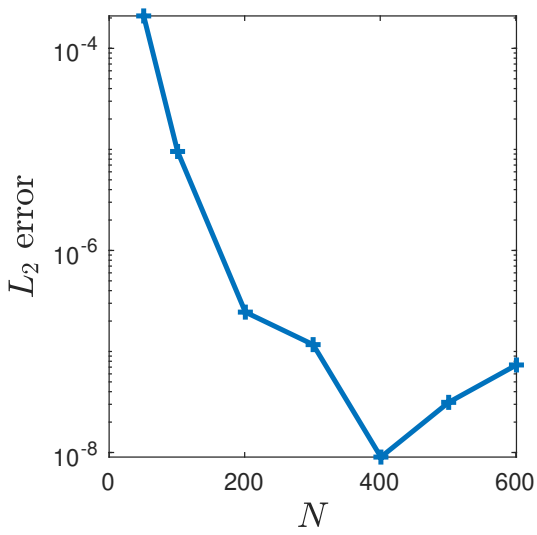

(b) Variation of $N = 51 - 601$ with constant $L = 1.0$

Figure 5.2.: Test case in 1D: Chebyshev collocation with exponential mapping, Variation of N and L.

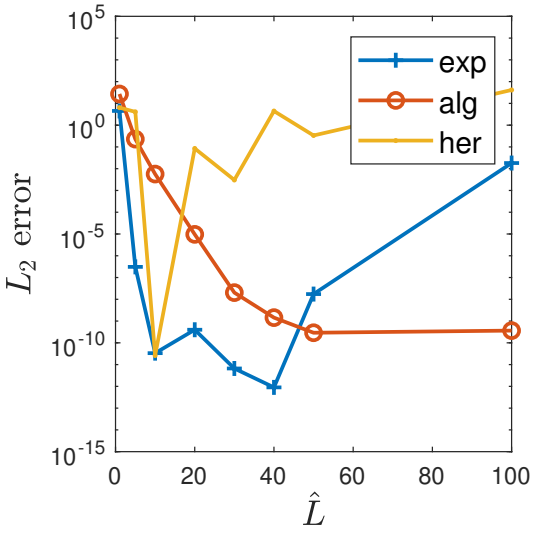

(a) Variation over the effective length $\hat{L}$, exponentially decaying test case

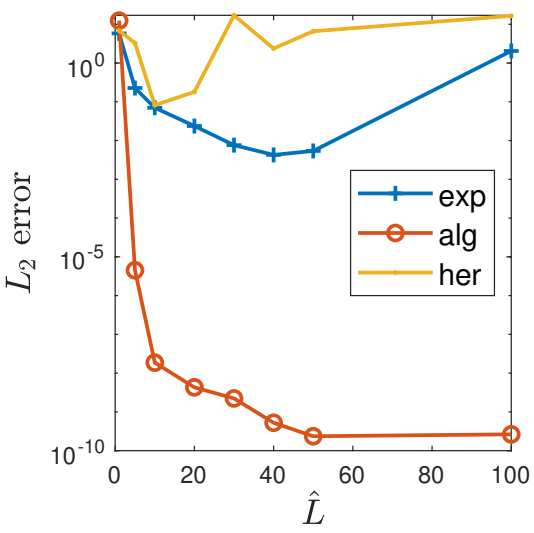

(b) Variation over the effective length $\hat{L}$, algebraically decaying test case

Figure 5.3.: Test case in 1D: Spectral collocation with Chebyshev polynomials with exponential and algebraic map, and Hermite polynomials. The calculations are done with $N = 100$ collocation points.

Choice of the polynomial The previous examples apply Chebyshev collocation with exponential mapping. It is interesting to see the difference between exponential maps, algebraic maps, and the use of Hermite polynomials. Figure 5.3a shows the results for the exponentially decaying test case (5.51) . The $L2$-error is plotted over the effective domain length. The Chebyshev collocation with an exponential map gives good results for moderate $\hat{L}$. The Hermite collocation is even more dependent on a good choice of L (or $\hat{L}$). The algebraic map gives relatively good results from a certain $\hat{L}$ and is not that much dependent on the choice of L from that point on.
Figure 5.3b shows the results for the algebraically decaying test case (5.52). Here we see, that the Chebyshev polynomials with exponential map and the Hermite polynomials do not give good results. By definition, the algebraic map is a good choice for algebraically decaying functions. Both test cases are also calculated with a simple domain truncation, which does not give any satisfactory results.

The test case with the algebraic decay shows that slow decay is a challenge in selecting the appropriate map. Another aspect is possible singularities in the solutions. As we focus on smooth solutions with a sufficiently fast decay, we do not consider this possibility here. The interested reader is referred to Boyd (2000) for an introduction.

5.5.2. Multidimensional examples (2D and 3D)

The discretization of problems in higher dimensions involves the use of Kronecker products (compare 5.23). To test the implementation for higher dimensions, we use a linear operator $\mathcal{L}$ which is similar to the linearized NEVP operator for linear shear. The test case is written as a

BVP with a manufactured solution $u(x_1, x_2)$ or $u(x_1, x_2, x_3)$, and a RHS given by $\mathcal{F}$ as

$$\mathcal{L}u = \mathcal{F}. \tag{5.53}$$

Test case 2D The linear operator $\mathcal{L}$ is obtained from (4.85) by setting $\lambda = 1$ and $A = 1$, which gives

$$\mathcal{L} = -\Delta - x_1 \frac{\partial \Delta}{\partial x_1} - x_2 \frac{\partial \Delta}{\partial x_2} + 2x_2 \frac{\partial \Delta}{\partial x_1}, \tag{5.54}$$

and the test solution reads

$$f = \exp\left(-ax_1^2 - bx_2^2\right), \qquad a, b \in \mathbb{R}^+, \tag{5.55}$$

where the parameters a and b control the decay rate. The corresponding RHS corresponding to 5.53 is given by

$$\begin{aligned} \mathcal{L}f = 8e^{-ax_1^2 - bx_2^2} \Bigg(& x_1^3 \left(x_1 - 2x_2\right) a^3 + x_1 \left(b x_1 x_2^2 - 2x_1 + 3x_2\right) a^2 \\ & + \left(-\frac{1}{2} + x_1(x_1 - 2x_2)b\right) \left(b x_2^2 - \frac{1}{2}\right) a + b^3 x_2^4 - 2b^2 x_2^2 + \frac{b}{4} \Bigg). \end{aligned} \tag{5.56}$$

Equation (5.53) is solved with boundary conditions $|u| \to 0$ as $|x_j| \to \infty$. The equation is discretized using Chebyshev collocation with exponential mapping. Note that algebraic maps gives rather badly scaled matrices which should be avoided. Technically speaking, the condition numbers are large, see Schäfer (1999) and Bornemann (2016) for a longer discussion on the topic of solving linear systems. Second order boundary conditions are applied. Note that the results showed better convergence than using third order boundary conditions. The linear system is solved and the L_2-error of the difference between the numerical and the analytical solution is shown in figure 5.4. Here the parameters are chosen to have different convergence rates in x_1 and x_2 directions. This test case is also used to test different mapping parameters for the different directions.

Test case 3D The linear operator in the 3D case from (4.85) with $\lambda = 1$ and $A = 1$ reads

$$\mathcal{L} = -\Delta - x_1 \frac{\partial \Delta}{\partial x_1} - x_2 \frac{\partial \Delta}{\partial x_2} - x_3 \frac{\partial \Delta}{\partial x_3} + 2x_2 \frac{\partial \Delta}{\partial x_1}, \tag{5.57}$$

with a test solution

$$u(x_1, x_2, x_3) = e^{-aq^2}, \qquad \text{with } q^2 = x_1^2 + x_2^2 + x_3^2 \tag{5.58}$$

and a RHS given by

$$\mathcal{F} = 8e^{-aq^2} a \left(0.75 + q^2(q^2 - 2x_1x_2)a^2 + (-3q^2 + 5x_1x_2)a\right) \tag{5.59}$$

with boundary conditions $|u| \to 0$ as $|x_j| \to \infty$. The equation is discretized using Chebyshev polynomials with exponential mapping (with Dirichlet boundary conditions). Additionally, a test case based on the Poisson equation is implemented. The Poisson equation with an exact solution (5.58) reads

$$\left(\frac{\partial^2}{\partial x_1^2} + \frac{\partial^2}{\partial x_2^2} + \frac{\partial^2}{\partial x_3^2}\right) u(x_1, x_2, x_3) = \left(4a^2q^2 - 6a\right) \exp(-aq^2) \tag{5.60}$$

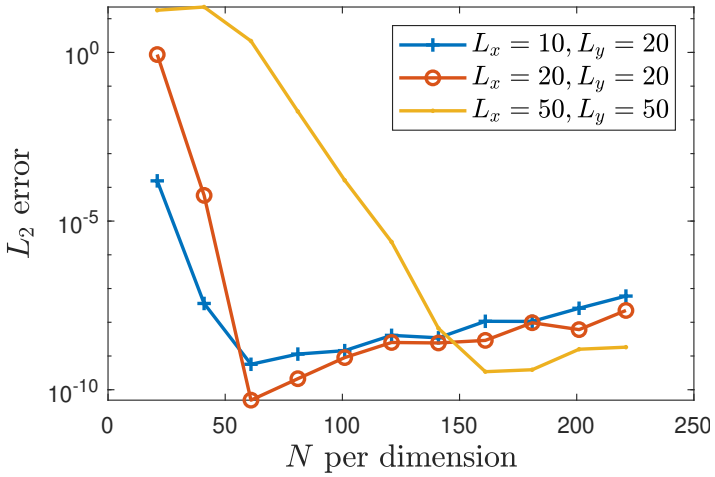

Figure 5.4.: Test case in 2D: L_2 error between the numerical and the analytical solution (5.55), shown for parameter $a = 0.1$ and $b = 0.01$, Chebyshev collocation with exponential map and N collocation points in each direction, the mapping parameters are shown in the legend.

The use of two test cases allows for comparing the convergence rate of third order derivatives with variable coefficients in (5.57) with second order derivatives in (5.60). The L_2-convergence of the residuals is shown in figure 5.5. We see that the residuals converge. The refinement is done up to $N = 91$ collocation points in each direction. Note that this corresponds to a discretized matrix with 90^6 entries in double precision, which requires in total approximately 3.9 terabyte [TB] of memory.

5.5.3. Eigenvalue filtering

The boundary value problem in (5.56) can be rewritten as a generalized eigenvalue problem

$$\mathcal{L}f = \lambda \mathsf{M} f \tag{5.61}$$

where the linear operator $\mathcal{L}$ is given in (5.54) and the solution f in (5.55). The operator $\mathcal{M}$ implies the multiplication of f by an expression depending on x_1 and x_2 as follows

$$\begin{aligned}\mathcal{M} = 8\Big(& x_1^3 \left(x_1 - 2x_2\right) a^3 + x_1 \left(b x_1 x_2^2 - 2x_1 + 3x_2\right) a^2 \\ & + \left(-\frac{1}{2} + x_1(x_1 - 2x_2)b\right)\left(b x_2^2 - \frac{1}{2}\right) a + b^3 x_2^4 - 2b^2 x_2^2 + \frac{b}{4}\Big).\end{aligned} \tag{5.62}$$

The problem (5.61) together with the boundary conditions $|f| \to 0$ as $|x| \to \infty$ constitutes a generalized eigenvalue problem. From (5.56) we know that $\lambda = 1.0$ and $f(x_1, x_2)$ given by (5.55) is an exact solution for the problem.
The GEVP (5.61) is discretized using Chebyshev polynomials with exponential mapping and the full eigenvalue spectrum for two resolutions $N = 61$ and $N = 81$ is calculated. After applying the boundary conditions we have a set of 3600 eigenvalues (for $N = 61$) and 6400 eigenvalues (for $N = 81$). The aim is to filter out spurious eigenvalues.

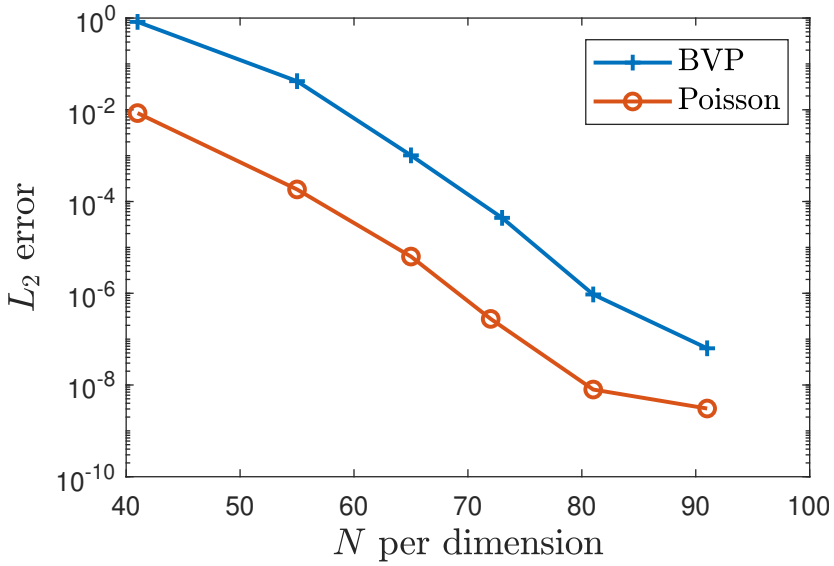

Figure 5.5.: 3D test case: L_2-error of the residuals, Chebyshev collocation, exponential mapping $L = 10$ for the 3D BVP from (5.53) with (5.57) and (5.59) and the Poisson equation from (5.60). The exact solution is given in (5.58) with $a = 1$.

EV(r_{ordinal})	EV(r_{nearest})	EV(r_{neighbor})
6.403e-06	1	-3.6352e-05
-5.5867e-06	-27.9764	-3.7768e-06
-1.2034e-05	0.10957	-2.3986e-06
-7.1652e-06	914.5045	-3.2599e-05
1.0416e-05	-211.4281	-0.00024621

Table 5.1.: Five eigenvalues with the best filtering metrics according to criterion r_{ordinal}, r_{nearest} and r_{neighbor}

Calculation of the metrics r_j In the first step, the spectrum from the two resolutions is compared. Following the approach of Boyd (1996) the value of r_j defined in (5.45) and (5.46) is calculated. In addition, we use the inverse of the nearest neighbor as a third filter criterion (i.e. without intermodal separation). The results after the filtering are shown in table 5.1 for the 5 eigenvalues having the best metric. The results show that the eigenvalue $\lambda = 1.0$ is only found by the metric r_{nearest}. However, if the correct eigenvalue is not known a priori, further analysis of the eigenpair is necessary. The corresponding eigenfunctions provide more information. Some solutions can be directly rejected by optical inspection (e.g. if they do not satisfy the boundary conditions). An automated selection can be done by calculating the Chebyshev coefficients.

Calculation of the Chebyshev coefficients The Chebyshev coefficients for the two-dimensional eigenfunction are calculated from the Chebyshev approximation formula (see (5.47) for the 1D case or Appendix A.3 its extension to 2D). This routine is successfully tested for 1D examples against existing implementations (e.g. *Chebfun*). The approximation of the five eigenvalues from Table 5.1 shows that only the eigenfunction for $\lambda = 1.0$ has rapidly decaying coefficients. The other four eigenfunctions do not have such a decay. The first 10 Chebyshev coefficients

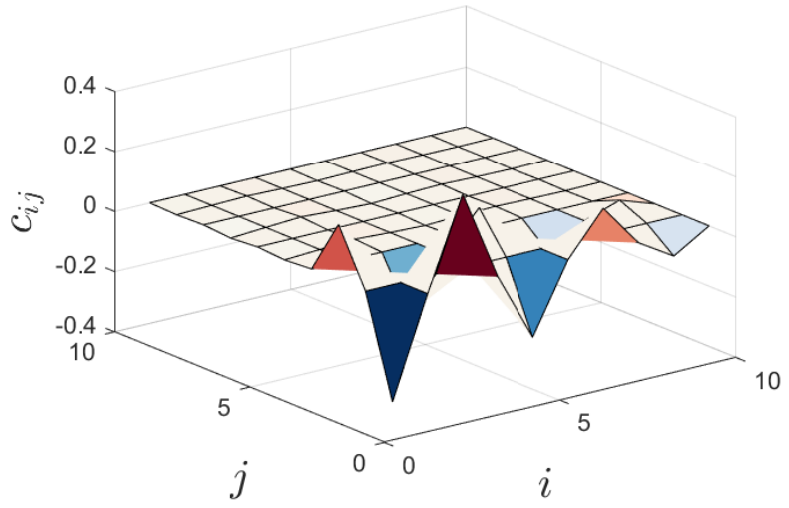

Figure 5.6.: Approximated Chebyshev coefficients of the filtered eigenfunction for $\lambda = 1.0$.

in both directions (in total 100 coefficients) are shown in Figure 5.6. Note that most of the information of the eigenfunction is therefore already stored in the leading coefficients. The odd coefficients are close to zero. This indicates a reflection symmetry $x \to -x$ and $y \to -y$, which is in line with the analytical solution (5.55). In this case, the discrete symmetry could be exploited to reduce the size of the discretized matrices, see e.g. Boyd (1986) and Boyd (2000) for some examples. Moreover, the Chebyshev coefficients can be used to calculate residuals by inserting the reconstructed series solution into the differential equation. However, this usually needs rapidly decaying coefficients, in the sense that higher-order coefficients are negligible. The reason is that the coefficients of Chebyshev polynomials are growing as 2^{k-1} for a truncated Chebyshev series of order k. This can be best seen from the recursion formula (5.13). Due to this growth of coefficients, the computed solution must have already a fine resolution. Otherwise, the numerical errors become too large. From the author's experience, higher-order contributions of non-zero Chebyshev coefficients often arise if the approximated solution does not perfectly satisfy the boundary conditions. This is the case for problems on unbounded domains and is observed frequently for the problems in this thesis. Therefore the practical use of residuals from a series reconstruction for the EVP is very limited in our experience.

This example shows that the value we seek for is only found by the metric r_{nearest}. The L_2 residual of the eigenfunction is $1.5 \cdot 10^{-3}$ and the difference between the numerical eigenvalue λ^N and the exact eigenvalue λ is $|\lambda - \lambda_N| = 3.70 \cdot 10^{-6}$. Our conclusion from this example is that the $r_{nearest}$ filter works best. In addition, we see the calculation of the Chebyshev coefficients is a valuable tool to identify spurious modes.

5.6. Summary

A spectral method based on mapped Chebyshev or Hermite polynomials can be used to discretize the linearized equations of the NEVP from Chapter 4. The discretized generalized eigenvalue

problem can be solved both for a full spectrum or iteratively around certain values of interest. As inhomogeneity is assumed in all spatial directions, this leads to large matrices, which makes the use of MPI routines necessary. The calculated eigenvalues should be carefully analyzed, as spurious modes frequently occur in generalized eigenvalue problems. Therefore different filtering techniques (e.g. distance metrics and decay of Chebyshev coefficients) are proposed. The test cases show that the discretization and filtering routines are correctly implemented for the 2D and 3D cases.

6. Results for the linearized eigenvalue problem

The numerical solution of the linearized NEVP from Chapter 4 is presented. The results are obtained with the software framework presented in Chapter 5.4 by first solving the eigenvalue problem for different numerical parameters (in particular collocation points and mapping parameters) and filtering the results afterward. The findings are discussed in the light of stability theory. In addition, a comparison with experimental and DNS data from turbulent flows is presented. As dimensionality may alter stability results, the present chapter is divided into results from 2D and 3D flows.

6.1. Two-dimensional flows

The approach for two-dimensional flows is the following: The eigenvalue equations for flows with constant velocity gradient from Chapter 4 are discretized using Chebyshev and Hermite polynomials. The full spectrum is computed, which reveals the location of all eigenvalues and possible branches in the spectrum Note that we numerically solve EVPs embedded in a completely new stability theory. Therefore we have little information on the spectrum a priori. In comparison, in normal mode theory (cf. ansatz (3.10) and (3.11)), it often suffices to seek eigenvalues near the neutral curve $\omega_i = 0$ to check for unstable modes. This is appropriate if the corresponding eigenvalue has already been intensively studied. However, this is the first numerical study of such a NEVP. Thus, we decided to resolve the full spectrum. This may also give information on branches or complex conjugate eigenvalues in the eigenvalue spectrum. Due to the occurrence of spurious modes in the solution, the calculations are done for different resolutions (number of collocation points).
The general approach is as follows:

1. The full spectrum is calculated for two different set of numerical parameters (e.g. different number of collocation points).
2. The data from the two spectra are filtered with a distance metric.
3. The eigenfunctions of the filtered eigenvalues are investigated and their Chebyshev coefficients are calculated.
4. The eigenpairs with sufficient decay from step 3 are further investigated (by using iterative solvers with shift-invert transformation for higher resolutions).

6.1.1. Linear shear

The full spectrum of (4.72) (with $\mathcal{N}_2 = 0$ from (4.73)) is solved for a resolution of $N = 141$ collocation points in each direction (Chebyshev collocation with exponential mapping). Figure 6.1 shows the full spectrum with a total of 19.600 eigenvalues. To filter the results, a calculation with $N = 121$ collocation points is done. Note that numerical eigenvalues with zero and infinite

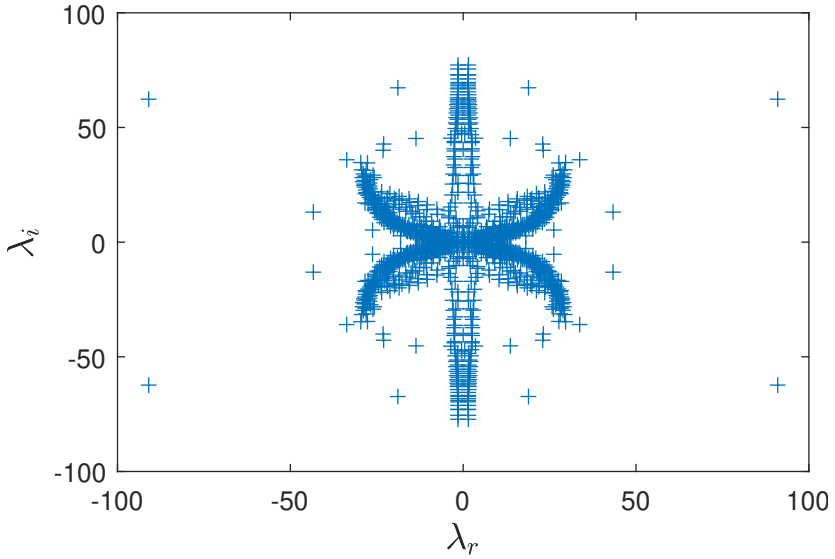

Figure 6.1.: Linear shear (2D): full spectrum, $N = 141$ Chebyshev collocation points in each direction with exponential map $L = 10$

values have been removed from the spectrum before the filtering. The corresponding filtering metric r_{nearest} from (5.46) is shown in Figure 6.2. As a cut-off for the filter was to be chosen, we selected all eigenvalues with $r_{\text{nearest}} > 10^4$ (in total 66 eigenvalues). We believe that this limit is a reasonable choice to filter correct eigenvalues. The filtered spectrum is shown in Figure 6.3. Here λ_r and λ_i denote the real and imaginary parts of λ, respectively. The filtered spectrum shows two interesting properties. First, all eigenvalues are real (in numerical double-precision, largest value with $\lambda = 0.16995$). Second, the filtered spectrum is symmetric with respect to $\lambda_r = 0$. Interestingly, we expect real eigenvalues and discussed this constraint already for the analytical solution (compare Chapter 4.2). Due to the (symmetry) transform with $e^{\lambda t}$, an imaginary part of λ would lead to oscillations and periodicity. The occurrence of the discrete reflection in the spectrum is an interesting finding. Note that the equation (4.72) itself is not invariant under $\lambda \to -\lambda$.

The influence of the shear rate A is given implicitly, as the shear rate has been absorbed in the eigenvalue. To allow a better physical interpretation of the results, we note that the physical eigenvalue $\lambda^{(P)}$ scales with the shear rate A and the numerically computed eigenvalue $\lambda^{(N)}$ by

$$\lambda^{(P)} = A\lambda^{(N)}. \tag{6.1}$$

Interpretation of the results From a physical perspective, positive real parts λ_r correspond to a growth of the kinetic energy $k \sim \exp(2\lambda t)$, cf. (4.4). Evidently, the kinetic energy grows exponentially. Note that this is the result of the linearized equations. Therefore the energy growth is not a solution for infinite times, but only for the shorter time scales until nonlinear effects are no longer negligible (from physical grounds an exponential growth can also be not infinitely long for a nonlinear equation). However, these findings indicate the existence of modes with growing perturbation energy. These modes can be interpreted as unstable modes. These findings are discussed in light of stability theory. Classical results show that the inviscid

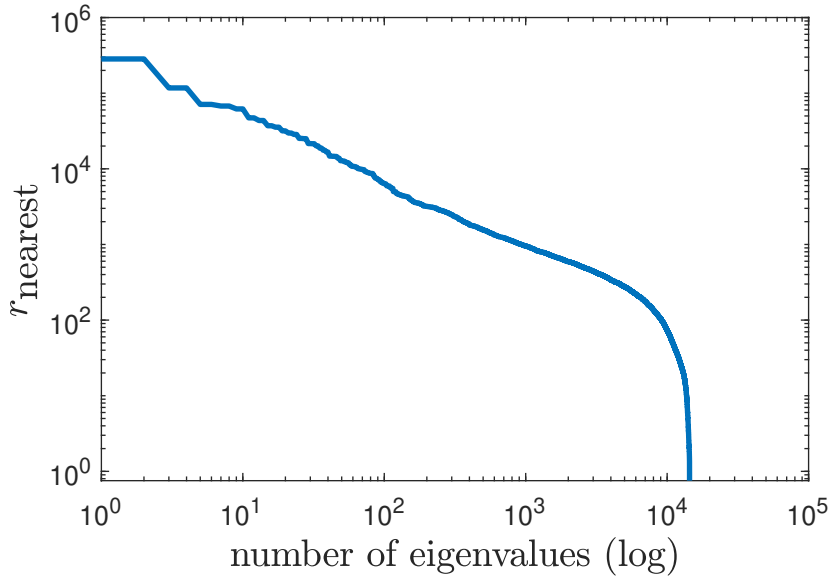

Figure 6.2.: Linear shear (2D): Metric r(nearest) over log(NEV) is the number of eigenvalues from the full spectrum

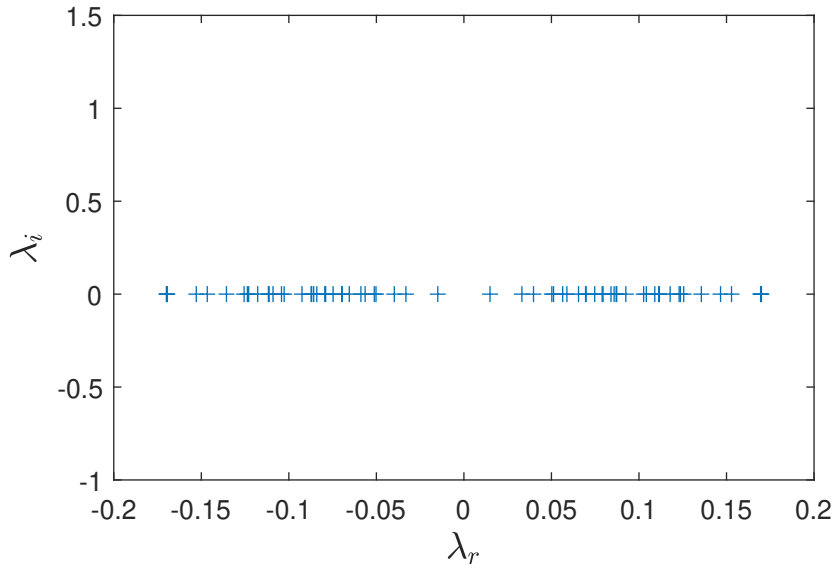

Figure 6.3.: Linear shear (2D): Filtered spectrum with $r_{\text{nearest}} > 10^4$

plane linear shear is stable. This follows directly from Rayleigh's inflection point theorem (3.25). Similarly, the plane Couette flow, i.e. a linear shear flow bounded by walls is stable (Schmid and Henningson, 2001). However, experiments and numerical simulations show a critical Reynolds number of Re ≈ 400. This indicates subcritical instability. Non-modal stability theories were used to explain this behavior. In that way, the solution of the NEVP reveals unstable modes (subcritical instability) for the two-dimensional inviscid linear shear flow. Further investigations should, therefore, investigate the eigenfunctions to further validate and verify these findings.
Interestingly, the filtered eigenvalues appear in pairs with the same absolute values but opposite signs. This indicates that there is a discrete symmetry $\lambda \to -\lambda$ in the spectrum of filtered eigenvalues. Alternatively, these values as complex conjugate pairs under multiplication by i, which means $i\lambda$. The latter view shows similarity to complex conjugate pairs in normal mode analysis, see e.g. Drazin (2002). Consequently we investigate whether if this discrete symmetry is also found in the equation. Therefore we consider (5.1),

$$-\lambda\Delta\tilde{u}_2' - \lambda\tilde{x}_k\frac{\partial\Delta\tilde{u}_2'}{\partial\tilde{x}_k} + \tilde{x}_2\frac{\partial\Delta\tilde{u}_2'}{\partial\tilde{x}_1} = 0. \tag{6.2}$$

which is restated here for sake of clarity. Substituting $\lambda \to -\lambda$ in (6.2) gives

$$\lambda\Delta\tilde{u}_2' + \lambda\tilde{x}_k\frac{\partial\Delta\tilde{u}_2'}{\partial\tilde{x}_k} + \tilde{x}_2\frac{\partial\Delta\tilde{u}_2'}{\partial\tilde{x}_1} = 0. \tag{6.3}$$

Obviously, the negative sign can not be entirely annihilated and the equation is not invariant. Alternatively, substituting both the eigenvalue $\lambda \to -\lambda$ and the eigenfunction $\tilde{u}_2' \to -\tilde{u}_2'$ in (6.2) by a reflection symmetry gives

$$\lambda\Delta\tilde{u}_2' + \lambda\tilde{x}_k\frac{\partial\Delta\tilde{u}_2'}{\partial\tilde{x}_k} - \tilde{x}_2\frac{\partial\Delta\tilde{u}_2'}{\partial\tilde{x}_1} = 0. \tag{6.4}$$

Again the equation changes under this transform, i.e. the equation is not invariant under the discrete transform. A possible explanation of the discrete symmetry in the spectrum may be due to the metric calculated by the filtering algorithm.
As mentioned, an interpretation from a turbulence perspective is possible if the perturbations are regarded as turbulence fluctuations. Note, however, that the flow physics for two- and three-dimensional turbulence differ (Boffetta and Ecke, 2012). To the author's knowledge, there is comparably little data available for two-dimensional turbulence. For example, we are aware of the work of Barkley and Tuckerman (1999) and references therein. However, note that most numerical work on *plane* Couette flow uses three-dimensional numerical domains (see e.g. Bech et al. (1995)). The eigenvalues are therefore interpreted in the context of three-dimensional turbulence in Chapter 6.2.1.

Eigenfunctions The eigenfunctions, or *modes* as they are referred to in normal mode stability theory, give insight into the structures of the perturbation velocities. In the following we select the filtered eigenvalue $\lambda = 0.14920$ having the best metric r_{nearest}, i.e. this value is the most reliable. To further validate the existence of this eigenvalue, calculations with higher resolutions (up to $N = 520$ collocation points per direction) are performed. The corresponding eigenfunction for u_2 is shown in Figure 6.4a. The approximated Chebyshev coefficients decay sufficiently fast, which is shown in Figure 6.4b for the leading 40 coefficients in each spatial

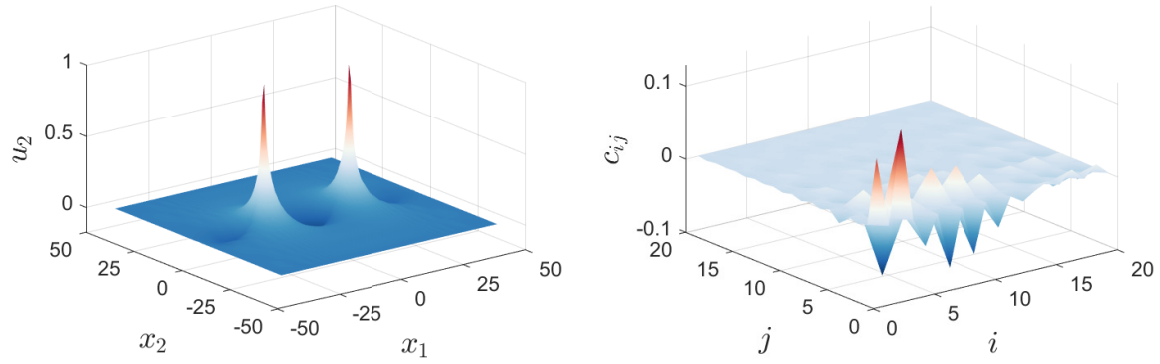

(a) Eigenfunction (velocity u_2)

(b) Chebyshev coefficients

Figure 6.4.: Numerical solution of the eigenfunction corresponding to leading eigenvalue $\lambda = 0.14920$

direction. To summarize, there are three arguments that this eigenvalue is non-spurious (filtering metric, persistence for higher resolutions, Chebyshev coefficients). It can also be shown that the negative eigenvalue, i.e. $-\lambda$, because it has a metric of the same order.
The eigenfunction for u_2 has two peaks. From a numerical perspective, it is recommended to use a mesh refinement in areas with strong gradients, i.e. near the peak. This is the subject of future work. To better show the structure, a slice of the eigenfunction in the center $x_2 = 0$ along the x_1-axis is shown in Figure 6.5 (a spline interpolation is used).
An interesting property of the eigenfunction is due to the scaling symmetry of the problem (4.72) (see also Oberlack (2018)), i.e. there is a freedom of spatial scaling. This is also reflected in the discretized equations. In the numerical implementation, the discretized equations with the same mapping parameter in both spatial directions (i.e. $L = L_x = L_y$) are equivalent for the same number of collocation points. However, for different mapping parameters in space ($L_x \neq L_y$) the discretizations are no longer equivalent. This can be easily shown by writing down the equations and applying the mappings.

6.1.2. Pure strain

The problem for pure planar strain (4.104) is solved. We performed various calculations using Chebyshev and Hermite collocation with different (or scaling) mapping parameters respectively. The filtered spectrum ($r > 10^4$) is shown for both Chebyshev (exponential mapping, $L = 10$) and Hermite collocation (scaling parameter $b = 0.35$) in Figure 6.6. A cluster of filtered eigenvalues around $\lambda = \pm 1$ can be observed. For the case of Chebyshev collocation, there are a few values with a real part around $\Re(\lambda) = 0.5$ Most of the eigenvalues are complex values. For physical reasons, we are interested in real-valued solutions and eigenvalues. For eigenvalues that occur as a complex conjugate pair, where λ is the eigenvalue and λ^* its complex conjugate, the real part can be recovered by a linear combination $2\lambda_r = \lambda + \lambda^*$. There is also the possibility that these eigenvalues later converge to unity, for unresolved solutions. Therefore one could follow a single eigenvalue and trace its trajectory while increasing the number of collocation points. However, for this problem, there is some indication for the value $\lambda = 1.0$ as shown for the analytical solution for (4.106). Therefore, with this guess, it is possible to insert $\lambda = 1.0$ directly into the eigenvalue problem which leads to a BVP for u_2.

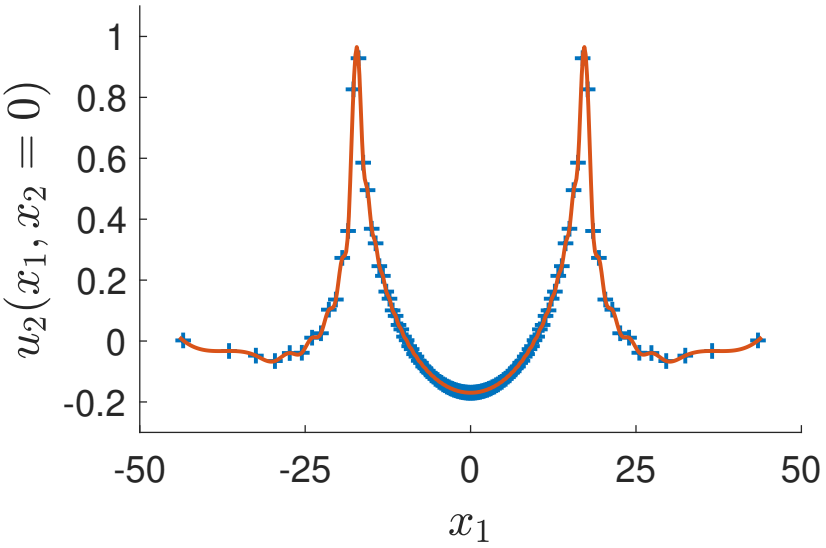

Figure 6.5.: Slice of the eigenfunction from figure 6.4a along the x_1 axis

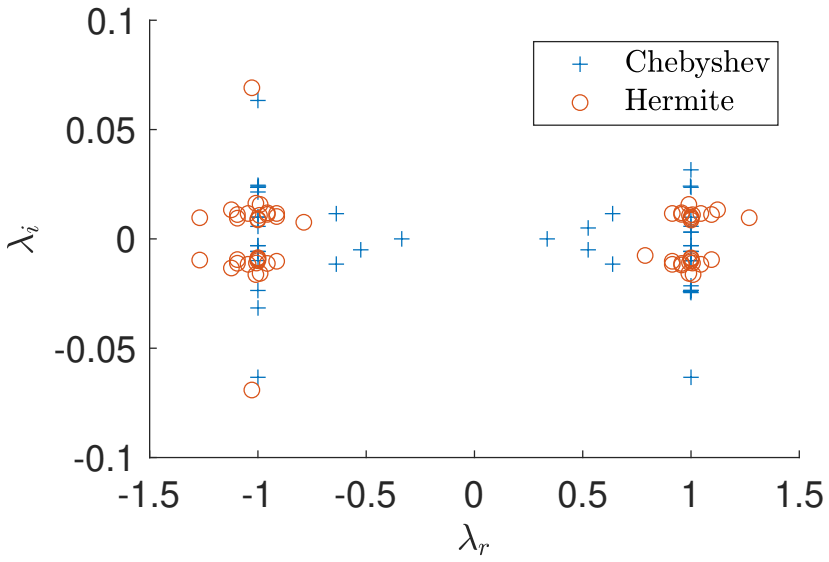

Figure 6.6.: Pure strain (2D): Filtered spectrum $r_{\text{nearest}} > 10^4$ for Chebyshev and Hermite collocation

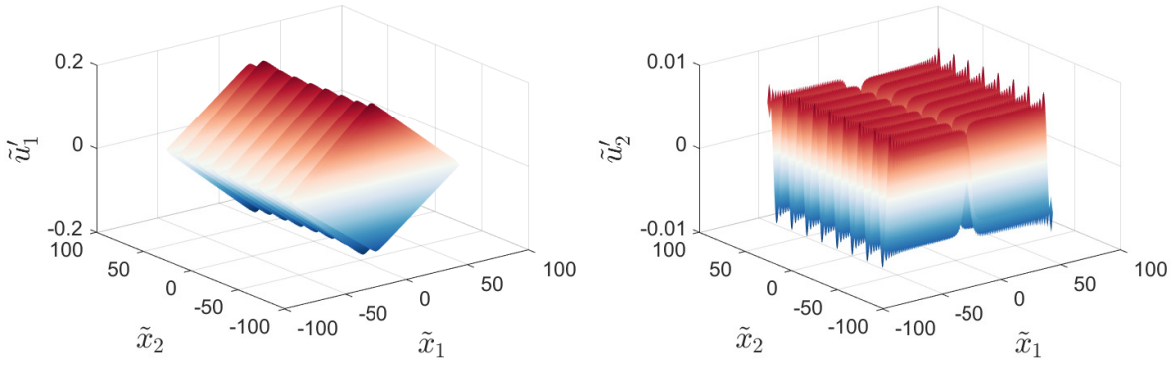

(a) Velocity u_1 (b) Velocity u_2

Figure 6.7.: Pure strain (2D): solution using Hermite collocation ($N = 240, b = 0.35$) for $\lambda = 1.0$, cf. (4.106)

The solutions are the eigenfunctions which can be further analyzed.

Analysis of eigenfunctions In the next step, the corresponding eigenfunctions are inspected around $\lambda = 1.0$. The observation is that the eigenfunctions from the Chebyshev collocation show high oscillations and do not satisfy the boundary conditions. To further validate the results, Chebyshev polynomials with algebraic map and Hermite collocation were used. To perform the calculations for higher resolutions, an iterative solver (ARPACK) is used for performance reasons. Note that a shift σ (cf. (5.40)) near the sought value, e.g. $\sigma = 1.01$ is usually better (which is due to the structure of the Arnoldi algorithm, refer to Embree (2009) for more details). In addition, the candidate eigenvalue $\lambda = 1.0$ is inserted directly into the equations and solved. The results are shown in Figure 6.7. Interestingly, the results qualitatively resemble the analytical solution (cf. Figure 4.3 in Chapter 4.3). Note that the analytical solution in (4.108) contains a free function and four constants $C_1 - C_4$. Formally, a linear system for the coefficients can be formulated where the coefficient matrix involves the point-wise evaluation of the special function. From this numerical solution, we see that Hermite collocation qualitatively captures the structure of the analytical solution while the mapped Chebyshev polynomials fail. This might have several reasons, for example, the distribution of grid points or the mapping parameter (as shown for the 1D test case). Another possible reason is the implementation of the boundary conditions. In contrast to Chebyshev polynomials, no boundary conditions need to be applied for Hermite collocation. We suppose that this makes a difference, as the eigenfunction does not decay at infinity and this causes large errors for mapped Chebyshev polynomials at the outer collocation points.

Discussion of the boundary conditions This observation raises the question if the prescribed boundary conditions for the problem should be refined. The reason for choosing boundary conditions of decay is to have bounded energy, given that the eigenfunctions have sufficient decay (compare rotational shear flow). However, there are examples within stability theory where the eigenfunction does not decay to zero, but rather to a constant value for $|\boldsymbol{x}| \to \infty$. This was observed in the stability analysis for boundary layer flows (Grosch and Salwen, 1978). The corresponding modes are called *improper eigenfunctions* (Friedrichs, 1950) and are bounded but not square-integrable on the infinite domain (Miura et al., 1968). Mathematical details of

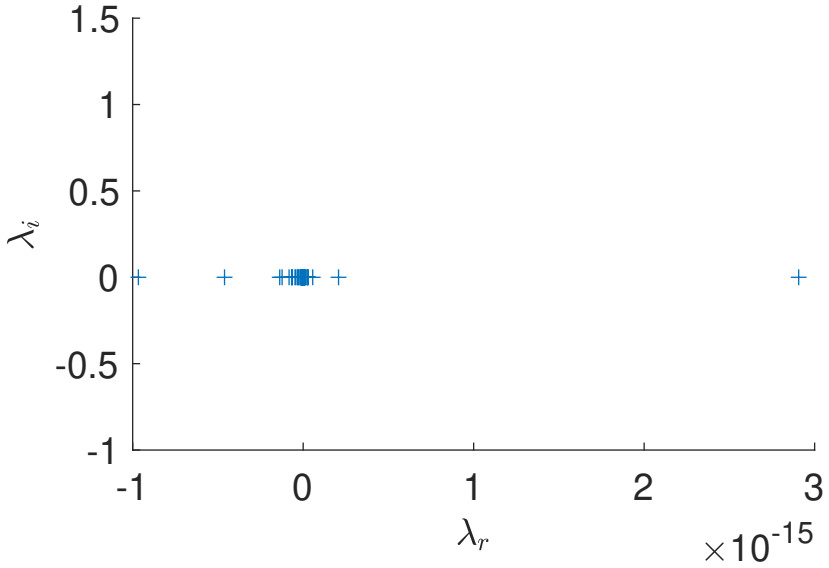

Figure 6.8.: Pure rotation 2D: Filtered spectrum, showing the 92 leading eigenvalues with $r_{\text{nearest}} > 10^5$ (unlike Figure 6.6 for linear shear where $r_{\text{nearest}} > 10^4$)

improper eigenfunctions are given in textbooks on spectral theory (cf. Friedman, 1990; Hanson and Yakovlev, 2002). These solutions are associated with a continuous spectrum of modes besides a discrete spectrum (if it exists). Another example of (eigen-)functions that asymptote to a constant for $|\boldsymbol{x}| \to \infty$ can be found in the theory of nonlinear waves. In general, soliton waves are nonlinear waves that asymptotically preserve their shapes even after interaction with other soliton waves (Ablowitz, 2011). Soliton waves that decay to a constant rather than zero are called *non-local*, cf. Boyd (1989), Boyd (1990), and Boyd (1991).
In future work, the problem should be studied with these more general boundary conditions. This needs careful implementation.

6.1.3. Pure rotation

The filtered eigenvalue spectrum (Chebyshev collocation with exponential map) for (4.133) is shown in Figure 6.8. Note the scaling of the axis which is 10^{-6} for the real part. Therefore the eigenvalues are near zero. All eigenfunctions have very strong oscillations in the Chebyshev coefficients, which is an indication for an under-resolved or spurious solution. As the rotation rate is combined with the eigenvalue, we cannot vary the rotation rate in terms of scaling. However, the direction of rotation can be changed. We, therefore, perform a calculation for the inverse rotation rate $\Omega \to -\Omega$. The filtered results also give eigenvalues near zero, with real parts smaller than 10^{-5}. All non-zero eigenvalues also have non-decaying Chebyshev coefficients. In conclusion, there is a strong indication, that $\lambda = 0$ is the numerical solution to the problem. The very small deviation from zero in the numerical results may be due to rounding errors.

Interpretation The solution $\lambda = 0$ is consistent with the rotation invariance for the 2D case, cf. symmetry (2.15). In addition, we consider the result from a turbulence perspective. Even though real-world turbulence is almost three-dimensional, the Taylor-Proudman theorem states for a sufficiently large rotation rate Ω, the flow is perpendicular to the rotation vector

and therefore two-dimensional (Chandrasekhar, 1961; Billant, 2021). For two-dimensional turbulence modeling the so-called frame-invariance is shown. For two-dimensional flows, the turbulent fluctuations in the momentum equation can be absorbed into the pressure term (Speziale, 1981; Speziale, 1989). This is consistent with the finding of the solution $\lambda = 0$ for the eigenvalue problem. Note that the frame-invariance does not hold for 3D flows. Experiments for isotropic turbulence show that the rotation rate decreases the decay rate (Mansour et al., 1992; Sagaut and Cambon, 2018).

6.2. Three-dimensional flows

The general approach for three-dimensional flows is different from two-dimensional flows. Due to the higher numerical cost (in particular storage) an iterative solver (Arnoldi method) is used instead of a QZ routine (full spectrum). Consequently, there is no information on the full spectrum available. The following approach is used for the large-scale 3D calculations:

1. Define an area of interest (if possible from theoretical considerations).
2. Calculate the eigenvalue in the area of interest. Use successive shifts in the domain of interest and make sure that the solutions of each shift overlap, similar to a method used e.g. in Timme (2020).
3. Repeat the calculations with different numerical parameters (e.g. a different number of collocation points).
4. Filter the set of eigenvalues using the methods described in chapter 5.3.

6.2.1. Linear shear

Area of interest from theory Iterative solvers seek solutions in certain areas of the spectrum. A turbulence perspective on the NEVP helps us to identify these areas. As discussed in Chapter 4, the study of homogeneous shear flows reveals growth of kinetic turbulent energy. Pope (2000) derived a simple balance for the turbulent kinetic energy as a function of time $k(t)$ and the difference in production of kinetic energy $\mathcal{P}$ and dissipation ϵ

$$\frac{dk}{dt} = \mathcal{P} - \epsilon \tag{6.5}$$

which can be rewritten as

$$\frac{\tau}{k}\frac{dk}{dt} = \frac{\mathcal{P}}{\epsilon} - 1, \tag{6.6}$$

and be solved as

$$k(t) = k(0)\exp\left(\frac{t}{\tau}\left(\frac{\mathcal{P}}{\epsilon} - 1\right)\right). \tag{6.7}$$

The results from the literature indicate that $\mathcal{P}/\epsilon \approx [1.4, ..., 1.8]$. Usually, a different notation is used, cf. Briard et al. (2016). Exponential growth is observed for finite times, i.e. the growth cannot be sustained infinitely long (Sagaut and Cambon, 2018). For short times scales, a Taylor expansion of the exponential term around $t = 0$ reveals a linear growth in leading order

	$\lambda_{N=60}$	$\lambda_{N=64}$	r_{nearest}
1	0.00609	0.00612	292.8
2	0.12995	0.12978	210.2
3	0.01771	0.01769	109.6

Table 6.1.: Linear shear (3D): three eigenvalues for the two different resolutions having the best metric r_{nearest}

(Rohr et al., 1988).
The aim is to use these predictions and compare them with the three-dimensional formulation of the linearized NEVP. One may argue that the linearization of the NEVP may limit the ability to predict turbulence phenomena. It should be noted that the Rapid Distortion Theory (RDT) also neglects the nonlinear terms as the forcing by shear dominates (Jacobitz et al., 1997; Hunt and Carruthers, 1990). The linearization is however only valid for $At = \mathcal{O}(1)$ (Jacobitz et al., 1997). Moreover, the linearized solution should serve as an initial guess for the full nonlinear equation (see chapter 7.3). We find the following area of interest for our numerical calculation. The kinetic energy of the fluctuations grows as $\exp(2\lambda t)$ (here, a different scaling of λ is used compared to equation 4.4). We compare the coefficients with those from the literature (Sagaut and Cambon, 2018) and find

$$2\lambda = \sigma A \tag{6.8}$$

For the numerical implementation of the linearized equation the eigenvalue is scaled by A^{-1}, i.e. $\lambda^N = \lambda/A$, where λ^N denotes the result from the numerical solution. Using this result, we find

$$\lambda^{(N)} = \frac{\sigma}{2} \tag{6.9}$$

according to the literature this gives theoretical values for $\lambda^{(N)} = [0.035, 0.165]$. Note that the filtered values from the 2D linear shear flow lie in the range $[-0.170, 0.170]$.

Results The approach to calculating the eigenvalues is the following. A parallel iterative solver is used to solve (4.72). Due to the sizes of the matrices for the three-dimensional case, an iterative solver is chosen. Keep in mind that routines for a full spectrum scale as $\mathcal{O}(N^3)$ for matrices of size $N \times N$ (cf. Chapter 5.2). A shift-invert technique is used and the sizes of the shifts σ were chosen to have overlapping solutions for each shift. This procedure is also used for problems with global stability analysis, cf. Timme (2020) and Nichols and Lele (2011). For this problem, the shifts were chosen as $[0.01, 0.05, 0.1, 0.15]$. As the calculated eigenvalues may still be spurious, the calculations are done for two resolutions with $N = 60$ and $N = 64$ collocation points in each spatial direction. Here we present the results for several shifts (different parameters $N = 61$ and $N = 65$, with $L = 10$) shown in Figure 6.9. The metrics for the two sets of eigenvalues are calculated. As there is a significant decrease in the metric after the first three eigenvalues, only these eigenvalues are considered. Note that the metrics r_{nearest} and r_{ordinal} both select the same three eigenvalues. These three leading eigenvalues are shown in Table 6.1. The analysis shows that there are three eigenvalues that change little for the two resolutions and are therefore are assumed to be physically relevant eigenvalues. In this way, eigenvalues in the domain of interest (compare to theory) are found. These values would explain an exponential growth of the kinetic energy in a view of turbulence

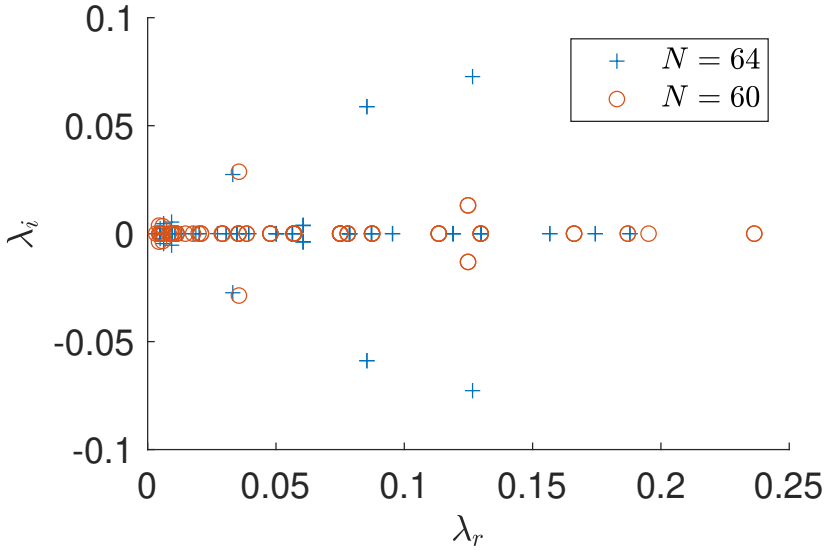

Figure 6.9.: Linear shear (3D): calculated eigenvalues with shifts along the real line, Chebyshev collocation with exponential map ($L = 10$) for $N = 60$ and $N = 64$ collocation points in each direction

theory. Additional investigations of the eigenfunctions and their Chebyshev coefficients are necessary to confirm these findings.

6.3. Summary

In this chapter, the numerical solution for the linearized NEVP is presented. The equations are successfully implemented and solved in an MPI solver for runs on $\mathcal{O}(1000)$ processors. The study of the linear shear shows the first promising results. First, the filtered values in the two-dimensional case reveal exponential growth. Second, the eigenfunction to the leading eigenvalue is obtained. For the three-dimensional case, we can show that there are three filtered eigenvalues that are in the range of experimentally observed eigenvalues. An analysis of the eigenfunctions should be performed in the next step. The effects of strain and rotation can also be included in the equation. Two-dimensional results for the calculation of these single effects are in accordance with theory.

7. Towards a solution for the nonlinear eigenvalue problem

In Chapter 4 a novel NEVP based on Lie symmetries is presented. The equations involve a non-linear term arising from the convective term of the Euler equation. The linearized dynamics are discussed in chapter 6. The aim is to understand the full nonlinear dynamics in stability theory, as finite amplitude perturbations can trigger turbulence (Pringle and Kerswell, 2010). This chapter gives an introduction to the numerical solution of nonlinear problems.
The dynamics of non-linear equations can be different from those of the linearized equation. The linear superposition of solutions no longer holds. Moreover, solutions of the equation can bifurcate at specific points in phase space. For an introduction to these phenomena refer for example to Strogatz (2018). In the scope of the present work, the term *nonlinear eigenvalue problem* refers to problems that are nonlinear in the eigenfunctions. However, the term *nonlinear eigenvalue problem* needs some clarification, as in general, the nonlinearity can apply to the eigenvalue, the eigenfunctions, and to both of them (Appell et al., 2004). An example of nonlinearity of the eigenvalue arises in structural mechanics and leads to the eigenvalue problem

$$\lambda^2 \mathsf{M} + \lambda \mathsf{C} + \mathsf{K} = 0, \tag{7.1}$$

where the eigenvalue is quadratic in leading order. This eigenvalue problem is used in the dynamic analysis of oscillating systems where $\mathsf{M}, \mathsf{C},$ and K denote the mass, damping, and stiffness matrix, respectively (Mehrmann and Voss, 2004). The numerical solution of (7.1) is widely discussed, for an extensive review refer to Mehrmann and Voss (2004).
By contrast, the NEVP considered in the present work is nonlinear in eigenfunctions, but the eigenvalue occurs linearly. Therefore the focus of this chapter is on this type of nonlinear problem. Mathematical theory is provided for some problems mostly where the eigenfunctions have a polynomial nonlinearity (Cerami, 1988; Lindqvist, 1993; Bognár, 2000). The spectrum of the eigenvalue problems can be studied with techniques from non-linear analysis, namely variational methods (Rayleigh's quotient), cf. Lindqvist (2008) and Appell et al. (2004). For the numerical solution of problems with nonlinear eigenfunctions, Newton-type methods are frequently used (Boyd, 2000). An example of nonlinear eigenfunctions in classical mechanics is a heavy rotating string problem (Kolodner, 1955). In theoretical physics, the nonlinear Schrödinger equation (Sulem and Sulem, 2004), the Korteweg-deVries equation (Miura, 1976) and Bratu's equation (Boyd, 1986; Boyd, 2000) are further examples.

7.1. Newton-Kantorovich method

We first summarize some basic ideas for solving nonlinear equations. The Newton method for nonlinear equations can be applied to differential equations, called the *Newton-Kantorovich method*, named after the work of Kantorovich and Akilov (1964). It has been successfully

applied in fluid mechanics, e.g. for the two-dimensional Navier-Stokes equation (Gabrielsen, 1975), wetting pheneomena (Smith, 1995), or vortical structures in shear flows (Haupt et al., 1993). This section is based on Boyd (2000) if not indicated otherwise.

Ordinary Newton method The ordinary Newton method can be used to compute the roots of an equation $f(x) = 0$. To this end, a Taylor expansion is used and truncated to linear terms. The linearization is done around a current guess $x^{(i)}$ as follows

$$f(x) = f\left(x^{(i)}\right) + f_x\left(x^{(i)}\right)\left(x - x^{(i)}\right) + \mathcal{O}\left(\left(x - x^{(i)}\right)^2\right), \tag{7.2}$$

where $f_x\left(x^{(i)}\right)$ is the derivative of f with respect to x at the point $x^{(i)}$. Neglecting higher order terms, an improved guess $x^{(i+1)}$ can be obtained from

$$x^{(i+1)} = x^{(i)} - \frac{f\left(x^{(i)}\right)}{f_x\left(x^{(i)}\right)}. \tag{7.3}$$

Newton-Kantorovich method A generalization of the ordinary Newton's method to differential equations is provided by the so-called Newton-Kantorovich method. Consider therefore the following differential equation

$$u_x = F(x, u(x)), \tag{7.4}$$

where F is an operator, acting on the solution $u(x)$ and u_x is the derivative of u with respect to x. Using Taylor expansion for the right hand side of (7.4) with respect to $u(x)$ at $u^{(i)}(x)$ yields

$$u_x = F\left(x, u^{(i)}(x)\right) + F_u\left(x, u^{(i)}(x)\right)\left(u(x) - u^{(i)}(x)\right) + \mathcal{O}\left(\left(u(x) - u^{(i)}(x)\right)^2\right). \tag{7.5}$$

The linear differential equation for the next iterate $u_x^{(i+1)}$ is given as

$$u_x^{(i+1)} - F_u u^{(i+1)} = F - F_u u^{(i)}. \tag{7.6}$$

The function F as well as its derivative F_u with respect to u are evaluated at $u^{(i)}$. Consequently, $u_x^{(i+1)}$ is found from a solution of linear differential equations.
First, we introduce the correction $\Delta(x)$ to the solution, which is defined as

$$u_x^{(i+1)} = u^{(i)}(x) + \Delta(x). \tag{7.7}$$

Consider then a nonlinear operator $\mathcal{N}$ acting on $u + \Delta$, which can be expanded as a Taylor series

$$\mathcal{N}(u + \Delta) \approx \mathcal{N}(u) + \mathcal{N}_u(u)\Delta + \mathcal{O}\left(\Delta^2\right) \tag{7.8}$$

where nonlinear terms (i.e. $\mathcal{O}\left(\Delta^2\right)$) are neglected in the following. The derivative $\mathcal{N}_u$, called *Fréchet derivative*, can be computed by

$$\mathcal{N}_u\Delta = \left.\frac{\partial\mathcal{N}(u + \epsilon\Delta)}{\partial\epsilon}\right|_{\epsilon=0}. \tag{7.9}$$

Non-linear problems can therefore be solved by treating the non-linear term with a Newton-Kantorovich method. For more details regarding the implementation of the Fréchet derivative refer to Birkisson and Driscoll (2012). The resulting linearized equation can be solved for the corrections and used to update the solution after each iteration. The stopping criterion for the iteration is usually based on an error norm for the residuals or the corrections.

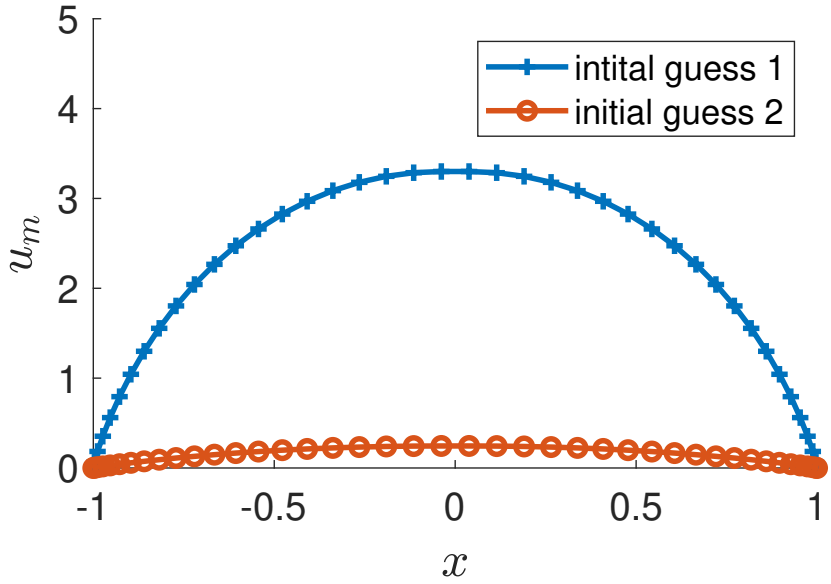

Figure 7.1.: Bratu's equation: two solutions for $\lambda = 0.4$, obtained with *Chebfun* for two different initial conditions (1) and (2).

7.2. Examples of non-linear eigenvalue problems

To solve a non-linear eigenvalue problem, it is important to understand the typical phenomena of this class of eigenvalue problems. Therefore two examples are presented in the following.

Bratu's equation In this section we consider the Liouville–Bratu–Gelfand equation (Liouville, 1853; Bratu, 1914; Gel'fand, 1959) in one dimension given by

$$u_{xx} + \lambda \exp(u) = 0 \qquad \text{with} \qquad u(\pm 1) = 0, \tag{7.10}$$

where λ is the eigenvalue. This equation describes for example the thermal heat explosion in chemical reactions (Trefethen et al., 2018). The problem (7.10) is frequently used as a test case for nonlinear eigenvalue problems, refer to Boyd (2011) for a review. In the spectral methods community, the eigenvalue problem is usually called *Bratu's equation* (Boyd, 2011) and we adopt this term in the following. An analytical solution to (7.10) is given by

$$u(x;\lambda) = \log\left(z^2 \operatorname{sech}^2\left(z\sqrt{\lambda/2}x\right)\right), \tag{7.11}$$

where the z is obtained implicitly from a transcendental equation

$$z = \cosh\left(\sqrt{\lambda/2}z\right). \tag{7.12}$$

The analytical solution for two different initial guesses is shown in Figure 7.1. The results are obtained with a nonlinear solver from the *Chebfun* package (Driscoll et al., 2014). The details on the algorithm are omitted here and can be found in Driscoll et al. (2014) and Birkisson (2013). Interestingly, the result shows that there are two eigenfunctions corresponding to the single eigenvalue $\lambda = 0.4$. This phenomenon is called bifurcation. The two different solutions

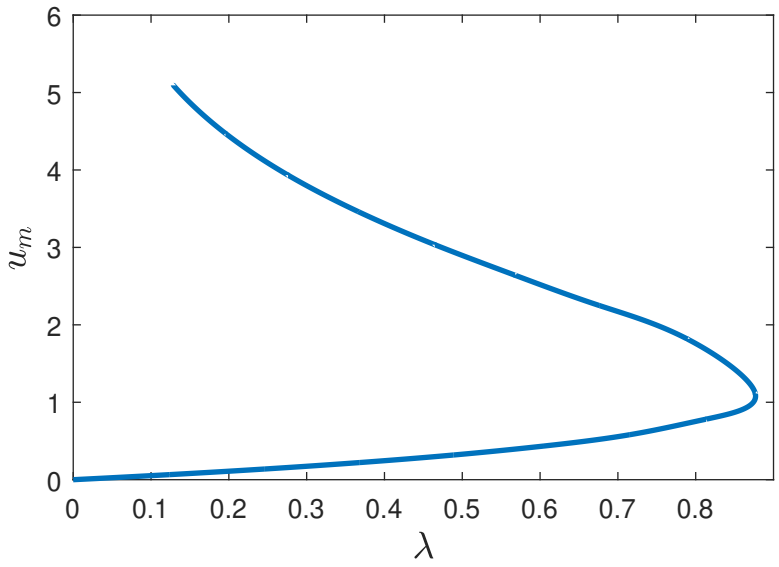

Figure 7.2.: Bratu's equation: bifurcation curve, obtained using a path following routine in *Chebfun*, based on a code from Trefethen et al. (2018).

are found by using different initial conditions, e.g. a simple polynomial with x^2 (initial guess 1) and a sine function (initial guess 2).
It can be easily shown numerically and analytically that the maximum value is $u_m = u(x = 0)$. The maximum value is taken as a measure to distinguish two eigenfunctions in the following. In contrast to linear eigenvalue problems, there is no longer freedom of scaling for the eigenfunctions. An observation is that there is a critical eigenvalue $\lambda_c \approx 0.87845$ (Boyd et al., 2003) associated with a saddle-node bifurcation (Trefethen et al., 2018). For eigenvalues $\lambda < \lambda_c$ there is a continuous spectrum of eigenvalues and every single eigenvalue corresponds to two solutions. At the critical value λ_c there is only one solution. For values $\lambda > \lambda_c$ no solution exists. This finding can be deduced from the solution of (7.12), compare (Boyd et al., 2003; Gheorghiu, 2020b). Figure 7.2 shows the bifurcation curve which is obtained numerically using path-tracking methods (Birkisson, 2013) based on a code presented in Trefethen et al. (2018). Note that the position of the saddle point depends on the domain length. For the domain [0,1] the saddle point is $4\lambda_c$.
The information on the bifurcation and continuous spectrum is useful to formulate the numerical algorithm. First, there are eigenvalues $\lambda_c > \lambda$ which do not have any solutions. Therefore the algorithm does usually not converge for initial guesses of $\lambda^{(0)} \gg \lambda_c$. Second, for a solution $\lambda < \lambda_c$, only the eigenfunction has to be iterated, but not the associated eigenvalue. This is due to the continuous spectrum of solutions. Boyd (2011) presents the following algorithm. The Fréchet derivative (defined in (7.9)) obeys the following form

$$\frac{\partial}{\partial \epsilon} \exp(u + \epsilon\delta)|_{\epsilon=0} = \delta \exp(u + \epsilon\delta)|_{\epsilon=0} = \delta \exp(u). \tag{7.13}$$

Therefore the algorithm to solve (7.10) by iteration reads (Boyd, 2011):

$$\delta_{xx}^{(k)} + \lambda \exp\left(u^{(k)}\right) \delta^{(k)} = u_{xx}^{(k)} + \lambda \exp\left(u^{(k)}\right), \qquad u^{(k+1)} = u^{(k)} - \delta^{(k)} \tag{7.14}$$

The solution depends on the initial conditions, as shown in the example. Technically, it is not difficult to extend this algorithm to higher dimensions. However, special care must be taken to identify the bifurcation points. Therefore Boyd (1986) iterated both the eigenvalue and the eigenfunctions. Some work has been done to identify the bifurcation in two-and three-dimensional Bratu's equation, cf. Karkowski (2013) and Ali and Ma (2020).

Van der Pol equation The solution of Bratu's equation shows that there are zero, one, or two solutions depending on the eigenvalue. In addition, a continuous spectrum of eigenvalue exists. However, this might not always be the case. Consider the Van der Pol equation, which describes a nonlinear oscillation, e.g. studied by Boyd (2000) and Amore et al. (2018). For this equation, only a single (discrete) eigenpair exists. The equation is given by

$$u_{tt} + u + \Gamma\left(1 - u^2\right) u_t = 0 \tag{7.15}$$

with a damping parameter (proportional to the velocity) Γ. The equation is an example of non-linear oscillation. Without the term $(1 - u^2)$, this equation would describe a (linear) spring-mass system. The amplitudes become periodic as t increases. The trajectories, therefore, tend to a point in phase space, which is called the limit cycle (Abell and Braselton, 2018). The Van der Pol equation is a classical example to study the limit cycle property (Davis, 1962). It is useful to make a substitution $t = \Omega\tau$ which leads to (Hunter and Tajdari, 1990)

$$\Omega^2 u_{\tau\tau} + u + \Gamma\Omega\left(1 - u^2\right) u_\tau = 0. \tag{7.16}$$

For a starting solution with a large amplitude, the solution rapidly turns to a solution with fixed frequency and amplitude. For the numerical solution, it is necessary to iterate both the eigenvalue (frequency) Ω and the eigenfunction u in each iteration. The nonlinear term is treated by a Fréchet derivative.
The Van der Pol equation has a translational invariance. It is therefore necessary to apply a phase condition $u_x(x = 0) = 0$ (Boyd, 2000). There are other examples of nonlinear wave equations that need constraints to eliminate certain symmetries, cf. Boyd (1996), Feng and Kawahara (2000), and Gameiro and Lessard (2017). This finding should be kept in mind when constructing algorithms for nonlinear equations.

Summary

The two examples show different properties of nonlinear eigenvalue equations. For both examples, the Newton-Kantorovich method can be applied algorithmically. Care must be taken for the initial guesses. Bratu's equation shows that the solutions depend on the eigenvalue, moreover, there are no solutions for eigenvalues larger than the critical eigenvalue. An interesting property is the existence of a continuous spectrum. However, the Van der Pol equation illustrates that nonlinear equations might also have discrete eigenpairs. In particular, the Van der Pol equation only admits a single eigenpair. To numerically solve this equation, both the eigenfunctions and the eigenvalue should be iterated. Moreover, the iteration of both quantities is a good idea when there is little or no information about bifurcation points.

7.3. Algorithm for the non-linear eigenvalue problem

We present an algorithm to solve the non-linear eigenvalue problem for linear shear given in (4.72) and (4.73). Here the prime and tilde are omitted for sake of readability. Both the

eigenfunctions and the eigenvalues are iterated, so that the corrections read

$$u_2 \to u_2 + \hat{u}_2, \tag{7.17}$$

$$\lambda \to \lambda + \hat{\lambda}. \tag{7.18}$$

The basic approach is as follows. First, the quantities u_2 and λ in (4.72) and (4.73) are replaced by the expressions (7.17), and (7.18). Then, nonlinear terms are neglected by using the Newton-Kantorovich method. The resulting linear system can be solved for the corrections $\hat{u}_2$ and $\hat{\lambda}$.

Nonlinear terms The nonlinear term (4.73) is rewritten as

$$\mathcal{N}_2 = -\underbrace{\frac{\partial \tilde{u}_2}{\partial \tilde{x}_2}\Delta\tilde{u}_2}_{A} + \underbrace{\tilde{u}_2\frac{\partial}{\partial \tilde{x}_1}\Delta\tilde{u}_2}_{B} + \underbrace{\tilde{u}_1\frac{\partial}{\partial \tilde{x}_1}\Delta\tilde{u}_2}_{C} - \underbrace{\frac{\partial \tilde{u}_2}{\partial \tilde{x}_1}\Delta\tilde{u}_1}_{D}. \tag{7.19}$$

This expression not only depends on u_2 but also on u_1 and in the three-dimensional case also on u_3 (or respectively on the vorticity η). Still, there are some differences concerning the nonlinearity of the terms in (7.19):

- A and B: These terms are non-linear in u_2, therefore the Newton-Kantorovich method must be applied.
- C and D: These terms are products of u_2 and u_1. If solving for $\hat{u}_2$ in the first step, u_1 from the previous iteration can be used.

This procedure is consistent with the handling of non-linear terms in the velocity-vorticity formulation (Kim et al., 1987). The Fréchet derivative for the term A with the correction $u_2 \to u_2 + \hat{u}_2$ can be calculated as follows

$$\mathcal{F}_A = \frac{\partial}{\partial\epsilon}\left[-\frac{\partial(u_2+\epsilon\hat{u_2})}{\partial x_2}\Delta\left(u_2+\epsilon\hat{u}_2\right)\right]\Bigg|_{\epsilon=0} \tag{7.20}$$

$$= \frac{\partial}{\partial\epsilon}\left[-\frac{\partial u_2}{\partial x_2}\Delta u_2 - \epsilon\frac{\partial u_2}{\partial x_2}\Delta\hat{u}_2 - \epsilon\frac{\partial \hat{u}_2}{\partial x_2}\Delta u_2 - \epsilon^2\frac{\partial \hat{u}_2}{\partial x_2}\Delta\hat{u}_2\right]\Bigg|_{\epsilon=0} \tag{7.21}$$

$$= \left[-\frac{\partial u_2}{\partial x_2}\Delta\hat{u}_2 - \frac{\partial \hat{u}_2}{\partial x_2}\Delta u_2 - 2\epsilon\frac{\partial \hat{u}_2}{\partial x_2}\Delta\hat{u}_2\right]\Bigg|_{\epsilon=0} \tag{7.22}$$

$$= -\frac{\partial u_2}{\partial x_2}\Delta\hat{u}_2 - \frac{\partial \hat{u}_2}{\partial x_2}\Delta u_2. \tag{7.23}$$

The calculation for the term B is analogous and yields

$$\mathcal{F}_B = \hat{u}_2\frac{\partial}{\partial x_1}\Delta u_2 + u_2\frac{\partial}{\partial x_1}\Delta\hat{u}_2. \tag{7.24}$$

The terms C and D can be simply evaluated by inserting $u_2 \to u_2 + \hat{u}_2$. The correction $\hat{u}_2$ is used to update the solution after each iteration and the correction for the velocity u_1 is calculated thereof. By using the result from (7.23) and (7.24) together with the terms C and D one obtains the expression

$$\begin{aligned}\mathcal{N}_2 \approx &-\frac{\partial u_2}{\partial x_2}\Delta\hat{u}_2 - \frac{\partial \hat{u}_2}{\partial x_2}\Delta u_2 + \hat{u}_2\frac{\partial}{\partial x_1}\Delta u_2 + u_2\frac{\partial}{\partial x_1}\Delta\hat{u}_2 + u_1\frac{\partial}{\partial x_1}\left(\Delta u_2 + \Delta\hat{u}_2\right)\\ &-\frac{\partial\left(u_2+\hat{u}_2\right)}{\partial x_1}\Delta u_1.\end{aligned} \tag{7.25}$$

Linear terms The linear operator is written as

$$\mathcal{L}_2(\lambda)[u_2] = -\lambda\Delta u_2 - \lambda x_k \frac{\partial \Delta u_2}{\partial x_k} + A x_2 \frac{\partial}{\partial x_1}\Delta u_2 \tag{7.26}$$

to indicate that the linear operator depends on λ and acts on the argument in square brackets $[...]$. As both the differential operator and the eigenvalue λ is linear, the corrections can be simply applied and give

$$\begin{aligned}\mathcal{L}_2\left(\lambda+\hat{\lambda}\right)[u_2+\hat{u}_2] = &-\left(\lambda+\hat{\lambda}\right)\Delta\left[u_2+\hat{u}_2\right] - \left(\lambda+\hat{\lambda}\right)x_k\frac{\partial\Delta\left[u_2+\hat{u}_2\right]}{\partial x_k} \\ &+ A x_2 \frac{\partial}{\partial x_k}\Delta\left[u_2+\hat{u}_2\right],\end{aligned} \tag{7.27}$$

where $\Delta[...]$ acts on the argument in the square brackets. The eigenvalue problem contains terms with both the eigenvalue and the eigenfunctions. Note that in contrast to the linearized case it is no longer possible to absorb the shear rate in the eigenvalue by using a substitution $\lambda/A \rightarrow \lambda$. Expanding the expression (7.27), sorting the terms, and ignoring all terms of order $\hat{\lambda}\hat{u}$ gives

$$\mathcal{L}_2(\lambda+\hat{\lambda})\left[u_2+\hat{u}_2\right] \approx \mathcal{L}_2(\lambda)\left[u_2\right] + \mathcal{L}_2(\lambda)\left[\hat{u}_2\right] - \hat{\lambda}\Delta u_2 - \hat{\lambda}x_k\frac{\partial\Delta u_2}{\partial x_k}. \tag{7.28}$$

It can be easily shown that neglecting the nonlinear terms is equivalent to applying Newton-Kantorovich method on these terms.

Linear system for iterations The equation can be discretized using spectral methods, e.g. a Chebyshev collocation method with exponential mapping. Sorting the terms from (7.25) and (7.28) gives a GEVP

$$\mathsf{A}\hat{\boldsymbol{u}}_2 + \hat{\lambda}\mathsf{B}\boldsymbol{u}_2 = \mathsf{C}\boldsymbol{u}_2, \tag{7.29}$$

where A, B, and C are matrices arising from the discretized operators. The aim is to solve (7.29) for the corrections $\hat{\boldsymbol{u}}_2$ and $\hat{\lambda}$, as the quantity $\boldsymbol{u}_2$ is known and the expression $\mathsf{B}\boldsymbol{u}_2$ has the dimension of a vector. To formulate a linear system we use an approach similar to Boyd (1986) and define

$$\hat{\boldsymbol{q}}^T = \left(\hat{\lambda}, \hat{\boldsymbol{u}}_2^*\right), \tag{7.30}$$

where the star $(*)$ indicates that the first entry has been eliminated. Introducing a new matrix D defined as

$$\mathsf{D} = \begin{pmatrix} | & \\ \mathsf{B}\boldsymbol{u}_2 & \mathsf{A}^* \\ | & \end{pmatrix}, \tag{7.31}$$

where A^* is matrix A with the first column being eliminated, we obtain a linear system for the corrections

$$\mathsf{D}\hat{\boldsymbol{q}} = \boldsymbol{r} \tag{7.32}$$

with $\boldsymbol{r} = \mathsf{C}\boldsymbol{u}_2$. The equation (7.32) can be solved by linear solvers, e.g. from LAPACK or PETSc (compare chapter 5.4)

Full algorithm All steps to solve the nonlinear problem are summarized in algorithm 1. The starting point is an initial guess, which can be obtained from solving the linearized equations (see chapter 6). In each step, (7.32) is solved and the solution is updated until convergence. The norm of the corrections may be used as a stopping criterion, i.e. if the norm of the changes is lower than a certain value, the iteration stops. Additionally, a maximum number of iterations can be specified.

Algorithm 1 Algorithm to solve the NEVP for linear shear

```
Initial guess (solution of the linearized equation)
u_2 ← u_2/‖u_2‖_2                                  ▷ Normalize u_2
while c > tol do
    u_1 ← f(u_2)                                   ▷ Obtain u_1 from the continuity equation
    Assemble r and D                               ▷ assemble linear system
    q̂ ← D/r                                        ▷ solve linear system (7.30)
    λ ← λ + q̂[1]                                   ▷ apply corrections
    q̂[1] ← 0
    u_2 ← u_2 + q̂
    u_2 ← u_2/‖u_2‖_2                              ▷ Normalize u_2
    c ← ‖q̂‖_2                                      ▷ Norm of corrections, for while loop
end while
```

The application of the algorithm to other base flows with constant velocity gradient (strain, rotation) is straightforward. The Fréchet derivative allows us to easily derive the necessary equations for these cases. The algorithm has been implemented in the software framework with MPI routines for matrix assembly and the solution of the linear system.

7.4. Future work

Oberlack (2018) noted that the nonlinear eigenvalue equation in primitive variables (velocity and pressure) has a scaling symmetry in space for pressure and velocity. In addition, there is a translation symmetry for the pressure, as only the pressure gradient occurs. It is proposed to use a unit norm for the velocities as a constraint. So far a constraint for the norm has been applied in the algorithm. However, the examples in Chapter 7.2 show that constraints have to be carefully applied for all symmetries, see also Boyd (2000). It should be further investigated if this constraint is sufficient or if further constraints have to be imposed. It might be helpful to study the nonlinear Schrödinger equation, which also has a scaling symmetry for the eigenfunctions, cf. Duyckaerts and Roudenko (2010). It may well be that the solution bifurcates. Therefore, the study of different eigenpairs as an initial condition is recommended. In addition, existing path tracking methods can be considered. Finally, a working algorithm allows studying of the full physics of the NEVP. In particular, we hope to get full information on the eigenvalues (which are interpreted as growth rates), the nonlinear eigenfunctions, and possible bifurcations.

8. Conclusion

The present work shows two main applications of Lie symmetries for stability theory. First, it is possible to extend the normal mode ansatz and to find new modes. Second, it is possible to derive a completely new nonlinear eigenvalue problem (NEVP). These two aspects are summarized in the following. Finally, directions for future work are shown.

Extension of normal mode stability theory In this thesis, we have shown that the Lie symmetries allow for a deeper mathematical understanding of the linear stability equations. In particular, they allow to explain and systematize existing ansatz functions. For example, the well-known normal mode ansatz implements a separation of variables that has a close link to the Lie symmetries. It is shown that the normal mode ansatz relies on three classical symmetries (translation in space and time and scaling of the dependent variable). Consequently, the Orr-Sommerfeld equation can be explained based on Lie symmetries. Moreover, the Kelvin mode solution is obtained from a symmetry analysis.
In addition, new ansätze can be found by the combination of additional (non-classical) Lie symmetries. This is shown in the work of Nold and Oberlack (2013), Nold et al. (2015), and Hau (2016) for a linear shear flow, where new modes are found. The same method was successfully applied to the asymptotic suction boundary layers (Yalcin et al., 2021), and to rotational shear flows (Gebler et al., 2021). For the latter case, it is shown that a stable solution with an algebraic rather than an exponential decay (as for the normal mode ansatz) in time is found. This is referred to as an algebraic mode solution. The stability results are in line with classical results so the algebraic modes are an interesting alternative ansatz in stability theory. The corresponding vorticity modes show a spiral-like behavior. In conclusion, Lie symmetry methods help to understand existing ansatz functions and generalize the modal approach such that new modes can be found.

On a new nonlinear eigenvalue problem The Lie symmetries of the Euler equations give rise to a completely new formulation of an NEVP. This formulation is completely new and the present thesis provides the first numerical results. An important aspect of the NEVP is a velocity decomposition into a mean flow with fluctuations, which shows a close link to problems in (linear) stability theory and to the Reynolds' decomposition for turbulent flows. The NEVP thus provides a theory to calculate the growth rate λ of the turbulent kinetic energy in homogeneous shear or the value of the van Kármán's constant κ.
In this work, unbounded flows with constant velocity gradient, for example, the cases of linear shear, strain, and rotation have been studied. Using analytical techniques, it is shown that the eigenvalue λ for linear shear scales linearly with the shear rate. A formal solution for the eigenfunctions is found, however, a free function therein could not be fully determined. Therefore, to gain further insight, the NEVP is solved numerically. For this, a software framework is implemented using parallel routines which allow to distribute large-scale matrices over several thousand processors. In the first step, the linearized NEVP is solved, where filtering has to be

applied to eliminate spurious eigenvalues.
The numerical solution of the 2D linear shear shows that the leading filtered eigenvalues are all real. The eigenvalues with positive real parts correspond to temporal growing solutions of the shear flow. The eigenvalue with the best filtering metric is found to be $\lambda = 0.14920$. The analysis of the corresponding eigenfunction for the velocity u_2 shows that a double peak structure is visible.
The solution of linear shear with 3D perturbations reveals eigenvalues in the range of values from the literature on turbulent homogeneous shear. This result has been obtained at a medium resolution of $N = 64$. The corresponding memory demand of the matrices makes the use of $\mathcal{O}(10^3)$ processors necessary. The investigation of the corresponding eigenfunctions is the subject of future work.
The results for pure strain indicate a solution of $\lambda = \pm 1.0$ which gives a closed-form solution. This special case arises from the structure of the equation, with a unit strain rate. The analytical solution is bounded at infinity but has no zero decay of the velocities. This type of eigenfunction does not satisfy the boundary conditions but may be referred to as an improper eigenfunction in accordance with the literature from linear stability theory.
Finally, it is shown that flows in rotating frames are affected by Coriolis forces which can be implemented in the equations. The numerical solution for pure rotation in 2D shows that the flow is unaffected by rotation, i.e. $\lambda = 0$. To gain further insight into the nonlinear dynamics, a nonlinear algorithm is developed in Chapter 7, which uses the linearized solution as an initial guess.

Outlook The present work is a basis for future research on the NEVP. We can identify three main questions for future work, which concern (1) the dynamics of the eigenfunctions, (2) the non-linear dynamics, and (3) the interaction with walls.
In Chapter 6, the eigenfunctions for linear shear and pure strain are presented. It would be interesting to investigate their temporal dynamics in transient flows. For example, in linear shear, the leading eigenfunctions can be taken as an initial perturbation in a direct numerical simulation (DNS) and its temporal evolution can be studied.
Moreover, the nonlinear algorithm presented in Chapter 7 can be applied by using the linearized solution as an initial guess. Consequently, the nonlinear evolution can be studied and possible bifurcations or mode-interactions can be analyzed.
Finally, the NEVP for wall-bounded flows can be investigated. For this, an NEVP for the log law region has been presented in the present work. Its numerical solution is the subject of future work.

A. Implementation details for Chebyshev collocation

A.1. Chebyshev differentiation matrices

The following formula to obtain the Chebyshev differentiation matrix is given by Canuto et al. (2007):

$$\left(\tilde{D}^1\right)_{jl} = \begin{cases} \frac{\bar{c}_j}{\bar{c}_l}\frac{(-1)^{j+l}}{x_j - x_l}, & j \neq l \\ -\frac{x_l}{2(1-x_l^2)}, & 1 \leq j = l \leq N-1 \\ \frac{2N^2+1}{6}, & j = l = 0 \\ -\frac{2N^2+1}{6} & j = l = N. \end{cases} \tag{A.1}$$

with

$$\bar{c}_j = \begin{cases} 2, & j = 0, N, \\ 1 & j = 1, ..., N-1 \end{cases} \tag{A.2}$$

A.2. Transform of differentiation matrices under mapping

For a mapped Chebyshev collocation, it is necessary to transform the derivatives. The following summary is adopted from Boyd (2000).

Algebraic map

The derivatives transform according to

$$u_x = \sqrt{Q} Q u_\xi / L, \tag{A.3}$$

$$u_{xx} = Q^2 \left(Q u_{\xi\xi} - 3\xi u_\xi\right) / L^2, \tag{A.4}$$

$$u_{xxx} = \sqrt{Q} Q^2 \left(Q^2 u_{\xi\xi\xi} - 9\xi Q u_{\xi\xi} + (12 - 15Q) u_\xi\right) / L^3, \tag{A.5}$$

where the auxiliary parameter is $Q = 1 - \xi^2$.

Exponential map

The derivatives transform according to

$$u_x = u_\xi \frac{Q}{L}, \tag{A.6}$$

$$u_{xx} = \left(Q u_{\xi\xi} - 2\xi u_\xi\right) \frac{Q}{L^2}, \tag{A.7}$$

$$u_{xxx} = \left(Q^2 u_{\xi\xi\xi} - 6\xi Q u_{\xi\xi} + (4 - 6Q) u_\xi\right) \frac{Q}{L^3}, \tag{A.8}$$

where the auxiliary parameter is $Q = 1 - \xi^2$.

A.3. Approximation of Chebyshev coefficients in 2D

The extension of the Chebyshev approximation to 2D cases is straightforward and can be found in the literature. The reader is referred to Glau and Mahlstedt (2019) and Thomas et al. (2012). For sake of simplicity assume that the number of collocation points is the same in both directions, i.e. $N_x = N_y = N$. The coefficients are given by c_{ij} from

$$c_{j_1,j_2} = \left(\frac{2}{N}\right)^2 \sum_{k_1=1}^{N} \sum_{k_2=1}^{N} u_2^N(x_{k_1}, x_{k_2}) T_{j_1}(x_{k_1}) T_{j_2}(x_{k_2}) \tag{A.9}$$

As can be seen from the one-dimensional formula (5.48), the coefficient c_0 is weighted by $1/2$. This extends to the two-dimensional case, where the boundaries of the coefficient matrix c_{ij} are weighted by $1/2$, except the corner points which are weighted by $1/4$. The function can be reconstructed by

$$u_2(x_{k_1}, x_{k_2}) \approx \sum_{k_1}^{N-1} \sum_{k_2}^{N-1} c'_{j_1,j_2} T_{j_1}(x_{k_1}) T_{j_2}(x_{k_2}) \tag{A.10}$$

with the modified coefficients with a weight factor at the end points given by

$$c'_{j_1,j_2} = \begin{cases} c_{j_1,j_2} & j_1, j_2 \in [1, .., N-1] \\ \frac{1}{2} c_{j_1,j_2} & j_1 \neq j_2 \text{ and } j_1 \in \{0, N\} \text{ or } j_2 \in \{0, N\} \\ \frac{1}{4} c_{j_1,j_2} & j_1 = j_2 \in \{0, N\} \end{cases} . \tag{A.11}$$

B. Derivations for the non-linear eigenvalue problem

B.1. Derivation of common term $\mathcal{M}$

B.1.1. Divergence

$$\nabla \cdot \mathcal{M} = \lambda \underbrace{\frac{\partial \tilde{u}_i}{\partial \tilde{x}_i}}_{=0} - \lambda \left(\frac{\partial \tilde{x}_k}{\partial \tilde{x}_i} \frac{\partial \tilde{u}_i}{\partial \tilde{x}_k} + \tilde{x}_k \underbrace{\frac{\partial \tilde{u}_i}{\partial \tilde{x}_k \partial \tilde{x}_i}}_{=0} \right) + \underbrace{\frac{\partial}{\partial \tilde{x}_i} \left(\tilde{u}_k \frac{\partial \tilde{u}_i'}{\partial \tilde{x}_k} \right)}_{\text{nonlinear terms}} + \frac{\partial^2 \tilde{p}'}{\partial \tilde{x}_i \partial \tilde{x}_i} \tag{B.1}$$

$$\nabla \cdot \mathcal{M} = \underbrace{\frac{\partial}{\partial \tilde{x}_i} \left(\tilde{u}_k \frac{\partial \tilde{u}_i'}{\partial \tilde{x}_k} \right)}_{\text{nonlinear terms}} + \frac{\partial^2 \tilde{p}'}{\partial \tilde{x}_i \partial \tilde{x}_i} \tag{B.2}$$

B.1.2. Divergence of $\mathcal{M}$

$$\nabla \cdot \mathcal{S} = \frac{\partial}{\partial \tilde{x}_1} \left(A \tilde{u}_2' + A \tilde{x}_2 \frac{\partial \tilde{u}_1'}{\partial \tilde{x}_1} \right) + \frac{\partial}{\partial \tilde{x}_2} \left(A \tilde{x}_2 \frac{\partial \tilde{u}_2'}{\partial \tilde{x}_1} \right) + \frac{\partial}{\partial \tilde{x}_3} \left(A \tilde{x}_2 \frac{\partial \tilde{u}_3'}{\partial \tilde{x}_1} \right) \tag{B.3}$$

$$= 2A \frac{\partial \tilde{u}_2'}{\partial \tilde{x}_1} + A \tilde{x}_2 \frac{\partial}{\partial \tilde{x}_1} \left(\underbrace{\frac{\partial \tilde{u}_1'}{\partial \tilde{x}_1} + \frac{\partial \tilde{u}_2'}{\partial \tilde{x}_2} + \frac{\partial \tilde{u}_3'}{\partial \tilde{x}_3}}_{=0} \right) \tag{B.4}$$

B.1.3. Laplacian of $\mathcal{M}$

$$\Delta \mathcal{M} = \Delta \left(\lambda \tilde{u}_i' - \lambda \tilde{x}_k \frac{\partial \tilde{u}_i}{\partial \tilde{x}_k} + \tilde{u}_k \frac{\partial \tilde{u}_i'}{\partial \tilde{x}_k} + \frac{\partial \tilde{p}'}{\partial \tilde{x}_i} \right) \tag{B.5}$$

B.1.4. Rotation

In the following we split the common part into a linear and a non-linear part

$$\mathcal{M} = \mathcal{M}^L + \mathcal{M}^N \tag{B.6}$$

The rotation of the linearized common part $\nabla \times \mathcal{M}^L$

$$\begin{aligned} &\frac{\partial}{\partial \tilde{x}_3} \left(\lambda \tilde{u}_1' - \lambda \tilde{x}_k \frac{\partial \tilde{u}_1'}{\partial \tilde{x}_k} + \frac{\partial \tilde{p}'}{\partial \tilde{x}_1} \right) - \frac{\partial}{\partial \tilde{x}_1} \left(\lambda \tilde{u}_3' - \lambda \tilde{x}_k \frac{\partial \tilde{u}_3'}{\partial \tilde{x}_k} + \frac{\partial \tilde{p}'}{\partial \tilde{x}_3} \right) \\ = &- \lambda \tilde{x}_k \frac{\partial \eta'}{\partial \tilde{x}_k} \end{aligned} \tag{B.7}$$

and of the nonlinear part

$$\nabla \times \mathcal{M}^L = \mathcal{N} = \tilde{u}_j \frac{\partial \eta}{\partial \tilde{x}_j} - \eta \frac{\partial \tilde{u}_2'}{\partial \tilde{x}_2} + \frac{\partial \tilde{u}_2'}{\partial \tilde{x}_3} \frac{\partial \tilde{u}_1}{\partial \tilde{x}_2} - \frac{\partial \tilde{u}_2'}{\partial \tilde{x}_1} \frac{\partial \tilde{u}_3}{\partial \tilde{x}_2} \tag{B.8}$$

Bibliography

Abell, M. L. and Braselton, J. P. (2018). *Introductory Differential Equations*. Fifth Edition. London: Elsevier.

Ablowitz, M. J. (2011). *Nonlinear Dispersive Waves: Asymptotic Analysis and Solitons*. Cambridge: Cambridge University Press.

Ali, M. R. and Ma, W.-X. (2020). "New Exact Solutions of Bratu Gelfand Model in Two Dimensions Using Lie Symmetry Analysis". In: *Chinese Journal of Physics* 65, pp. 198–206. DOI: 10.1016/j.cjph.2020.01.008.

Amore, P., Boyd, J. P., and Fernández, F. M. (2018). "High Order Analysis of the Limit Cycle of the van Der Pol Oscillator". In: *Journal of Mathematical Physics* 59.1, p. 012702. DOI: 10.1063/1.5016961.

Anco, S. C. and Bluman, G. (2002). "Direct Construction Method for Conservation Laws of Partial Differential Equations Part I: Examples of Conservation Law Classifications". In: *European Journal of Applied Mathematics* 13.5, pp. 545–566. DOI: 10.1017/S095679250100465X.

Anderson, E., Bai, Z., Bischof, C., Blackford, L. S., Demmel, J., Dongarra, J., Du Croz, J., Greenbaum, A., Hammarling, S., McKenney, A., and Sorensen, D. (1999). *LAPACK Users' Guide*. Third. Society for Industrial and Applied Mathematics.

Appell, J., De Pascale, E., and Vignoli, A. (2004). *Nonlinear Spectral Theory*. Ed. by A. Bensoussan, R. Conti, A. Friedman, K.-H. Hoffmann, M. A. Krasnoselskii, L. Nirenberg, A. Vignoli, and J. Appell. De Gruyter Series in Nonlinear Analysis and Applications. Berlin, New York: Walter de Gruyter.

Ash, R. L. and Khorrami, M. R. (1995). "Vortex Stability". In: *Fluid Vortices*. Ed. by S. I. Green. Dordrecht: Springer Netherlands, pp. 317–372.

Avila, K., Moxey, D., de Lozar, A., Avila, M., Barkley, D., and Hof, B. (2011). "The Onset of Turbulence in Pipe Flow". In: *Science* 333.6039, pp. 192–196. DOI: 10.1126/science.1203223.

Avila, M. (2012). "Stability and Angular-Momentum Transport of Fluid Flows between Corotating Cylinders". In: *Physical Review Letters* 108.12. DOI: 10.1103/PhysRevLett.108.124501.

Bailey, P. B., Gordon, M. K., and Shampine, L. F. (1978). "Automatic Solution of the Sturm-Liouville Problem". In: *ACM Transactions on Mathematical Software* 4.3, pp. 193–208. DOI: 10.1145/355791.355792.

Baltensperger, R. and Trummer, M. R. (2003). "Spectral Differencing with a Twist". In: *SIAM Journal on Scientific Computing* 24.5, pp. 1465–1487. DOI: 10.1137/S1064827501388182.

Balay, S. et al. (2021). *PETSc/TAO Users Manual*. Tech. rep. ANL-21/39 - Revision 3.16. Argonne National Laboratory.

Balbus, S. A. (2011). “A Turbulent Matter”. In: *Nature* 470, p. 475.

Balbus, S. A. (2017). “When Is High Reynolds Number Shear Flow Not Turbulent?” In: *Journal of Fluid Mechanics* 824, pp. 1–4. DOI: 10.1017/jfm.2017.327.

Barkley, D. and Tuckerman, L. S. (1999). “Stability analysis of perturbed plane Couette flow”. In: *Physics of Fluids* 11.5, pp. 1187–1195. DOI: 10.1063/1.869987.

Batchelor, G. K. and Gill, A. E. (1962). “Analysis of the Stability of Axisymmetric Jets”. In: *Journal of Fluid Mechanics* 14.04, p. 529. DOI: 10.1017/S0022112062001421.

Bech, K. H., Tillmark, N., Alfredsson, P. H., and Andersson, H. I. (1995). “An investigation of turbulent plane Couette flow at low Reynolds numbers”. In: *Journal of Fluid Mechanics* 286, pp. 291–325. DOI: 10.1017/s0022112095000747.

Billant, P. and Gallaire, F. (2005). “Generalized Rayleigh Criterion for Non-Axisymmetric Centrifugal Instabilities”. In: *Journal of Fluid Mechanics* 542.-1, p. 365. DOI: 10.1017/S0022112005006464.

Billant, P. (2021). “Is the Taylor–Proudman Theorem Exact in Unbounded Domains? Case Study of the Three-Dimensional Stability of a Vortex Pair in a Rapidly Rotating Fluid”. In: *Journal of Fluid Mechanics* 920. DOI: 10.1017/jfm.2021.431.

Birkisson, A. and Driscoll, T. A. (2012). “Automatic Fréchet Differentiation for the Numerical Solution of Boundary-Value Problems”. In: *ACM Transactions on Mathematical Software* 38.4, pp. 1–29. DOI: 10.1145/2331130.2331134.

Birkisson, A. (2013). “Numerical Solution of Nonlinear Boundary Value Problems for Ordinary Differential Equations in the Continuous Framework”. PhD thesis. Oxford: Oxford University.

Birkhoff, G. (1960). *Hydrodynamics*. Princeton, New Jersey: Princeton University Press.

Bitev, V. O. (1972). “Group Properties of the Equations of Navier-Stokes”. In: *Collection: Numerical Methods of the Mechanics of Fluids, Novosibirsk, Academy of Sciences of USSR* 3, pp. 13–17.

Blackford, L. S., ed. (1997). *ScaLAPACK User’s Guide*. Software, Environments, Tools. Philadelphia: SIAM.

Bluman, G. W., Cheviakov, A. F., and Anco, S. C. (2010). *Applications of Symmetry Methods to Partial Differential Equations*. Vol. 168. Applied Mathematical Sciences. New York, NY: Springer New York.

Boffetta, G. and Ecke, R. E. (2012). “Two-Dimensional Turbulence”. In: *Annual Review of Fluid Mechanics* 44.1, pp. 427–451. DOI: 10.1146/annurev-fluid-120710-101240.

Bognár, G. (2000). “EIGENVALUE PROBLEM FOR A CLASS OF NONLINEAR PARTIAL DIFFERENTIAL EQUATION”. In: *Systems Analysis Modelling Simulation* 37.4, p. 14.

Boisvert, R. E., Ames, W. F., and Srivastava, U. N. (1983). “Group Properties and New Solutions of Navier-Stokes Equations”. In: *Journal of Engineering Mathematics* 17.3, pp. 203–221. DOI: 10.1007/BF00036717.

Bornemann, F. (2016). *Numerische lineare Algebra: eine konzise Einführung mit MATLAB und Julia*. Springer Studium Mathematik Bachelor. Wiesbaden: Springer Spektrum.

Boyd, J. P., Rangan, C., and Bucksbaum, P. H. (2003). “Pseudospectral Methods on a Semi-Infinite Interval with Application to the Hydrogen Atom: A Comparison of the Mapped

Fourier-sine Method with Laguerre Series and Rational Chebyshev Expansions". In: *Journal of Computational Physics*, p. 19.

Boyd, J. P. (2000). *Chebyshev and Fourier Spectral Methods*. Second. New York: Dover Publications.

Boyd, J. P. (2011). "One-Point Pseudospectral Collocation for the One-Dimensional Bratu Equation". In: *Applied Mathematics and Computation* 217.12, pp. 5553–5565. DOI: 10.1016/j.amc.2010.12.029.

Boyd, J. P. (1986). "An Analytical and Numerical Study of the Two-Dimensional Bratu Equation". In: *Journal of Scientific Computing* 1.2, pp. 183–206. DOI: 10.1007/BF01061392.

Boyd, J. P. (1987). "Spectral Methods Using Rational Basis Functions on an Infinite Interval". In: *Journal of Computational Physics* 69.1, pp. 112–142. DOI: 10.1016/0021-9991(87)90158-6.

Boyd, J. P. (1989). "New Directions in Solitons and Nonlinear Periodic Waves: Polycnoidal Waves, Imbricated Solitons, Weakly Nonlocal Solitary Waves, and Numerical Boundary Value Algorithms". In: *Advances in Applied Mechanics*. Vol. 27. Elsevier, pp. 1–82.

Boyd, J. P. (1990). "A Numerical Calculation of a Weakly Non-Local Solitary Wave: The Phi Breather". In: *Nonlinearity* 3.1, pp. 177–195. DOI: 10.1088/0951-7715/3/1/010.

Boyd, J. P. (1991). "Weakly Non-Local Solitons for Capillary-Gravity Waves: Fifth-degree Korteweg-de Vries Equation". In: *Physica D: Nonlinear Phenomena* 48.1, pp. 129–146. DOI: 10.1016/0167-2789(91)90056-F.

Boyd, J. P. (1996). "Traps and Snares in Eigenvalue Calculations with Application to Pseudospectral Computations of Ocean Tides in a Basin Bounded by Meridians". In: *Journal of Computational Physics* 126.1, pp. 11–20. DOI: 10.1006/jcph.1996.0116.

Bratu, G. (1914). "Sur Les Équations Intégrales Non Linéaires". In: *Bulletin de la Société Mathématique de France* 42, pp. 112–142.

Brethouwer, G. (2005). "The Effect of Rotation on Rapidly Sheared Homogeneous Turbulence and Passive Scalar Transport. Linear Theory and Direct Numerical Simulation". In: *Journal of Fluid Mechanics* 542.-1, p. 305. DOI: 10.1017/S0022112005006427.

Briard, A., Gomez, T., Mons, V., and Sagaut, P. (2016). "Decay and Growth Laws in Homogeneous Shear Turbulence". In: *Journal of Turbulence* 17.7, pp. 699–726. DOI: 10.1080/14685248.2016.1191641.

Burde, G. I., Nasibullayev, I. S., and Zhalij, A. (2007). "Stability Analysis of a Class of Unsteady Nonparallel Incompressible Flows via Separation of Variables". In: *Physics of Fluids* 19.11, p. 114110. DOI: 10.1063/1.2814296.

Canuto, C., Quarteroni, A., Hussaini, M. Y., and Zang, T. A. (2007). *Spectral Methods: Evolution to Complex Geometries and Applications to Fluid Dynamics*. Ed. by J. .-. Chattot, P. Colella, W. E, R. Glowinski, M. Holt, Y. Hussaini, P. Joly, H. B. Keller, J. E. Marsden, D. I. Meiron, O. Pironneau, A. Quarteroni, J. Rappaz, R. Rosner, P. Sagaut, J. H. Seinfeld, A. Szepessy, and M. F. Wheeler. Scientific Computation. Berlin, Heidelberg: Springer Berlin Heidelberg.

Cantwell, B. (2002). *Introduction to Symmetry Analysis*. Cambridge Texts in Applied Mathematics. Cambridge, UK ; New York: Cambridge University Press.

Canuto, C., ed. (2006). *Spectral Methods: Fundamentals in Single Domains*. Scientific Computation. Berlin ; New York: Springer-Verlag.

Canuto, C., ed. (1988). *Spectral Methods in Fluid Dynamics*. Corr. 3rd print. Springer Series in Computational Physics. Berlin ; New York: Springer-Verlag.

Cerami, G. (1988). "A Note on a Nonlinear Eigenvalue Problem". In: *Annali di Matematica Pura ed Applicata* 150.1, pp. 119–127. DOI: 10.1007/BF01761465.

Charru, F. (2011). *Hydrodynamic Instabilities*. Cambridge: Cambridge University Press.

Chandrasekhar, S. (1961). *Hydrodynamic and Hydromagnetic Stability*. Dover ed. New York: Dover Publications.

Cheviakov, A. F. (2010). "Symbolic Computation of Local Symmetries of Nonlinear and Linear Partial and Ordinary Differential Equations". In: *Mathematics in Computer Science* 4.2-3, pp. 203–222. DOI: 10.1007/s11786-010-0051-4.

Choi, J., Demmel, J., Dhillon, I., Dongarra, J., Ostrouchov, S., Petitet, A., Stanley, K., Walker, D., and Whaley, R. (1996). "ScaLAPACK: A Portable Linear Algebra Library for Distributed Memory Computers — Design Issues and Performance". In: *Computer Physics Communications* 97.1-2, pp. 1–15. DOI: 10.1016/0010-4655(96)00017-3.

Craik, A. D. D. and Criminale, W. O. (1986). "Evolution of Wavelike Disturbances in Shear Flows: A Class of Exact Solutions of the Navier-Stokes Equations". In: *Proceedings of the Royal Society A: Mathematical, Physical and Engineering Sciences* 406.1830, pp. 13–26. DOI: 10.1098/rspa.1986.0061.

Crawford, J. D. and Knobloch, E. (1991). "Symmetry and Symmetry-Breaking Bifurcations in Fluid Dynamics". In: *Annual Review of Fluid Mechanics* 23.1, pp. 341–387. DOI: 10.1146/annurev.fl.23.010191.002013.

Criminale, W. O., Jackson, T. L., and Joslin, R. D. (2003). *Theory and Computation of Hydrodynamic Stability*. Cambridge: Cambridge University Press.

Criminale, W. O. and Drazin, P. G. (1990). "The Evolution of Linearized Perturbations of Parallel Flows". In: *Studies in Applied Mathematics* 83.2, pp. 123–157. DOI: 10.1002/sapm1990832123.

Criminale, W. (1991). *Initial-Value Problems and Stability in Shear Flows*. Tech. rep. University of Washington, Seattle.

Dahmen, W. and Reusken, A. (2008). *Numerik für Ingenieure und Naturwissenschaftler*. Springer-Lehrbuch. Berlin, Heidelberg: Springer Berlin Heidelberg.

Daviaud, F., Hegseth, J., and Bergé, P. (1992). "Subcritical transition to turbulence in plane Couette flow". In: *Physical Review Letters* 69.17, pp. 2511–2514. DOI: 10.1103/physrevlett.69.2511.

Davis, H. T. (1962). *Introduction to Nonlinear Differential and Integral Equations*. New York, NY: Dover Publications.

Don, W. S. and Solomonoff, A. (1997). "Accuracy Enhancement for Higher Derivatives Using Chebyshev Collocation and a Mapping Technique". In: *SIAM Journal on Scientific Computing* 18.4, pp. 1040–1055.

Drazin, P. G. and Reid, W. H. (2004). *Hydrodynamic Stability*. Cambridge: Cambridge University Press.

Drazin, P. G. (2002). *Introduction to Hydrodynamic Stability*. Cambridge: Cambridge University Press.

Drazin, P. G. (1958). "The Stability of a Shear Layer in an Unbounded Heterogeneous Inviscid Fluid". In: *Journal of Fluid Mechanics* 4.02, p. 214. DOI: 10.1017/S0022112058000409.

Driscoll, T. A., Bornemann, F., and Trefethen, L. N. (2008). "The Chebop System for Automatic Solution of Differential Equations". In: *BIT Numerical Mathematics* 48.4, pp. 701–723. DOI: 10.1007/s10543-008-0198-4.

Driscoll, T. A., Hale, N., and Trefethen, L. N. (2014). *Chebfun Guide*. Oxford: Pafnuty Publications.

Duyckaerts, T. and Roudenko, S. (2010). "Threshold Solutions for the Focusing 3D Cubic Schrödinger Equation". In: *Revista Matemática Iberoamericana*, pp. 1–56. DOI: 10.4171/RMI/592.

Eckhardt, B. and Pandit, R. (2003). "Noise Correlations in Shear Flows". In: *The European Physical Journal B - Condensed Matter* 33.3, pp. 373–378. DOI: 10.1140/epjb/e2003-00178-3.

Eckhardt, B., Schneider, T. M., Hof, B., and Westerweel, J. (2007). "Turbulence Transition in Pipe Flow". In: *Annual Review of Fluid Mechanics* 39.1, pp. 447–468. DOI: 10.1146/annurev.fluid.39.050905.110308.

Embree, M. (2009). "The Arnoldi Eigenvalue Iteration with Exact Shifts Can Fail". In: *SIAM Journal on Matrix Analysis and Applications* 31.1, pp. 1–10. DOI: 10.1137/060669097.

Farrell, B. F. and Ioannou, P. J. (1996). "Generalized Stability Theory. Part I: Autonomous Operators". In: *Journal of the Atmospheric Sciences* 53.14, pp. 2025–2040. DOI: 10.1175/1520-0469(1996)053<2025:GSTPIA>2.0.CO;2.

Farrell, B. (1987). "Developing Disturbances in Shear". In: *Journal of Atmospheric Sciences* 44.16, pp. 2191–2199.

Feng, B.-F. and Kawahara, T. (2000). "Stationary Travelling-Wave Solutions of an Unstable KdV–Burgers Equation". In: *Physica D: Nonlinear Phenomena* 137.3-4, pp. 228–236. DOI: 10.1016/S0167-2789(99)00183-9.

Fjørtoft, R. (1950). *Application of Integral Theorems in Deriving Criteria of Stability for Laminar Flows and for the Baroclinic Circular Vortex*. Grøndahl & søns boktr., I kommisjon hos Cammermeyers boghandel.

Fornberg, B. (1996). *A Practical Guide to Pseudospectral Methods*. Cambridge Monographs on Applied and Computational Mathematics 1. Cambridge ; New York: Cambridge University Press.

Fransson, J. H. M. and Alfredsson, P. H. (2003). "On the Disturbance Growth in an Asymptotic Suction Boundary Layer". In: *Journal of Fluid Mechanics* 482, pp. 51–90. DOI: 10.1017/S0022112003003926.

Friedrichs, K. O. (1950). "Criteria for Discrete Spectra". In: *Communications on Pure and Applied Mathematics* 3.4, pp. 439–449. DOI: 10.1002/cpa.3160030407.

Friedman, B. (1990). *Principles and Techniques of Applied Mathematics*. New York: Dover Publications.

Funaro, D. (1992). *Polynomial Approximation of Differential Equations*. Ed. by H. Araki, E. Brézin, J. Ehlers, U. Frisch, K. Hepp, R. L. Jaffe, R. Kippenhahn, H. A. Weidenmüller, J. Wess, J. Zittartz, and W. Beiglböck. Vol. 8. Lecture Notes in Physics Monographs. Berlin, Heidelberg: Springer Berlin Heidelberg.

Gabrielsen, R. (1975). *An Effective Solution to the Nonlinear, Nonstationary Navier-Stokes Equations for Two Dimensions*. Tech. rep.

Gameiro, M. and Lessard, J.-P. (2017). "A Posteriori Verification of Invariant Objects of Evolution Equations: Periodic Orbits in the Kuramoto–Sivashinsky PDE". In: *SIAM Journal on Applied Dynamical Systems* 16.1, pp. 687–728. DOI: 10.1137/16M1073789.

Gardner, D. R., Trogdon, S. A., and Douglass, R. W. (1989). "A Modified Tau Spectral Method That Eliminates Spurious Eigenvalues". In: *Journal of Computational Physics* 80.1, pp. 137–167. DOI: 10.1016/0021-9991(89)90093-4.

Gebler, T., Plümacher, D., Kahle, J., and Oberlack, M. (2021). "Algebraic Stability Modes in Rotational Shear Flow". In: *Fluid Dynamics Research* 53.6, p. 065509. DOI: 10.1088/1873-7005/ac44f9.

Gel'fand, I. (1959). "Some Problems in the Theory of Quasi-Linear Equations". In: *Uspekhi Mat. Nauk* 14.2, pp. 87–158.

Gentleman, W. M. (1972). "Implementing Clenshaw-Curtis Quadrature, II Computing the Cosine Transformation". In: *Communications of the ACM* 15.5, pp. 343–346. DOI: 10.1145/355602.361311.

George, W. K. (2007). "Is There a Universal Log Law for Turbulent Wall-Bounded Flows?" In: *Philosophical Transactions of the Royal Society A: Mathematical, Physical and Engineering Sciences* 365.1852, pp. 789–806. DOI: 10.1098/rsta.2006.1941.

Georgescu, A. (2010). *Hydrodynamic Stability Theory*. Place of publication not identified: Springer.

Gheorghiu, C.-I. (2018). *Spectral Collocation Solutions to Problems on Unbounded Domains*.

Gheorghiu, C.-I. (2020a). "Accurate Spectral Collocation Computation of High Order Eigenvalues for Singular Schrödinger Equations". In: *Computation* 9.1, p. 2. DOI: 10.3390/computation9010002.

Gheorghiu, C.-I. (2020b). "Accurate Spectral Collocation Solutions to Some Bratu's Type Boundary Value Problems". In: *arXiv:2011.13212 [cs, math]*. arXiv: 2011.13212 [cs, math].

Glau, K. and Mahlstedt, M. (2019). "Improved Error Bound for Multivariate Chebyshev Polynomial Interpolation". In: *International Journal of Computer Mathematics* 96.11, pp. 2302–2314. DOI: 10.1080/00207160.2019.1599364.

Golub, G. H. and van der Vorst, H. A. (2000). "Eigenvalue Computation in the 20th Century". In: *Journal of Computational and Applied Mathematics* 123.1-2, pp. 35–65. DOI: 10.1016/S0377-0427(00)00413-1.

Golub, G. H. and Van Loan, C. F. (2013). *Matrix Computations*. Fourth Edition. Baltimore: The John Hopkins University Press.

Golubitsky, M. and Schaeffer, D. G. (1985). *Singularities and Groups in Bifurcation Theory*. Ed. by J. E. Marsden, L. Sirovich, and F. John. Vol. 51. Applied Mathematical Sciences. New York, NY: Springer New York.

Goldstein, M. E. (2020). "Theoretical Foundation of Rapid Distortion Theory on Transversely Sheared Mean Flows". In: *Fluids* 5.2, p. 62. DOI: 10.3390/fluids5020062.

Görtler, H. (1940). "Über den Einfluß der Wandkrümmung auf die Entstehung der Turbulenz". In: *ZAMM - Zeitschrift für Angewandte Mathematik und Mechanik* 20.3, pp. 138–147. DOI: 10.1002/zamm.19400200303.

Görtler, H. (1955). "Dreidimensionale Instabilität Der Ebenen Staupunktströmung Gegenüber Wirbelartigen Störungen". In: *50 Jahre Grenzschichtforschung*. Ed. by H. Görtler and W. Tollmien. Braunschweig: Friedrich Vieweg.

Gottlieb, D. and Orszag, S. A. (1977). *Numerical Analysis of Spectral Methods: Theory and Applications*. Nachdr. CBMS-NSF Regional Conference Series in Applied Mathematics 26. Philadelphia, Pa: Soc. for Industrial and Applied Mathematics.

Green, J. (2008). "Laminar Flow Control - Back to the Future?" In: *38th Fluid Dynamics Conference and Exhibit*. Seattle, Washington: American Institute of Aeronautics and Astronautics. DOI: 10.2514/6.2008-3738.

Grosch, C. E. and Salwen, H. (1978). "The Continuous Spectrum of the Orr-Sommerfeld Equation. Part 1. The Spectrum and the Eigenfunctions". In: *Journal of Fluid Mechanics* 87.01, p. 33. DOI: 10.1017/S0022112078002918.

Grossmann, S. (2000). "The Onset of Shear Flow Turbulence". In: *Reviews of Modern Physics* 72.2, pp. 603–618. DOI: 10.1103/RevModPhys.72.603.

Hahn, W. (1967). *Stability of Motion*. Berlin, Heidelberg: Springer Berlin Heidelberg.

Hall, P., Malik, M. R., and Poll, D. I. A. (1984). "On the Stability of an Infinite Swept Attachment Line Boundary Layer". In: *Proceedings of the Royal Society of London. Series A, Mathematical and Physical Sciences* 395.1809, pp. 229–245.

Hämmerlin, G. (1955). "Zur Instabilitätstheorie Der Ebenen Staupunktströmung". In: *50 Jahre Grenzschichtforschung*. Ed. by H. Görtler and W. Tollmien. Braunschweig: Friedrich Vieweg.

Hanson, G. W. and Yakovlev, A. B. (2002). *Operator Theory for Electromagnetics*. New York, NY: Springer New York.

Hau, J.-N., Oberlack, M., and Chagelishvili, G. (2017). "On the Optimal Systems of Subalgebras for the Equations of Hydrodynamic Stability Analysis of Smooth Shear Flows and Their Group-Invariant Solutions". In: *Journal of Mathematical Physics* 58.4, p. 043101. DOI: 10.1063/1.4980055.

Haupt, S. E., McWilliams, J. C., and Tribbia, J. J. (1993). "Modons in Shear Flow". In: *Journal of the Atmospheric Sciences* 50.9, pp. 1181–1198. DOI: 10.1175/1520-0469(1993)050<1181:MISF>2.0.CO;2.

Hau, J.-N. (2016). "On the basic phenomena of acoustic wave generation and dynamics in compressible shear flows". PhD thesis.

Heinrichs, W. (1999). "Spectral Approximation of Third-Order Problems". In: *Journal of Scientific Computing* 14, pp. 275–289.

Hernandez, V., Roman, J. E., and Vidal, V. (2005). “SLEPc: A Scalable and Flexible Toolkit for the Solution of Eigenvalue Problems”. In: *ACM Transactions on Mathematical Software* 31.3, pp. 351–362. DOI: 10.1145/1089014.1089019.

Hiemenz, K. (1911). “Die Grenzschicht an Einem in Den Gleichformigen Flussigkeitsstrom Eingetauchten Geraden Kreiszylinder”. In: *Dinglers Polytech. J.* 326, pp. 321–324, 344–348, 357–362, 372–376, 391–393, 407–410.

Hocking, L. M. (1975). “Non-Linear Instability of the Asymptotic Suction Velocity Profile”. In: *The Quarterly Journal of Mechanics and Applied Mathematics* 28.3, pp. 341–353. DOI: 10.1093/qjmam/28.3.341.

Holmes, P., Lumley, J. L., Berkooz, G., and Rowley, C. W. (2012). *Turbulence, Coherent Structures, Dynamical Systems and Symmetry*. Second. Cambridge: Cambridge University Press.

Howarth, L. (1934). *On the Calculation of Steady Flow in the Boundary Layer near the Surface of a Cylinder in a Stream*. Tech. rep. AERONAUTICAL RESEARCH COUNCIL LONDON (UNITED KINGDOM).

Howard, L. N. (1961). “Note on a Paper of John W. Miles”. In: *Journal of Fluid Mechanics* 10.04, p. 509. DOI: 10.1017/S0022112061000317.

Hughes, T. H. and Reid, W. H. (1965). “On the Stability of the Asymptotic Suction Boundary-Layer Profile”. In: *Journal of Fluid Mechanics* 23.4, pp. 715–735.

Hunt, J. C. R. and Carruthers, D. J. (1990). “Rapid Distortion Theory and the ‘Problems’ of Turbulence”. In: *Journal of Fluid Mechanics* 212.-1, p. 497. DOI: 10.1017/S0022112090002075.

Hunter, C. and Tajdari, M. (1990). “Singular Complex Periodic Solutions of Van Der Pol’s Equation”. In: *SIAM Journal on Applied Mathematics* 50.6, pp. 1764–1779.

Hydon, P. E. (2000). *Symmetry Methods for Differential Equations: A Beginner’s Guide*. Cambridge Texts in Applied Mathematics. New York: Cambridge University Press.

Isaza, J. C. and Collins, L. R. (2009). “On the Asymptotic Behaviour of Large-Scale Turbulence in Homogeneous Shear Flow”. In: *Journal of Fluid Mechanics* 637, pp. 213–239. DOI: 10.1017/S002211200999053X.

Jacobitz, F. G., Sarkar, S., and Van Atta, C. W. (1997). “Direct Numerical Simulations of the Turbulence Evolution in a Uniformly Sheared and Stably Stratified Flow”. In: *Journal of Fluid Mechanics* 342, pp. 231–261. DOI: 10.1017/S0022112097005478.

Janßen, R. (1986). “Elliptic Problems on Unbounded Domains”. In: *SIAM Journal on Mathematical Analysis* 17.6, pp. 1370–1389. DOI: 10.1137/0517097.

Ji, H., Burin, M., Schartman, E., and Goodman, J. (2006). “Hydrodynamic Turbulence Cannot Transport Angular Momentum Effectively in Astrophysical Disks”. In: *Nature* 444.7117, pp. 343–346. DOI: 10.1038/nature05323.

Jiménez, J. (2013). “Near-Wall Turbulence”. In: *Physics of Fluids* 25.10, p. 101302. DOI: 10.1063/1.4824988.

Jost, J. and Li-Jost, X. (1998). *Calculus of Variations*. Cambridge Studies in Advanced Mathematics 64. Cambridge, UK ; New York: Cambridge University Press.

Joslin, R. D. (1998). “Aircraft Laminar Flow Control”. In: *Annual Review of Fluid Mechanics* 30.1, pp. 1–29. DOI: 10.1146/annurev.fluid.30.1.1.

Juniper, M. P., Hanifi, A., and Theofilis, V. (2014). “Modal Stability Theory”. In: *Applied Mechanics Reviews* 66.2. DOI: 10.1115/1.4026604.

Kahle, J. (2017). “Masterarbeit Thema: Stability Analysis of Taylor-Couette Flow Using Lie-Symmetry and Fokas’ Methods”. MA thesis.

Kambe, T. (2007). *Elementary Fluid Mechanics*. Hackensack, N.J. ; London: World Scientific.

Kantorovich, L. and Akilov, G. (1964). *Functional Analysis in Normed Spaces*. New York, NY: Pergamon Press.

Karkowski, J. (2013). “Numerical Experiments with the Bratu Equation in One, Two and Three Dimensions”. In: *Computational and Applied Mathematics* 32.2, pp. 231–244. DOI: 10.1007/s40314-013-0007-9.

Kelvin, L. (1887). “Stability of Fluid Motion: Rectilineal Motion of Viscous Fluid between Two Parallel Planes”. In: *The London, Edinburgh, and Dublin Philosophical Magazine and Journal of Science* 24.147, pp. 188–196. DOI: 10.1080/14786448708628078.

Kerswell, R. R. (2005). “Recent Progress in Understanding the Transition to Turbulence in a Pipe”. In: *Nonlinearity* 18.6, R17–R44. DOI: 10.1088/0951-7715/18/6/R01.

Kerswell, R. R. (2015). “Instability Driven by Boundary Inflow across Shear: A Way to Circumvent Rayleigh’s Stability Criterion in Accretion Disks?” In: *Journal of Fluid Mechanics* 784, pp. 619–663. DOI: 10.1017/jfm.2015.613.

Kerswell, R. (2018). “Nonlinear Nonmodal Stability Theory”. In: *Annual Review of Fluid Mechanics* 50.1, pp. 319–345. DOI: 10.1146/annurev-fluid-122316-045042.

Khapko, T., Kreilos, T., Schlatter, P., Duguet, Y., Eckhardt, B., and Henningson, D. S. (2013). “Localized Edge States in the Asymptotic Suction Boundary Layer”. In: *Journal of Fluid Mechanics* 717. DOI: 10.1017/jfm.2013.20.

Khorrami, M. R., Malik, M. R., and Ash, R. L. (1989). “Application of Spectral Collocation Techniques to the Stability of Swirling Flows”. In: *Journal of Computational Physics* 81.1, pp. 206–229. DOI: 10.1016/0021-9991(89)90071-5.

Kim, J., Moin, P., and Moser, R. (1987). “Turbulence Statistics in Fully Developed Channel Flow at Low Reynolds Number”. In: *Journal of Fluid Mechanics* 177, pp. 133–166. DOI: 10.1017/S0022112087000892.

Kitsios, V. (2010). “Recovery of Fluid Mechanical Modes in Unsteady Separated Flows”. PhD thesis.

Kleinjung, J. (2019). “Stability Theory in Accretion Disks”. MA thesis. TU Darmstadt.

Klingenberg, D., Oberlack, M., and Pluemacher, D. (2020). “Symmetries and Turbulence Modeling”. In: *Physics of Fluids* 32.2, p. 025108. DOI: 10.1063/1.5141165.

Knüpfer, A., Rössel, C., Mey, D. an, Biersdorff, S., Diethelm, K., Eschweiler, D., Geimer, M., Gerndt, M., Lorenz, D., Malony, A., Nagel, W. E., Oleynik, Y., Philippen, P., Saviankou, P., Schmidl, D., Shende, S., Tschüter, R., Wagner, M., Wesarg, B., and Wolf, F. (2012). “Score-P: A Joint Performance Measurement Run-Time Infrastructure for Periscope, Scalasca, TAU, and Vampir”. In: *Tools for High Performance Computing 2011*. Springer Berlin Heidelberg, pp. 79–91. DOI: 10.1007/978-3-642-31476-6_7.

Kolodner, I. I. (1955). “Heavy Rotating String—a Nonlinear Eigenvalue Problem”. In: *Communications on Pure and Applied Mathematics* 8.3, pp. 395–408. DOI: 10.1002/cpa.3160080307.

Kopriva, D. A. (2009). *Implementing Spectral Methods for Partial Differential Equations*. Scientific Computation. Dordrecht: Springer Netherlands.

Kressner, D. (2005). *Numerical Methods for General and Structured Eigenvalue Problems*. Vol. 46. Berlin/Heidelberg: Springer-Verlag.

Kundu, P. K., Cohen, I. M., and Dowling, D. R. (2012). *Fluid Mechanics*. 5th ed. Waltham, MA: Academic Press.

Kuznetsov, V. V. and Pukhnachev, V. V. (2009). “A New Family of Exact Solutions of Navier-Stokes Equations”. In: *Doklady Physics* 54.3, pp. 126–130. DOI: 10.1134/S1028335809030069.

Lehoucq, R., Sorensen, D. C., and Yang, C. (1997). *ARPACK Users’ Guide: Solution of Large Scale Eigenvalue Problems with Implicitly Restarted Arnoldi Methods*.

Lin, S.-J. and Pierrehumbert, R. T. (1988). “Does Ekman Friction Suppress Baroclinic Instability?” In: *Journal of the Atmospheric Sciences* 45.20, pp. 2920–2933. DOI: 10.1175/1520-0469(1988)045<2920:DEFSBI>2.0.CO;2.

Lin, R.-S. and Malik, M. R. (1996). “On the Stability of Attachment-Line Boundary Layers. Part 1. The Incompressible Swept Hiemenz Flow”. In: *Journal of Fluid Mechanics* 311.-1, p. 239. DOI: 10.1017/s0022112096002583.

Lin, Z. (2003). “Instability of Some Ideal Plane Flows”. In: *SIAM Journal on Mathematical Analysis* 35.2, pp. 318–356. DOI: 10.1137/S0036141002406266.

Lindqvist, P. (2008). “A Nonlinear Eigenvalue Problem”. In: *Topics in Mathematical Analysis*. Ed. by P. Ciatti. Vol. 3. Singapore: World Scientific.

Lin, C. (1955). *The Theory of Hydrodynamic Stability*. Cambridge University Press.

Lindqvist, P. (1993). “Note on a Nonlinear Eigenvalue Problem”. In: *The Rocky Mountain Journal of Mathematics* 23.1, pp. 281–288.

Liouville, J. (1853). “Sur l’équation Aux Différences Partielles”. In: *Journal de mathématiques pures et appliquées* 18, pp. 71–72.

Mack, L. M. (1984). *Boundary-Layer Linear Stability Theory*. Tech. rep. Pasadena, California: California Institute of Technology, Jet Propulsion Lab.

Manning, M. L., Bamieh, B., and Carlson, J. M. (2008). “Descriptor Approach for Eliminating Spurious Eigenvalues in Hydrodynamic Equations”. In: *arXiv:0705.1542 [physics]*. arXiv: 0705.1542 [physics].

Mansour, N. N., Cambon, C., and Speziale, C. G. (1992). “Theoretical and Computational Study of Rotating Isotropic Turbulence”. In: *Studies in Turbulence*. Ed. by T. B. Gatski, C. G. Speziale, and S. Sarkar. New York, NY: Springer New York, pp. 59–75.

Marusic, I., McKeon, B. J., Monkewitz, P. A., Nagib, H. M., Smits, A. J., and Sreenivasan, K. R. (2010). “Wall-Bounded Turbulent Flows at High Reynolds Numbers: Recent Advances and Key Issues”. In: *Physics of Fluids* 22.6, p. 065103. DOI: 10.1063/1.3453711.

Marsden, J. E. and Ratiu, T. S. (1999). *Introduction to Mechanics and Symmetry: A Basic Exposition of Classical Mechanical Systems*. Ed. by J. E. Marsden, L. Sirovich, M. Golubitsky, and W. Jäger. Vol. 17. Texts in Applied Mathematics. New York, NY: Springer New York.

Maschho, K. J. and Sorensen, D. C. (1996). "PARPACK: An E Cient Portable Large Scale Eigenvalue Package for Distributed Memory Parallel Architectures". In: p. 10.

Mäulen, J. and Werner, P. (1983). "Lösungen der poissongleichung und harmonische vektorfelder in unbeschränkten gebieten". In: *Mathematical Methods in the Applied Sciences* 5.1, pp. 233–255. DOI: 10.1002/mma.1670050117.

McFadden, G., Murray, B., and Boisvert, R. (1990). "Elimination of Spurious Eigenvalues in the Chebyshev Tau Spectral Method". In: *Journal of Computational Physics* 91.1, pp. 228–239. DOI: 10.1016/0021-9991(90)90012-P.

Meerbergen, K. and Roose, D. (1996). "Matrix Transformations for Computing Rightmost Eigenvalues of Large Sparse Non-Symmetric Eigenvalue Problems". In: *IMA Journal of Numerical Analysis* 16.3, pp. 297–346. DOI: 10.1093/imanum/16.3.297.

Mehrmann, V. and Voss, H. (2004). "Nonlinear Eigenvalue Problems: A Challenge for Modern Eigenvalue Methods: Nonlinear Eigenvalue Problems: A Challenge for Modern Eigenvalue Methods". In: *GAMM-Mitteilungen* 27.2, pp. 121–152. DOI: 10.1002/gamm.201490007.

Meneveau, C. (2011). "Lagrangian Dynamics and Models of the Velocity Gradient Tensor in Turbulent Flows". In: *Annual Review of Fluid Mechanics* 43.1, pp. 219–245. DOI: 10.1146/annurev-fluid-122109-160708.

Millikan, C. B. (1939). "A Critical Discussion of Turbulent Flows in Channels and Circular Tubes". In: *Proceedings of fifth International Congress for Applied Mechanics, 1939*.

Miller, J. W. (1977). *Symmetry and Separation of Variables*. Reading: Addison-Wesley.

Mirzayev, J. (2016). "Asymptotic Suction Boundary Layer". MA thesis. TU Darmstadt.

Mishra, A. A. and Girimaji, S. S. (2015). "Hydrodynamic Stability of Three-Dimensional Homogeneous Flow Topologies". In: *Physical Review E* 92.5. DOI: 10.1103/PhysRevE.92.053001.

Miura, R. M., Gardner, C. S., and Kruskal, M. D. (1968). "Korteweg-de Vries Equation and Generalizations. II. Existence of Conservation Laws and Constants of Motion". In: *Journal of Mathematical Physics* 9.8, pp. 1204–1209. DOI: 10.1063/1.1664701.

Miura, R. M. (1976). "The Korteweg-deVries Equation: A Survey of Results". In: *SIAM Review* 18.3, p. 48.

Moffatt, H. K. (1965). "The Interaction of Turbulence with Strong Wind Shear". In: *Atmospheric Turbulence and Radio Waves Propagation, Proc. Intern. Collq. Moscow, 1965*, pp. 139–156.

Nichols, J. W. and Lele, S. K. (2011). "Global Modes and Transient Response of a Cold Supersonic Jet". In: *Journal of Fluid Mechanics* 669, pp. 225–241. DOI: 10.1017/S0022112010005380.

Noether, E. (1918). "Invarianten Beliebiger Differentialausdrücke". In: *Nachrichten von der Gesellschaft der Wissenschaften zu Göttingen, mathematisch-physikalische Klasse* 1918, pp. 37–44.

Nold, A. and Oberlack, M. (2013). “Symmetry Analysis in Linear Hydrodynamic Stability Theory: Classical and New Modes in Linear Shear”. In: *Physics of Fluids* 25.10, p. 104101. DOI: 10.1063/1.4823508.

Nold, A., Oberlack, M., and Cheviakov, A. F. (2015). “On New Stability Modes of Plane Canonical Shear Flows Using Symmetry Classification”. In: *Journal of Mathematical Physics* 56.11, p. 113101. DOI: 10.1063/1.4934726.

Oberlack, M., Hoyas, S., Kraheberger, S. V., Alcántara-Ávila, F., and Laux, J. (2022). “Turbulence Statistics of Arbitrary Moments of Wall-Bounded Shear Flows: A Symmetry Approach”. In: *Physical Review Letters* 128.2. DOI: 10.1103/PhysRevLett.128.024502.

Oberlack, M. (2000). “Symmetrie, Invarianz Und Selbstähnlichkeit in Der Turbulenz”. PhD thesis. RWTH Aaachen.

Oberlack, M. (2001). “A Unified Approach for Symmetries in Plane Parallel Turbulent Shear Flows”. In: *Journal of Fluid Mechanics* 427, pp. 299–328.

Oberlack, M. (2018). *Antrag DFG SPP1881 2. Phase: Asymptotic Suction Boundary Layer - Nonlinear Eigenfunctions, Nonlinear Stability and Coherent Structures*.

Oberlack, M. (2020). *Antrag ERC Advanced Grant 2020: Research Proposal: Symmetry Based Turbulence Theory*.

Oberlack, M. (1994). “Herleitung Und Lösung Einer Längenmaß- Und Dissipations-Tensorgleichung Für Turbulente Strömungen”. PhD thesis. Aachen: Rheinisch-Westfälische Technische Hochschule.

Oberlack, M. (1997). *Invariant Modeling in Large-Eddy Simulation of Turbulence*. Tech. rep. Stanford: Center for Turbulence Research.

Obrist, D. and Schmid, P. J. (2003a). “On the Linear Stability of Swept Attachment-Line Boundary Layer Flow. Part 1. Spectrum and Asymptotic Behaviour”. In: *Journal of Fluid Mechanics* 493, pp. 1–29. DOI: 10.1017/S0022112003005779.

Obrist, D. and Schmid, P. J. (2003b). “On the Linear Stability of Swept Attachment-Line Boundary Layer Flow. Part 2. Non-modal Effects and Receptivity”. In: *Journal of Fluid Mechanics* 493, pp. 31–58. DOI: 10.1017/S0022112003005780.

Olver, P. J. (2000). *Applications of Lie Groups to Differential Equations*. 2. ed., 1., softcover printing. Graduate Texts in Mathematics 107. New York: Springer.

Olver, F. W. J., ed. (2010). *NIST Handbook of Mathematical Functions*. Cambridge ; New York: Cambridge University Press : NIST.

Olver, F. W. J. (1974). *Introduction to Asymptotics and Special Functions*. Elsevier.

Olver, P. J. (1986). *Applications of Lie Groups to Differential Equations*. Ed. by P. R. Halmos, F. W. Gehring, and C. C. Moore. Vol. 107. Graduate Texts in Mathematics. New York, NY: Springer US.

Olver, P. J. (1992). “Symmetry and Explicit Solutions of Partial Differential Equations”. In: *Applied Numerical Mathematics* 10.3-4, pp. 307–324. DOI: 10.1016/0168-9274(92)90047-H.

Ondich, J. (1995). “The Reducibility of Partially Invariant Solutions of Systems of Partial Differential Equations”. In: *European Journal of Applied Mathematics* 6.04. DOI: 10.1017/S0956792500001881.

Örlü, R., Fransson, J. H., and Henrik Alfredsson, P. (2010). “On near Wall Measurements of Wall Bounded Flows—The Necessity of an Accurate Determination of the Wall Position”. In: *Progress in Aerospace Sciences* 46.8, pp. 353–387. DOI: 10.1016/j.paerosci.2010.04.002.

Orr, W. M. (1907a). “The Stability or Instability of the Steady Motions of a Perfect Liquid and of a Viscous Liquid. Part I: A Perfect Liquid”. In: 27, pp. 9–68.

Orr, W. M. (1907b). “The Stability or Instability of the Steady Motions of a Perfect Liquid and of a Viscous Liquid. Part II: A Viscous Liquid”. In: 27, pp. 69–138.

Orszag, S. A. (1971). “Accurate Solution of the Orr–Sommerfeld Stability Equation”. In: *Journal of Fluid Mechanics* 50.4, pp. 689–703. DOI: 10.1017/S0022112071002842.

Peyret, R. (2002). *Spectral Methods for Incompressible Viscous Flow*. Ed. by S. S. Antman, J. E. Marsden, and L. Sirovich. Vol. 148. Applied Mathematical Sciences. New York, NY: Springer New York.

Polyanin, A. D. and Zhurov, A. I. (2022). *Separation of Variables and Exact Solutions to Nonlinear PDEs*. Oxon: Chapman and Hall/CRC.

Polyanin, A. D. (2001). “Exact Solutions to the Navier-Stokes Equations with Generalized Separation of Variables”. In: *Doklady Physics* 46.10, pp. 726–731. DOI: 10.1134/1.1415590.

Pope, S. B. (2000). *Turbulent Flows*. Cambridge: Cambridge University Press.

Prandtl, L. (1932). “Zur Turbulenten Strömung in Rohren Und Längs Platten”. In: *Ergebnisse Der Aerodynamischen Versuchsanstalt Zu Göttingen Lfg. 4*. Berlin, Boston: De Gruyter, pp. 18–29.

Press, W. H., ed. (1996). *FORTRAN Numerical Recipes*. 2nd ed. Cambridge [England] ; New York: Cambridge University Press.

Pringle, C. C. and Kerswell, R. R. (2010). “Using Nonlinear Transient Growth to Construct the Minimal Seed for Shear Flow Turbulence”. In: *Physical Review Letters* 105.10. DOI: 10.1103/PhysRevLett.105.154502.

Puhnachev, V. V. (1960). “Group Properties of the Equations of Navier-Stokes in the Plane”. In: *Journal of Appl. Mech. and Tech. Phys* 1, pp. 83–90.

Pukhnachev, V. V. (2021). “Partial Invariance and Problems with Free Boundaries”. In: *Symmetries and Applications of Differential Equations: In Memory of Nail H. Ibragimov (1939–2018)*. Ed. by A. C. J. Luo and R. K. Gazizov. Singapore: Springer Singapore, pp. 251–267.

Rayleigh, L. (1917). “On the Dynamics of Revolving Fluids”. In: *Proceedings of the Royal Society A: Mathematical, Physical and Engineering Sciences* 93.648, pp. 148–154. DOI: 10.1098/rspa.1917.0010.

Rayleigh, L. (1879). “On the Stability, or Instability, of Certain Fluid Motions”. In: *Proceedings of the London Mathematical Society* s1-11.1, pp. 57–72. DOI: 10.1112/plms/s1-11.1.57.

Reynolds, O. (1883). “III. An Experimental Investigation of the Circumstances Which Determine Whether the Motion of Water Shall Be Direct or Sinuous, and of the Law of Resistance in Parallel Channels”. In: *Proceedings of the Royal Society of London* 35.224-226, pp. 84–99. DOI: 10.1098/rspl.1883.0018.

Roache, P. J. (2019). “The Method of Manufactured Solutions for Code Verification”. In: *Computer Simulation Validation: Fundamental Concepts, Methodological Frameworks, and*

Philosophical Perspectives. Ed. by C. Beisbart and N. J. Saam. Cham: Springer International Publishing, pp. 295–318.

Rogallo, S. (1981). "Numerical Experiments in Homogeneous Turbulence". In: p. 93.

Rohr, J. J., Itsweire, E. C., Helland, K. N., and Atta, C. W. V. (1988). "An Investigation of the Growth of Turbulence in a Uniform-Mean-Shear Flow". In: *Journal of Fluid Mechanics* 187, pp. 1–33. DOI: 10.1017/S002211208800031X.

Rosteck, A. (2014). "Scaling Laws in Turbulence - A Theoretical Approach Using Lie-Point Symmetries". PhD thesis. Darmstadt: Technische Universität Darmstadt.

Rosenhead, L. (1963). *Laminar Boundary Layers*. Oxford University Press.

Rotta, J. C. (2010). *Turbulente Strömungen*. Vol. 8. Göttinger Klassiker Der Strömungmechanik. Göttingen: Göttingen University Press.

Sagaut, P. and Cambon, C. (2018). *Homogeneous Turbulence Dynamics*. Cham: Springer International Publishing.

Sanjon, C. (2005). "Stability of Taylor-Couette Flow". MA thesis.

Saric, W. S., Reed, H. L., and White, E. B. (2003). "Stability and Transition of Three-dimensional Boundary Layers". In: *Annual Review of Fluid Mechanics* 35.1, pp. 413–440. DOI: 10.1146/annurev.fluid.35.101101.161045.

Schmid, P. J. and Henningson, D. S. (2001). *Stability and Transition in Shear Flows*. Springer.

Schlichting, H. and Gersten, K. (2006). *Grenzschicht-Theorie*. Berlin: Springer.

Schlatter, P. and Örlü, R. (2011). "Turbulent Asymptotic Suction Boundary Layers Studied by Simulation". In: *Journal of Physics: Conference Series* 318.2, p. 022020. DOI: 10.1088/1742-6596/318/2/022020.

Schmid, P. J. and Henningson, D. S. (1994). "Optimal Energy Density Growth in Hagen–Poiseuille Flow". In: *Journal of Fluid Mechanics* 277.-1, p. 197. DOI: 10.1017/S0022112094002739.

Schmid, P. J. (2007). "Nonmodal Stability Theory". In: *Annual Review of Fluid Mechanics* 39.1, pp. 129–162. DOI: 10.1146/annurev.fluid.38.050304.092139.

Schecter, S. (1976). "Bifurcations with Symmetry". In: *The Hopf Bifurcation and Its Applications*. Vol. 19. New York, NY: Springer New York, pp. 224–229.

Schneider, W. (1978). *Mathematische Methoden der Strömungsmechanik*. Wiesbaden: Vieweg-Teubner Verlag.

Schäfer, M. (1999). *Numerik im Maschinenbau*. Springer-Lehrbuch. Berlin: Springer.

Shariff, K. (2009). "Fluid Mechanics in Disks Around Young Stars". In: *Annual Review of Fluid Mechanics* 41.1, pp. 283–315. DOI: 10.1146/annurev.fluid.010908.165144.

Shakura, N. (2018). *Accretion Flows in Astrophysics*. New York, NY: Springer Berlin Heidelberg.

Shen, J. and Wang, L.-L. (2009). "Some Recent Advances on Spectral Methods for Unbounded Domains". In: *Commun. Comput. Phys.*, p. 47.

Shen, J., Tang, T., and Wang, L.-L. (2011). *Spectral Methods*. Vol. 41. Springer Series in Computational Mathematics. Berlin, Heidelberg: Springer Berlin Heidelberg.

Shi, L., Hof, B., Rampp, M., and Avila, M. (2017). "Hydrodynamic Turbulence in Quasi-Keplerian Rotating Flows". In: *Physics of Fluids* 29.4, p. 044107. DOI: 10.1063/1.4981525.

Silvis, M. H. (2020). “Physics-Based Turbulence Models for Large-Eddy Simulation: Theory and Application to Rotating Turbulent Flows”. PhD thesis. University of Groningen.

Skufca, J. D., Yorke, J. A., and Eckhardt, B. (2006). “Edge of Chaos in a Parallel Shear Flow”. In: *Physical Review Letters* 96.17. DOI: 10.1103/PhysRevLett.96.174101.

Smith, M. K. (1995). “Thermocapillary Migration of a Two-Dimensional Liquid Droplet on a Solid Surface”. In: *Journal of Fluid Mechanics* 294, pp. 209–230.

Solomonoff, A. (1992). “A Fast Algorithm for Spectral Differentiation”. In: *Journal of Computational Physics* 98.1, pp. 174–177. DOI: 10.1016/0021-9991(92)90182-X.

Spalart, P. R. and McLean, J. D. (2011). “Drag Reduction: Enticing Turbulence, and Then an Industry”. In: *Philosophical Transactions of the Royal Society A: Mathematical, Physical and Engineering Sciences* 369.1940, pp. 1556–1569. DOI: 10.1098/rsta.2010.0369.

Speziale, C. G. (1981). “Some Interesting Properties of Two-Dimensional Turbulence”. In: *Physics of Fluids* 24.8, p. 1425. DOI: 10.1063/1.863560.

Speziale, C. G. (1989). “Turbulence Modeling in Noninertial Frames of Reference”. In: *Theoretical and Computational Fluid Dynamics* 1, pp. 3–19.

Squire, H. B. (1933). “On the Stability for Three-Dimensional Disturbances of Viscous Fluid Flow between Parallel Walls”. In: *Proceedings of the Royal Society of London. Series A, Containing Papers of a Mathematical and Physical Character* 142.847, pp. 621–628. DOI: 10.1098/rspa.1933.0193.

Stewart, G. W. (2002). “A Krylov–Schur Algorithm for Large Eigenproblems”. In: *SIAM Journal on Matrix Analysis and Applications* 23.3, pp. 601–614. DOI: 10.1137/s0895479800371529.

Straughan, B. (2004). *The Energy Method, Stability, and Nonlinear Convection*. Ed. by S. S. Antman, J. E. Marsden, and L. Sirovich. Vol. 91. Applied Mathematical Sciences. New York, NY: Springer New York.

Strogatz, S. H. (2018). *Nonlinear Dynamics and Chaos*. Zeroth. New York, NY: CRC Press.

Sulem, C. and Sulem, P.-L., eds. (2004). *The Nonlinear Schrödinger Equation: Self-Focusing and Wave Collapse*. Vol. 139. Applied Mathematical Sciences. New York, NY: Springer New York.

Sun, L. (2007). “General Stability Criterion for Inviscid Parallel Flow”. In: *European Journal of Physics* 28.5, pp. 889–895. DOI: 10.1088/0143-0807/28/5/012.

Sundermeyer, K. (2014). *Symmetries in Fundamental Physics*. Cham: Springer International Publishing.

Swaters, G. E. (2000). *Introduction to Hamiltonian Fluid Dynamics and Stability Theory*. New York: Chapman and Hall/CRC.

Synge, J. L. (1938). “On the Stability of a Viscous Liquid between Rotating Coaxial Cylinders”. In: *Proceedings of the Royal Society A: Mathematical, Physical and Engineering Sciences* 167.929, pp. 250–256. DOI: 10.1098/rspa.1938.0130.

Takagi, D. and Strickler, J. R. (2020). “Active hydrodynamic imaging of a rigid spherical particle”. In: *Scientific Reports* 10.1. DOI: 10.1038/s41598-020-58880-0.

Tavoularis, S. and Corrsin, S. (1981). “Experiments in Nearly Homogenous Turbulent Shear Flow with a Uniform Mean Temperature Gradient. Part 1”. In: *Journal of Fluid Mechanics* 104, pp. 311–347. DOI: 10.1017/S0022112081002930.

Taylor, G. I. (1923). “Stability of a Viscous Liquid Contained between Two Rotating Cylinders”. In: *Philosophical Transactions of the Royal Society A: Mathematical, Physical and Engineering Sciences* 223.605-615, pp. 289–343. DOI: 10.1098/rsta.1923.0008.

Theofilis, V., Fedorov, A., Obrist, D., and Dallmann, U. C. (2003). “The Extended GrtlerHmmerlin Model for Linear Instability of Three-Dimensional Incompressible Swept Attachment-Line Boundary Layer Flow”. In: *Journal of Fluid Mechanics* 487, pp. 271–313. DOI: 10.1017/s0022112003004762.

Theofilis, V. (2003). “Advances in Global Linear Instability Analysis of Nonparallel and Three-Dimensional Flows”. In: *Progress in Aerospace Sciences* 39.4, pp. 249–315. DOI: 10.1016/S0376-0421(02)00030-1.

Theofilis, V. (2011). “Global Linear Instability”. In: *Annual Review of Fluid Mechanics* 43.1, pp. 319–352. DOI: 10.1146/annurev-fluid-122109-160705.

Theofilis, V. (1998). “On Linear and Nonlinear Instability of the Incompressible Swept Attachment-Line Boundary Layer”. In: *Journal of Fluid Mechanics* 355, pp. 193–227. DOI: 10.1017/s0022112097007660.

Thomas, P. S., Somers, M. F., Hoekstra, A. W., and Kroes, G.-J. (2012). “Chebyshev High-Dimensional Model Representation (Chebyshev-HDMR) Potentials: Application to Reactive Scattering of H2 from Pt(111) and Cu(111) Surfaces”. In: *Physical Chemistry Chemical Physics* 14.24, p. 8628. DOI: 10.1039/c2cp40173h.

Timme, S. (2020). “Global Instability of Wing Shock-Buffet Onset”. In: *Journal of Fluid Mechanics* 885. DOI: 10.1017/jfm.2019.1001.

Townsend, A. (2014). “Computing with Functions in Two Dimensions”. PhD thesis. University of Oxford.

Trefethen, L. N., Birkisson, A., and Driscoll, T. A. (2018). *Exploring ODEs*. New York: Society for Industrial & Applied Mathematics.

Trefethen, L. N., Trefethen, A. E., Reddy, S. C., and Driscoll, T. A. (1993). “Hydrodynamic Stability Without Eigenvalues”. In: *Science, New Series* 261.5121, pp. 578–584.

Trefethen, L. N. (2000). *Spectral Methods in MATLAB*. Software, Environments, Tools. Philadelphia, PA: Society for Industrial and Applied Mathematics.

Volponi, F. and Yoshida, Z. (2002). “Remarks on Kelvin’s Solutions of Shear-flow Systems – a Generalized Modal Approach –”. In: *Journal of the Physical Society of Japan* 71.8, pp. 1870–1874. DOI: 10.1143/JPSJ.71.1870.

Volkmer, H. (1988). *Multiparameter Eigenvalue Problems and Expansion Theorems*. Lecture Notes in Mathematics. Berlin Heidelberg: Springer.

von Kármán, T. (1930). “Mechanische Ähnlichkeit Und Turbulenz”. In: *Wiss. Göttingen, Math. Phys. Klasse* 58.

Weideman, J. A. and Reddy, S. C. (2000). “A MATLAB Differentiation Matrix Suite”. In: *ACM Transactions on Mathematical Software (TOMS)* 26.4, pp. 465–519. DOI: 10.1145/365723.365727.

Weideman, J. A. C. and Trefethen, L. N. (1988). “The Eigenvalues of Second-Order Spectral Differentiation Matrices”. In: *SIAM Journal on Numerical Analysis* 25.6, pp. 1279–1298. DOI: 10.1137/0725072.

Winternitz, P. and Fris, I. (1965). “Invariant Expansions of Relativistic Amplitudes and Subgroups of the Proper Lorentz Group”. In: *Yadern. Fiz.* 1.

Yaglom, A. M. (2012). *Hydrodynamic Instability and Transition to Turbulence*. Ed. by U. Frisch. Vol. 100. Fluid Mechanics and Its Applications. Dordrecht: Springer Netherlands.

Yalcin, A., Turkac, Y., and Oberlack, M. (2021). “On the Temporal Linear Stability of the Asymptotic Suction Boundary Layer”. In: *Physics of Fluids* 33.5, p. 054111. DOI: 10.1063/5.0048208.

Yalcin, A. (2018). *Unpublished Notes on the Derivation for a Nonlinear Eigenvalue Problem*. Tech. rep.

Yoshida, Z. (2005). “Kinetic Theory for Non-Hermitian Dynamics of Waves in Shear Flow”. In: *Physics of Plasmas* 12.2, p. 024503. DOI: 10.1063/1.1849799.

Zebib, A. (1987). “Removal of Spurious Modes Encountered in Solving Stability Problems by Spectral Methods”. In: *Journal of Computational Physics* 70.2, pp. 521–525. DOI: 10.1016/0021-9991(87)90193-8.

Zhalij, A., Burde, G. I., and Nasibullayev, I. S. (2006). “Separation of Variables in the Hydrodynamic Stability Equations”. In: *Journal of Physics A: Mathematical and General* 39.22, pp. 7141–7160. DOI: 10.1088/0305-4470/39/22/024.

Zhalij, A. (2002). “On Separable Pauli Equations”. In: *Journal of Mathematical Physics* 43.3, pp. 1365–1389. DOI: 10.1063/1.1436563.

Zhalij, A. (1999). “On Separable Fokker-Planck Equations with a Constant Diagonal Diffusion Matrix”. In: *Journal of Physics A: Mathematical and General* 32.42, pp. 7393–7404. DOI: 10.1088/0305-4470/32/42/311.

Zhdanov, R. and Zhalij, A. (1999a). “On Separable Schrödinger Equations”. In: *Journal of Mathematical Physics* 40.12, pp. 6319–6338. DOI: 10.1063/1.533095.

Zhdanov, R. and Zhalij, A. (1999b). “Separation of Variables in the Kramers Equation”. In: *Journal of Physics A: Mathematical and General* 32.20, pp. 3851–3863. DOI: 10.1088/0305-4470/32/20/315.